Alternative marine energy carrier impact on ship powering and the environment

A comparative conceptual LCA of the operational stage of ship types with alternative marine energy carriers

A.M. Snaathorst

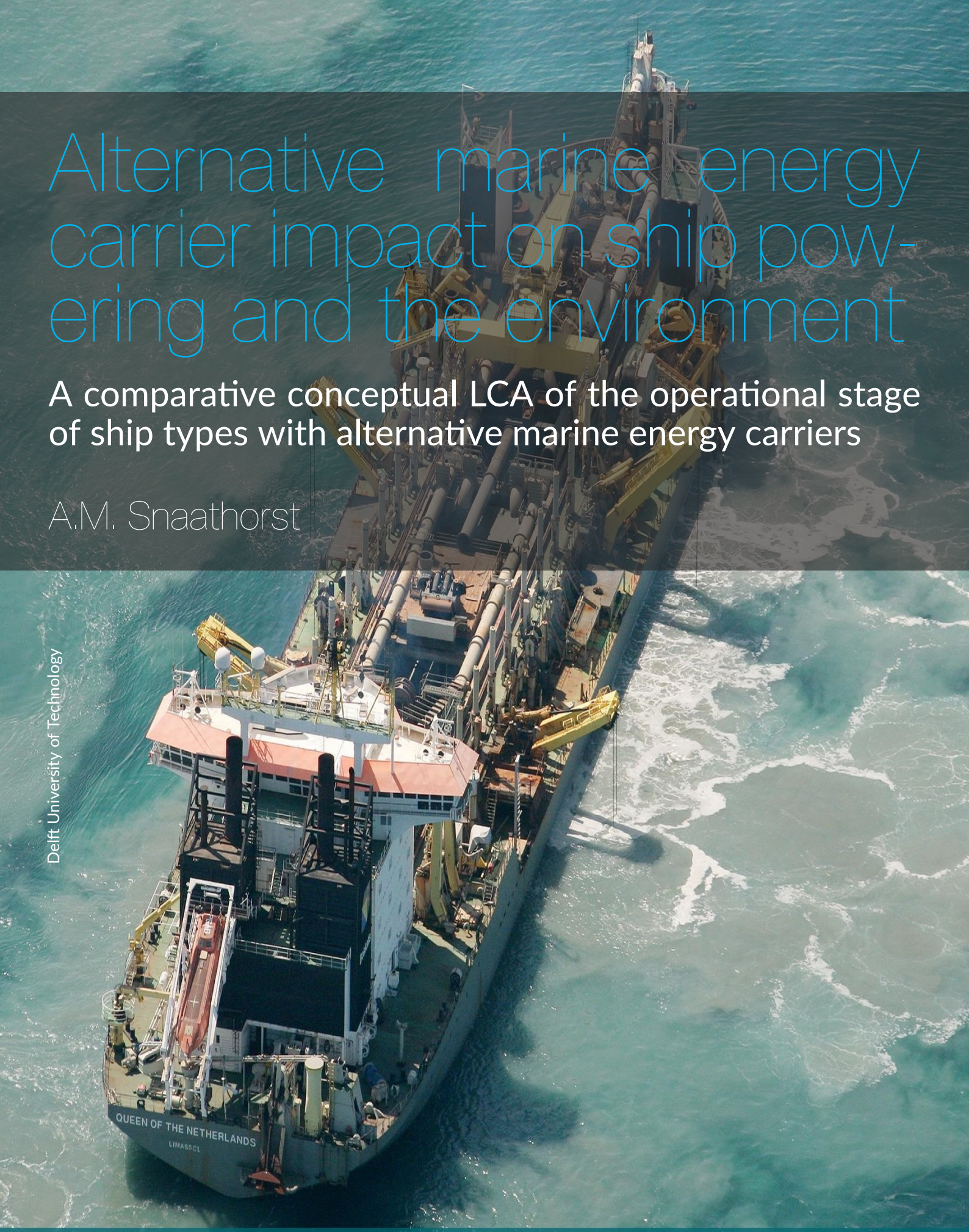

Delft University of Technology

TU Delft

VUYK ENGINEERING

Alternative marine energy carrier impact on ship powering and the environment

A comparative conceptual LCA of the operational stage of ship types with alternative marine energy carriers

by

A.M. Snaathorst

Performed at

Vuyk Engineering Rotterdam

This thesis **MT.22/23.020.M** is written to obtain the degree of MSc in Marine Technology
in the specialization of *Ship Design* and *Maritime Operations & Management*
at the faculty of 3mE at Delft University of Technology

Delft, Monday 23rd January, 2023

Thesis exam committee

Chair & TU Delft supervisor/professor	Dr.ir. J.F.J. Pruyn
TU Delft staff member	Dr.ir. L. van Biert
Vuyk Engineering supervisor	Ir. A.J.T.H. Bot

Author details

Student number	4345584

An electronic version of this thesis is available at `http://repository.tudelft.nl/`.

TU Delft

Preface

As a young child, I was always fascinated by the world of engineering and technology without even realizing it. From building machines with Lego's to designing and building rafts, I knew that I wanted to pursue a career in this field. So, it is with great excitement and a sense of accomplishment that I present my master's thesis, a culmination of my studies and efforts in Marine Technology at the Delft University of Technology. It is my wish that the work contained within these pages will make a meaningful contribution to my program specializations Ship Design, and Maritime Operations and Management, and serve as a foundation for future research and innovation.

I would like to begin to thank my university daily supervisor, Jeroen Pruyn, for his guidance and insights during the course of this project. I am forever grateful for his expertise and mentorship. Additionally, I am grateful to have had the opportunity to collaborate with Vuyk Engineering Rotterdam on my master's thesis research. Working with such a renowned and respected organization in the marine engineering industry has been an invaluable learning experience for me. Not only have I gained invaluable understanding into the latest technologies and methodologies in the field, but I have also had the chance to observe and participate in the inner workings of a successful engineering company. I would like to thank my company daily supervisor, Sander Bot, for his support and cooperation during my time at Vuyk Engineering Rotterdam. His industry experience have greatly enhanced the practical applications of my research.

Lastly, I would like to thank my family, girlfriend and friends for their unconditional love and support. The constant source of encouragement has pulled me through the late nights spent writing and researching. Their contributions to my academic and personal growth have been immeasurable. This thesis would not have been possible without the support of all of these wonderful individuals.

A.M. Snaathorst
Rotterdam, January 2023

Summary

The maritime industry is responsible for 3% of the annual global CO_2 emissions, which is a cause of global warming and the consequent climate change due to the use of fossil fuel oil. Without any intervention, these emissions will further rise, and therefore the International Maritime Organization has implemented greenhouse gas emission restrictions with the goal of eliminating them before the end of this century. Consequently, fossil fuel oil will be forced out of the ship powering market for what are now considered alternative marine energy carriers (AMECs). The predicted AMECs of the near future are still fuel oil, but it is quickly making way for LNG, hydrogen based fuels, alcohol fuels, batteries, and bio/renewable versions of these energy carriers. However, all these AMECs have a lower contained volumetric and gravimetric energy density compared to fuel oil. As a result, ship designs would require more volume and weight to accommodate the same amount of effective energy to perform the same operational requirements. In general, a larger and heavier ship results in higher propulsion powering and thus a higher energy carrier consumption.

It is generally acknowledged that the use of AMECs for equal power is more environmentally friendly. However, to the authors' knowledge, it has not been researched if this is still the case when taking the increased energy carrier consumption into account for constant operational requirements. In ample cases, there is the compromise of cargo volume, service speed, sailing range, or a combination of these operational requirements to accommodate the additional AMEC bunker space. Maritime design and engineering company Vuyk Engineering Rotterdam has identified this issue and values sustainable solutions in their vessel designs and strive to become more environmentally friendly. To support Vuyk's environmental ambition, the goal of this research is to determine the full environmental impact of AMECs on ships while taking the powering impact into account with regards to conventional fuel oil.

Two models have been developed to determine the powering impact and the environmental impact of the future predicted AMECs. The powering impact assessment model generates new ship designs for existing ships for their constant operational requirements. This assessment is performed on bulk carriers, tankers, container ships and trailing suction hopper dredgers. The design generation procedure applies the additional required AMEC bunker space to the original design to optimize for the least additional resistance, while adhering to the dimension trends of the ship type. The AMEC types considered are fuel oil, methanol, LNG, liquid hydrogen, ammonia, and lithium ion batteries. The environmental impact assessment model consists of a comparative life cycle assessment of the operational stage of a ship with the AMECs. For each AMEC type, a conventional version and a bio/renewable version are investigated.

The results show that the average additional main engine brake power increase for methanol, LNG, liquid hydrogen, ammonia and batteries are +2.3%, +1.1%, +8.6%, +3.7%, and +235.3% respectively. The results for the gross environmental impact show that conventional methanol, conventional liquid hydrogen, conventional ammonia, and conventionally charged lithium ion batteries perform worse than conventional fuel oil in terms of global warming. When taking the powering increase per ship type into account, only renewably charged lithium ion batteries transition from a performance that is better to worse in terms of global warming for all ship types. The criteria for the recommended AMEC for the environment is suggested to perform better in terms of the three environmental endpoint areas of protection and global warming - all while taking the powering impact into account. Renewable liquid hydrogen and renewable ammonia are the only AMECs that comply with this criteria, and therefore these are the recommended energy carriers for the least amount of damage to human health, ecosystems and natural resource availability.

Contents

List of Figures

List of Tables

1

Introduction and problem analysis

The maritime industry is responsible for 3% of the annual global CO_2 emissions, which is a cause of global warming and the consequent climate change due to the use of fossil fuel oil [70]. Ship engines run on fossil fuels and emit CO_2 which is the primary green house gas (GHG) responsible for climate change [70]. In 2013 the International Maritime Organization (IMO) enforced a regulation to reduce GHG emissions from newly built international shipping vessels. As a result the measure encourages the use of more energy efficient propulsion methods and equipment on board. However in 2015 the United Nations (UN) set out the treaty in the Paris Agreement to take further urgent action as the total global GHG emissions were not declining. The IMO therefore presented a new strategy to reduce GHG emissions from international shipping by 50% annually by the year 2050. Consequently new and stricter GHG emission regulations followed that also apply to existing vessels. The new regulations boosted technical research and innovative development regarding energy consumption by engine manufactures and ship designers. Accordingly alternative marine energy carriers (AMECs) which result in less or no GHG emissions become more lucrative in order to comply with the regulations. It is projected that conventional fuel oil in ships will be reduced by more than 50% by the year 2050 [91]. Be that as it may, the regulations only apply to direct GHG emissions and it does not take into account the emissions from the production process. It could be possible that the production and usage emissions of an AMEC are greater than that of conventional marine fuel oil. Thus not achieving the goal of reducing GHG emissions as a whole. In addition, AMECs have a lower contained energy density than fuel oil and therefore ships will have to become larger and heavier to travel the same distance with the same cargo space. As a result more power is necessary and the energy consumption will increase. Accordingly an AMEC that does produce less GHG emissions might result in higher emissions due to the increased energy consumption. Furthermore climate change is not the only environmental impact as there are also other emissions resulting in other effects. It could be possible that the overall climate change impact is reduced by switching to an AMEC, but then resulting in an other environmental issue. In conclusion, there is a need to research the broader environmental effects of AMECs including the effect on energy consumption.

Maritime design and engineering company Vuyk Engineering Rotterdam has also identified these issues. Vuyk specializes in dredging, heavy lift, subsea and offshore vessels which do not have to comply with the IMO's GHG regulation as those vessels are not shipping vessels. However, there is a possibility that these vessel types might also have to comply in the future, just like the regulation expansion from new to existing shipping vessels in the past. In addition, Vuyk Engineering and their clients value sustainable solutions in their vessel designs and strive to become more environmentally friendly. The goal of this research is to determine the full environmental impact of AMECs in ships while taking the powering impact into account with regards to conventional fuel oil.

This chapter consists of a literature research to analyze the extended problem into greater detail and the research project description. First the current situation regarding changing ship design aspects is explained using a model in section 1.1. Thereafter each aspect of ship design contributing to the changing vessel specifications is investigated into greater detail in sections 1.2 to 1.5. After this follows an analysis on the possible environmental consequences of the changing ship design aspects in section 1.6. Finally,

the research project is described for its novelty, scope, methodology and reporting in section 1.7.

1.1. The current situation

According to Vossen et al. the ship design or mission requirements of a vessel are composed of four aspects [136]. The four aspects are *Available Technology*, *Operational Requirements*, *External Requirements*, and *Commercial Aspects* and are illustrated in figure 1.1. With these four aspects the current situation can be depicted more clearly where the *External Requirements* are affecting the other aspects and causing a change in ship design. As a result, there are various environmental consequences.

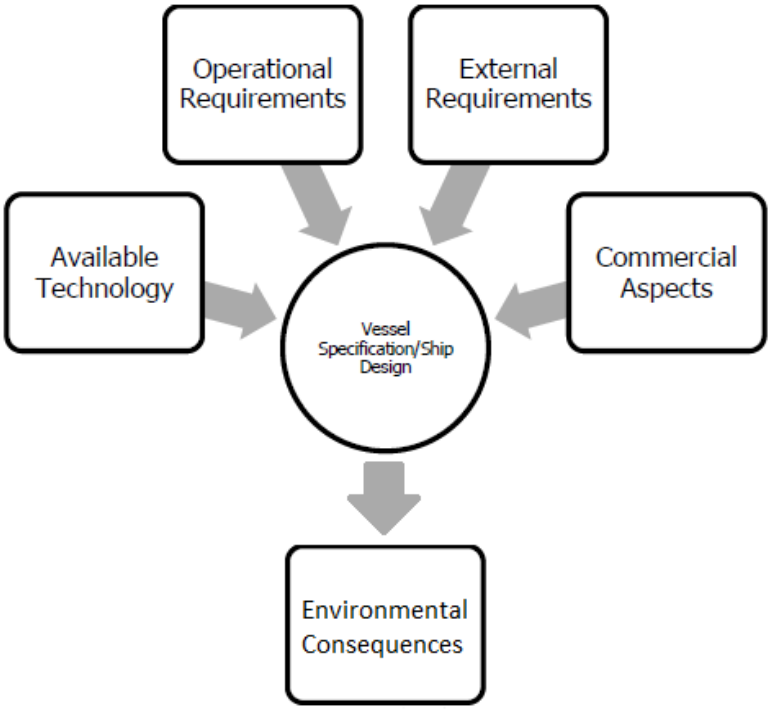

Figure 1.1: Ship design aspects by Vossen et al. (2013) adapted by author

The *External Requirements* of ship design concern the domestic and international rules and regulations. They are governed on national level (flag administration) and international level (IMO) for safety, security and environmental motivations. The IMO's environmental emission regulations for ships are becoming significantly stricter and will progress further in the future [131]. This change in *External Requirements* is causing an out roll of new powering technologies to comply with these regulations and consequently it is changing the *Available Technology* aspect. This aspect affecting the ship design is driven by the available equipment and building materials on the market. The new powering technologies are accompanied by AMECs and thus changing the *Commercial Aspects* of ships. The *Commercial Aspects* of ship design concern the profitability of its service. The demand for newly built ships is amongst others driven by the international oil and gas prices which determines the fuel cost. In addition the domestic and global economic status drives the future outlook of the demand for new ships. However now that other energy carriers have entered the market, the prices and availability of conventional fuels and AMECs will change. Unlike the others, the *Operational Requirements* division is affected to a lesser extent. The *Operational Requirements* concern the requirements to perform the vessel's tasks. When focusing on new ships and their design, the main dimensions are not necessarily a part of that. They are considered to be the result of the four ship design aspects rather than a given requirement. However the ship dimensions do not necessarily affect the operational transportation service demand from a client, as long as the original task can still be performed. Therefore the *Operational Requirements* aspect remains the same for newly built ships with AMECs.
To summarize this section, the *External Requirements*, *Available Technology* and *Commercial Aspects* of ship design are changing, while the *Operational Requirements* remain the same. This affects the vessel specifi-

cations of newly built ships and might bring environmental consequences with it. This situation is driven by the IMO's GHG regulations which are further investigated in greater detail in the next section.

1.2. External requirements

Ships must comply with global and domestic regulations and thus are affected by these external requirements. The IMO is a specialized agency within the UN which governs the global regulations for safety, security and environmental performance for the maritime industry. In 1973, the International Convention for the Prevention of Pollution from Ships (MARPOL) was adopted into the IMO [65]. This is the first international external requirement concerning the environment for ships. MARPOL is the most important international convention for preventing pollution of the marine environment by ships due to operational or unintentional causes. This convention covers many types of pollution by ships, such as toxic chemicals, oils, packaging, wastes, air emissions and other harmful substances and went into force in 1978.

In 1997, Annex VI: Prevention of Air Pollution from Ships protocol was added into MARPOL and went into force in 2005 [69]. From these regulations, sulphur oxide (SOx) and nitrogen oxide (NOx) emissions from ship exhausts are limited, and purposeful emissions of ozone-depleting compounds are prohibited. Furthermore designated Emission Control Areas (ECAs) have been introduced for more rigorous rules for SOx, NOx, and particulate matter. These areas are close to the shore and therefore the emission have a higher impact on human health. Only until 2011 did the IMO introduce an amendment to Annex VI to reduce GHG emissions from international shipping vessels in order to combat global warming and consequently climate change [63]. This is done by making the Energy Efficiency Design Index (EEDI) for newly built ships and the Ship Energy Efficiency Management Plan (SEEMP) for all ships mandatory. The amendment went into force in 2013 where it progressively restricts CO_2 emissions which must be monitored by ship operators and owners. The EEDI results in more efficient energy use from engines and equipment through emission limits while the SEEMP provides improvement approaches to become more energy efficient.

The UN set out seventeen Sustainable Developent Goals (SDGs) in 2015 of which goal thirteen advocates to "Take urgent action to combat climate change and its impacts" [128]. As the IMO is a body of the UN, the current emissions regulations on GHG needed to become stricter to coincide regulation and vision. Therefore, in 2018, the Marine Environment Protection Committee (MEPC) of the IMO adopted a the Initial Strategy which ratifies the commitment to reduce GHG emissions from international shipping while continuing efforts to phase them out as quickly as practicable during the next century. The Initial Strategy by the IMO on the reduction of GHG emission from ships states:

"The initial GHG strategy envisages, in particular, a reduction in carbon intensity of international shipping (to reduce CO_2 emissions per transport work, as an average across international shipping, by at least 40% by 2030, pursuing efforts towards 70% by 2050, compared to 2008); and that total annual GHG emissions from international shipping be reduced by at least 50% by 2050 compared to 2008." [64]

The emission pathway from international shipping according to the IMO's GHG Initial Strategy, can be seen in figure 1.2. The EEDI only affects newly built ships to reduce emissions, however that is not enough to meet the GHG strategy. It can be seen in the figure that the 'Business-as-usual emissions' pathway first slightly decreases until 2020 but thereafter significantly increases. Therefore to close the gap, the most recent regulations were adopted in 2021 for already existing ships: the Energy Efficiency Existing Ships Index (EEXI) and the Carbon Intensity Indicator (CII). Due to these measures it is inevitable for the shipping industry and shipbuilding sector to face some radical changes, including tightening regulations and the use of alternative fuels [76].

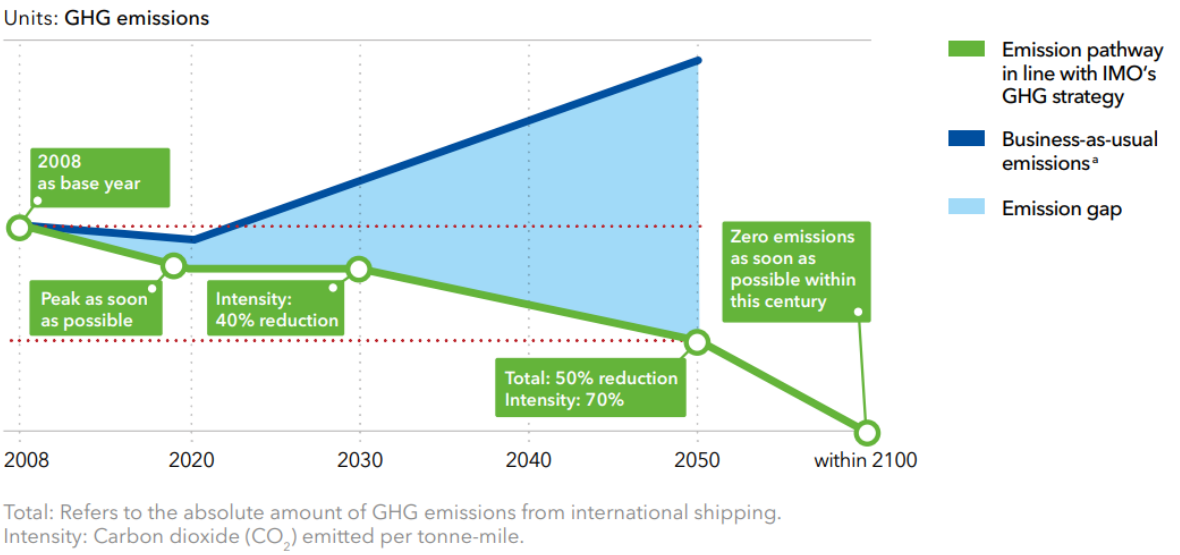

Figure 1.2: IMO's Initial Strategy GHG emission pathway [31]

The EEXI and CII regulations will go into force in 2023, while the last phase of the EEDI goes into effect shortly later in 2025. The most relevant air pollution regulations have been considered and an overview of them is given in table 1.1. It is possible to comply with these considered regulations by using alternative fuels which result in less direct GHG emissions. In order to understand how these AMECs can benefit, the working principles of these regulations are presented in the following subsections.

Table 1.1: Timeline overview of air pollution regulations in the IMO

Adopted	Enforced	Regulation
1973	1978	MARPOL - Convention for prevention of pollution from ships
1997	2005	Annex VI - Prevention of air pollution
2011	2013	EEDI and SEEMP
2018		Initial Strategy on reduction of GHG emissions (not regulation)
2021	2023	EEXI and CII

1.2.1. The EEDI and SEEMP regulations

The EEDI for newly built ships encourages the use of more energy efficient equipment and engines for various ship types, and sizes and specifies a minimum energy efficiency level per capacity distance (e.g. tonne-km). The EEDI regulation is proposed to boost technical research and innovative development of all mechanisms regarding fuel efficiency for vessels in their design phase [107]. It is however only mandatory for ships of 400 GT and above. The attained EEDI is a numerical value for a ship design and is expressed in grams of CO_2 per tonne-km and it is calculated according to the simplified equation 1.1. The attained EEDI must be lower than the required EEDI per equation 1.2. The attained EEDI formula takes energy saving technology into account and also accounts correction factor for certain design elements, for instance an ice class [43]. These design elements negatively impact the propulsion performance and therefore result in more CO_2 emissions. However these design elements are necessary for safety purposes. Accordingly these ships deserve a correction factor in the attained EEDI to make the playing field even for all ships. The attained EEDI formula is the same for all ships, but the required EEDI is calculated differently per ship type.

$$\text{Attained EEDI} = \frac{\text{CO}_2 \text{ emissions}}{\text{Transported work}} \quad \left[\frac{g\ CO_2}{t \cdot km}\right] \tag{1.1}$$

$$\text{Attained EEDI} \leq \text{Required EEDI} \tag{1.2}$$

The calculation of the attained EEDI in more detail is computed according to equation 1.3 [21]. The total CO_2 emissions are dependent on the ship's energy consumers and energy savers. They are related to the engine power (P), fuel conversion factor to CO_2 (C_F) and specific fuel consumption of the engine (SFC). The transported work is dependent on the capacity, service speed (V_S) and correction factors (f). The denominator in the equation contains the previously determined constant operational factors. Therefore the parameters in the numerator are deciding factor for direct emissions. Consequently the influencing factors for direct emissions are the power which corresponds to the energy consumers, conversion factor which corresponds to the energy carrier type, and the specific fuel consumption which corresponds to the engine (power plant) efficiency.

$$\text{Attained EEDI} = \frac{\sum(P \cdot C_F \cdot SFC)_{consumers} - \sum(P \cdot C_F \cdot SFC)_{savers}}{Capacity \cdot V_S \cdot f} \quad \left[\frac{g\ CO_2}{t \cdot km}\right] \tag{1.3}$$

The required EEDI is calculated according to equation 1.4 and differs per ship type and size [10]. The EEDI regulation went into effect on January 1st 2013 where new ships needed to meet the required EEDI for the next two years, called *Phase 0*. Every five years after *Phase 0*, the required EEDI is tightened by an additional 10%. The EEDI requirement during the different phases is illustrated in figure 1.3. This regulation is aimed to increase the energy efficiency of ships over time. However according to a study by Transport & Energy, 71% of container ships, 69% of general cargo ships, 26% of tankers, and 13% of gas carriers built between 2013 and 2017 already comply with the *Phase 3* requirement (-30% emissions) [1]. On the contrary, for bulk carriers this is only 1%. This exposes the inequality of the regulation and also the lost potential to further reduce its emissions in ships (e.g. container ships) that already meet the harshest requirement.

$$\text{Required EEDI} = a \cdot b^{-c} \cdot (100\% - phase\ \%) \quad [g\ CO_2/t \cdot nm] \tag{1.4}$$

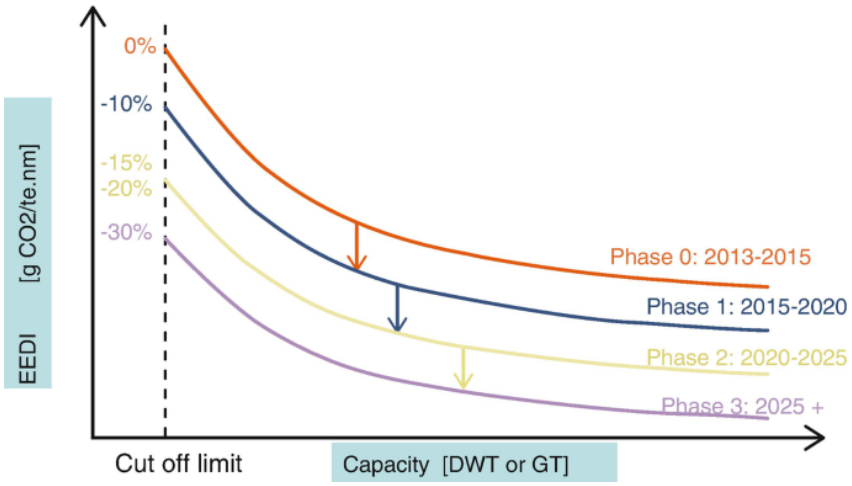

Figure 1.3: An illustration of the required EEDI phases over time [64]

The required EEDI is calculated by three parameters (a, b and c), of which parameter a and c are fixed values [67]. Parameter b is the deadweight tonnage (DWT) of a ship. The DWT is the total carrying capacity of a ship at loaded design draft. The DWT is the sum of all the free weights on board, thus excluding the weight of the ship itself: DWT is the weight of cargo, fuel, fresh water, ballast water, provisions, passengers, and crew [127]. The formula for the DWT is expressed in equation 1.5. According to McKinsey Energy Insights, the cargo weight is approximately 95% of the DWT [97]. Therefore it is not calculated exclusively with the cargo weight and thus does not fully represent the emissions of the transport of the cargo. As not all ship types must comply with the EEDI, such as TSHDs, the EEDI is not relevant for them. However, the IMO's Initial Strategy states that all ships must have zero GHG emissions before 2100, thus non-compliant ship types will also have to surrender to the alternative energy carriers in the future.

$$DWT = m_{cargo} + m_{fuel} + m_{freshwater} + m_{ballast\ water} + m_{provisions} + m_{passengers} + m_{crew} \quad (1.5)$$

The SEEMP is an operational strategy that creates a system to increase a ship's energy efficiency in a profitable way. The SEEMP also offers an approach for managing the efficiency performance of a fleet over time utilizing a software indicator as a monitoring tool [62]. The software tool facilitates ship operators to monitor the ship's fuel consumption and efficiency to determine how an operational or technical implementation change will affect it. This strategy will drive ship operators to not be able to slack in the future when going into a stricter EEDI phase.

1.2.2. The EEXI and CII regulations

To further reduce emissions from ships, the IMO has adopted the Energy Efficiency Existing Ships Index (EEXI) and the Carbon Intensity Indicator (CII) that will go into force on the first of January 2023. As the name already states, the EEXI is for already existing ships and the CII is for existing and newly built ships. Existing ships did not have to comply with the EEDI regulation, but significant emission reduction is still possible for these vessels. Therefore these indexes have come into practice to strengthen the IMO's GHG strategy goals and to coincide with the UN's Paris Agreement. The EEXI regulation works in the same principle as the EEDI regulation: where the attained EEXI must be lower than the required EEXI. The attained EEXI is calculated according to the same formula as the attained EEDI in equation 1.3. The required EEXI is similar to the required EEDI, however a reduction factor (X) has been introduced and is calculated according to equation 1.7. The reduction factors are not equal over all ship types and also not within a ship type. A higher DWT results in a higher reduction factor. The parameters a, b, and c within the required EEXI are the same as for the required EEDI. The required EEXI is only subjected to phase 0 (0% reduction) of the required EEDI and does not change over time.

$$\text{Attained EEXI} = \text{Attained EEDI} \leq \text{Required EEXI} \quad [g\ CO_2/t \cdot nm] \quad (1.6)$$

$$\text{Required EEXI} = \left(1 - \frac{X}{100}\right) \cdot a \cdot b^{-c} \quad [g\ CO_2/t \cdot nm] \quad (1.7)$$

The EEDI is required to all shipping vessels that are 400 GT and above. This is not the case for the EEXI, where it is required for a minimal DWT dependent per ship type. In addition to the EEXI regulation, the ship owners of existing ships must also provide an SEEMP to ensure that the regulation will be met in the future. According to ClassNK, on the day that the EEXI will go into force, 84% of the ships that are compliant need to take technical action to comply with the ruling [25]. However, the EEXI will only reduce CO_2 emissions from the 2030 fleet by 0.8% - 1.6% compared to no EEXI regulation [112].

The CII is an annual carbon emissions registration- and rating system for all shipping vessels above 5000 GT regardless of when they were built. The CII is calculated according to equation 1.8 [28]. In comparison, the EEDI and EEXI focuses on the physical ship properties, while the CII focuses on the operational properties. Particularly on the efficiency of transported passengers or cargo. With the collected CII's from all compliable ship types, a ship can be given a operational carbon intensity rating. The CII rating ranges from A (best) to E (worst) and is illustrated in figure 1.4. The CII rating system is based on the relative performance rather than a predefined value. Due to the fuel and distance registry going into affect in 2023, the distribution scale of CII's is currently unknown. In addition, the first assessment will take place in 2024 and thereafter the carbon emission targets will be set in 2025 for the duration of 2027 to 2030. Even though there is much unknown about the scale distribution, the idea is that a ship that is rated an E for a single year or rated a D for three consecutive years, must take immediate action to achieve a C rating the next year [28]. This approach will be applied in the SEEMP. Once again the denominator in the equation contains the previously determined constant operational factors. Therefore the parameters in the numerator are deciding factor for direct emissions. Consequently the influencing factors for direct emissions are the same as in the EEDI and EEXI regulation.

$$\text{CII} = \frac{\text{Annual fuel consumption} \cdot \text{CF}}{\text{Annual distance traveled} \cdot \text{Capacity}} \cdot f \quad [g\ CO_2/t \cdot nm] \quad (1.8)$$

Where:

Annual fuel consumption (t) of fuel type
CF: Conversion Factor of fuel type to emissions (t CO_2/t fuel)
Annual distance traveled (nm)
Capacity: Deadweight tonnage (DWT) (or Gross Tonnage (GT) for passenger ships)
f: Corrections factor (-) *To be developed*

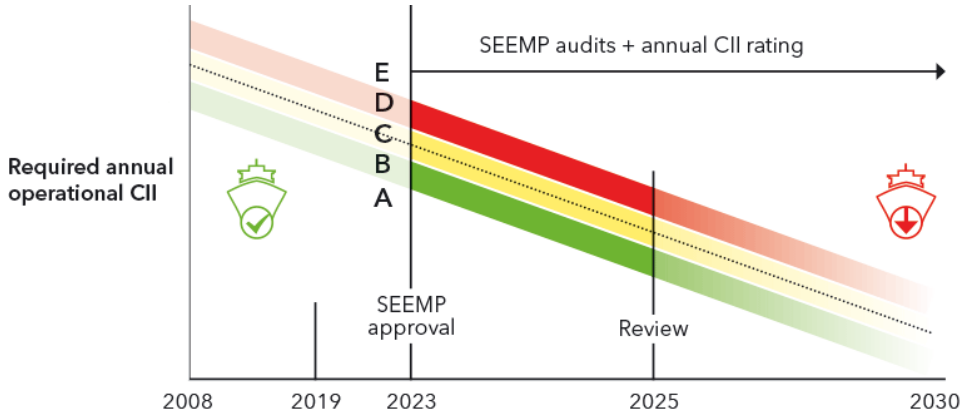

Figure 1.4: The CII rating system over time [28]

The main difference between the CII compared to the EEDI/EEXI is that the CII uses the total distance travel while the EEDI/EEXI uses the ship's service speed. Therefore the EEDI/EEXI is a predetermined fixed value based on the physical properties of the ship, whereas the CII is a combination of the physical properties of the ship and the operational use. Wang et al. found that in some situations the current indicator method creates a paradox where in theory total carbon emissions can increase while simultaneously lowering a ship's average [139]. Since the indicator is distance based, a ship operator can travel longer distances while sailing empty. As a result it lowers the average emissions due to the lower fuel consumption in this empty state. However this does come at the expense of the additional fuel cost to perform this technicality. Overall the IMO does expect the total carbon emissions by shipping sector to decrease with the implementation of the CII. In addition, the CII will be reviewed in 2025 and therefore it can be remodeled to fix issues. Just like the EEDI/EEXI, AMECs can result in less or no carbon emissions by changing the input chemicals and consequently the resulting output emissions.

To summarize this section, the direct GHG emission regulations are being expanded to existing ships and becoming stricter as well for new ships. The regulations are currently intended for combustible and carbon containing fuels and therefore have a common calculation method. Energy carriers such as hydrogen, ammonia and batteries do not emit GHGs and therefore their EEDI, EEXI or CII would equal zero. However, GHGs are emitted during the production and distribution of these energy carriers, especially when produced from fossil sources. Both calculation methods are related to the propulsive energy consumption, non-propulsive energy consumption, energy carrier type, power plant efficiency, service speed, carrying capacity, sailing distance/endurance, and design elements. Of these eight ship features, five are considered to remain constant when changing to a different energy carrier: ship type (design elements), service speed, sailing range/endurance, non-propulsive energy consumption, and carrying capacity. The three features that are considered to change are the propulsive energy consumption, energy carrier type and power plant efficiency. These features are strictly related to the available technology. In the following section, the available technology in the maritime industry and the future outlook of it is further investigated.

1.3. Available technology

Currently fossil fuels dominate the marine power generation market and 100% of the bunkered fuels in the Port of Rotterdam originates from fossil sources in the year 2020 [51]. 99% of those bunker sales

were oil fuels, such as heavy fuel oil, marine diesel oil and marine gas oil which are used in the internal combustion engine. However fuel oils are not the only available technology to power a ship. Therefore any other energy carrier other than oil fuel is considered to be alternative. Previously the term 'energy carrier' and 'fuel' were used interchangeably, however they are not the same. Energy carriers are substances or phenomenons that contain energy and can produce mechanical work, for instance batteries. Fuels are specifically combustible substances that produce heat or power. Meaning that all fuels are energy carriers, but not all energy carriers are fuels.

The emissions of fossil fuels are harmful to the environment, reduce resource availability and cause human health issues [110]. The emissions of the combustion of these fuels have a 3% annual share on the global warming effect and cause climate change [70]. Oil fuels have been used in marine power plants for over a hundred years. One of the many reasons is due to it having the highest energy density from all the marine energy carriers [30]. Due to the fossil fuel market dominance there is an unsustainable technology lock-in and therefore a voluntary switch to less harmful energy carriers is unlikely [134]. However, the implementation of GHG emission regulations has caused a global quest to find alternative energy carrier solutions to comply with these laws. At present much research is being done on alternative energy carriers, power plants and emission reduction technologies. This is not only the case for the maritime industry, but the whole global energy sector is shifting towards non-fossil energy solutions.

The designed service life of a ship is typically 20 to 30 years [27], meaning the physical life expectancy of a ship can be 30+ years. Consequently, a ship built today could still be in service in the year 2050 when the total GHG emissions need to be reduced by 50%. In the operational stage or also known as the service life, the chosen energy carrier results in certain emissions based on its chemical composition and usage. Kameyama et al. found that the operational stage contributes to 98.3% of the total environmental impact of a Panamax bulk carrier powered by oil fuel [77]. The shipbuilding and dismantling & recycling stage contributes less than 2% to the total environmental impact as can be seen in figure 1.5.

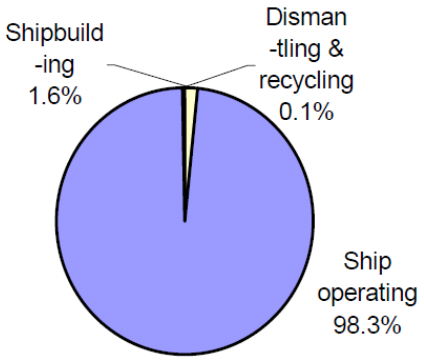

Figure 1.5: Panamax bulker environmental impact share per stage [77]

1.3.1. Future marine energy carrier outlook

Ship energy carriers play an important role to reach the IMO's GHG strategy goal of reducing emissions by 50% in 2050. Liu and Duru compiled five different projections by various institutions on future marine energy carriers and constructed an average scenario which can be seen in figure 1.6 [91]. From the average future scenario in figure 1.6 it can be seen that oil fuels from fossil sources account for approximately 98% of energy use by energy carriers in the maritime market today. However in the 2050 projection, that share will be down to only $\sim$45%. Moreover, it is also projected that hydrogen in combination with a fuel cell will have a 20% average share of energy use of all energy carriers. The use of ammonia in a fuel cell has been categorized in the projection as hydrogen by Liu and Duru. In the projection by the University Maritime Advisory Services (UMAS), the fuel cell energy carrier share is even as high as 75%. Furthermore battery powered ships are also expected to be present, although at a very small share of $\sim$2%. Therefore the conventional marine power plant is partially making its way for fuel cell and full electric powering technologies. As mentioned previously, a ship built today will probably still be in service in 2050 and thus making this energy transition a slow process.

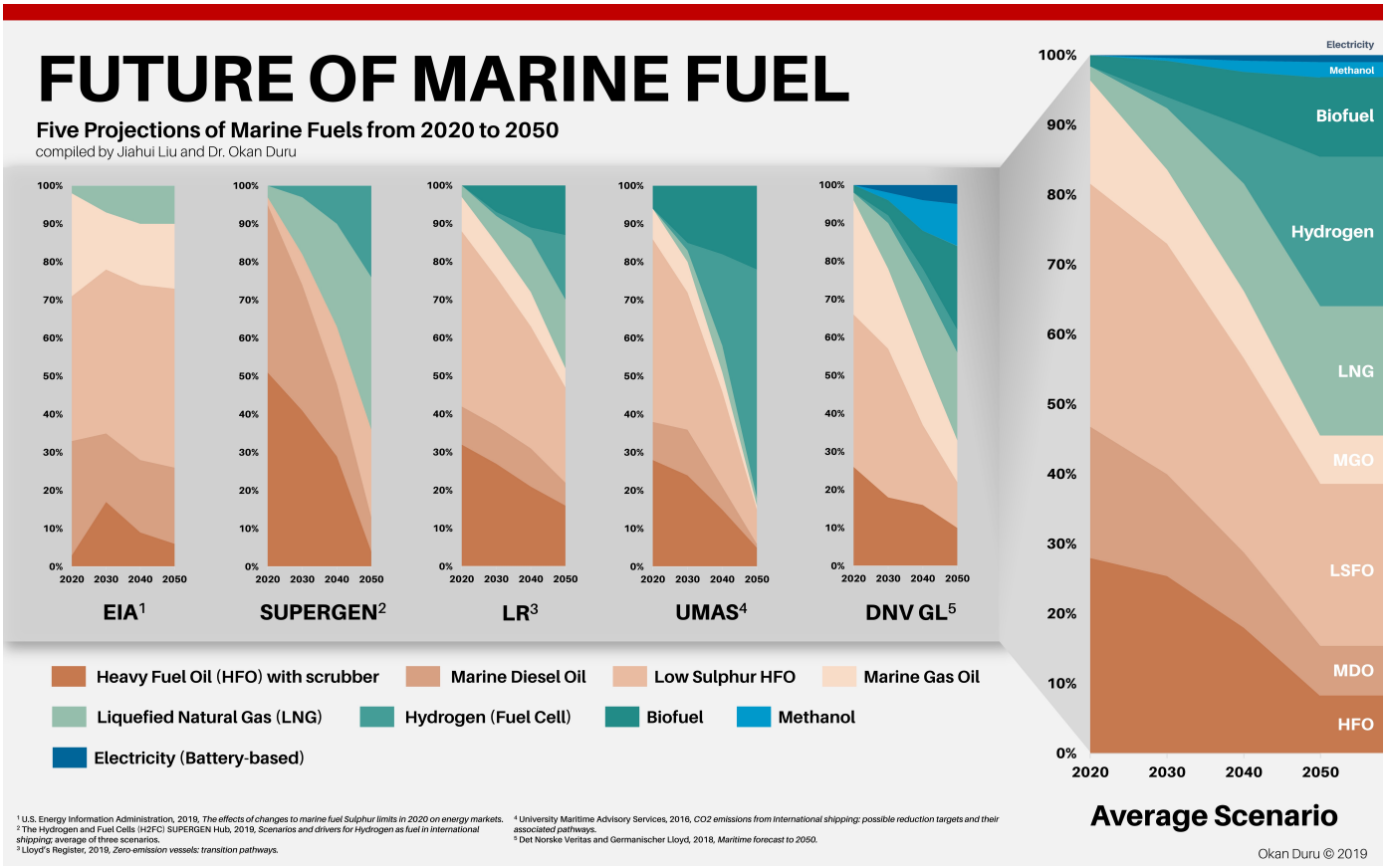

Figure 1.6: Future marine fuel projections from 2020-2050 [91]

[1] U.S. Energy Information Administration (EIA)
[2] Sustainable Power Generation and Supply initiative (SUPERGEN)
[3] Lloyd's Register (LR)
[4] University Maritime Advisory Services (UMAS)
[5] Det Norske Veritas and Germanischer Lloyd (DNV GL)

DNV-GL has established seven high priority parameters and an additional four key parameters which determine the future outlook of marine fuels [30]. The seven high priority parameters are: energy density, technological maturity, local emissions, GHG emissions, energy cost, capital cost/converter storage, and bunkering availability. The four additional parameters are: flammability, toxicity, regulations & guidelines, and global production capacity & locations. The other companies and institutions from figure 1.6 have similar parameters to DNV GL's in their projection reports. This research focuses on the effects of these energy carriers on the ship powering and the environment, and not on the proportions of the energy carriers in the maritime sector. Therefore the presence of an energy carrier in the future is more relevant rather than the share of it.

To summarize this section, there is a technology lock-in by fossil fuel oil accompanied by the internal combustion engine in the maritime power generation market. The use of this fuel contributes to almost all the environmental impact during a ship's lifetime. However, due to the stricter GHG emission regulations by the IMO, AMECs can offer a solution and therefore change the available technology in ships. The expected future marine energy carrier types are alcohol, LNG, hydrogen, ammonia and batteries. These new energy carrier types are accompanied by new energy converters such as fuel cells. Therefore the supply and demand of these substances and powering technologies will change the commercial aspect of the maritime powering market. In the next section, the energy carrier types are investigated for their contribution to the commercial aspect of ship design.

1.4. Commercial aspects

Financial performance is the key to being successful in the shipping market and shipowners must take three key variables into account according to Stopford: revenue from chartering/operating the ship, cost of operating/owning the ship, and method of financing the business [117]. As mentioned previously, the demand for newly built ships is amongst others driven by the international prices for oil and gas together with the cost of manufacturing [136]. The oil and gas prices eventually determine the conventional fuel oil costs of a ship. According to Stopford, voyage costs account for 40% of the total cost of operations/ownership. Of the voyage costs, 76% originates from fuel costs and totalling at 27% of the total cost of operations/ownership [117]. Lindstad even states that fuel cost accounts for 50% of the total cost of operations/ownership [89]. Therefore introducing alternative energy carrier types that do not originate form oil and gas will change the supply and demand of all energy carriers. Consequently the cost of ship operations changes and subsequently the commercial aspect of ship design as well.

Energy carrier types are not interchangeable as their energy conversion method differs. Energy carriers that are combusted in the internal combustion engine are instantly converted to mechanical work to drive the propeller. The first internal combustion for the propulsion of a ship was launched over 100 years ago and since then the efficiency and compactness of the propulsion plant has improved significantly [42]. On the contrary, the first fuel cell powered ship was only launched in 2021 and its still in its infancy [41]. Usually all energy carrier types (except batteries) contain a specific amount of energy that is that is constant by weight. However they must be contained in order to be 'carried', hence the term 'energy carrier'. Therefore the size and weight of the storage tank and necessary bunker handling systems influences the energy density.

1.4.1. Energy density

Marine energy carriers have different chemical properties which determines the power plant configuration, components, and processes. Therefore conventional oil fuels cannot easily be interchanged with non oil fuels in the same power plant installation. The caloric value of a fuel is one of the most important properties for combustion engine performance and it is defined as the amount of heat of combustion for a unit quantity of fuel [8]. During the combustion process not all of the fuel is transformed into usable heat, but some energy remains in the exhaust. Therefore the lower heating value (LHV) portrays the net energy availability in an energy carrier. The LHVs of a selection of energy carriers are given in table 1.2. Hydrogen has the highest LHV of 120.2 MJ/kg and it is 2.5 times the LHV of methane (LNG) which is the second highest. Nevertheless, these LHVs do not include the storage tank and necessary bunker handling systems. Generally, all energy carrier types (except batteries) contains a specific amount of energy that is generally constant by weight. However they must be contained in order to be 'carried', hence the term 'energy carrier'. Therefore the size and weight of the storage tank and necessary bunker handling systems alters the energy density.

Table 1.2: Conventional and alternative marine carrier properties [137]

Property	Unit	MGO	HFO	Methane	Methanol	Hydrogen	Ammonia
Chemical composition		C_xH_x	C_xH_x	CH_4	CH_3OH	H_2	NH_3
Boiling point	°C, 1bar	180...360	180...360	-166	65	-253	-33
Density (liquid)	kg/m^3	900	991	450	790	76.9	696
LHV	MJ/kg	42.7	40.2	48	19.9	120.2	22.5
Flashpoint	°C	>60	> 60	-188*	11*	-	132
Auto-Ignition	°C	210	256-262	580	470	536	651
Water solubility		No	No	No	Complete	n/a	n/a

* LFL: Low-Flashpoint Liquid per SOLAS II-2/4, 2.1.1

Unfortunately for hydrogen, its storage tank and necessary bunker handling systems are heavy and voluminous relative to hydrogen. Consequently this reduces the amount of available energy per volume and weight. Therefore the energy carrier densities in their contained form are an important aspect to their spatial characteristics. Figure 1.7 illustrates the volumetric (MJ/L) and gravimetric (MJ/kg) energy density of marine energy carriers including and excluding storage tanks and necessary systems. The dots

represent the energy carriers in uncontained form and the arrows display the shift in energy density after including the storage tank and necessary systems. The graph is divided into four sections and has diesel as its middle point as it is the most similar to conventional fuel oil. All the contained energy carriers in the top left section require less volume, but are heavier than diesel. The contained energy carriers in the bottom right section require more volume, but are lighter than diesel. The top right section is where the superior contained energy carrier would be, however there are none. A contained energy carrier in this section would require less volume and less weight compared to diesel. The bottom left section is where the inferior contained energy carriers are. In this section the contained energy carriers require more volume and more weight compared to diesel. It should be noted that the shift (arrow) of the contained energy densities of various energy carriers such as diesel, coal, and CNG 200 are not displayed in figure 1.7. The values of the contained energy densities are given in table 1.3. **From this it can be concluded that all the AMECs shift into the bottom left quadrant and therefore require more volume and weight for equal energy content as fuel oil.**

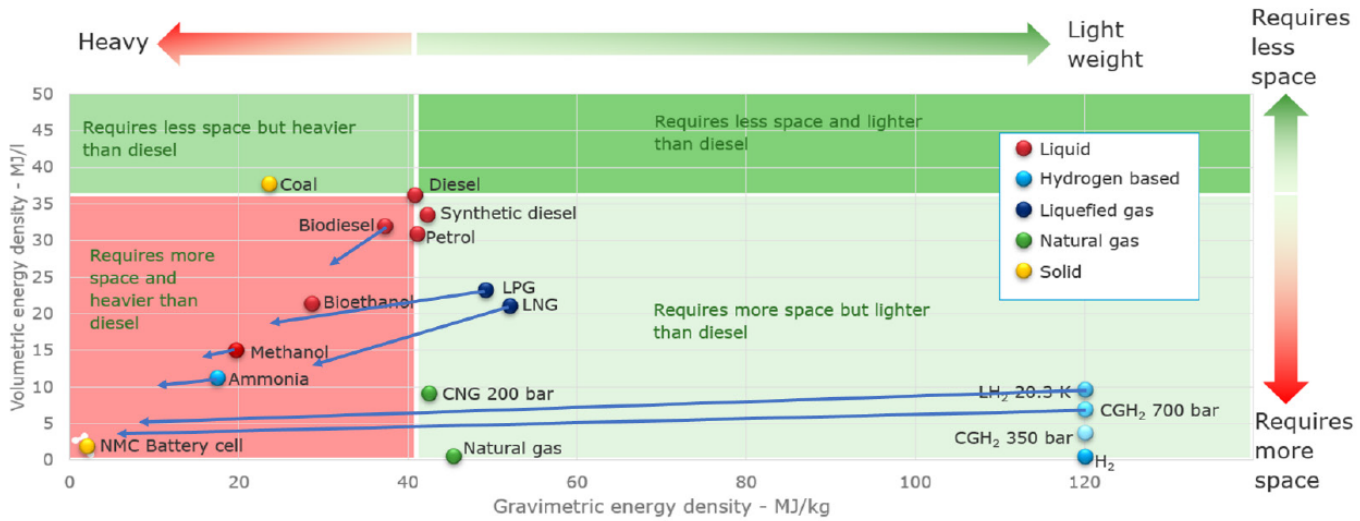

Figure 1.7: Comparison of gravimetric and volumetric storage density of energy carriers [30]

Table 1.3: Contained gravimetric and volumetric energy densities of energy carriers [138]

Energy carrier	Abbr.	Contained volumetric energy density (MJ/L)	Contained gravimetric energy density (MJ/kg)
Marine Diesel Oil	MDO	33.200	29.650
Bio Diesel	HVO	31.900	31.064
Synthetic Diesel	GTL	30.890	31.064
Marine Gas Oil	MGO	29.500 [a]	29.900 [a]
Methanol	MeOH	13.634	14.533
Dimethyl Ether	DME	13.300	19.800
Liquefied Natural Gas	LNG	13.170	28.370
Ammonia	NH_3	9.450	11.700
Compressed Natural Gas	CNG	8.500	4.500
Liquefied Hydrogen	LH_2	4.600	11.700
Compressed Hydrogen	CH_2	3.730	6.600
Lithium battery	Li-NMC	0.220	0.330

[a] Biert (2016) [11]

An important observation can be made that liquefied and compressed gaseous energy carriers have storage tanks that highly impacts the volumetric and gravimetric energy densities. In spite of hydrogen having the highest gravimetric energy density in uncontained form, it is not the case in contained form. All the

contained energy carriers other than coal will require more volume and more weight compared to diesel (fuel oil). Therefore if a ship were only to replace its fuel oil bunker space with an AMEC in contained form inside the main hull for the same amount of energy content, it would increase in size and in weight. The efficiency of the power plants is one factor that is not taken into account yet. However certain energy carriers can be used in different power plants with different efficiencies and resulting in various effective energy densities. For example, the uncontained volumetric energy density of diesel compared to ammonia is $\sim$2.8 times larger. Therefore it is expected that 2.8 times the volume of ammonia is necessary for the same energy content. Nevertheless, according to Castro et al. the required ammonia volume compared to diesel is only twice as much (-30%) [22]. For this reason other factors such as power plant efficiency must be taken into account as a case study in this research. Moreover, this does not even take the storage tank and necessary bunker handling systems into account which requires the use of the contained volumetric energy density.

1.4.2. Ship design and size

The vessel specifications are the starting point to the design process of a ship. There are many models of the ship design process, therefore it is crucial to find an appropriate and applicable model of the design stage. This will help to understand when an energy carrier is introduced in the process and how that influence the rest of a ship's life. In 1959, Evans constructed the design spiral to illustrate the naval architecture process of vessels [36]. To this day the design spiral is still applicable and is considered the classical approach to the ship design process [114]. However, due to technological advancement and the increasing complexity of ships there are many variations of the design stages. The design spiral is depicted in figure 1.8 with the starting point *mission requirements* on top. The *mission requirements* are to be considered the same as the *vessel specification/ship design* from the four aspects in figure 1.1 from section 1.1 'The current situation'.

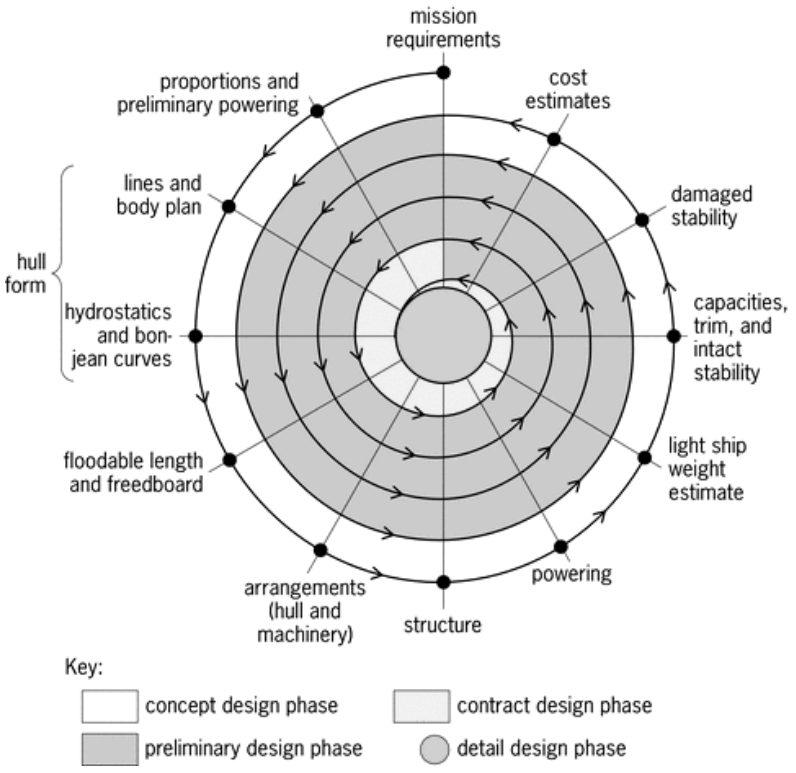

Figure 1.8: Ship design spiral [36]

As a result of the additional volume and weight of an AMEC for the same amount of energy content, a ship will increase in total internal volume and lightweight ship. Consequently it also leads to a higher resistance and thus more engine power is necessary to propel the ship at the same service speed. A higher engine power also results in a higher energy consumption and thus additional bunkering is necessary to compensate for the increased energy consumption to have the same endurance range.

The first step of the numeric ship sizing process in figure 1.9 starts with the carrying capacity (payload) and accompanying equipment to estimate a ship's total internal volume. However the historical data is based on ships powered by conventional fuel oil and thus there is no to very little historical sizing data available on ships with AMECs. Consequently there is no other choice than to use fuel oil powered ship data as a starting point. Since there is no step in the process accounting for the selecting of an energy carrier, it is assumed that this would take place in the 'Selection of machinery' as the power plant components (machinery) are dependant on the energy carrier. Taking into account the constant operational ship requirements, the change in the 'Selection of machinery' step impacts the following three steps: 'Complement', 'Auxiliary power and services' and 'Tank volume'. An AMEC power plant can require complementary space for safety reason or just because the machinery is larger compared to the conventional. For this same reasoning the space requirement for the auxiliary power and services are impacted as well. Finally, the tank volume of an AMEC is calculated with its energy characteristics and efficiencies of the accompanying power plant.

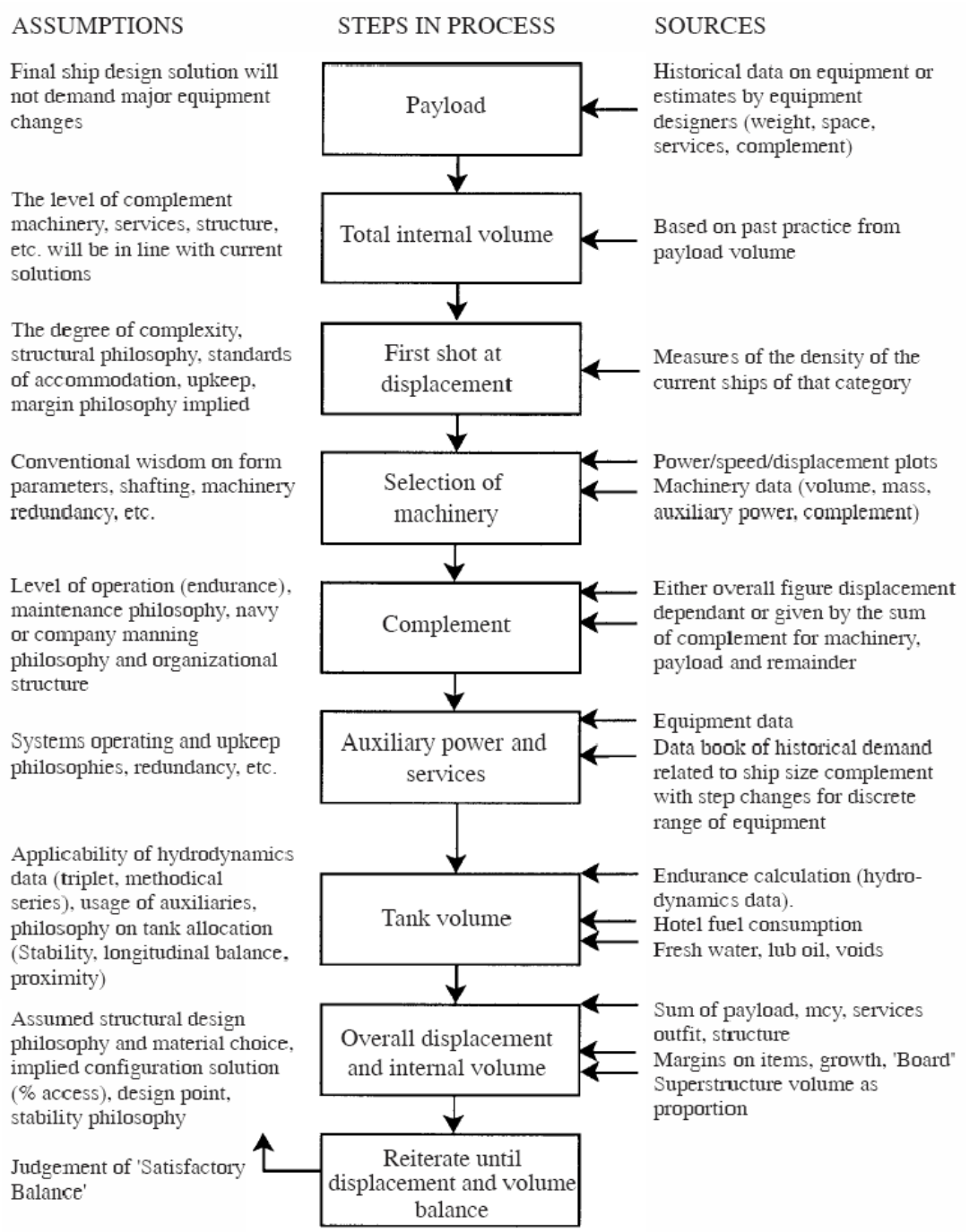

Figure 1.9: A simple numeric ship sizing iterative sequence with feedback [7]

1.4.3. Ship resistance and propulsion

A ship that moves through the water and air is subjected to the forces acting on the outer hull surface. These forces by the water and air are a reaction to the ship's size, shape and speed. All of the forces combined are known as the total hull resistance. The total hull resistance is the sum of the resistance components: viscous resistance, wave making resistance and air resistance. The viscous and wave making resistance are a result of the underwater volume of the ship and the air resistance is a result of the volume above the waterline. The underwater volume and above water volume are related to the main ship dimensions and its shape. The main ship dimensions being the length (L), beam (B), depth (D), and draft (T). The resistance component proportion to the total resistance is speed dependant and visualized in figure 1.10. At lower ship speeds the viscous resistance proportion is the highest, while at higher ship

speeds the wave making resistance is dominant. The viscous resistance is the friction between the water and the hull. Therefore a higher wetted surface area results in a higher viscous resistance at the same speed. Just like the viscous resistance, the air resistance also has a near-linear correlation to the ship speed. The mechanism of the air resistance component is similar to the viscous resistance, but it involves the air friction and pressures above the waterline.

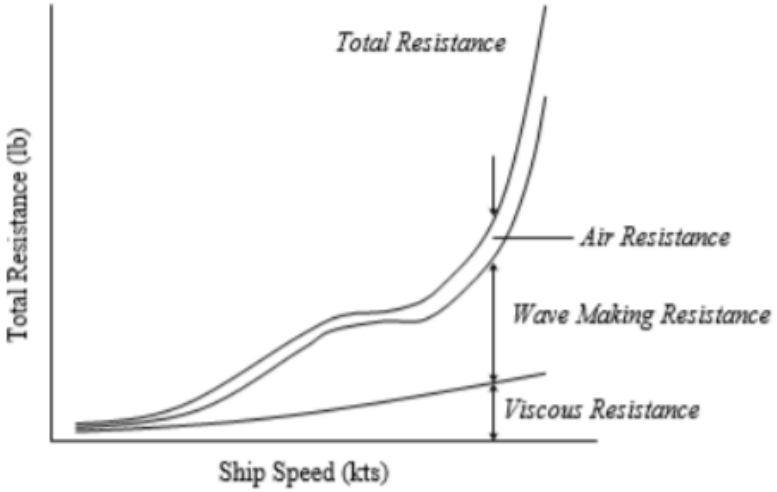

Figure 1.10: Components of hull resistance with varying speed [130]

The wave making resistance is not near-linear correlated to the ship speed and it highly shape dependant. As the name suggests, it involves the resistance caused by the resulting waves by the ship moving through the water. The waves are created by the pressure build up at the bow and pressure release at the stern of the ship. The wave making resistance curve first rises at an increasing rate, then flattens out and then rises at an increasing rate again. This slope discontinuity is the result of the bow and stern waves first being in phase, then out of phase and then in phase again. When the bow and stern waves are in phase they enhance each other and when they are out of phase they cancel each other out [18]. In 1868 William Froude found a relation between the wave making resistance and wave length. He found that the higher the ship speed with respect to to the waterline length, the higher the wave making resistance. The relation is known as the Froude number and it is expressed in equation 1.9.

$$F_n = \frac{V_S}{\sqrt{g \cdot L}} \quad [-] \tag{1.9}$$

In section 1.4.1 it was concluded that the contained energy density of the AMECs are all lower than conventional fuel oil. As a consequence the tank volume and weight will increase for the same operational ship requirements. In section 1.4.2 it was concluded that the overall internal volume will thus increase for the additional tank volume. Accordingly, to accommodate the increased overall internal volume, the ship's main dimensions will change as well. All the resistance components are related to the underwater and above water volumes and therefore a change in the main dimensions will result in a change the ship's total resistance. However the air resistance only contributes a small portion of the total resistance and thus the most valuable main dimensions are length (L), beam (B) and draft (T).

The Froude number is a parameter which is often optimized in ship design in order to lower the total resistance according to Wilson et al. [144]. To lower the Froude number and therefore the wave making resistance, the ship speed (V_S) has to decrease or the ship length (L) has to increase according to the equation. The additional length will result in a lower wave making resistance but also in a higher viscous resistance as there is more surface area. It will only result in a lower total resistance in the speed range where the wave making resistance is dominant. One of the constant operational conditions considered is the ship speed. Therefore increasing the ship's length to accommodate for the additional overall inter-

nal volume is a solution within the Froude number parameter to decrease the wave making resistance. However it is not practical to accommodate all the additional volume in the length as it would cause high bending moments in the ship's structure. In a study by Lindstad et al. in 2013, they evaluated the cost and emissions associated with various fuel oil powered bulk vessel designs with equal carrying capacity (DWT), focusing on the vessel's beam, length, hull slenderness, and bow section length [89]. The results show that more slender designs with lower block coefficients are the most energy efficient and reduce the added resistance significantly. The added resistance is the extra resistance caused by winds and waves and can be increased about 10–40% compared to calm water [80]. In a follow up study on slender body designs in 2014, the results show that slender designs reduce emissions and increase the profit [90].
The total ship resistance is a parameter for determining the effective towing power (P_E). This is the required power to tow the ship at a given speed. The effective towing power is calculated by multiplying the total ship resistance (R_{TOT}) by the ship speed (V_S). With the given propulsion plant components, the propulsion main engine brake power can be determined. In section 1.2.1 it was determined that the engine brake power is a parameters for the energy carrier consumption and direct emissions. Accordingly, a ship that increases in total resistance will also increase in energy carrier consumption and subsequently also cost of operation/ownership. This results in an iterative issue where the increased energy carrier consumption needs to be compensated by additional energy carrier bunker volume to operate for the same amount of time or distance. This ship resizing problem is in agreement with the numeric ship sizing process by Andrews and Dicks within figure 1.9 [7].

To summarize this section, the introduction of AMECs will change the cost of ship operations/ownership and therefore the commercial aspect of ship design. However energy carrier types are not interchangeable as their energy conversion method differs. An additional issue to the increased energy carrier types is the storage and handling properties. All AMECs have a lower volumetric and gravimetric energy density than conventional fuel oil. Therefore it is anticipated that more bunkering is necessary for the same operational conditions. The additional bunker volume and weight result in a larger overall internal volume and ship weight. Accordingly the main ship dimensions increase and yield a higher total ship resistance and consequently engine powering. The higher powering causes an iterative issue where additional bunkering is required to compensate for the increased consumption for the same operational conditions. In conclusion, an AMEC can lead to increased energy carrier consumption and therefore increasing the operational cost and additionally could cancel out the GHG emission reduction which it was intended to solve. It was determined that the operational conditions must remain the same to have the same operational requirements, but it was not yet explained how that is applied. Therefore the operational requirements and conditions are elaborated and applied in the following section.

1.5. Operational requirements

There is not a one size fits all ship design that fulfils all the requirements for the shipping industry. Therefore merchant ship types are categorized based on their function even though they are all constructed using the same naval architecture principles [106]. According to Levander, the function of a shipping vessel can be divided into two main categories: inherent ship functions and payload functions [85]. The function categories and sub categories are depicted in figure 1.11. The inherent ship functions are related to safely transporting the payload from one port to another in a timely manner, while the payload functions are related to the handling of the payload content. In this section, the operational requirements affecting the ship design are analyzed and questioned whether they change if a ship substitutes its fuel with an AMEC.

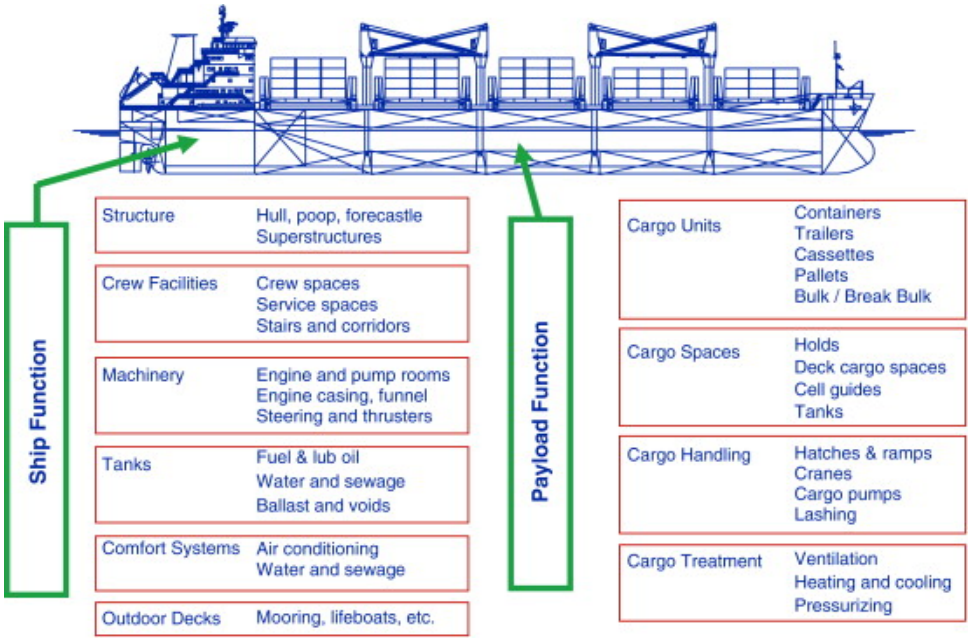

Figure 1.11: Shipping vessel function categories [85]

1.5.1. Ship functions and ship design

According to Levander, first the inherent ship functions and payload functions are selected in this system based design process. Thereafter the required areas and volumes for the ship to house all systems are then determined. There is no requirement for pre-selected main dimensions, hull lines, or typical layouts using this design approach [85]. From there on the total internal volume and first estimate of weight are calculated. With that information the main dimensions and ship form are selected using historical data based on performance and operating economics. In section 1.4, it was determined that the operational key variables to financial performance (operating economics) are revenue and cost of operations [117]. In that same section it was also established that fuel cost is a major contributor and it is directly related to the main ship dimensions, hull form and ship speed. Therefore to strive for the highest profit given the same operational requirement (constant speed), the main dimensions and hull form are selected which generate the lowest fuel cost. The approach by Levander is almost identical to the numeric ship sizing sequence by Andrews and Dicks, especially the use of historical data [7]. In conclusion, Levander, Andrews and Dicks, and Vossen et al. are all in agreement that the main ship dimensions are motivated by external factors, are based on historical data and are not pre-selected by default. Essentially all historical ship data is based on vessels powered by fuel oils as AMEC types are still in their infancy. However that does not signify that the powering and dimensional historical data is inaccurate for achieving lowest energy carrier consumption and thus cost. Therefore the historical powering and dimensional ship data is still useful in determining the ship dimensions powered with AMEC types.

1.5.2. Constant operational requirements

The five considered operational conditions result in the same operational requirements for a new design. The operational requirements are not necessarily determined, but are considered by using an existing ship and substituting the fuel oil with an AMEC for equal effective energy. The equal effective energy is the product of the lower heating value and the power plant efficiency. Accordingly additional bunker volume and weight is necessary due to the lower gravimetric and volumetric density of AMECs. As a reminder, the five constant operational conditions are listed below. The ship type must remain constant because it is defined by the payload function and accompanying design elements and trends. A ship that increases in internal volume due to switching to an AMEC should not contain new or less design elements that it is considered a different ship type. The original internal volume minus the bunker volume must remain constant as the original internal volume houses all the inherent ship functions and payload function systems, excluding the bunker volume. The service speed, sailing range/endurance and non propulsive energy users are related to the energy carrier consumption and therefore determine the varying bunker volume. They must remain constant to comply with the inherent ship function of transporting the payload

from one port to another in a timely matter and handling the payload.

Ship type (design elements/dimension trends)
Original internal volume minus the bunker volume
Service speed
Sailing range/endurance
Non propulsive energy consumers (cargo handling/treatment)

It is considered that the original ship design results in the lowest energy consumption feasible for its given multi objective operational requirements. Accordingly, the new lowest energy consumption equilibrium for the new ship design will be near for the additional volume and weight. For that reason the new ship dimensions will be within the maximum expansion of a single dimension to accommodate for the additional volume and weight. In simpler explanation, a single dimension (L, B, or D) can be increased to a maximum distance while the other dimensions remain constant to accommodate for the additional volume and weight. For example only increasing the length ($L + \Delta L_{max}$, B, D). Or it can be achieved by increasing multiple dimensions to anywhere less the than the maximum to accommodate the additional volume and weight. Traditionally ships are designed to maximize its dimensions to the spatial limits for locks, canals, bridges, etc. Therefore, it is possible that the newly generated ship designs exceed the spatial limitations and consequently it cannot perform its operational tasks. For the purpose of determining new ship designs based on existing ships, the spatial limits are not taken into account as an operational requirement. A method of avoiding this spatial limit issue is by surrendering cargo space for bunker space, however this does change the operational requirements.

In a master's thesis by Bodewes in 2020, he modeled the refit design impact on a general cargo vessel for various AMECs and assessed the energy carrier cost and GHG emissions [14]. The model approached the additional bunkering volume for equal amount of effective energy to be added by lengthening in the midship section. According to Bodewes this was done because the beam was restricted, however there is no mentioning of increasing the ship's depth as an option. By using an existing ship the operational requirements were kept constant. However, the added resistance and powering impact due to lengthening on the effective energy were not taken into account. Additionally, the contained energy density was correctly used, but only the efficiency of the prime mover was used to calculate the effective energy. Moreover this research is intended for refit purposes and accordingly does not take new design options as a possibility.

In a recent study by Terün, Kana and Dekker, an ultra large container vessel (ULCV) is subjected to various AMECs intended for the same power plant to investigate the cost and GHG emission performance [118]. The additional bunker volume and weight is determined using the same range at the same service speed. The power plant efficiency is assumed to be the same and therefore also the efficiency, however all auxiliary loads were neglected. The additional volume and weight is added to the ULCV by lengthening in the midship section and substituting container bays for tanks. Therefore the operational requirements are not kept constant. Moreover the added resistance of the lengthening was not taken into account in the fuel consumption and neither the indirect GHG emissions.

To summarize this section, to keep the operational requirements constant, five operational conditions have been determined to remain the same. The constant operational conditions are related to existing ships substituting their fuel oil with an AMEC for equal effective energy. As a result the ship's weight and internal volume will increase and causes the main dimensions to increase as well. This further increases the energy carrier consumption and therefore more bunkering is necessary to keep the same sailing range/endurance. This results in an iterative issue where the increased energy carrier consumption needs to be compensated by additional bunkering and then causes increased consumption again. Therefore also causing an accelerated emission issue by the AMECs. Up until now, only direct GHG emissions are taken into account as an environmental impact, yet global warming is not the only environmental effect nor are direct emissions the only contributor. In the next section, other environmental effects of energy carriers are investigated including the non-direct emissions. Furthermore, the approach to quantitatively assessing the environmental impact is researched as well.

1.6. Environmental consequences

The green house gas reduction strategy by the IMO is the initial driver for the change in vessel specifications/ship design in order to stop global warming effects. As mentioned previously, global warming is not the only effect on the environment. Kameyama et al. found that within operational stage of a ship, the direct emissions of conventional fuel oil account for 81% of the total environmental effects while the production and distribution only accounts for 19% [77]. A well known previous global environmental effect caused by humans is the depletion of the ozone layer and without it it would cause damage to exposed life forms from the sun's ultraviolet light [32]. Since the phasing out of the ozone depleting substances (ODSs) by the Montreal Protocol, an international treaty by the UN, the ozone layer is finally healing [115]. It was a simple solution by phasing out the chemicals which caused the ozone depletion and using alternatives. However the alternatives to ODSs are potent green house gasses [132]. Thus solving one environmental effect and causing another. Therefore it is necessary to determine the types and magnitude of the environmental effects of the production and use of AMECs.

1.6.1. Life cycle assessment (LCA)

Life cycle assessment (LCA) is a methodology for quantitatively assessing the environmental and social impacts of a system, product, service or process over its full life time [37]. The environmental impact is measured in effects on ecological consequences, resource use and human health. An LCA takes all the materials, resources and consumed energy into account over all the life cycle stages and it also takes transportation into consideration. When researching a life cycle, the life system boundaries need to be known. Figure 1.12 displays the ecological loop with the system boundaries of cradle, gate and grave. From the time natural resources are mined from the earth (cradle) and processed through each consecutive stage of manufacture, transport, product usage, and finally disposal (grave), a 'cradle-to-grave' assessment evaluates impacts at each stage of a product's life cycle's trajectory. It is also possible to do an assessment on only a part of a life cycle (gate-to-gate), namely a conceptual LCA [37]. In such a conceptual LCA, the environmental impact results are valuable for comparative reporting. Since this research is focused on determining the environmental impacts of AMECs during the operational stage of a ship's life cycle it is deemed as a conceptual LCA.

Hausschild et al. provide a comprehensive description in their book *Life Cycle Assessment* on the theory and practice of LCAs [50]. According to them there are four essential phases to an LCA, which are: 1 - The goal and scope definition, 2 - The life cycle inventory analysis (LCI), 3 - The life cycle impact assessment (LCIA), and 4 - The life cycle result interpretation. Major components of the goal and scope definition phase include defining the system boundaries, function of the output, the unit of comparison, and the reference flow of the inventory. The LCI phase consists of compiling the inventory process data sets for the in- and output materials, energy, resources and emissions. Activities in this phase include process identification, planning and collection of data, constructing and quality check of the data, uncertainty preparation, and reporting. The LCIA phase consists of conducting the impact assessment on the environment for a system in a quantitative manner. It include selecting impact categories, impact classification, characterization, normalization, and weighting. The final phase consists of identifying the critical environmental issues, evaluation of the analyzed results, sensitivity analysis, conclusions, and further recommendations. The major components of this phase include high impact process identification, completeness and quality analysis, consistency examination over all the systems in the LCA, and a sensitivity analysis.

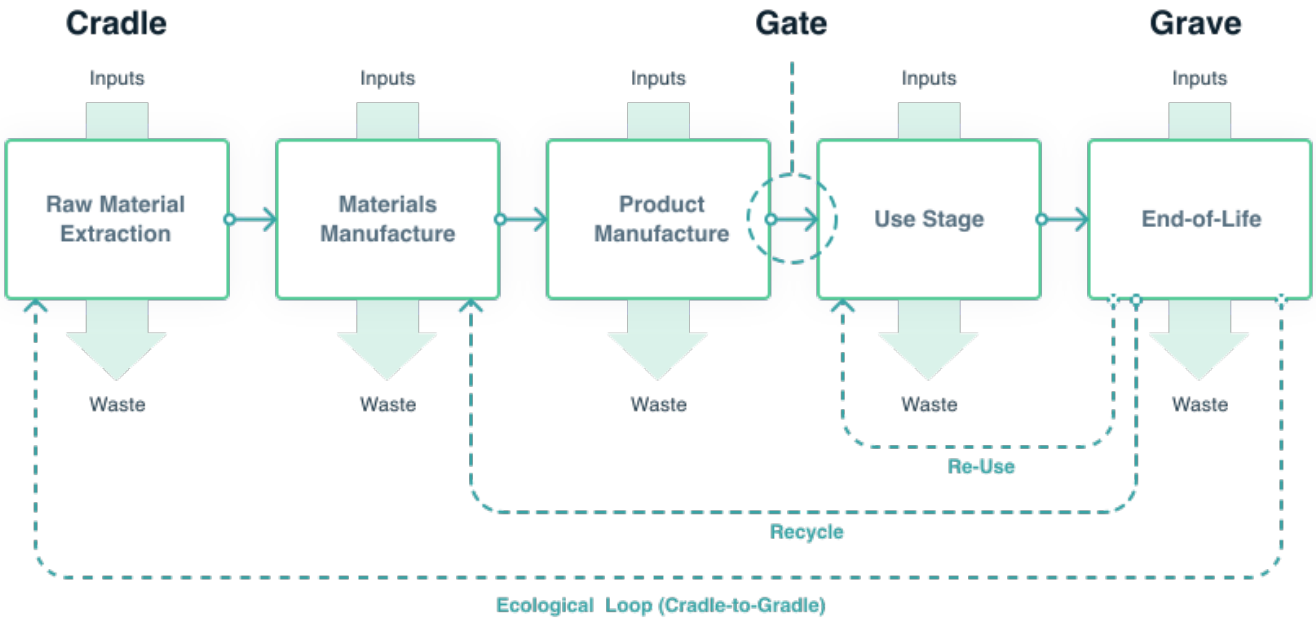

Figure 1.12: The ecological loop and system boundaries [105]

The cradle-to-grave principle is similar to the well-to-wake pathway principle, except it is the generalized for all products and processes in an ecological perspective. The well-to-wake pathway is specific to energy carriers and GHG emissions in the maritime industry. The cradle-to-grave concept takes all environmental effects into account, while well-to-wake only takes the emissions into consideration in a global warming impact perspective. Nevertheless, the well-to-wake pathway targets the impact from the contributors from the moment of extraction to disposal. Therefore the well-to-wake pathway is the cradle-to-grave system boundary for an LCA. The GHG emissions contribute to global warming, mainly carbon dioxide, but also contributes to the acidification of the ocean [109]. Acidification is also one of the environmental impacts in an LCA. This shows how an LCA takes more into consideration than just global warming, even though it is the driver of this research.

LCA is the most extensive and dominant method for studying the environmental impacts throughout a product's full life cycle. The LCA methodology is globally recognized by the International Organization for Standardization (ISO) for its environmental management procedure in the ISO14040 standard [71]. A comparable method of studying a product or process's life cycle is a Life Cycle Screening (LCS). An LCS focuses on the finding the key issues in a part of a life cycle to optimize it with new technologies in a environmental perspective [39] [38]. According to Hung et al. the LCS method is intended for upcoming technologies where the technology has a low readiness level [60]. Castro et al. found that an internal combustion engine fueled by ammonia is not technically ready for application [22]. However, this technical readiness grading is featured in their 2019 study and in the mean time engine manufacturer MAN Energy Solutions is launching an ammonia internal combustion engine in 2024 [104].

In 2021, Bilgili was the first to perform a quantitative comparative LCA on AMECs in a life cycle perspective [12]. In his research he performed an LCA using the SimaPro 9 software in combination with the Ecoinvent database and the ReCiPe 2016 method on a selection of AMECs. Unlike other studies that focused on pollutant emissions (especially GHG), he focused on the damage of the pollutant to human health. He concluded that biogas is the best in terms of human health in the short, medium and long term. However, the comparative LCA study does have limitations, such as the functional unit of comparison was determined as 1 ton or equivalent volume of fuel. Therefore not taking the power plant efficiency or the contained energy density. Therefore the operational requirements were not taken into account to compare on the same playing field. Additionally, the largest limitation in his study is the differing LCA research scope. Bilgili uses the results from other LCA researches and compiles them. Consequently, it is unknown what is and is not included in the scope of these studies and how the inputs and wastes were measured. Differing research scopes can cause different results for the same system and therefore as well when comparing various energy carriers.

1.6.2. Well-to-wake pathway

It is possible that a specific energy carrier can be sourced, produced and distributed in a variety of pathways. All these pathways have a different effect and magnitude on the environment. There is ample research done on global warming effects of GHG emissions originating from marine energy carriers. AMEC emissions in the maritime industry can be categorized into two phases of its life cycle: well-to-tank (WTT) and tank-to-wake (TTW) [46]. The well-to-tank phase consists of the extraction, processing, transportation and distribution of the energy carrier. This phase is not specific to the maritime industry. However, the tank-to-well phase consists of the use of the energy carrier in the maritime industry. During these two phases harmful green house gasses are emitted into the atmosphere and the two phases together form the full life cycle: well-to-wake (WTW). The emissions from the tank-to-wake phase are the primary cause of global warming, but without the preceding well-to-tank phase it would not exist [108]. If the primary goal is to stop contributing to global warming, accordingly the use of fossil resources for energy carriers must stop. However, an energy carrier such as hydrogen does not contribute to global warming in the tank-to-wake phase as there are no emissions. Yet, if it is sourced from natural gas, then the well-to-tank phase is the primary contributor to global warming. As in this phase there are not any GHG emissions. Therefore, the full well-to-wake pathway for every chosen energy carrier must be taken into account to determine the full environmental effect. The possible well-to-tank pathways from source to energy carrier can be seen in figure 1.13.

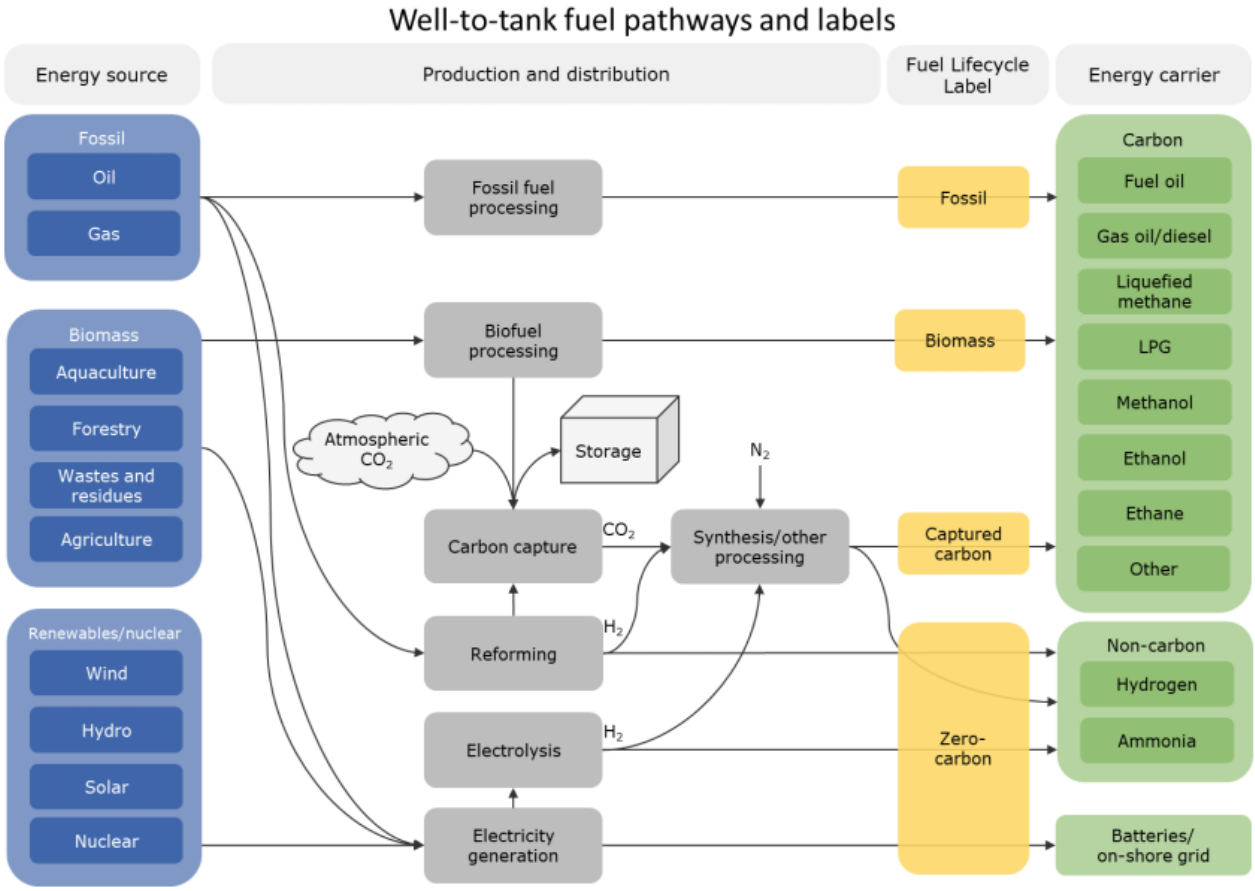

Figure 1.13: Overview of main well-to-tank energy carrier pathways and labels [61]

In a 2019 study by DNV-GL on the comparison of alternative marine, it was concluded that renewable hydrogen in a fuel cell power plant has the least GHG emissions in the well-to-wake pathway/system boundary [30]. The functional unit of comparison was determined as 1 kWh shaft output and therefore taking the power plant efficiency into account. Unfortunately the research was only performed on the global warming environmental impact.

1.6.3. Environmental impact method: ReCiPe 2016

Depending on which LCA method is used, there are environmental impact results which come forth from the LCIA phase. These impact categories are the environmental effects and are mostly similar to one and other. One of the LCA methods is ReCiPe 2016 and it is developed in collaboration with the Dutch National Institute for Public Health and the Environment (RIVM), Radboud University Nijmegen, Norwegian University of Science and Technology, and PRé Sustainability. ReCiPe 2016 uses impact categories at two levels: midpoint and endpoint. There are eighteen midpoint impact categories which can be reduced down to three endpoint categories. The midpoint and endpoint categories and their relationship are displayed in figure 1.14.

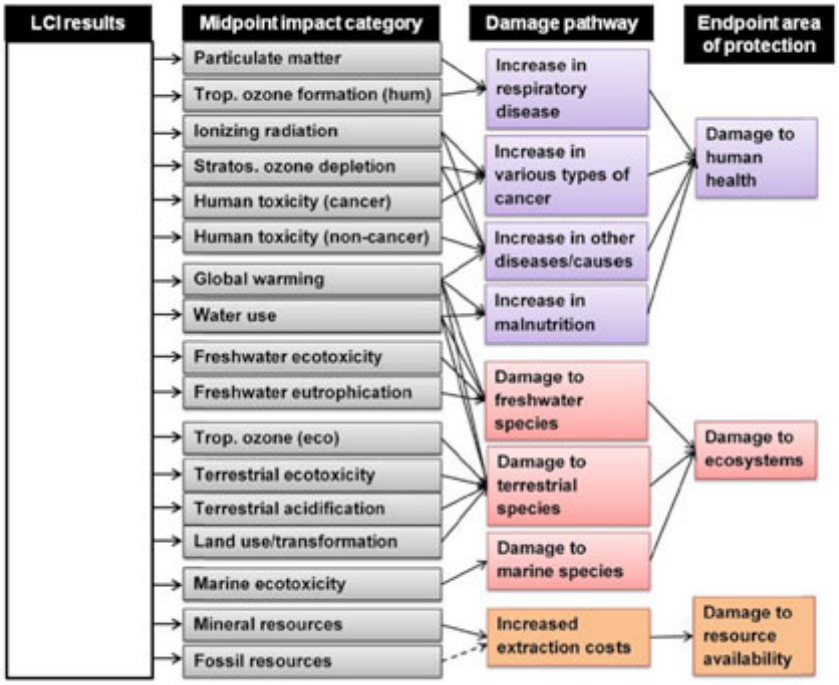

Figure 1.14: Overview and relation from midpoint (18) to endpoint (3) in ReCiPe 2016 [58]

The midpoint impact categories are classified by their identical environmental impact mechanism. For example, carbon dioxide (CO_2) absorbs infrared radiation (light) from the earth and emits thermal radiation. As a result the earth heats up and causes the climate to change. CO_2 is characterized as the global warming potential and expressed in terms of thermal energy for a year per square meter ($W{\cdot}yr/m^2$) also known as the characterization factor (CF). Other chemicals can also have this mechanism, but in a different magnitude, such as methane. The global warming potential of 1 kg methane is 84 worse than 1 kg of CO_2 over the course of 20 years time. That is why a normalization factor of 84 is used to translate this effect for methane for the same weight. Therefore the environmental impact measurement is in kilograms of CO_2 to the atmosphere. In addition, one midpoint impact category can influence the other, for example climate change can cause dry periods without rain and thus will cause increased use of water consumption for the agriculture sector. Therefore weighting factors are used to convert characterizations across the midpoint impact categories. The three endpoint impact categories are classified by their identical damage mechanism. The reduction from eighteen to three impact categories provides better information to compare results in a broader perspective, however this yields higher uncertainty than the midpoint indicators [59]. The translation from midpoint to endpoint impact category is also done through weighting factors by their identical damaging mechanism. Luckily, by using the ReCiPe through a software, the characterization, normalization and weighting is done automatically.

To perform a conceptual LCA on an AMEC through the ReCiPe 2016 method, all the in- and output materials, energy, resources and emissions need to be identified of the life cycle in a life cycle inventory (LCI) analysis. This involves compiling the inventory processes and collection of data. The data is sourced from databases as a finished result or self constructed from intermediate results from previous LCAs. The Delft

University of Technology offers a free license to the LCA software SimaPro 9. This software can perform LCAs through different LCA methods and LCI databases. The software includes the ReCiPe 2016 method and many different databases. One of those LCI databases is the Ecoinvent database which is provided by the Ecoinvent Association. The Ecoinvent Association is a non-profit dedicated to high quality environmental data for environmental assessments [35]. The database contains more than 19,000 life cycle inventory data entries and is updated every year. According to openLCA Nexus, an online repository for LCA data, "Ecoinvent is a very transparent, consistent and most popular database containing industrial life cycle inventory data on energy supply, resource extraction, material supply, chemicals, metals, agriculture, waste management services, and transport services" [45]. By using the Ecoinvent database for the LCI phase in combination with the ReCiPe 2016 method will result in the LCIA results. This process can be automated by using the SimaPro 9 software. To fully understand what the environmental impacts are from the ReCiPe 2016 method, the endpoint and midpoint impact categories are briefly explained in the following subsections.

1.6.4. Endpoint area of protection

The three endpoint areas of protection are a convenient outcome to compare life cycle impact assessments as they contain less end factors. The endpoint areas are a result of the damage pathways from the midpoint categories. Every midpoint impact category has a conversion factor to result in the endpoint area.

Human health Damage to human health is the result of the years of life that are lost or that a human is disabled as a result of a disease or accident. This can be caused by an increase in respiratory disease, increase in various types of cancer, increase in other diseases/cause, or increase in malnutrition resulting from a midpoint category. The unit of characterization for damage to human health is disability-adjusted loss of years (DALY).

Natural environment Damage to ecosystems is the result of loss in quality of an ecosystem. This can be caused by damage to freshwater, terrestrial or marine species. The unit of characterization for damage to ecosystems is local species loss integrated over time (species x year).

Resource scarcity Damage to resource availability is the result of the extra cost involved for future mineral and fossil resource extraction due to its scarcity. This can be caused by increased extraction costs and fossil energy cost. The unit of characterization for damage to resource availability is US dollars ($) in valued in 2013.

1.6.5. Midpoint impact categories

The eighteen midpoint categories contain the characterization identity of the emitted substances. The emitted substances are gathered from the life cycle inventory (LCI) and their environmental impact is categorized by these eighteen categories.

Climate change Climate change is the result of green house gas emissions into the atmosphere. Therefore the atmospheric green house gas concentration rises. The radiative forcing capacity of these green house gasses causes an increase in the global mean temperatures. It results in climates all around the world to change. As an effect it damages human health as it causes a change in disease distribution and flooding. It also disappears terrestrial species due to change in biome distribution, and it disappears fresh water fish due to changes in river discharge. The unit of characterization for climate change is kg of CO_2 equivalent to the air.

Stratospheric ozone depletion Stratospheric ozone depletion is the result of Ozone Depleting Substance (ODS) emissions into the atmosphere. Therefore the ODS concentration in the troposphere and stratosphere rises. The ODSs interact with ozone and decrease atmospheric ozone concentrations which causes more ultraviolet B (UVB) radiation to reach the earths surface. The UVB radiation increases the chance of getting skin cancer and cataracts. Therefore increasing damage to human health. The unit of characterization for ozone depletion is kg of CFC-11 equivalent to the air.

Ionizing radiation Ionizing radiation is the result of radionuclide emissions into the biosphere. Therefore the radionuclide concentration increases in the biosphere and the dispersion causes it to come in contact with the human population. The exposure of radionuclides increases the chance of getting cancer and other hereditary effects. Therefore these effects damage the human health. The unit of characterization for ionizing radiation is kBq Cobalt-60 equivalent to the biosphere.

Fine particulate matter formation Fine particulate matter formation is the result of aerosol emissions of up to 2.5 μm into the atmosphere. These aerosols include nitrogen oxides (NO_x), ammonia (NH_3), sulfur dioxide (SO_2) which cause secondary aerosols to form in the air. Therefore the aerosol concentration increases in the atmosphere which then can be inhaled by the human population. The fine particulate matter causes an increase in mortality cases and thus damages human health. The unit of characterization for fine particulate matter is kg $PM_{2.5}$ equivalent to the atmosphere.

Photochemical ozone formation Photochemical ozone formation is the result of nitrogen oxides (NO_x) and non-methane volatile organic compounds (NMVOC) into the atmosphere. Therefore these chemical concentrations in the atmosphere increase which transform to ozone in the air. The ozone can be inhaled by the human population, leading to higher cases of mortality. Consequently damaging human health. In addition, plants can also uptake ozone and die off, leading to disappearing plant species. Thus damaging terrestrial ecosystems as well. The unit of characterization for photochemical ozone formation is kg NO_x equivalent into the atmosphere.

Terrestrial acidification Terrestrial acidification is the result of inorganic substance emissions into the atmosphere which eventually deposit into the soil. The concentration of these substances in the soil cause the soil to acidify and eventually killing specific plant species. Therefore the terrestrial acidification damages terrestrial ecosystems. The unit of characterization for terrestrial acidification is kg SO_2 equivalent into the atmosphere.

Freshwater eutrophication Fresh water eutrophication is the result of nutrient emissions, for instance phosphorus and nitrogen, into fresh bodies of water or soil. The nutrient concentration increases in the water and soil. Autotrophic organisms, for instance photosynthesizing bacteria and algae, as well as heterotrophic species such as bottom feeders and fish, thrive on these nutrients while other organisms do not. This causes an imbalance in the organism and species population in these fresh bodies of water. Therefore the freshwater eutrophication damages freshwater ecosystems. The unit of characterization for freshwater eutrophication is kg phosphorus (P) equivalent into freshwater.

Marine eutrophication Marine eutrophication is the result of diffusion and direct emission of dissolved inorganic nitrogen (DIN) to soil, rivers and coastal environments. The DIN concentration increases in the coastal water which were previously limited. Therefore certain organisms and species thrive and uptake other limiting nutrients. This increases the disappearance of marine species, especially demersal fish. Therefore marine eutrophication damages marine ecosystems. The unit of characterization for marine eutrophication is kg nitrogen (N) equivalent into rivers and coastal waters.

Toxicity Toxicity is the result of chemical emissions to the biosphere. The chemical concentration increases in the habitable environment. The increased concentration of chemicals is exposed to humans and other species. Therefore it can cause species to die off and potentially disappear in its habitat. Thus damaging ecosystems in fresh water, marine and terrestrial environment. In addition it can cause increased incidence of carcinogenic and non-carcinogenic diseases in human health. Thus damaging human health. The unit of characterization for toxicity is kg 1,4-dichlorobenzene (1,4-DCB) equivalent into the air, freshwater, seawater, and industrial soil.

Water use Water use is the result of fresh water consumption from the environment. The fresh water consumption results in a reduction of fresh water availability. This can lead to three damage pathways. The first being that it can cause a water shortage for irrigation and eventually resulting in an increase in malnutrition. Therefore damaging human health. The second damage pathway due to water use is the reduction in plant diversity as result of drought which kill off plants. Thus disappearing terrestrial species. The third damage pathway due to freshwater use is the reduction in river discharge rate and thus

resulting in disappearing freshwater species. The last two damage pathways cause damage to terrestrial ecosystems. The unit of characterization for water use is m^3 fresh water consumption from the biosphere.

Land use Land use is the result of change of land cover and land use intensification from habitable land. Change in land cover leads to loss of habitat and thus resulting in potentially disappearing terrestrial species. Land use intensification leads to loss of habitat as well and also to soil disturbance, thus also resulting in potentially disappearing terrestrial species. Therefore land use causes damage to ecosystems. The unit of characterization for land use is m^2 arable land use equivalent annually from the biosphere.

Mineral resource scarcity Mineral resource scarcity is the result of mineral resource extraction which leads to a decrease in concentration of that mineral (ore grade) worldwide. The demand for the mineral will increase as it becomes more valuable and therefore it will be extracted from sites with higher concentrations. Once these highly concentrated sites are depleted, it will cause the extraction to be done at less accessible sites which causes the cost of extraction to increase. Therefore mineral resource scarcity causes damage to resource availability. The unit of characterization for mineral resource scarcity is kg copper (Cu) equivalent from the earth.

Fossil resource scarcity Fossil resource scarcity is the result of fossil resource extraction. Fossil source concentration are similar around the world and therefore are not susceptible to concentration differences. However, it will cause the extraction to be done at less accessible sites one the easily accessible ones are depleted which causes the cost of extraction to increase as well. Therefore fossil resource scarcity causes damage to resource availability. The unit of characterization for fossil resource scarcity is kg oil equivalent from the earth.

To summarize this section, the direct emissions during the use of energy carriers does not represent the total emissions as the production and distribution needs to be accounted for. Therefore the life cycle system boundaries are determined as the well-to-wake pathways which is the equivalent of the cradle-to-grave trajectory in an energy carrier perspective. With the well-to-wake pathways an LCA can be performed to determine the environmental impacts and their magnitude. The software SimaPro 9 that automates the LCI phase to the LCIA phase is accessible to perform the LCA. Within SimaPro 9 the Ecoinvent database for the LCI phase and the ReCiPe 2016 method for the LCIA are available.

1.7. Research project

To conclude the extended problem analysis on ship design/vessel specifications, the *External Requirements* are actively changing through GHG emission regulations and thus involuntarily impacting the *Available Technology* and *Commercial Aspect* while the *Operational Requirements* do not change. Consequently the main dimensions of a ship will increase due to equal effective energy from AMECs, resulting in higher propulsion powering and cause increased energy carrier consumption. Additionally the regulations only apply to direct GHG emissions, however the indirect emissions also account for a significant proportion. Moreover, there are many other environmental impacts by emissions over the full life of energy carriers. Therefore a comparative environmental assessment on AMECs which takes into account the increased AMEC consumption needs to be researched to determine the total *Environmental Consequences*.

1.7.1. Knowledge gap in literature

Based on the extended problem analysis, there is ample individual research on AMECs and their powering technologies, energy saving ship designs and propulsion, and maritime environmental assessments. Nevertheless there are only a few studies in which two of these three elements are taken into account. According to the author's knowledge there are no studies taking all three elements into account. However, as demonstrated, current AMEC properties and their powering technologies require additional bunker volume and weight to maintain the same operational requirements. Consequently this affects the ship design and additional propulsion power is necessary, resulting in more energy carrier consumption. It consequently causes increased direct and indirect emissions that impact the environment in many different ways than just global warming. Accordingly, the main goal of this research is to determine the total environmental impact including the powering impact by AMECs.

The flaws of the existing literature have already been discussed in the extended problem analysis. Nevertheless, the existing literature contains valuable approaches which can be combined in order to achieve the main goal. The studies by Terün, Kana and Dekker, and Bodewes maintain the operational requirement of service speed and sailing range/endurance and define this by calculating the effective energy of the bunkered fuel [118] [14]. They also use the contained energy densities of the AMECs and the power plant efficiencies to determine the additional bunkering volume and weight. This approach will also be used, but with more accurate power plant efficiencies and auxiliary powers. The additional volume and weight can best be applied to strive for the lowest propulsion power possible. Lindstad et al. determined that higher length-beam ratios for ships with equal carrying capacity are the most energy efficient [89] [90]. Additionally, Liu and Pananikolauo determined that the added ship resistance decreases for lower Froude numbers, which can be achieved by increasing the length of a ship [92]. They also demonstrated that increasing the beam-draft ratio for a constant speed further reduces the added ship resistance. Therefore both methods are useful for modelling the additional bunkering volume and weight of the AMECs. Levander, Andrews and Dicks, and Vossen et al. all conclude that ship designs are based on historical data and therefore the maximum dimensions will be determined using historical ship design aspects [85] [136] [7]. Terün, Kana and Dekker used the Holtrop & Mennen method and also the propulsion chain method by Klein Woud and Stapersma to parametrically determine the ship resistance and necessary propulsion [118]. These are accurate and practical methods to determine the resistance and propulsion while keeping the design aspects of the ship types into account. Lastly, Bilgili uses SimaPro 9 software in combination with the Ecoinvent database and the ReCiPe 2016 method to conduct a comparative LCA on various AMECs [12]. SimaPro 9 including the Ecoinvent database and the ReCiPe 2016 method are also available and necessary to conduct an environmental assessment.

Project goal
To achieve the main goal of this research and support the energy carrier selection of the future by the maritime industry, a main research question and sub-questions are established to be answered in the methodology. The goal of this research project is to determine the full environmental impact of AMECs in ships while taking the powering impact into account with regards to conventional fuel oil powered ships. The main research question states:

What is the impact on the ship's propulsion powering and consequently the environment by alternative marine energy carriers?

The sub research questions state:

- What are the power plant efficiencies and energy densities of the current and future (A)MEC types?
- What are the historical design elements/dimension trends of ship types?
- How can the resistance and propulsion power be calculated while taking the design elements per ship type into account?
- How can the total bunker volume and weight change by the AMEC types be determined while maintaining the same operational requirements?
- How can the total bunker volume and weight change be applied to the ship design while striving for the lowest propulsion power as possible within a ship type?
- How can the magnitudes of the environmental impacts be determined of the operational stage of a ship for current and future (A)MECs?

1.7.2. Research approach

A case study will be constructed containing four ships with six energy carrier types. Four ship types have been selected for this research: bulk carriers, tankers, container ships, and trailer suction hopper dredgers. The first three ship types account for 85% of the global seagoing merchant vessels of 100 GT and above in 2021 [129]. Therefore this project will relate to the largest share of seagoing vessels. In addition, these vessel are subjected to the emission regulations by the IMO and therefore are more likely to be involved in being powered by AMECs. However, it is expected that other ship types that do not have to comply now will also have to follow in the future. Hence, trailer suction hopper dredgers (TSHDs) have been included as well to represent the ships that are not subjected to the emission regulations and the non international shipping vessels. Twelve ships of which their main design and energy parameters are known are compiled per ship type to be analyzed how an energy carrier type will impact the design

and consequently the energy carrier consumption.

Six energy carrier types have been selected for their current and future predicted presence with accompanying power plant in the maritime industry from section 1.3.1. The selected energy carrier types are fuel oil (current/original), methanol, LNG, liquid hydrogen, ammonia, and charged batteries. The power plants of the energy carriers are investigated for their components, performance and total efficiency. Each energy carrier type has a different uncontained and contained energy density. The uncontained energy density is used to determine the volume and weight of the energy carrier on board and it is a part of the variable free weights (DWT). The contained energy density includes the tank system as well and it is used to determine the additional volume and weight to the ship's overall internal volume and lightweight ship (design). A change to the design of the ship results in a change in the ship resistance, main engine power and consequently the energy carrier consumption. Therefore the design impact of an energy carrier type is modeled to determine the powering (=consumption) impact. The design impact model strives to generate a new design which causes the least additional powering. This is done by taking into account that a higher length-beam ratio is favorable in terms of resistance. Consequently, the ship design generation procedure will apply the additional required AMEC bunker space by first lengthening, thereafter heightening, and lastly widening the ship.

The six energy carrier types can be produced from many different sources and processes and therefore two sources with their accompanying production processes are selected. The first source of the energy carrier type originates from their conventional origin while the second source originates from biomass or renewables. For electricity as an energy carrier in the form of batteries, the environmental impact of the production of a lithium ion battery (LIB) will be included in the assessment. This is done because the extraction and production of LIBs is known to be severely environmentally unfriendly.

Model description
A model is fabricated to determine the total environmental impact for a ship with constant operational requirements for the twelve energy carriers. The model consists of two main components which are performed separately: the powering impact per energy carrier type and the environmental impact per energy carrier. the total research model is displayed in figure 1.15. The two impact assessments result in the total environmental impact of an energy carrier. The total model uses five separate inputs/data. The powering impact assessment component uses four inputs. The first input is detailed information of a sample set of existing ships per ship type (1). Together with the second input, the dimension trends per ship type (2), the new design of a ship can be determined which corresponds to historical design data. The third and fourth inputs are the energy densities (3) and power plant efficiencies (4) per energy carrier type. With these four inputs, the iterative powering impact assessment can be conducted which consists of three sub-models: a resistance approximation-, propulsion power approximation- and ship design generator. The environmental impact component uses three inputs of which two are the same from the powering impact inputs. The first is the well-to-wake characteristics per energy carrier (5). The second and third inputs are the energy densities (3) and power plant efficiencies (4) per energy carrier type which are the same from the powering impact component. With these three inputs, an LCA can be performed which yield the environmental effects.

The powering impact assessment component and its inputs of the model result in the total installed power changes in the ship by an energy carrier type. The total installed power is direct related to the energy carrier consumption. Therefore a higher total installed power yields a higher energy carrier consumption and therefore also higher emissions. The environmental impact assessment component and its inputs of the model result in the quantifiable net environmental effect of the energy carrier. The purpose of AMECs is to reduce the environmental effects compared to conventional fuel oil. However, if the AMEC causes the total powering to be increased to the point that the environmental effects of the additional AMEC consumption surpasses the environmental effects of conventional fuel oil, the opposite is achieved. Additionally, the focus of AMECs in the maritime industry is focused on climate change/global warming, however the regulations do not take other environmental impact types into account. Therefore AMECs could possibly solve one effect and cause another one. With this model the total environmental impact can be determined and compared to conventional fuel oil in different ship types.

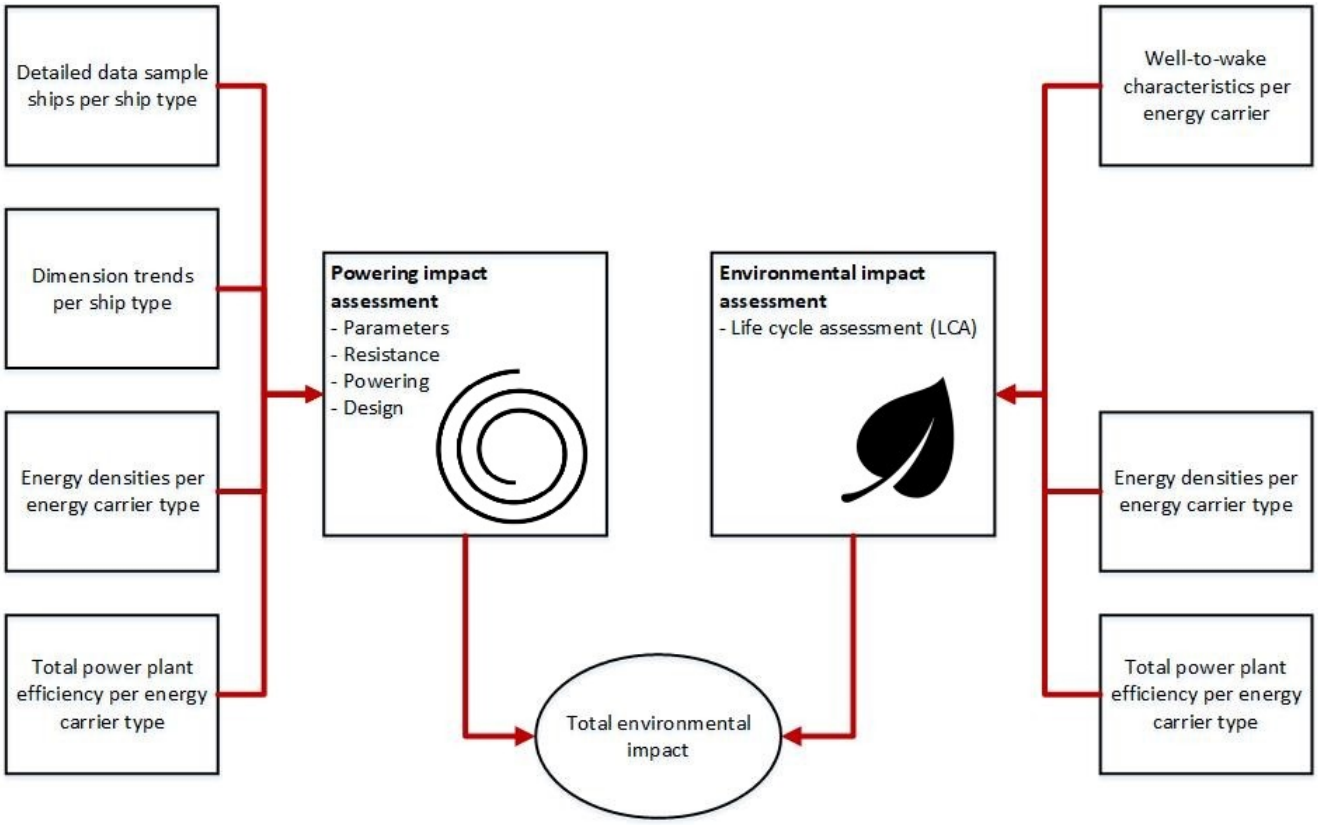

Figure 1.15: Total research model

1.7.3. Research scope and methodology

The scope of this research is bounded to the constant operational requirements. This can be achieved by maintaining the operational conditions. While the main dimensions of a ship can be an operational requirement, it is considered that they are driven by the other operational requirements. This is in agreement with the ship design requirements considered by Vossen et al. [136]. As reminder from section 1.1, the operational conditions are:

Ship type (design elements/dimension trends)
Original internal volume minus the bunker volume
Service speed
Sailing range/endurance
Non propulsive energy consumers (ship functioning and cargo handling/treatment)

In order to answer the sub research questions and subsequently the main research question, a research methodology is constructed to achieve the research goal. The research methodology consists of three parts where the first part is the data collection and case study set up. With the information from the case study generation (part one), the powering impact assessment (part two) and the environmental impact

assessment (part three) can be performed independently. The methodology is as follows:

1. Data collection & case study generation
   (a) Well-to-wake characteristics per energy carrier
   (b) Energy densities per energy carrier type
   (c) Total power plant efficiency per energy carrier type
   (d) Detailed data of sample ships per ship type
   (e) Dimension trends per ship type
2. Propulsion power impact assessment
   (a) Resistance approximation method on sample ships
   (b) Propulsion power approximation method on sample ships
   (c) Design impact assessment on sample ships
   (d) Parameter: iterative process of resistance, propulsion power and design
3. Environmental impact assessment
   (a) LCA of energy carriers

1.7.4. Report structure

In chapter 2, the case study is presented. In the case study chapter, the input data for both the powering impact and environmental impact assessment are determined. In the following chapter 3, the powering impact assessment of the AMEC types on the ship types is conducted and the results are discussed. In chapter 4, the environmental impact assessment of the (A)MECs are determined for equal shaft output. The powering impact and environmental impact results are combined to determine the total environmental impact. The total environmental impact results are discussed and a conclusion on the total research given in the next chapter 5.

2

Case study

Fuel oil currently dominates the marine powering industry. In section 1.3.1, it was determined that the energy carrier types of the future are relatively certain but their share is less predictable. Therefore the future presence of the energy carrier types will be considered as the deciding factor to investigate their powering and environmental effects. The energy carrier types selected are fuel oil, methanol, LNG, liquid hydrogen, ammonia, and electricity in batteries. LNG, methanol, liquid hydrogen and ammonia are carried in a liquid state. However only liquefied natural gas (LNG) and liquid hydrogen (LH_2) are specifically titled 'liquid/liquefied' because they also are available in compressed gaseous state (CNG and CGH_2), whereas methanol and ammonia are not. The energy densities in compressed state are lower than in their liquid state and therefore are less favorable for spatial reasons. The energy carrier types are subjected to the four selected ship types: bulk carriers, tankers, container ships and TSHDs. The merchant shipping vessels account for the largest share of seagoing vessel and are compliant with the IMO's GHG regulations. Therefore they are more involved with AMECs and their powering technologies. TSHDs are not shipping vessels and thus do not need to comply with the regulations. However the goal by the IMO is to have zero carbon emissions by 2100 and therefore non compliant ship types will eventually have to follow. In this chapter, the data collection and case study generation is presented to be subjected to powering impact and environmental assessment. In section 4.1.1, the conventional and alternative energy carrier types and their power plants are investigated. In section 2.2, the ship types are investigated for their design elements and dimension trends from historical data.

2.1. Energy carrier types and power plants

In simple terms, energy carriers are substances or phenomenons that are 'carried' to power a mobile power plant. In section 1.6.2, it was determined that a single energy carrier type can be sourced, processed and used in many different ways. Therefore for each energy carrier type, two different sources are selected. The first source of each energy carrier type is from the conventional origin and the second from biomass or renewable origin. It is generally known that the conventional source fully or partially originates from fossil reserves whereas the biomass or renewable sources are more diverse. Consequently the source also determines the production process and thus the emissions from well-to-tank differ as well per single energy carrier. For every energy carrier type, the usage in the power plant from tank-to-wake is the same.

In this section, the energy carriers are described for their method of production, energy producing mechanism (usage), safety hazards and notorious environmental issues. For every energy carrier type, the components related to the total power plant efficiency and the auxiliary power required for those components are investigated. The total power plant efficiency and the required auxiliary power are used in the powering impact assessment. The source and production methods of the energy carriers are used in the environmental impact assessment. The energy carrier types, specific energy carrier, state, source and power plant type to be investigated are displayed in table 2.1

Table 2.1: Energy carrier, processed state, source and power plant to be investigated

Energy carrier type	Marine energy carrier	Carried state	Source	Power plant
Fuel oil	Diesel BioDiesel	-	Fossil Biomass	Mechanical
Methanol	Methanol Bio Methanol	Liquefied	Fossil Biomass	Mechanical
LNG	Natural gas Bio Natural gas	Liquefied	Fossil Biomass	Mechanical
Liquid hydrogen	Hydrogen eHydrogen	Liquefied	Fossil Renewable	Electric
Ammonia	Ammonia eAmmonia	Liquefied	Fossil Renewable	Electric
Electricity + LIB	Electricity mix Electricity renewable	Li-ion battery	Regional mix Renewable	Electric

2.1.1. Fuel oil

As the name already advocates, fuel oil is an oil intended as a fuel to be combusted in an internal combustion engine or burned to generate heat. It is a group name for all petroleum distillates in liquid oil form. It is the most common energy carrier in the maritime industry and it comes in different forms. The dominant source of fuel oil is petroleum (crude oil) where the fuel oil is separated from other hydrocarbons, for instance butane and propane by the process of distillation. In this process, the crude oil is heated and the lighter hydrocarbons will boil before the heavier hydrocarbons and rise. The heaviest hydrocarbons will stay at the bottom of the distillation tank and removed resulting in heavy fuel oil. Heavy fuel oil (HFO) is therefore also known as a residual oil and it is extremely viscous compared to other fuel oils. It requires to be heated in order to become more fluid-like to flow through pipes. In addition, HFO is the remnant of the distillation process and therefore it is the cheapest oil fuel on the market. Therefore it is commonly used in the maritime sector as large quantities are necessary. However, HFO also contains the highest amount of contaminants which are more polluting than other oil fuels. If ingested it could be fatal and thus it is also very to toxic to aquatic lifeforms [98]. Another source of fuel oil is vegetable oil. In the production process oil is extracted from biomass such as palm trees. The vegetable oil hydrocarbon chains are too short to be immediately used as a fuel and thus a chemical is used to combine them to create long chains similar to fuel oil resulting in biodiesel. Biodiesel is however problematic when coming in contact with water as it can slightly absorb water and cause combustion problems. Due to biodiesel originating from biomass, it is labeled as a biofuel, however it is criticized for the environmental impact it has. Natural forest are burned or cut down in order to make space for palm tree plantations. Only a small portion of bunkered fuel oil is bio-fuel oil or a distillate from the bunker sales from the Port of Rotterdam and thus not widely applied [52].

Fuel oil has a contained volumetric energy density ($\rho_{V\ E\ con}$) of 33.20 MJ/L and a contained gravimetric energy density ($\rho_{G\ E\ con}$) of 29.65 MJ/kg [138]. Together, the contained density (ρ_{con}) is 1.12 kg/L.

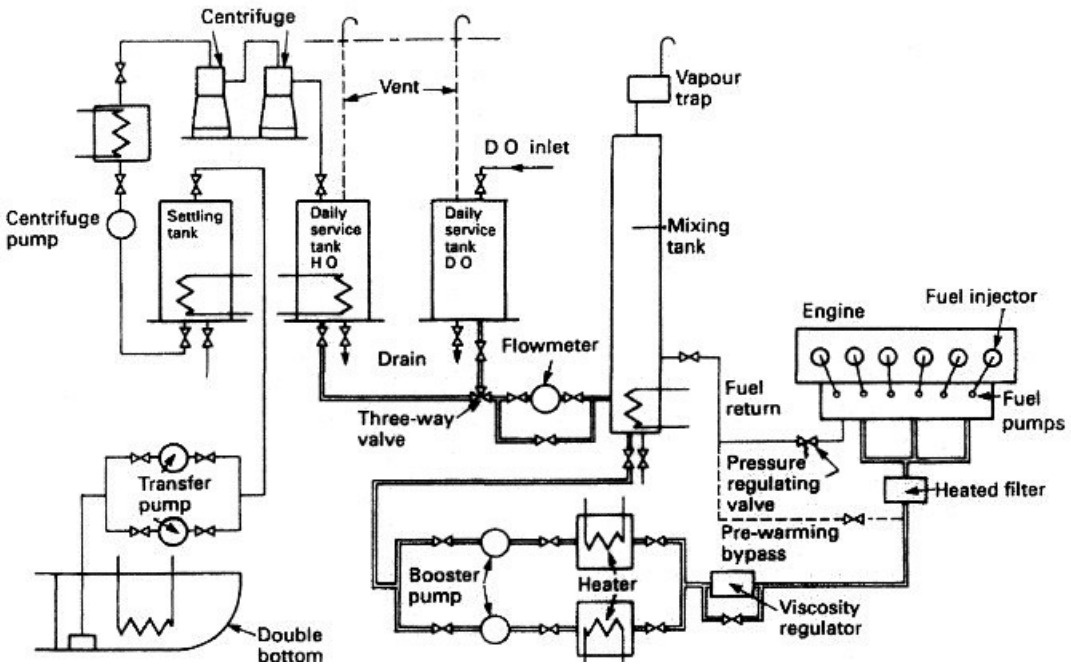

Figure 2.1: Generalized fuel oil power plant system [93]

Fuel oil power plant system
Heavy fuel oil is bunkered externally through the fuel oil transfer system to the settling tank. At the point of bunkering the fuel is heated to be less viscous, making it easier to flow and pump. In the settling tank residues and/or water settle to the bottom to be discarded and thereafter pumped through the transfer pump to the storage tank. When fuel is demanded from the storage tank, the fuel oil gets pumped through the transfer pump and to the settling tank again for the fuel oil treatment system. In this system the fuel oil is cleaned through a two stage process. The fuel oil is purified and clarified in a heated centrifuge and transferred to the heated service tank. This system decontaminates the heavy fuel oil more rigorously than the settling tank. From the settling tank, the fuel oil is transferred to the fuel oil supply system where the flow and fluid characteristics are monitored and controlled more precisely to the specifications of the internal combustion engine. Finally the fuel is pumped to the main or auxiliary engines where it will drive the propeller, generator or other mechanical consumers. The heating of the heavy fuel oil is done by contained pressurized steam originating from a boiler which uses fuel oil and/or exhaust waste heat recovery system. Other fuel oils do not need the fuel oil treatment system as they are not as viscous and do not contain as many impurities. In order to start the whole fuel oil system, a purer fuel oil distillate is used such as marine diesel oil (MDO) to make the heavy fuel oil usable. Therefore a small amount of diesel oil is bunkered. All the pumps and centrifuges are powered by the generator which is driven by the fuel oil. Likewise the heating system is also powered by fuel oil in the boiler. This displays how the additional energy necessary from using cheap heavy fuel oil is still more profitable than using MDO where the heating and treatment is not necessary due to its lower viscosity and purity.

Power plant components and total efficiency The fuel oil power plant efficiency is primarily dependent on the internal combustion engine cycle. A slow speed 2-stroke diesel engine has an efficiency up to 49,34%, while a medium speed 4-stroke diesel engine has an efficiency of 41% [102] [20]. It is assumed that there are not any other energy losses in the fuel oil power plant system and the total power plant efficiency (η_{PP}) is 49.34%. Additionally to main engine power, the auxiliary power (PP_{aux}) is estimated to be 5% of the main engine power to drive all the components necessary for the power plant [101]. In ships that fully run on MDO, there are not any components involving the processing of heavy fuel oil. Therefore the minimal auxiliary power is decided to be 1% for simplicity to power the necessary pumps.

2.1.2. Methanol

Methanol is an alcohol and belongs to the category of low flashpoint fuels. Therefore it turns into a vapour in ambient conditions, making it highly flammable. In addition, the vapour is also corrosive to the respiratory system and can also cause suffocation if the vapour displaces oxygen [6]. It can be combusted in the same internal combustion engine as fuel oil with minor modifications. Methanol is synthesized by the hydrogenation process of carbon dioxide which can originate from fossil natural gas or biomass. Methanol fuel originating from biomass is therefore also a biofuel. Methanol fuel contains significantly less impurities than fuel oil and therefore burns cleanly. It burns so clean that the flame is invisible and there is no smoke formation, causing the fuel to be a safety issue [95]. It also contains some contaminants which cause the fuel to be corrosive on metals. Even though methanol can be combusted in the same internal combustion engine as fuel oil, a small amount of pilot fuel is necessary to improve the ignition and combustion process. This can done with diesel oil at 1% of the injected fuel [20]. Methanol is already applied in the maritime industry as an energy carrier. Especially on methanol carriers such as the Manchac Sun (IMO: 9724013) and the Mari Couva (IMO: 9848584) where it is already on board as a cargo. However, it is less applied to other ships and as can be seen by the Port of Rotterdam bunker sales, it is barely sold at at all [51].

Methanol has a contained volumetric energy density ($\rho_{V\ E\ con}$) of 13.83 MJ/L and a contained gravimetric energy density ($\rho_{G\ E\ con}$) of 15.67 MJ/kg [138]. This is calculated using 99% pure methanol and 1% fuel oil for the pilot fuel. Together, the contained density (ρ_{con}) is 0.88 kg/L.

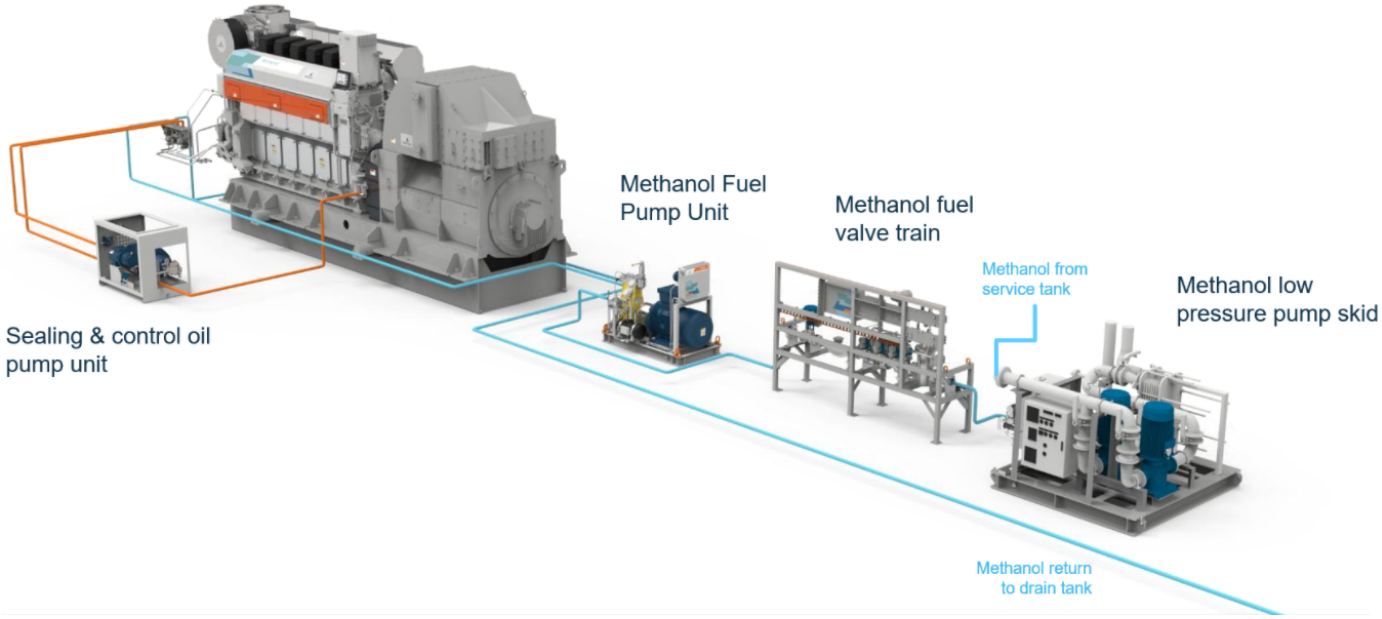

Figure 2.2: Methanol power plant system MethanolPac by Wärtsila [26]

Methanol power plant system

Methanol is bunkered externally through the bunkering skid to be purified and drained from impurities during the bunkering process, where it continues to the methanol tank. As methanol is a low flash point fuel, all piping must be be double walled for inerting with nitrogen to lessen the chance of ignition. Consequently a nitrogen generator is used for the inerting. From the fuel tank it is transferred by the low pressure pump to the methanol preparation room through where the methanol is cooled and excess flow is recirculated back to the tank. The methanol further continues to the fuel valve train where the flow is filtered and the pressure is controlled with a block and bleed arrangement. Finally, the methanol is supplied to the fuel pump unit which receives signals from the engine to adjust its speed and deliver the correct amount of fuel accordingly. The low pressure pump, fuel valve train, and fuel pump unit are all located in the fuel preparation room which is enclosed by a coffer dam with nitrogen to further reduce the risk off ignition. Additionally, a sealing and control oil pump unit located in the engine room filters and controls the flow, pressure and temperature of the lubrication oil of the engine.

Power plant components and total efficiency The methanol internal combustion engine in figure 2.2 is the Wärtsila 32 and it is fuel flexibility allows for it to operate not only on methanol, but also on HFO, MDO and liquid biofuels [141]. It is assumed that there are not any other energy losses in the fuel oil power plant system and therefore the same power plant efficiencies as fuel oil apply. Meaning a total power plant efficiency (η_{PP}) of 49.34% for a 2-stroke engine and 41% for a 4-stroke engine. Additionally to main engine power, the auxiliary power (PP_{aux}) is estimated to be 3% of the main engine power to drive all the components necessary for the power plant [17].

2.1.3. LNG

Liquefied natural gas (LNG) is natural gas that has been liquefied by cooling it to approximately -162 degrees Celsius and thereby decreasing the volume by almost 600 fold. Just like fuel oil and methanol, natural gas is highly flammable and used in internal combustion engines or burned to generate heat. Just like methanol, a small amount of pilot fuel is necessary to improve the combustion process in the engine. Natural gas can be extracted from fossil wells deep in the ground and predominantly contain methane, but also small amounts of other hydrocarbon gases. The bio version of natural gas is called biogas and it is usually produced from biomass through a process where microorganisms break down the biomass and release methane in return. Biogas can be produced from a wide variety of organic wastes, making it a volatile production process. The difference in biodiesel and biogas is that biogas can be produced from wastes rather than fresh agricultural biomass. Therefore biogas does not require agricultural plantations which contributes to land use and can cause deforestation. LNG comes with a few hazardous elements due to it chemical properties, but also because of its containment state [5]. Natural gas is also a low flashpoint fuel and therefore extremely flammable by the slightest ignition in the presence of oxygen. In addition, LNG is stored under pressure and therefore it can explode by a tank breach. The gas is also colorless and odorless and therefore it is difficult to detect, thus it can cause suffocation by oxygen displacement. LNG has become an increasingly popular fuel in the maritime industry. From 21,242 m^3 in sales in 2018 to 603,690 m^3 in sales in 2021 in the Port of Rotterdam [52] [51]. It is especially popular for its lower price compared to fuel oil for its energy content, however since the war in Ukraine that is not the case anymore. Additionally, natural gas contains significantly less contaminants and therefore burns more cleanly than fuel oil and emits less CO2. Nonetheless, 0.2 to 3 percent of natural gas slips from the combustion process and is released into the atmosphere [19]. Yet, methane is 34 times more potent than CO2 in its global warming properties [58].

LNG has a contained volumetric energy density ($\rho_{V\ E\ con}$) of 13.37 MJ/L and a contained gravimetric energy density ($\rho_{G\ E\ con}$) of 28.38 MJ/kg [138]. This is calculated using 99% pure LNG and 1% fuel oil for the pilot fuel. Together, the contained density (ρ_{con}) is 0.47 kg/L.

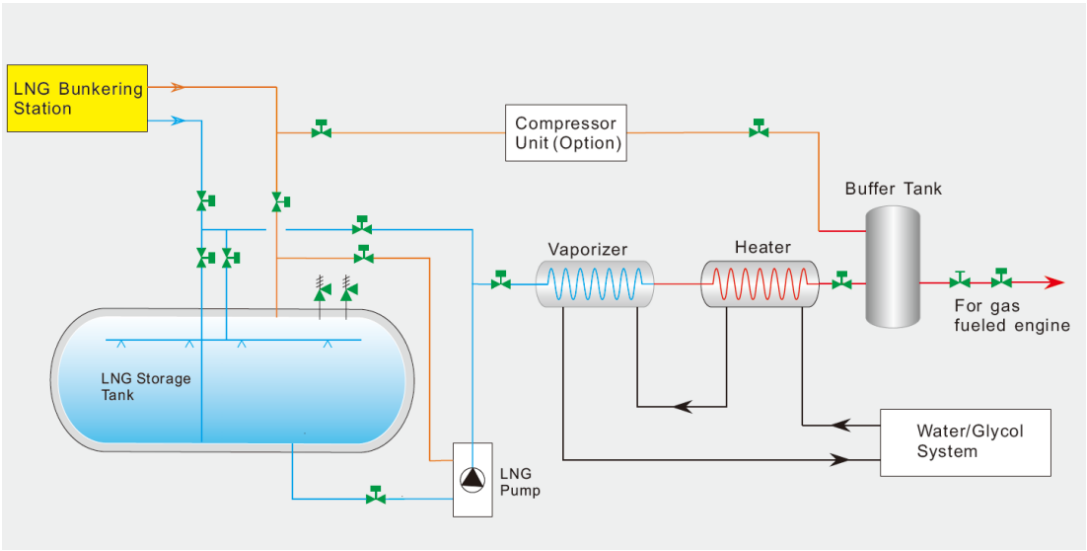

Figure 2.3: Partial generalized LNG power plant system [86]

LNG power plant system
The LNG power plant is similar to the methanol power plant, mainly due to the low flash point property of LNG. LNG is also bunkered through the bunkering skid to be refined from impurities in the bunkering process. The LNG flows to the cylindrical tanks under high pressure. Since its a low flash point fuel all piping must be double walled with inert gas in between such as nitrogen to minimize the chance of ignition. Therefore a nitrogen generator can be used to extract the nitrogen from the air. The LNG is extracted from the tank by the LNG pump and pumped to the vaporizer where the liquid returns to a gaseous state in the fuel preparation room. The natural gas has extremely low temperature at this point and thus it is passed through a heater. The now heated gas is supplied to the buffer tank where it can continue to the fuel valve train or excess natural gas can be resupplied to the LNG tank by a compressor. The fuel valve train controls the pressure of the flow through a block and bleed arrangement to the internal combustion engine in the engine room. Additionally, a sealing and control oil pump unit located in the engine room filters and controls the flow, pressure and temperature of the lubrication oil of the engine.

Power plant components and total efficiency The LNG power plant efficiency is also dependent on the efficiency of the internal combustion engine. With an efficiency of 49.34% for a 2-stroke diesel engine and 41% for a 4-stroke diesel engine. Unlike fuel oil and methanol, the natural gas slip will be taken into account as a loss at an average of 1.6%. Therefore the total LNG power plant efficiency (η_{PP}) for a 2-stroke diesel engine configuration is 48.55% and 40.34% for a 4-stroke diesel engine configuration. It is assumed that there are not any other energy losses in the LNG power plant system other than slip and engine efficiency. Additionally to main engine power, the auxiliary power (PP_{aux}) is estimated to be 3% of the main engine power to drive all the components necessary for the power plant [17].

2.1.4. Liquid hydrogen

Liquid hydrogen (LH_2) is hydrogen gas that is liquefied by cooling it to approximately -253 degrees Celsius. Hydrogen is extremely flammable without a visible flame and may also form an explosion [4]. It can be used in an internal combustion engine as well as in a fuel cell. Be that as it may, hydrogen internal combustion engines have a much lower overall efficiency than a fuel cell [15]. Hydrogen is predominantly produced by methane pyrolysis, where fossil natural gas is reacted in a catalyst and breaks down into hydrogen gas and solid carbon without any other byproducts. Although it is produced from natural gas, hydrogen itself does not contain any carbon. An other method of production is through water electrolysis, where an electrical current is passed through pure water and oxygen gas forms at the anode side while hydrogen forms at the cathode side. Hydrogen internal combustion engines are not used in the maritime industry, but hydrogen fuel cells are an upcoming technology of interest as fuel cell efficiencies and reliability keep improving further. The reaction of hydrogen and oxygen in a fuel cell solely emits water and thus the reaction has negligible impact on the environmental.

Liquid hydrogen has a contained volumetric energy density ($\rho_{V\ E\ con}$) of 4.6 MJ/L and a contained gravimetric energy density ($\rho_{G\ E\ con}$) of 11.7 MJ/kg [138]. Together, the contained density (ρ_{con}) is 0.39 kg/L.

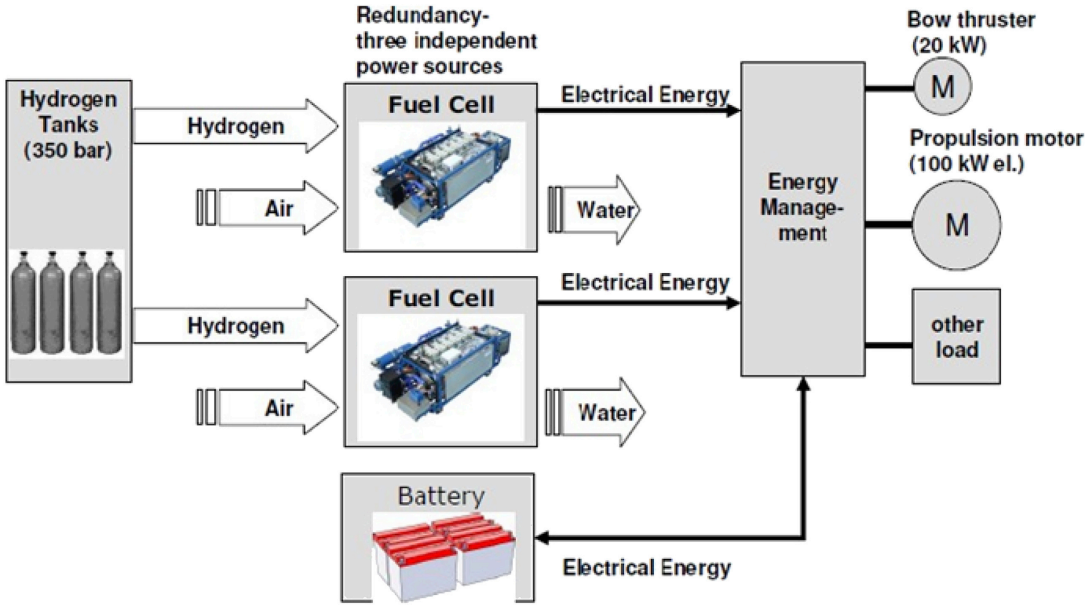

Figure 2.4: Generalized hydrogen power plant system [126]

Liquid hydrogen power plant system
The liquid hydrogen is bunkered through a skid to remove any impurities during bunkering. It is also a low flashpoint fuel and therefore double walled piping with inert nitrogen gas in between walls is necessary. The hydrogen is pumped from the tank to the fuel preparation room where is vaporized and heated before entering the fuel valve train to control the pressure. Thereafter it enter the fuel cell on side while air enters through the other side. There are different types of fuel cells available, yet a solid oxide fuel cell (SOFC) is most applicable due to its high thermal efficiency, high electrical efficiency and long term stability. The fuel cell is kept at a constant temperature and therefore it is cooled by an air blower. The hydrogen and oxygen react in the fuel cell which produces a direct current electricity. The electrical energy is transferred to the energy management system (main switchboard) where the electricity is distributed, transformed and converted to all electrical consumers. The main electrical consumer is the electric propulsion motor on a ship.

Power plant components and total efficiency The hydrogen power plant contains significantly more parts that contribute to the overall efficiency than the previous three power plants. A marine SOFC system with hydrogen has a net electrical efficiency of 47.1% [133]. The total losses in the main switchboard are from the average electrical distribution losses at 0.45%, the average losses due to transforming at 1.05%, and the average converting losses at 2% [75]. Finally the electric motor has an average load loss of 3.5% [75]. The total hydrogen power plant efficiency (η_{PP}) comes down to 43.88%. Additionally to main engine power, the auxiliary power (PP_{aux}) is estimated to be 11% of the main engine power to drive all the components necessary for the power plant [49].

2.1.5. Ammonia

Liquid ammonia is ammonia gas that is liquefied by cooling it to approximately -33 degrees Celsius. Ammonia is also flammable, but ammonia internal combustion engines are practically non existent due to the unstable combustion conditions it requires. Due to its flammability and low boiling point, it is a low flashpoint fuel. It can be used directly in solid oxide fuel cells (SOFC) or only as an energy carrier where it is cracked into nitrogen and hydrogen before entering a proton exchange membrane fuel cell (PEMFC). The PEMFC is currently the most commercialized fuel cell type due to its lower cost and power flexibility. Ammonia is predominantly produced through the Haber-Bosch process, where nitrogen and hydrogen react under specific temperature and pressure to form ammonia. The hydrogen used in this process generally originates from the methane pyrolysis process as mentioned in the previous section 2.1.4. Ammonia can also be synthesized electrochemically with water and nitrogen. This process can be done with renewable energy and therefore making the production process a sustainable method. In addition to ammonia being flammable and explosive, ammonia is also extremely toxic and can cause respiratory damage, suffocation,

eye damage, and can easily kill aquatic life [3]. Currently, there are not any ships powered by ammonia, however the Kriti Future (IMO: 9924326) is ammonia-ready. This means that the engine is designed to be easily converted to run on ammonia. Moreover, the Viking Energy (IMO: 9258442) is planned to be refitted to be powered by ammonia fuel cells in 2024. Ammonia emissions have severe impacts on the environment [48]. For example, ammonia emissions negatively affect biodiversity as the result of an over-abundance of nutrients. In addition, it also causes increased soil acidity and oxygen depletion of fresh water ecosystems.

Ammonia has a contained volumetric energy density ($\rho_{V\ E\ con}$) of 9.45 MJ/L and a contained gravimetric energy density ($\rho_{G\ E\ con}$) of 11.7 MJ/kg [138]. Together, the contained density (ρ_{con}) is 0.81 kg/L.

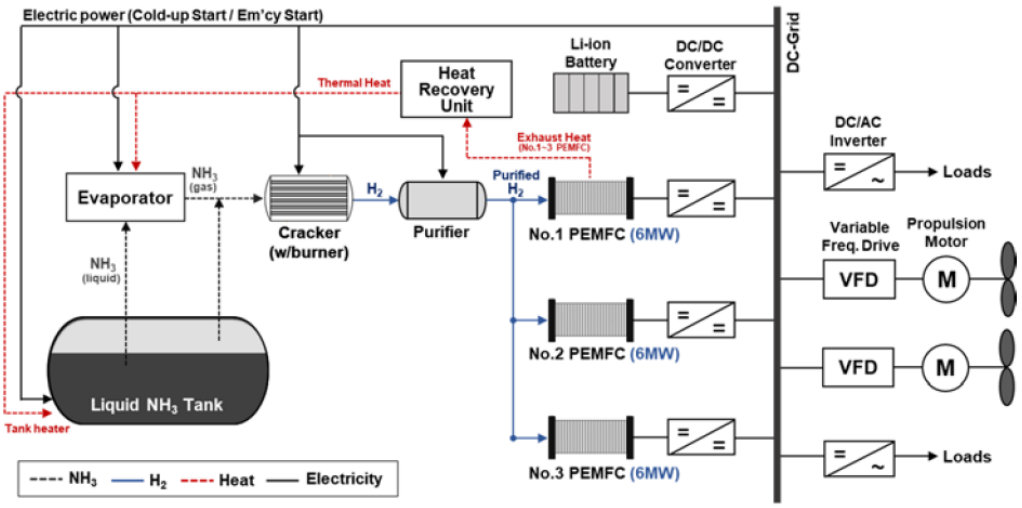

Figure 2.5: Generalized ammonia power plant system [79]

Ammonia power plant system
The liquid ammonia power plant is practically the same as the liquid hydrogen power plant, however there are major two practical fuel cell options. The first option is to 'crack' the ammonia into hydrogen and nitrogen, and use the hydrogen in a PEMFC rather than a SOFC. The CAPEX of a PEMFC is approximately a fifth of a SOFC for the same output, while the OPEX is the same [79]. However in this configuration an ammonia cracker and hydrogen purifier needs to be installed before the PEMFC as in figure 2.5. In an SOFC configuration the cracker and purifier would be removed.

Power plant components and total efficiency The ammonia power plant is comparable to the hydrogen power plant. A marine SOFC system with ammonia has a net electrical efficiency of 55.1% [133]. The total losses in the main switchboard are from the average electrical distribution losses at 0.45%, the average losses due to transforming at 1.05%, and the average converting losses at 2% [75]. Finally the electric motor has an average load loss of 3.5% [75]. The total ammonia power plant efficiency (η_{PP}) comes down to 51.33%. Additionally to main engine power, the auxiliary power (PP_{aux}) is estimated to be 11% of the main engine power to drive all the components necessary for the power plant [49].

2.1.6. Electrically charged lithium ion batteries

Li-ion batteries are a type of rechargeable battery which contains lithium ions which can discharge electrons to create an electrical current and charge again to serve as an energy carrier. Li-ion batteries are widely used in small electronic mobile devices such as cell phones, but also in larger machines as electric vehicles. Li-ion is extracted from two different sources. The first source is from water brine basins under the ground which contain the lithium ions which are pumped up and extracted by evaporating the water. The remaining solution continues to further refining. The second method is from ore mining where it is extracted from the rock and further processed. Additional minerals such as nickel, cobalt, manganese, and graphite are necessary to produce the battery. The actual battery production is extremely energy intensive containing many parts which are shipped form all around the world. During the use of the

batteries there are no direct emissions, however depending on the source of the electricity there are indirect emissions. For example, electrically charging the batteries where the electricity originates from a coal power plant will have considerably more emissions than originating from renewable sources. A very small share of ships use li-ion batteries for propulsion in the maritime industry. Ships that do use batteries as energy carrier are generally ferries that travel a fixed short distance. Batteries can also be useful for non-propulsive uses such as peak shaving where the energy load of the ship is highly inconsistent. Therefore only using the battery during infrequent times when the electrical load demanded is higher than the installed electrical power is a good solution. Li-ion batteries are extremely harmful to the environment if not disposed properly as they contain poisonous minerals. These toxic minerals mines have also been associated to child labour, birth defects, fresh water contamination, and extreme land use.

Electricity in LIB has a contained volumetric energy density ($\rho_{V\ E\ con}$) of 0.22 MJ/L and a contained gravimetric energy density ($\rho_{G\ E\ con}$) of 0.33 MJ/kg [138]. Together, the contained density (ρ_{con}) is 0.67 kg/L.

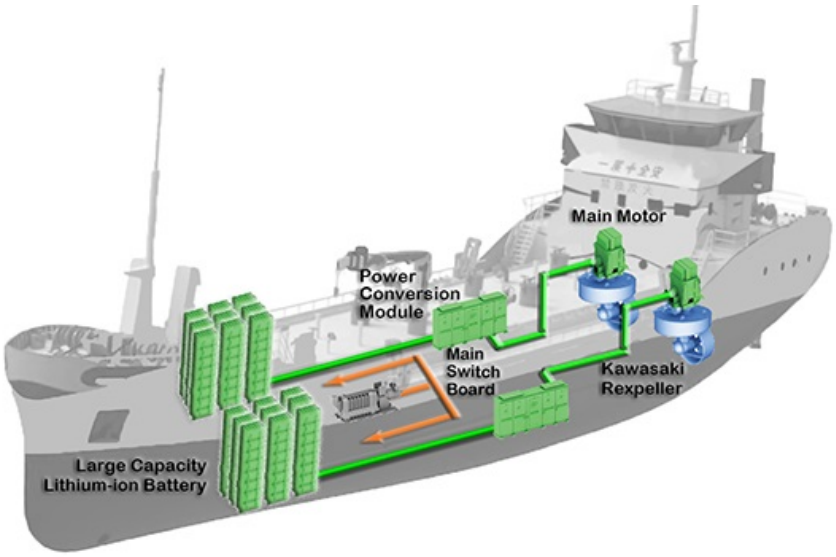

Figure 2.6: Generalized Li-ion battery power plant system [78]

Li-ion battery power plant system
A li-ion battery power plant contains a few major components. The main switchboard is the center of the whole system. Through this component the batteries are charged through a cable from ashore. The discharging of the batteries to supply energy to all the consumers also passes through the main switchboard. The battery stack contains a battery management system and cooling fans. Moreover, the largest energy consumer is the electric main motor which drives the propeller.

Power plant components and total efficiency Lithium-ion batteries are subjected to energy losses due to self discharging and heat loss, thus having an overall average efficiency of 92% [145]. The total losses in the main switchboard are from the average electrical distribution losses at 0.45%, the average losses due to transforming at 1.05%, and the average converting losses at 2% [75]. Finally the electric motor has an average load loss of 3.5% [75]. The total li-ion battery power plant efficiency (η_{PP}) comes down to 85.70%. Additionally to main engine power, the auxiliary power (PP_{aux}) is estimated to be 1% of the main engine power to drive all the components necessary for the power plant [34].

2.1.7. Overview energy carrier types and power plants

The energy carriers and their accompanying power plants that are going to be used in the ship powering assessment have been presented in the previous sections. Fuel oil, methanol, and LNG are converted to mechanical energy in the internal combustion engine. Therefore they have direct emissions. Hydrogen and ammonia are first converted to electrical energy through an SOFC and thereafter converted to

mechanical energy by an electrical motor. The li-ion batteries do not need any converting as the electrical energy is stored within them. The electrical energy can be instantly converted to mechanical power through the electric motor. The power plants containing the internal combustion engine have a similar power plant efficiency as there no to minor components causing energy losses. The energy carriers that contain an electric motor in their configuration are all affected by the losses in the switch board, which are assumed to be the same regardless of the energy carrier. Therefore the energy carrier losses and the fuel cell efficiency play an important role on the total power plant efficiency respectively. The SOFC has a significantly higher auxiliary power necessity as the fuel cell operates at a high temperature needing a high cooling power. The resulting total power plant efficiencies, minimal auxiliary power necessities and energy carrier densities are displayed in table 2.2. Additionally the volumetric ($\rho_{V\ E}$) and gravimetric ($\rho_{G\ E}$) energy densities of the energy carrier types in the contained and uncontained form are displayed as well. All the densities and efficiencies are necessary for the powering impact assessment and the environmental impact assessment.

Table 2.2: Overview (A)MEC type densities and power plant efficiencies

	Power plant		Contained			Uncontained		
	η_{PP} -	PP_{aux} -	$\rho_{V\ E\ con}$ MJ/L	$\rho_{G\ E\ con}$ MJ/kg	ρ_{con} kg/L	$\rho_{V\ E\ uncon}$ MJ/L	$\rho_{G\ E\ uncon}$ MJ/kg	ρ_{uncon} kg/L
Fuel oil (original)	*49.34%	**5%	33.20	29.65	1.12	35.70	41.00	0.87
Methanol	49.34%	3%	13.83	15.67	0.88	15.60	19.90	0.78
LNG	48.55%	3%	13.37	28.38	0.47	22.37	49.20	0.45
Liq. hydrogen	43.88%	11%	4.60	11.70	0.39	7.55	120.00	0.06
Ammonia	51.33%	11%	9.45	11.70	0.81	12.70	22.00	0.58
Elec. + LIB	85.70%	1%	0.22	0.33	0.67	2.98	0.50	5.96

* 41% for pure MDO in 4-stroke diesel engines
** 1% for pure MDO in 4-stroke diesel engines

2.1.8. Sensitivity analysis power plant efficiencies

The total power plant efficiency is the product sum of the efficiencies of the power plant components. Therefore the decision of selecting the average from an efficiency range for a single component can influence the total power plant efficiency. In the fuel oil and methanol power plant configurations, it was considered that only the ICE contributes to the total power plant efficiency. Therefore the uncertainty for the fuel oil and methanol power plant efficiency calculation is zero. However, in the other power plants there are more components contributing to the total power plant efficiency. The power plant efficiencies are calculated for the pessimistic scenario with the components containing the lowest efficiencies and for the optimistic containing the highest efficiencies. Only in the case of the hydrogen power plant where the permeation rate of 1% loss per day is used, does the pessimistic scenario account for every five weeks (35 days) of bunkering and optimistic scenario account for every three weeks (21 days) of bunkering. The power plant efficiency ranges are displayed in table 2.3. The lithium ion battery power plant has the highest uncertainty due to the largest efficiency spread.

Table 2.3: Sensitivity marine power plant efficiencies

Energy carrier	Average efficiency	Pessimistic	Optimistic	Spread
Fuel oil	49.34%	49.34%	49.34%	0.00%
Methanol	49.34%	49.34%	49.34%	0.00%
LNG	48.55%	47.86%	49.24%	0.69%
Hydrogen	33.11%	29.80%	36.78%	3.67%
Ammonia	51.33%	49.56%	53.14%	3.58%
Li-ion battery	85.70%	76.46%	95.47%	9.77%

2.2. Ship types and design aspects/trends

Bulk carriers, tankers and container ships together account for 85% of the global seagoing merchant vessels of 100 GT and above in 2021 [129]. These ship types must therefore comply with the EEDI, EEXI and CII regulation. In addition, trailing suction hopper dredgers (TSHD) are also included in the research to represent the non merchant vessels and for the interest of Vuyk Engineering. Currently ships such as TSHDs do not have to comply with these regulations. However, in order to fulfill the goal of having zero carbon emissions before the end of the century in the maritime industry, they will eventually also have to comply. In addition, a TSHD is a specialty work ship and therefore their operational mode is completely different from merchant ships. Such specialty and non-merchant ships are underrepresented in studies concerning sustainability as they are exempt from IMO's emission regulations. A high detailed data sample of twelve ships per ship type is acquired to represent bulk carriers, tankers, container ships and TSHDs in the powering impact assessment. The twelve sample ships per ship type do not represent the design aspects of a ship type enough and therefore a larger data set is acquired for the dimension trends.

Sampled ships Highly detailed information of ships is not easily to come by publicly. Therefore the data for the sampled merchant ships is acquired through the magazine Significant Ships by The Royal Institution of Naval Architects. The 2015 to the 2020 edition are openly available for Marine Technology students of the Delft University of technology. Significant Ships is an annual publication of the 50 most innovative and important commercial ships launched in the year of the edition of at least 100 m in length. In addition, a detailed technical drawing is mostly included of each ship. The data of the TSHDs is acquired through Vuyk Engineering as most of the sample ships have been fully or partly designed by Vuyk Engineering. Additionally, to verify the data from Significant Ships and Vuyk Engineering, the World Fleet Register by Clarksons is used. This is done because the data from Significant Ships is submitted voluntarily by shipbuilders, designers or owners and can be altered or classified [124]. The World Fleet Register by Clarksons is the market leading online vessel reference tool and provides comprehensive, authoritative and timely information in a powerful and user friendly format. However, it contains less or inconsistent information compared to the Significant Ship entries.

Design aspect ship type Clarksons World Fleet Register has also been used to determine the length-beam (L/B) ratios per ship type. This is necessary to constrain the design impact assessment to adhere to design aspects of the ship type. In section 1.4.3 it was determined that the additional volume and weight can best be applied in a specific way to strive for the lowest propulsion power possible. Lindstad et al. determined that higher length-beam ratios for ships with equal carrying capacity are the most energy efficient [89]. Additionally, Liu and Pananikolauo determined that the added ship resistance decreases for lower Froude numbers, which can be achieved by increasing the length of a ship [92]. Therefore lengthening a ship to what is deemed plausible and thereafter increasing the beam to accommodate for the additional volume and weight is the considered method. What is deemed 'plausible' is considered through a maximum length-beam ratio trend. The merchant ship trend data sets from Clarksons are filtered to correspond to the sampled ships from Significant Ships and therefore they had to be built between 2015 and 2020, and be at least 100 meters in length. The TSHD data set is filtered to contain ships that were built after the year 2000 and be at least 50 meters in length. The time constraint for TSHDs is to adhere to the length-beam ratios of ships still in service. The length constraint is to adhere to TSHDs that are primarily intended for coastal services rather than ports and rivers. The results of the data gathered for the sample ships and the length-beam ratios per ship type are presented in the following sections.

The linear equation parameters are selected to intersect the highest length-beam ratio of a highly dense coordinate (dark blue) at higher ship lengths. The slope is adjusted in order for the highest length-beam ratios of a highly dense coordinates at lower ship lengths to be lower than the line. This approach is chosen as it is expected that ships with higher lengths are less or not capable of being lengthened further compared to widening.

2.2.1. Bulk carriers

Bulk carriers, also known as bulkers, are merchant vessels which transport dry non-packed cargo in its cargo holds, such as ores, coal, and grains. Each hold has a hatch on top to prevent containment from the external environment. Bulk carrier often are categorized by their maximum size to fit through a specific

canal or lock. Some bulkers have their own cranes on deck to load and unload their cargo and therefore being independent of terminal equipment in ports. Bulk carriers generally travel fully loaded to a port, unload all cargo and travel unloaded (in ballast) to the next port to be fully loaded again. Their voyage distribution is therefore ∼40% of the time in loaded condition, ∼35% of the time in ballast condition, and ∼25% of the time in port [9]. The service speed of bulk carriers in loaded condition is 14 ± 0.5 knot for all sampled ships. The sampled ships for this research are presented in table 2.4. A typical bulk carrier with cranes from the sampled ships is displayed in the figure below.

Table 2.4: Bulk carrier sample ships

Name	IMO
CIELO D'ITALIA	9539274
TRUE LOVE	9697143
VENTURE GOAL	9670731
RB JORDANA	9730816
GREAT INTELLIGENCE	9800623
YUAN HE HAI	9806873
SAO DIANA	9822255
ADMIRAL SCHMIDT	9838838
CHINA STEEL LIBERTY	9832975
DIETRICH OLDENDORFF	9860350
SARA	9837119
BEATE OLDENDORFF	9853022

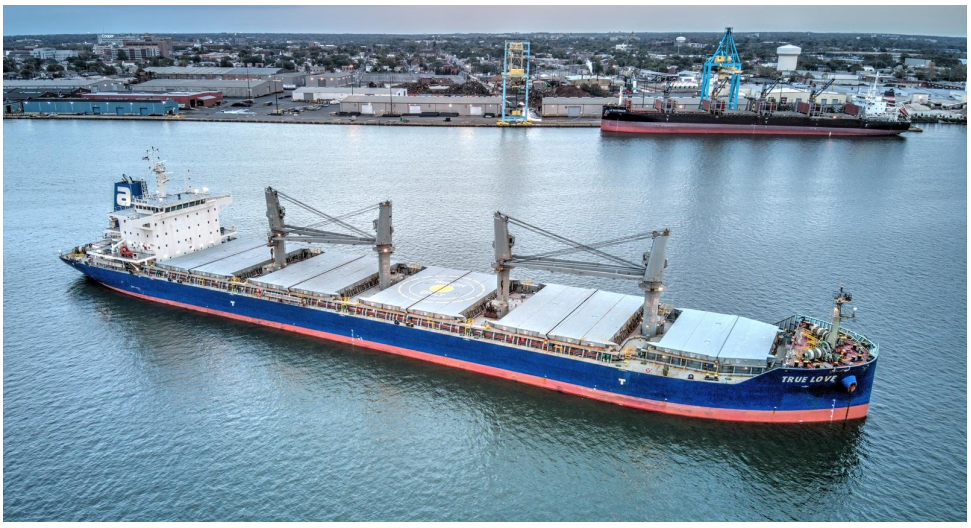

Bulk carrier (TRUE LOVE) with cranes [83]

Length-beam ratio trend bulk carriers

There are 2823 entries which fulfill the filter criteria for bulk carriers from the World Fleet Register by Clarksons. The length overall ranges between 130.00 m and 362.00 m. The beam ranges between 20.20 m and 65.00 m. As the length and beam are going to be adjusted for the additional volume for an alternative marine energy carrier, the length overall over beam per length overall (Loa/B per Loa) of bulk carriers is plotted in figure 2.7. The blue dots represent the Clarksons entries of which the darker the color represents a higher density. The red squares represent the sampled bulk carriers from table 2.4. The maximum Loa/B for bulk carriers has been set to equation 2.1 and it is displayed in figure 2.7 as the dashed blue line.

$$L_{OA}/B_{\,MAX,\,BULKERS} = -0.0125858 \cdot L_{OA} + 10.1251 \quad [-] \tag{2.1}$$

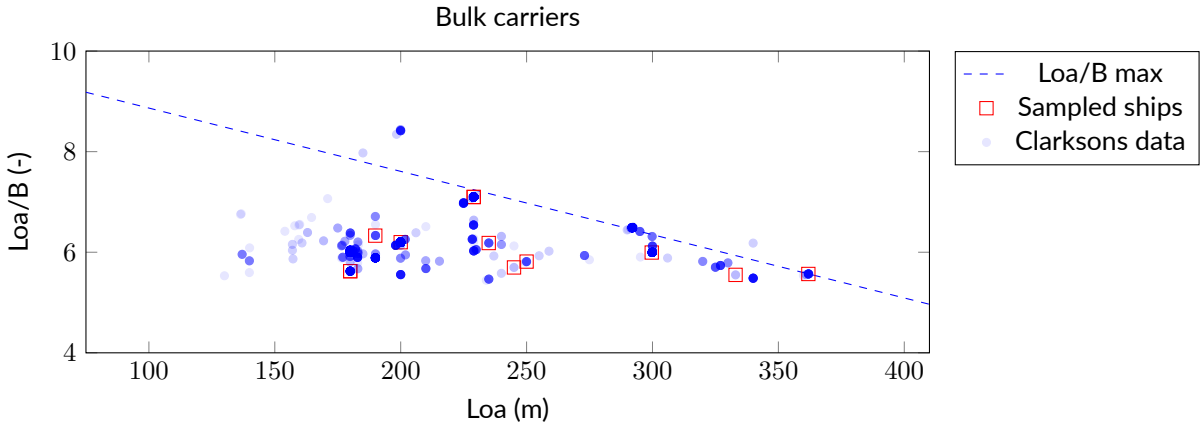

Figure 2.7: Length-beam ratio of Clarksons data and sampled bulk carriers

2.2.2. Tankers

Tankers are merchant ships which transport liquid cargo in pressure tight cargo holds and can be divided into sub-types for their unique property within their fluid state: oil tankers, chemical tankers, gas carriers and combination carriers [140]. Due to the liquid state of the cargo, the fluid can be pumped into the vessel. Oil tankers carry a range of oil types such as crude to petroleum derivatives. Heavy petroleum products are highly viscous and therefore need to be heated to become less viscous in order to be pumped. Therefore tankers carrying heavy oil product have many heating elements in their holds. Chemical tankers carry highly toxic chemicals and therefore have special safety features to minimize the risk of the chemicals escaping. Gas carriers transport liquefied gasses that are cooled to extremely low temperatures. Chemical tankers and gas carriers both have inert gas plants on board which mostly produce nitrogen from the air. The nitrogen gas flows through double walled piping and other spaces to minimize the risk of the product igniting or reacting if it escapes. Tankers generally travel fully loaded to a port, unload all cargo and travel unloaded (in ballast) to the next port to be fully loaded again. This is similar to bulk carriers. The voyage distribution of tankers is dependent on its size, unlike bulk carriers. For instance, a Handysize tankers spend $\sim$30% of the time in loaded condition, $\sim$15% of the time in ballast condition, and $\sim$55% of the time in port [9]. A Suezmax tankers spend $\sim$35% of the time in loaded condition, $\sim$35% of the time in ballast condition, and $\sim$30% of the time in port [9]. Larger tankers spend more time in laden, more time in ballast, and less time in port. The service speed of tankers in loaded condition is 14 ± 1 knot which is similar to bulk carriers. The sampled ships for this research are presented in table 2.5. A typical tanker from the sampled ships is displayed in the figure below.

Table 2.5: Tankers sample ships

Name	IMO
ASPHALT SPLENDOR	9763332
D&K ABDUL RAZZAK KHALID ZAID	9700213
KMARIN RESPECT	9683001
HERON	9730086
WHITE STAR	9799109
CABO VICTORIA	9778674
IBERIAN SEA	9815604
NAUTICAL DEBORAH	9794836
HILI	9851830
BOW ORION	9818515
SOLAR SHARNA	9877614
TOVE KNUTSEN	9868376

Tanker (ASPHALT SPLENDOR) [119]

Length-beam ratio trend tankers
There are 1299 entries which fulfill the filter criteria for tankers from the World Fleet Register by Clarksons. The length overall ranges between 99.71 m and 339.50 m. The beam ranges between 16.00 m and 60.04 m. As the length and beam are going to be adjusted for the additional volume for an alternative marine energy carrier, the length overall over beam per length overall (Loa/B per Loa) of tankers is plotted in figure 2.8. The blue dots represent the Clarksons entries of which the darker the color represents a higher density. The red squares represent the sampled tankers from table 2.5. The maximum Loa/B for tankers has been set to equation 2.2 and it is displayed in figure 2.8 as the dashed blue line.

$$L_{OA}/B_{\,MAX,\,TANKERS} = -0.0080163 \cdot L_{OA} + 8.3795 \quad [-] \tag{2.2}$$

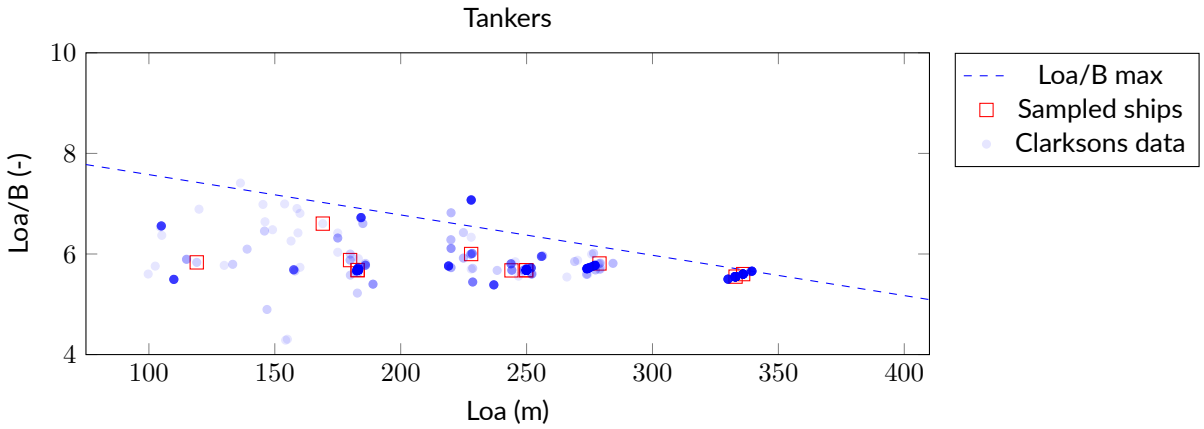

Figure 2.8: Length-beam ratio of Clarksons data and sampled tankers

2.2.3. Container ships
Container ships are merchant vessels which transport fixed sized metal box containers that are stowed in its holds below deck and on top of the hatch covers on deck. The containers comply with an ISO standard for their size measurements in order to improve intermodal transport for trucks, trains and ships. The containerization makes handling of cargo standardized and requires less specialization. A container ship's capacity is measured in the amount of twenty foot equivalent units (TEU). The containers are fitted on top of each other, mostly assisted by cell guides for easy stacking. Some containers are climate controlled or refrigerated (reefers) for perishable cargo. These containers have generators to produce electricity for the air conditioner, however on board a ship there are designated spaces for these reefers to be plugged in. Some container ships have cranes on the deck which gives the advantage of being able to sail to ports

which do not have a container terminal availability. Container ships do not travel fully loaded and fully unloaded because empty containers must be transported back to the where export is higher than import. Their voyage distribution is therefore ∼70% of the time in loaded condition, ∼0% of the time in ballast condition, and ∼30% of the time in port [9]. The service speed of container ships in loaded condition is 21 ± 2 knots for all sampled ships, which is significantly higher than bulkers and tankers. The sampled ships for this research are presented in table 2.6. A typical container ship from the sampled ships is displayed in the figure below.

Table 2.6: Container sample ships

Name	IMO
AL MURABBA	9708837
CMA CGM ARKANSAS	9722651
CAPE AKRITAS	9706190
MAERSK BERMUDA	9697014
EVER BLISS	9786932
OOCL HONG KONG	9776171
DANIEL K INOUYE	9719056
SABRE TRADER	9817884
MSC JOSSELINE	9842061
SEATRADE GREEN	9810915
KMTC SEOUL	9882205
YM CELEBRITY	9864502

Container ship (EVER BLISS) [121]

Length-beam ratio trend container ships

There are 788 entries which fulfill the filter criteria for container ships from the World Fleet Register by Clarksons. The length overall ranges between 99.71 m and 339.50 m. The beam ranges between 16.00 m and 60.04 m. As the length and beam are going to be adjusted for the additional volume for an alternative marine energy carrier, the length overall over beam per length overall (Loa/B per Loa) of container ships is plotted in figure 2.9. The blue dots represent the Clarksons entries of which the darker the color represents a higher density. The red squares represent the sampled container ships from table 2.6. The maximum Loa/B for container ships has been set to equation 2.3 and it is displayed in figure 2.9 as the dashed blue line.

$$L_{OA}/B_{\,MAX,\,CONTAINER} = 0.0047341 \cdot L_{OA} + 5.8620 \quad [-] \tag{2.3}$$

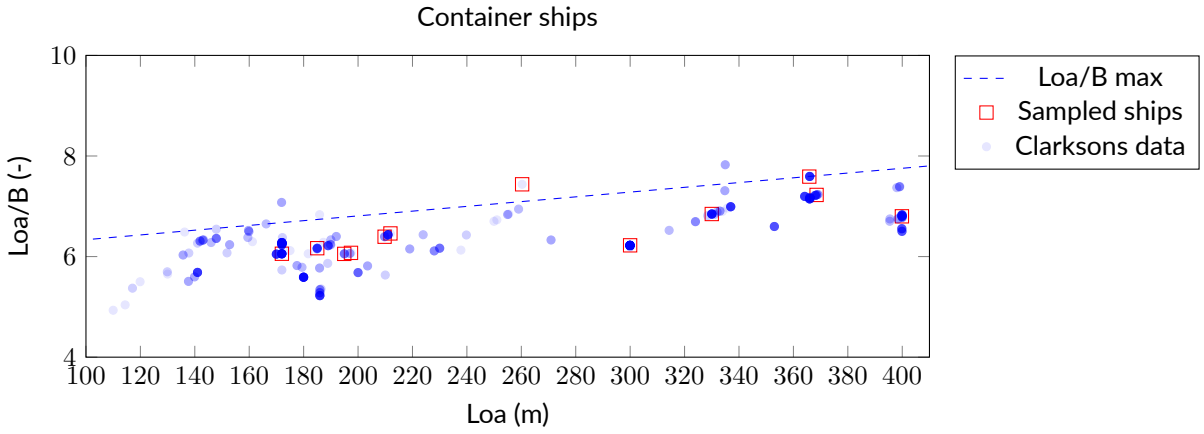

Figure 2.9: Length-beam ratio of Clarksons data and sampled container ships

2.2.4. Trailing suction hopper dredgers

Trailing suction hopper dredgers (TSHD) are self propelled ships which trail the bottom of a body of water with a suction pipe and a drag head to extract the bottom soil material. The soil and water mixture is then pumped into the hold (hopper) where the material settles to the bottom while the redundant water flows over board. The material in the hoppers can be dumped through doors on the bottom, pumped through a piping system connected to the pump ashore system on the bow, spouted out through a nozzle on the bow (rainbowing), or even pumped back through the trailing pipe for precision dumping. TSHD are especially used to deepen and maintain waterways, the reclamation of land, and beach nourishment. They generally work within 15 nautical miles from shore and do not have a common pattern in their voyage distribution like the merchant ships. The service speed of TSHD in loaded condition is 17 ± 2 knots for all sampled ships, however in trailing condition the speed is between 2 and 3 knots [135]. The sampled ships for this research are presented in table 2.7. A typical trailing suction hopper dredger from the sampled ships is displayed in the figure below.

Table 2.7: TSHDs sample ships

Name	IMO
BONNY RIVER	9810939
CHARLES DARWIN	9538079
CONGO RIVER	9574523
GALILEO GALILEI	9872365
HAM 318	9229556
INAI KENANGA	9568782
LEIV EIRIKSSON	9429584
PRINS DER NEDERLANDEN	9263899
QUEEN OF THE NETHERLANDS	9164031
VASCO DA GAMA	9187473
VOX MAXIMA	9454096
WILLEM VAN ORANJE	9449065

Trailing suction hopper dredger (QUEEN OF THE NETHERLANDS) [111]

Length-beam ratio trend TSHD
There are 139 entries which fulfill the filter criteria for TSHDs from the World Fleet Register by Clarksons. The length overall ranges between 99.71 m and 339.50 m. The beam ranges between 16.00 m and 60.04 m. As the length and beam are going to be adjusted for the additional volume for an alternative marine energy carrier, the length overall over beam per length overall (Loa/B per Loa) of TSHD is plotted in figure 2.10. The blue dots represent the Clarksons entries of which the darker the color represents a higher density. The red squares represent the sampled TSHDs from table 2.7. The maximum Loa/B for TSHD has been set to equation 2.4 and it is displayed in figure 2.10 as the dashed blue line.

$$L_{OA}/B_{\,MAX,\,TSHD} = -0.0068975 \cdot L_{OA} + 7.2756 \quad [-] \tag{2.4}$$

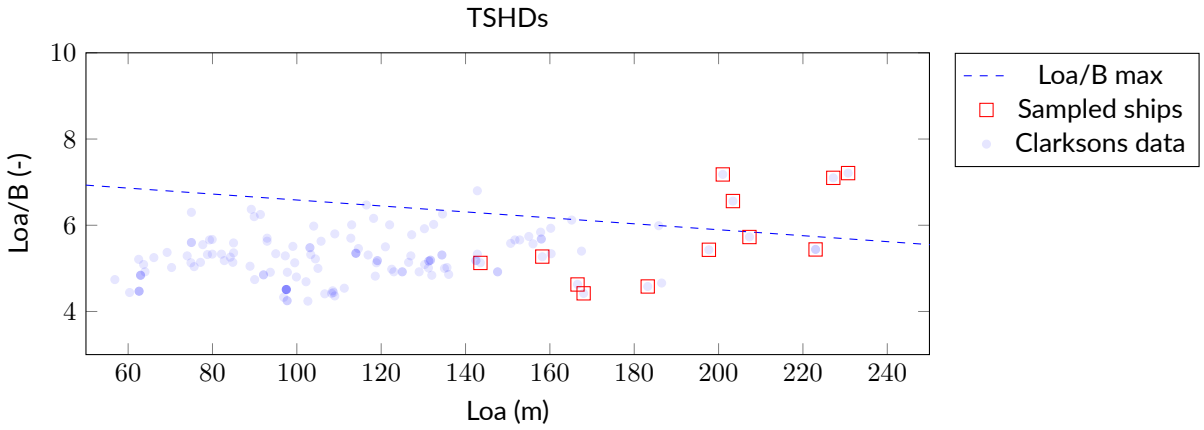

Figure 2.10: Length-beam ratio of Clarksons data and sampled TSHD

2.2.5. Parameters sampled ships

To approximate the resistance, propulsion powering and design impact of the ship powering impact assessment, the parameters of the sampled ships in table 2.8 are acquired. The data is gathered through the magazine Significant Ships, from Vuyk Engineering and from Clarksons Fleet Register. Not all the parameters are used in the design impact, but are also used to compare the original ship geometry and weight to the new. The data of the parameters of the sampled ships are displayed per ship type in appendix A.

Table 2.8: Sampled ship parameters

Parameter	Symbol	Unit
Length overall	L_{OA}	m
Length between perpendiculars	L_{PP}	m
Beam moulded	B	m
Depth moulded	D	m
Draft	T	m
Gross tonnage	GT	gt
Deadweight tonnage	DWT	t
Ship speed	V_S	kt
Diameter propeller	D_P	m
Fuel oil bunker volume	V_{BUNK}	m^3
TEU capacity	n_{TEU}	-
Cargo capacity volume	V_{CC}	m^3
Total main engine power (MCR)	P_{ME}	kW
Number of main engines	k_{ME}	-
Total auxiliary engine power (MCR)	P_{AE}	kW
Total shaft generator/PTO power	P_{PTO}	kW
Bulbous bow presence	BB	-
Number of propellers	k_p	-
Number of bow thruster tunnels	n_{TH}	-

To assess the volume impact of a ship, the overall internal volume (V_{INT}) is calculated. The overall internal volume can be calculated using the inverse formula for the calculation of the given gross tonnage (GT). The formula for the gross tonnage in equation 2.5 is from the International Convention on Tonnage Measurement of Ships [66]. The inverse formula is therefore given in equation 2.6 in which *W* is the Lambert function.

$$GT = V_{INT} \cdot (0.2 + 0.02 \cdot \log_{10}(V_{INT})) \quad [gt] \tag{2.5}$$

$$V_{INT} = \frac{50 \cdot ln(10) \cdot GT}{W(5 \cdot 10^{14} \cdot ln(10) \cdot GT)} \quad [m^3] \tag{2.6}$$

The lightweight ship (m_{LIGHT}) is also assessed to determine the weight impact of a ship and calculated according to equation 2.7. The lightweight ship is equal to the gravimetric displacement (Δ) minus the deadweight tonnage (DWT). The gravimetric displacement is equal to the volumetric displacement multiplied by the density of seawater (ρ_{sw}). The volumetric displacement is calculated in the resistance approximation method in section 3.1.1 according to equation equation 3.6.

$$\begin{aligned} m_{LIGHT} &= \Delta - DWT \quad [t] \\ &= \nabla \cdot \rho_{sw} - DWT \quad [t] \end{aligned} \tag{2.7}$$

The energy operational profiles of TSHDs is considerably diverse compared to shipping vessels. The main engines generally deliver power to other power consumers than just the propeller. In some cases the main engines drives the propeller, dredging sand pump and a generator all at the same time or separately through a gearbox. Therefore the total auxiliary engine power (P_{AE}) is determined to be the total installed engine power ($P_{TOT\ INSTALLED}$) minus the calculated main engine power (MCR) ($P_{ME\ CALC}$) according to equation 2.8. The total installed power is sourced from Clarksons. The generator/PTO power (P_{PTO}) therefore must equal zero, however this does not change the usage of the sample parameter as it is used to calculate the total auxiliary engine power.

$$P_{AE} = P_{TOT\ INSTALLED} - P_{ME\ CALC} \quad [kW] \tag{2.8}$$

2.2.6. Overview maximum length-beam trend ratios per ship type

The length-beam ratio trends per ship type is constructed using the World Fleet Register by Clarksons Research [24]. The Clarksons data is filtered for ships $\geq$ 100 meters in length and built between 2015 and 2020 to coincide with the Significant Ships entry conditions for the commercial vessels. The length-beam ratios of the Clarksons ships and Significant Ships data are displayed in figures 2.7, 2.8, 2.9, and 2.10 for bulk carriers, tankers, container ships, and TSHDs respectively. The maximum length-beam ratio constraint formula is displayed in equation 2.9 and the parameters per ship type are displayed in table 2.9. The linear equation parameters are to intersect the highest length-beam ratio of a highly dense coordinate (dark blue) at higher ship lengths. The slope is adjusted in order for the highest length-beam ratios of a highly dense coordinates at lower ship lengths to be lower than the line. This approach is chosen as it is expected that ships with higher lengths are less capable of being lengthened further compared to widening. The maximum length-beam ratio trends will be used specifically in the common design impact assessment as a part of total powering impact assessment.

$$L_{OA}/B_{MAX,\ ship\ type} = a \cdot L_{OA} + b \quad [-] \tag{2.9}$$

Table 2.9: Maximum length-beam ratio contraint parameters per ship type

Ship type	a	b
Bulk carriers	-0.0125858	10.1251
Tankers	-0.0080163	8.3795
Container ships	0.0047341	5.8620
TSHDs	-0.0068975	7.2756

3

Ship powering impact assessment

The main objective of the ship powering impact assessment is to determine the powering increase caused by the AMECs with the same operational requirements. The constant operational requirements are defined by constraining the physical conditions related to the original ship volume and weight, and the varying energy carrier volume and weight. The total powering impact assessment is done on each sampled ship of the four ships types using each of the six energy carrier types. The total powering impact assessment model consists of three calculation sub-models. The first sub-model calculates the ship *resistance*. The second sub-model calculates the *propulsion power*. The third sub-model calculates the additional bunker volume and weight and generates a *design impact* model. The additional bunker volume and weight includes the storage tank and necessary bunker handling systems. The resistance calculation model is according to the Holtrop & Mennen method compiled by Birk [13]. The propulsion power calculation model is according to the propulsion chain method by Klein Woud & Stapersma [81]. The additional bunker volume and weight calculation is based on the constant operational requirements and modeled based on the energy efficient ship design characteristics from section 1.4.

In this chapter, first the full model is described as an iterative process in the form of a spiral using the sub-models. Additionally the sub-models are described into higher detail for their required input parameters and procedure. Throughout the third sub-model detailed description, the bulk carrier Cielo D'Italia (IMO 9539274) is used as an example to understand the process more clearly. The Cielo D'Italia is the first in the list of the sampled bulk carriers and its detailed information is displayed in table A.1 in appendix A. For the first and second sub-model, only the total ship resistance and main engine brake power are given respectively, because these models are generally understood in the ship design industry. Finally the results are presented of the powering impact of an energy carrier type on a ship type.

3.1. Model description

In the simplest explanation, the total ship powering impact assessment model is comparable to the ship design spiral in section 1.4.2. This is because of the iterative sizing issue explained in section 1.4.2. The powering impact assessment model is displayed in figure 3.1. The model starts with the original (0) ship design parameters which already fulfils all the operational requirements. With the parameters, the original resistance is approximated using the resistance calculation sub-model. With the original resistance, the original propulsion powering is approximated in the power approximation sub-model. Thereafter the first step of the design generation model is conducted by substituting the fuel oil (1) with an AMEC based on equal effective energy. The additional bunker space is applied to the original design by first lengthening, thereafter heightening, and if necessary widening. With the first revision design, the first revision parameters necessary to conduct the resistance and power approximation sub-model. With the first revision powering impact results, the second step of the design impact model is conducted by upscaling the AMEC bunkering (2) based on the first revision powering impact results. Once again, the design procedure is applied in the same manner and the final ship parameters, resistance and powering are determined using the sub-models. In theory the total powering impact assessment iterative process can be repeated infinitely until the powering impact and design are in equilibrium. However, for simplicity the assessment model goes through two design generation cycles.

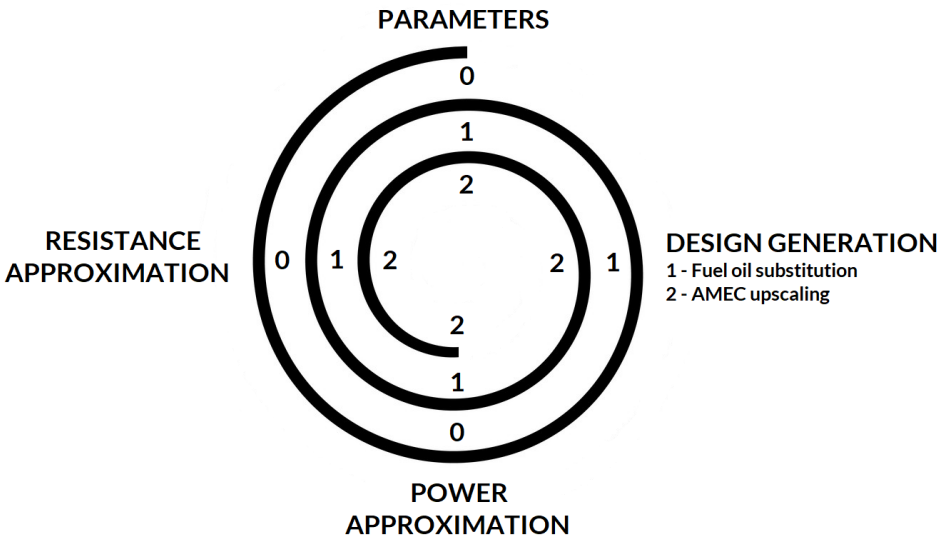

Figure 3.1: Ship powering impact assessment model

3.1.1. Resistance sub-model

The approximate resistance prediction method by Holtrop and Mennen is considered to be efficient and accurate for determining the required propulsive power [103]. The method is based on a regressional statistical analysis from random model tests and full scale ship trials [57]. The method is established on the basis of five papers by Holtrop alone or Holtrop and Mennen together which are presented in table 3.1. Some papers are re-assessments of previous papers to further increase the accuracy of the approximation. The resistance and powering calculation process is based on a wide range of existing mono-hull ships and therefore the method is not applicable to atypical vessels. In order to compute the resistance approximation method, a limited amount of required design parameters are necessary. There are also optional parameters for additional ship characteristics such as bilge keels, stabilizer fins and bow thruster tunnels near the water surface. The required and optional parameters can be found in table 3.2.

Table 3.1: The papers necessary for the Holtrop & Mennen resistance and power prediction method

Title	Author	Year	Reference
A statistical analysis of performance test results	J Holtrop	1977	[55]
A statistical power prediction method	J Holtrop & GGJ Mennen	1978	[56]
An approximate power prediction method	J Holtrop & GGJ Mennen	1982	[57]
A statistical re-analysis of resistance and propulsion data	J Holtrop	1984	[53]
A statistical resistance prediction method with a speed dependent form factor	J Holtrop	1988	[54]

As mentioned, some estimation equations have been re-assessed for higher accuracy, therefore making the method puzzling to find the most recent equations. Luckily Lothar Birk dedicated a whole chapter in his book *Fundamental of Ship Hydrodynamics: Fluid Mechanics, Ship Resistance and Propulsion* with all the necessary equations present and in their newest form [13]. The Holtrop & Mennen method is extremely suitable in this situation due to the small amount of parameters necessary [96]. The assessment can reasonably estimate the resistance and powering for the following conditions according to equations 3.1, 3.2 and 3.3 according to Birk [13].

$$F_n = \frac{V_s}{\sqrt{g \cdot L_{WL}}} \leq 0.45 \quad [-] \tag{3.1}$$

$$0.55 \leq C_P = \frac{C_B}{C_M} \leq 0.85 \quad [-] \tag{3.2}$$

$$3.9 \leq \frac{L_{WL}}{B} \leq 9.5 \quad [-] \tag{3.3}$$

With the input parameters, the Holtrop & Mennen method computes the total ship resistance ($\mathbf{R_{TOT}}$) as a sum of all the resistance components, which are:

- Frictional resistance ($\mathbf{R_F}$)
- Appendage resistance ($\mathbf{R_{app}}$)
- Wave making and wave breaking resistance ($\mathbf{R_W}$)
- Pressure resistance due to bulbous bow near water surface ($\mathbf{R_B}$)
- Pressure resistance due to immersed transom ($\mathbf{R_{TR}}$)
- Model-ship correlation resistance ($\mathbf{R_A}$)
- Air resistance ($\mathbf{R_{AA}}$)

Required input
The resistance approximation method by Holtrop & Mennen requires a certain amount of ship parameters, listed in table 3.2. These parameters are known to the ship designer in the initial design phase. However most of the parameters are unknown to the public and therefore are approximated. The approximation formulas for these required input parameters are given within the Holtrop & Mennen method, or in Lothar Birk's chapter, or found in other literature. After table 3.2 the approximation formulas from the table are presented and described. All the required input parameters are either already given from the sampled ship parameters or approximated using these sampled ship parameters. The sampled ship parameters per ship type are located in appendix A.

Table 3.2: Required input parameters for the Holtrop-Mennen resistance approximation method [13]

Parameter	Symbol	Unit	Value/Source
Length waterline	L_{WL}	m	Calculated according to equation 3.4 [a]
Moulded beam	B	m	Sampled parameter
Moulded mean draft	T	m	Sampled parameter
Moulded mean draft at aft	T_A	m	Assumed to be $T_A = T$ (Sampled parameter)
Moulded mean draft at fore	T_F	m	Assumed to be $T_F = T$ (Sampled parameter)
Block coefficient	C_B	-	Calculated according to equation 3.5 [b]
Volumetric displacement	∇	m^3	Calculated according to equation 3.6
Midship section coefficient	C_M	-	Calculated according to equation 3.7 [b]
Prismatic coefficient	C_P	-	Calculated according to equation 3.8 [c]
Waterplane area coefficient	C_{WP}	-	Calculated according to equation 3.9 [d]
Longitudinal center of buoyancy	lcb	%	Calculated according to equation 3.10 [c]
Area of ship above waterline	A_V	m^2	Calculated according to equation 3.11
Immersed transom area	A_T	m^2	Calculated according to equation 3.16
Transverse area of bulbous bow	A_{BT}	m^2	Calculated according to equation 3.17 [e]
Height of center of A_{BT}	h_B	m	Calculated according to equation 3.18
Propeller diameter	D_p	m	Sampled parameter
Stern shape parameter	C_{stern}	-	Normal shape for simplicity and constant
Ship design speed	V_s	m/s	Sampled parameter
Wetted surface area	S	m^2	Calculated according to equation 3.19
Half angle of waterline entrance	i_E	$^\circ$	Calculated according to equation 3.21
Wetted surface area appendages	S_{app}	m^2	Calculated according to equation 3.24
Number of bow thruster tunnels	n_{TH}	-	Sampled parameter
Diameter of bow thruster tunnel	d_{TH}	m	Calculated according to equation 3.31
Bulbous bow presence	BB	Yes/No	Sampled parameter
Number of propellers	k_P	1 / 2	Sampled parameter

[a] MAN Energy Solutions (2018) [94]
[b] Jensen (1994) [74]
[c] Guldhammer and Harvald (1974) [47]
[d] Schneekluth (1998) [113]
[e] Castro et al. (1997) [23]

$$L_{PP} = [0.96 - 0.98] \cdot L_{WL} \quad \approx \quad L_{WL} = \frac{L_{PP}}{0.97} \quad [m] \tag{3.4}$$

$$C_B = -4.22 + 27.8 \cdot \sqrt{F_n} - 39.1 \cdot F_n + 46.6 \cdot F_n^3 \quad [-] \tag{3.5}$$

The block coefficient formula in equation 3.5 is only applicable to shipping vessels. According to Vlasblom, the block coefficient for TSHDs lies between 0.78 - 0.85 and therefore the average of 0.815 is used [135].

$$\nabla = C_B \cdot L_{WL} \cdot B \cdot T \quad [m^3] \tag{3.6}$$

$$C_M = \frac{1}{1 + (1 - C_B)^{3.5}} \quad [-] \tag{3.7}$$

$$C_P = \frac{C_B}{C_M} \quad [-] \tag{3.8}$$

$$C_{WP} = \frac{1 + 2 \cdot C_B}{3} \quad [-] \tag{3.9}$$

$$lcb_{optimal} = -(0.44 \cdot F_n - 0.094) \quad [\% \quad w.r.t. \quad \frac{1}{2} L_{WL}] \tag{3.10}$$

The area of ship above the waterline in its projected speed direction (A_V) is approximated by equation 3.11. For simplicity, the deckhouse (A_{dh}) is approximated by multiplying the width by the height of the deckhouse (h_{dh}). The width is approximated as 75% of the moulded beam (B). The height of the deckhouse is calculated by using the SOLAS requirements of minimum bridge visibility [68], which is displayed in figure 3.2. The regulation states that the view of the sea surface from the bridge is not to be hidden by more than two times the length of the ship or 500 m, whichever is less. Using simple trigonometry rules for similar triangles, the main ship parameters, a forecastle height equal to twice the height of tween deck for a main public room (2.9 m) [142], and the bridge located at 15% of the overall length (L_{OA}), the minimum bridge height for visibility can be approximated. As this height is the minimum, an additional height of a tween deck will be added for trim and safety reasons. The trigonometry rule for similar triangles for ships less than 250 m is presented in equation 3.12 and for ships larger or equal than 250 m is presented in equation 3.14. The deckhouse height above the main deck for ships below 250 meters is equal to equation 3.13 and ships of 250 m and above equal to equation 3.15. This method is not fully accurate for container ships as the visibility from the bridge at the aft would be obstructed by the containers on top of the main deck. This would result in a higher bridge. However, the air resistance only contributes approximately for 2% of the total resistance [140], therefore the additional air resistance on top of this method for container ships is expected to have an even smaller effect on the total ship resistance. Accordingly, this method is also applied to container ships.

$$A_V = B \cdot (D - D_p) + 0.75 \cdot B \cdot h_{dh} \quad [m^2] \tag{3.11}$$

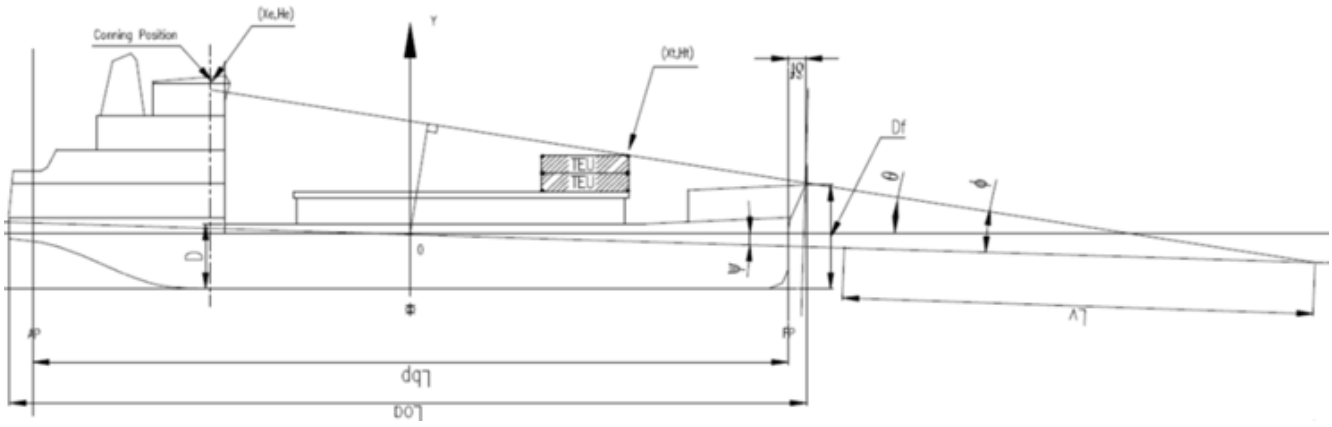

Figure 3.2: SOLAS bridge visibility law [99]

$$\frac{h_{dh} + D - D_p}{2 \cdot L_{OA} + 0.85 \cdot L_{OA}} = \frac{D - D_p + 2 \cdot 2.9}{2 \cdot L_{OA}} \tag{3.12}$$

$$h_{dh} \quad (L_{OA} < 250m) \quad = \frac{D - D_p + 2 \cdot 2.9}{2 \cdot L_{OA}} \cdot (2.85 \cdot L_{OA}) - D + D_p + 2.9 \quad [m] \tag{3.13}$$

$$\frac{h_{dh} + D - D_p}{500 + 0.85 \cdot L_{OA}} = \frac{D - D_p + 2 \cdot 2.9}{500} \tag{3.14}$$

$$h_{dh} \quad (L_{OA} \geq 250m) \quad = \frac{D - D_p + 2 \cdot 2.9}{500} \cdot (500 + 0.85 \cdot L_{OA}) - D + D_p + 2.9 \quad [m] \tag{3.15}$$

The immersed transom area is approximated by using the formula for the area of an oval $A = a \cdot b \cdot \pi$. Parameters a and b are the long and short radius of an oval respectively. Where the immersed transom area is half of the oval area, where a is estimated to be Half (50%) of the moulded beam (B) and b estimated to be an eighth (12.5%) of the draft (T).

$$A_T = \frac{1}{2} \cdot (0.5 \cdot B) \cdot (0.125 \cdot T) \cdot \pi \quad [m^2] \tag{3.16}$$

The bulbous bow is useful for reducing the wave making resistance for the condition 0.9 $\leq V/\sqrt{L} \leq$ 1.9 according to Wigley [143], which coincides with the Holtrop-Mennen acceptable conditions from equation 3.1. The transverse area of the bulbous bow (A_{BT}) from Castro et al. in equation 3.17 also contains a bulbous bow breadth coefficient (C_{BB}), where typical values are 0.170 $\leq C_{BB} \leq$ 0.200 [82]. For the reason that the minimum and maximum value are close to each other, the average is taken at 0.185 for C_{BB}. If a bulb is not present, the transverse area of the bulbous bow is set to zero.

$$A_{BT} = C_{BB} \cdot B \cdot T \cdot C_M \quad = \quad 0.185 \cdot B \cdot T \cdot C_M \quad [m^2] \tag{3.17}$$

The height of the center of the bulbous bow h_B must be less than $0.6 \cdot T_F$ according to Birk [13]. According to Ghani and Wilson there are three typical transverse bulbous bow shapes, seen in figure 3.3. The average h_B of all the three bulb types is equal to the center of the O-type bow. Therefore, for simplicity reasons, h_B will be set to half of the draft (T), which also fulfils the condition by Birk.

$$h_B = 0.5 \cdot T \quad [m] \tag{3.18}$$

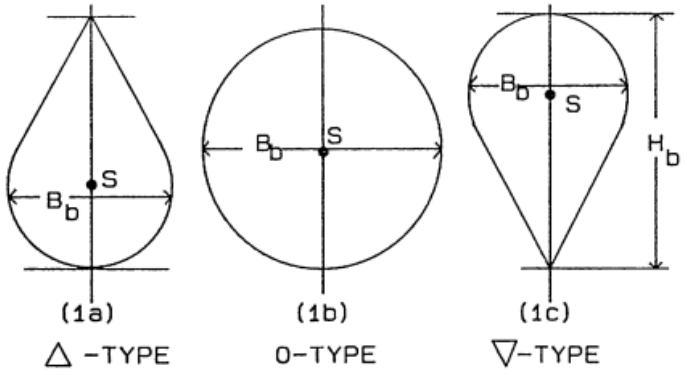

Figure 3.3: Typical bulbous bow transverse shapes [2]

The wetted surface area (S) according to Holtrop is calculated according to equation 3.19 [54]. An earlier version of the wetted surface area equation was first presented in a previous paper by Holtrop and Mennen in 1982, but was later updated for higher accuracy [54].

$$S = L_{WL} \cdot (2T + B)\sqrt{C_M} \cdot \left[0.615989 \cdot c_{23} + 0.111439 \cdot C_M^3 + 0.000571111 \cdot C_{stern} + 0.245357 \cdot \frac{c_{23}}{C_M}\right] + 3.45538 \cdot A_T + \frac{A_{BT}}{C_B} \cdot \left(1.4660538 + \frac{0.5839497}{C_M}\right) \quad [m^2] \tag{3.19}$$

With the factor c_{23} according to Holtrop and Mennen for equation 3.19 [57]:

$$c_{23} = 0.453 + 0.4425 \cdot C_B - 0.2862 \cdot C_M - 0.003467 \cdot \frac{B}{T} + 0.3696 \cdot C_{WP} \quad [-] \tag{3.20}$$

The half angle of waterline entrance (i_E) according to Holtrop and Mennen is calculated according to equation 3.21 [57].

$$i_E = 1 + 89 \cdot e^a \quad [-] \tag{3.21}$$

With the factor a according to Holtrop and Mennen for equation 3.21 [57]:

$$a = -\left(\frac{L_{WL}}{B}\right)^{0.80856} \cdot (1 - C_{WP})^{0.30484} \cdot (1 - C_P - 0.0225 \cdot l_{CB})^{0.6367} \cdot \left(\frac{L_R}{B}\right)^{0.34574} \cdot \left(\frac{100 \cdot \nabla}{L_{WL}^3}\right)^{0.16302} \quad [-] \tag{3.22}$$

With the length of run (L_R) according to Holtrop for equation 3.22 [53]:

$$L_R = L_{WL} \cdot \left(\frac{1 - C_P + 0.06 \cdot C_P \cdot l_{CB}}{4 \cdot C_P - 1}\right) \quad [m] \tag{3.23}$$

The total wetted surface area of the appendages (S_{app}) is calculated by summing the approximate surface area of the rudder(s) (A_R), bilge keels (A_B), and skeg(s) (A_S) according to equation 3.24. There are no other appendages considered for all ship types in this research. The resistance of the suction pipe and mouth of the TSHD cannot be calculated with the Holtrop & Mennen method. However the trailing speed is 2-3 knots with the suction pipe and head in the water and the non trailing speed is around 16 knots. Therefore it is assumed that the resistance of the suction pipe and head at 2-3 knots is equal to the resistance at its service speed.

$$S_{app} = A_R + A_B + A_S \quad [m^2] \tag{3.24}$$

The rudder surface area (A_R) recommended by DNV-GL is given in equation 3.25 [29]. Factor C_1 will be equal to 1.0 for container ships and bulk carriers and tankers with less than 50.000 tonnes of displacement. For bulk carriers and tankers with a displacement of 50.000 t and over will have a C_1 factor of 0.9. TSHDs will have a C_1 factor of 1.7 as they have similar characteristics to a trawler where they are dragging an object through the water. Factors C_2, C_3, and C_4 will be set to 1.0 as it is not expected that special rudder types, profiles or arrangements are used.

$$A_R = C_1 \cdot C_2 \cdot C_3 \cdot C_4 \cdot \frac{1.75 \cdot L \cdot T}{100} \quad [m^2] \tag{3.25}$$

C_1 = Factor for ship type
= 1.0 in general
= 0.9 for bulk carriers and tankers having a displacement over 50.000 t
= 1.7 for tugs and trawlers
C_2 = Factor for rudder type
= 1.0 in general
= 0.9 for semi-spade rudder
= 0.7 for high lift rudders
C_3 = Factor the rudder profile
= 1.0 for NACA profiles and plate rudders
= 0.8 for hollow profiles and mixed rudders
C_4 = Factor for the rudder arrangement
= 1.0 for rudders in the propeller jet
= 1.5 for rudders outise the propeller jet

It is assumed that every ship has bilge keels of 20 cm over the full parallel body (L_X) on each side. Therefore the bilge keel surface area (A_B) is calculated according to equation 3.26.

$$A_B = 2 \cdot 0.2 \cdot L_X \quad [m^2] \tag{3.26}$$

The parallel middle body (L_X) is approximated by subtracting the length of run (L_R) and the length of entrance (L_E) from the length of waterline (L_{WL}), according to equation 3.27.

$$L_X = L_{WL} - L_R - L_E \quad [m] \tag{3.27}$$

With the length of run (L_R) according to equation 3.23 and the length of entrance (L_E) calculated by equation 3.28 according to Lindblad [87].

$$L_E = L_{WL} \cdot (1.975 - 2.27 \cdot C_B) \quad [m] \tag{3.28}$$

The skeg (sometimes referred to as gondola) surface area (A_S) is estimated as the surface area of a triangle, where the length of the base is equal to the length of the skeg (L_S) and the height is equal to the propeller diameter (D_p). The surface area of one face is therefore a half times the base times the height. For the full surface area and thus both faces of the triangle, it is multiplied by two. The estimation is calculated according to equation 3.29 and is dependent on the amount of propellers (k_p).

$$A_S = k_p \cdot 2 \cdot 0.5 \cdot L_S \cdot D_p \quad [m^2] \tag{3.29}$$

With the length of the skeg (L_S) approximated according to equation 3.30. The length of the skeg is estimated to be the length of the run minus the part behind the rudder axis which is equal to ($L_{WL} - L_{PP}$). However, the skeg does not really cover the full distance from the rudder axle to where the parallel middle body starts and therefore an estimated length equal to the propeller diameter is subtracted.

$$L_S = L_R - (L_{WL} - L_{PP}) - D_p \quad [m] \tag{3.30}$$

The final parameter necessary to perform the Holtrop & Mennen method is the diameter of the bow thruster tunnel (D_{TH}). If there are bow thrusters present, the diameter of the tunnel will be approximated as a quarter of the draft (T), according to equation 3.31.

$$D_{TH} = 0.25 \cdot T \quad [m] \tag{3.31}$$

Procedure
The Holtrop & Mennen is a lengthy procedure with hardly any additional input other than the required input from the previous section. The full Holtrop & Mennen procedure is reported in appendix B. The total ship resistance is the sum of all the resistance components calculated in the method according to equation 3.32.

$$R_{TOT} = R_F + R_{app} + R_W + R_B + R_{TR} + R_A + R_{AA} \quad [kN] \tag{3.32}$$

Cielo D'Italia According to the resistance approximation method by Holtrop & Mennen, the Cielo D'Italia has a total ship resistance of 1 351 kN. The detailed intermediate results of the ship resistance are displayed in table B.2 in appendix B.

3.1.2. Propulsion power sub-model

Holtrop and Mennen's method does not provide the final powering prediction, because it is also dependent on the propeller(s), configuration and ship geometry. However, the Holtrop & Mennen method does provide the hull-propeller interaction parameters, which are the wake fraction factor (w), thrust deduction fraction (t), and the relative rotative efficiency (η_R). Together with the total ship resistance, propeller characteristics, and the power plant configuration, the necessary power types can be calculated according to the propulsion chain in figure 3.4 by Klein Woud and Stapersma. The thrust towing power ($\mathbf{P_T}$), open water propeller power ($\mathbf{P_O}$), and shaft power ($\mathbf{P_S}$) are not necessary as there is an alternative route within the chain to calculate the final main engine brake power which can be seen in figure 3.4. The different powers calculated in the propulsion chain are:

- Effective towing power ($\mathbf{P_E}$)
- Thrust towing power ($\mathbf{P_T}$) (not necessary)
- Open water propeller power ($\mathbf{P_O}$) (not necessary)
- Propeller power ($\mathbf{P_P}$)
- Delivered power ($\mathbf{P_D}$)
- Shaft power ($\mathbf{P_S}$) (not necessary)
- Main engine brake power ($\mathbf{P_B}$)

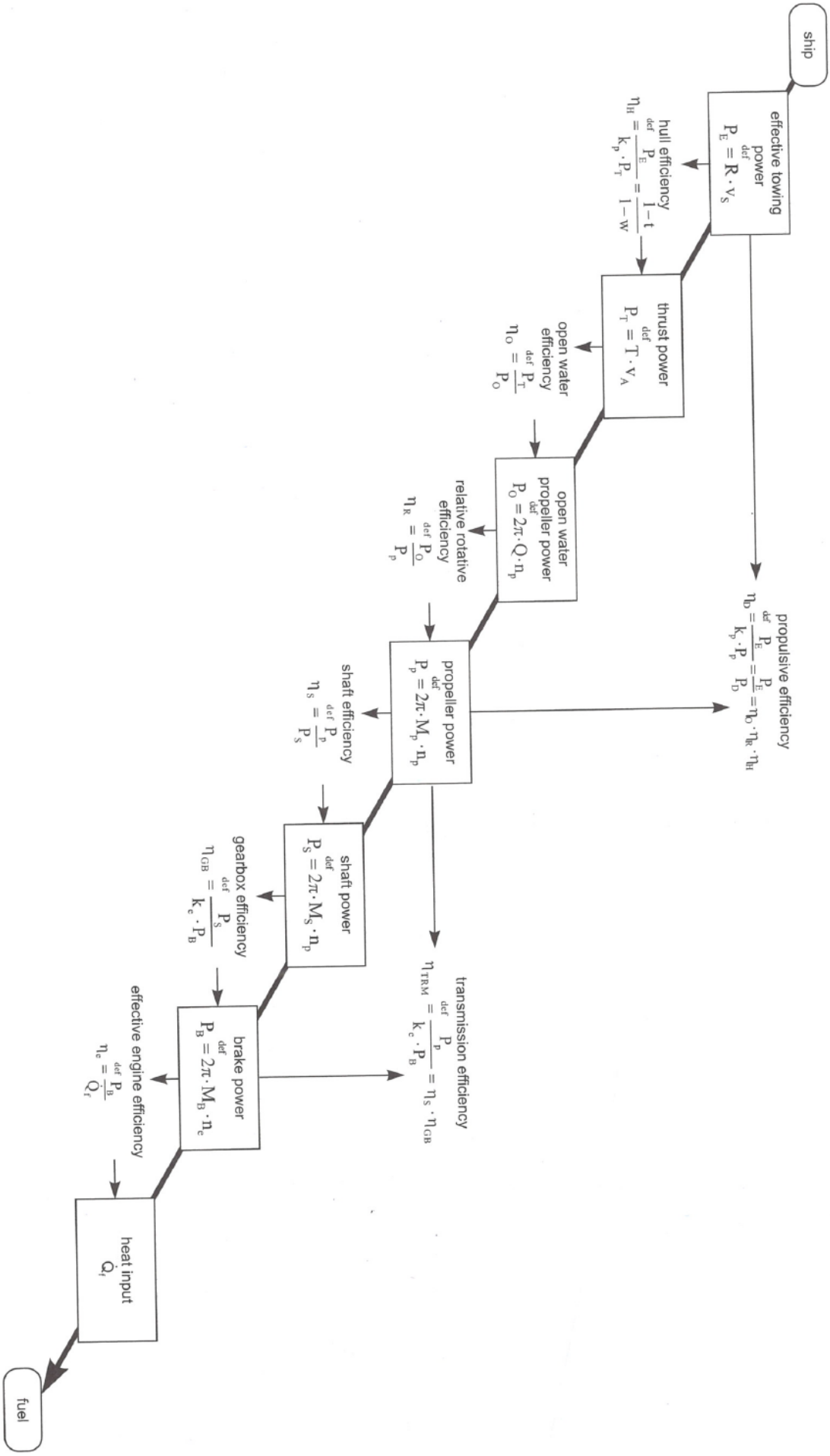

Figure 3.4: Propulsion chain generally intended for fossil fuel power plants [81]

Required input
The required input for the propulsion power sub-model originate from the ship sample data or are estimated using literature data. The required input parameters and value/source are displayed in table 3.3. The total ship resistance (R_{TOT}), thrust deduction factor (t), wake fraction factor (w), and relative rotative efficiency (η_R) are parameters which are estimated within the Holtrop & Mennen method.

Table 3.3: Required input parameters for propulsion chain [81]

Parameter	Symbol	Unit	Value/Source
Number of propellers	k_p	-	Sampled parameter
Number of main engines per shaft	k_{ME}	-	Sampled parameter
Ship design speed	V_s	m/s	Sampled parameter
Total ship resistance	R_{TOT}	kN	Value from Holtrop & Mennen
Thrust deduction factor	t	-	Value from Holtrop & Mennen
Wake fraction factor	w	-	Value from Holtrop & Mennen
Relative rotative efficiency	η_R	-	Value from Holtrop & Mennen
Open water efficiency	η_O	-	Approximated $\eta_O \approx 0.625$ [94]
Hull efficiency	η_H	-	Calculated according to equation 3.33
Shaft efficiency	η_S	-	Dependent on the propulsion plant
Gearbox efficiency	η_{GB}	-	Dependent on the propulsion plant
Engine margin	EM	%	EM = 12.5% [140]

The open water efficiency (η_O) is typically between 0.55 and 0.7 according to MAN Energy Solutions [94]. The actual efficiency is dependent on the propeller characteristics which is matched by the propeller designer to the ship characteristics. The open water efficiency of modern propellers is classified by the designers and therefore the average of typical values is used at 0.625.

The hull efficiency (η_H) is the ratio between the effective towing power (P_E) and the thrust towing power (P_T). It essentially refers to the connection between the thrust deduction factor (t) and the wake fraction factor (w).

$$\eta_H = \frac{P_E}{P_T} = \frac{1-t}{1-w} \quad [-] \tag{3.33}$$

The shaft efficiency (η_S) is based on the ship type. According to *Basic principles of ship propulsion* by MAN Energy Solutions, the shaft efficiency for directly coupled engines, the shaft efficiency is $\eta_S \approx 0.99$ for short shafts, which is common in bulk carriers and tankers. The shaft efficiency is $\eta_S \approx 0.98$ for long direct coupled shafts and is common in container ships. If a reduction gear is installed, the shaft efficiency is $\eta_S \approx 0.955$ and it is common in TSHDs [94].

The gearbox efficiency (η_{GB}) is dependent on the propulsion plant arrangement. If the propeller is directly coupled to the engine, there is no gearbox and thus η_{GB}= 1. This direct coupling is the case for bulk carriers, tankers and container ships, . According to MAN Energy Solutions, single step gearboxes have a power loss of 1 to 2% and for more complex gearboxes, the power loss is 3 to 5% [94]. TSHDs commonly have an engine that drives the propeller and the dredging pump according to Vlasblom [135]. In addition, TSHDs that have a pump ashore installation need an extra transmission within the gearbox and thus have an extra axis [135]. Therefore the gearbox for the TSHD is considered a complex gearbox with a power loss of 4%, resulting in $\eta_{GB} \approx 0.96$.

The engine margin (EM) is a power reserve on top of the necessary brake power. It is recommended to have a margin to lower maintenance costs, lower fuel consumption and have extra power for increased speed [140]. Generally the engine margin is between 10% and 15%, therefore the average is used at 12.5% [94].

Procedure
The propulsion chain starts by calculating the effective towing power (P_E) with the total ship resistance (R_{TOT}) and design speed (V_S) according to equation 3.34.

$$P_E = R_{TOT} \cdot V_S \quad [kW] \tag{3.34}$$

The thrust towing power (P_T) is calculated according to equation 3.35 with the necessary total thrust (T) and speed of advance (V_A). The necessary total thrust does not equal the total ship resistance because the water in front of the propeller is 'sucked' into the propeller, creating an additional resistance on the hull. This additional resistance is constructed using the thrust deduction factor (t). The speed of advance (V_A) is the speed of the water entering the propeller at behind ship conditions. Due to the water flow direction following the hull boundary, the water does not flow straight into the propeller. The flow into the propeller will therefore be less than the ship's speed and this speed reduction is constructed using the wake fraction factor (w).

$$\begin{aligned}
P_T =& T \cdot V_A \quad [kW] \\
P_T =& \frac{R_{TOT}}{(1-t)} \cdot V_A \quad [kW] \\
P_T =& \frac{R_{TOT}}{(1-t)} \cdot V_S \cdot (1-w) \quad [kW] \\
P_T =& R_{TOT} \cdot V_S \cdot \frac{1-w}{1-t} \quad [kW] \\
P_T =& \frac{R_{TOT} \cdot V_S}{\eta_H} \quad [kW] \\
P_T =& \frac{P_E}{\eta_H} \quad [kW]
\end{aligned} \tag{3.35}$$

The delivered power to all the propeller(s) (P_D) is calculated with the thrust towing power (P_T), open water propeller efficiency (η_O) and the relative rotative efficiency (η_R) according to equation 3.36.

$$P_D = \frac{P_T}{\eta_O \cdot \eta_R} \quad [kW] \tag{3.36}$$

The delivered power to a single propeller (P_P) is the total delivered power (P_D) divided by the number of propellers (k_p) according to equation 3.37.

$$P_P = \frac{P_D}{k_p} \quad [kW] \tag{3.37}$$

The total shaft power (P_S) is the total delivered power to all the propellers divided by the shaft efficiency (η_S) according to equation 3.38. The shaft power of a single shaft is the total shaft power divided by the number of shafts which is equal to the number of propellers.

$$P_S = \frac{P_D}{\eta_S} \quad [kW] \tag{3.38}$$

The total main engine brake power (P_B) is the total shaft power divided by the gearbox efficiency (η_{GB}) according to equation 3.39. The main engine brake power of a single engine is the total main engine brake power divided by the number of engine (k_{ME}).

$$P_B = \frac{P_S}{\eta_{GB}} \quad [kW] \tag{3.39}$$

The maximum continuous rated power (P_{MCR}) is the total main engine brake power including an engine margin (EM). The maximum continuous rated engine power is the maximum power of the main engine(s) installed in the ship.

$$P_{MCR} = \frac{P_B}{1 - EM} \quad [kW] \tag{3.40}$$

Cielo D'Italia According to the propulsion chain method by Klein Woud and Stapersma, the Cielo D'Italia requires a main engine brake power (P_B) of 10.964 kW. The detailed intermediate results of the propulsion chain are displayed in table B.3 in appendix B. With an engine margin of 12.5%, the maximum continuous rated engine power (P_{MCR}) is 12.531 kW, which is 14% higher than the given total main engine power (P_{ME}) from the sampled ship parameters. However, according to the article from Significant Ships 2015, the Cielo D'Italia has a 20% lower fuel consumption in relation to comparable ships due to its extremely efficient design particulars [119].

3.1.3. Design generation sub-model

The design generation is done twice in the total model approach. The additional contained AMEC bunker volume and weight is first calculated before each revision and thereafter applied to the original design. It is performed once to accommodate for the substitution of fuel oil bunker space with that of an AMEC (first revision). The second time it is performed to accommodate the upscaling of the AMEC bunker space proportionate to the propulsion power increased caused by the first revision ship design.

In order to maintain the operational requirements, the effective energy of the AMEC type must remain the same as that of fuel oil. The method of calculating the original effective energy is explained in the next section. To calculate the bunkered volume and weight associated to the AMECs, the following parameters are necessary for both steps of the design impact: the contained volumetric energy density ($\rho_{V\ E\ con}$), contained gravimetric energy density ($\rho_{G\ E\ con}$), density contained (ρ_{con}), power plant efficiency (η_{PP}), and power plant auxiliary engine power (PP_{aux}). The values of the parameters are displayed in table 2.2 from the case study chapter.

Lindstad et al. determined that higher length-beam ratios for ships with equal carrying capacity are the most energy efficient [89] [90]. Additionally, Liu and Pananikolauo determined that the added ship resistance decreases for lower Froude numbers, which can be achieved by increasing the length of a ship [92]. For that reason, to accommodate the additional AMEC bunker space, the ship is first lengthened at the midship transverse plane area (a). Thereafter heightened at the water plane area (b) and if necessary widened in the center plane area (c). The sequence design generation sequence is depicted in figure 3.5. The lengthening is constrained to a maximum length-beam ratio within the length-beam ratio trend per ship type.

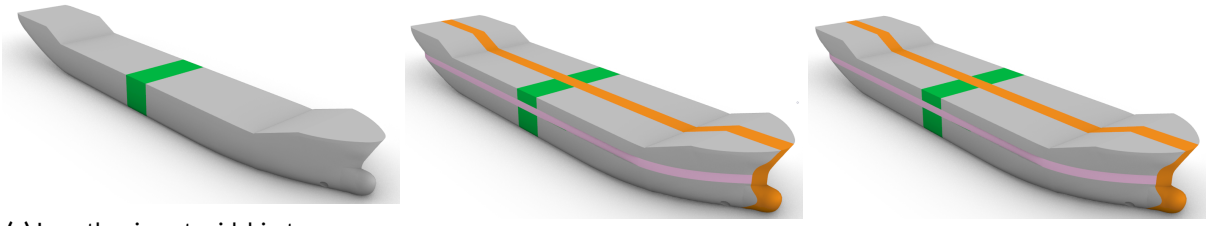

(a) Lengthening at midship transverse plane area

(b) Lengthening at water plane area

(c) Widened at center plane area

Figure 3.5: The design generation sequence to accommodate additional AMEC bunker space

Step one: Fuel oil substitution

The total effective energy ($E_{eff,\ total}$) of the bunkered fuel oil on board is calculated with the given fuel oil bunker volume ($V_{BUNK,\ FO}$), the contained volumetric energy density ($\rho_{V\ E,\ FO\ con}$) and the power plant efficiency ($\eta_{PP,\ FO}$). It is assumed that the given bunker volume is in contained form. The total effective energy is calculated according to equation 3.41.

$$E_{eff,\ total} = V_{BUNK,\ FO} \cdot \rho_{V\ E,\ FO\ con} \cdot \eta_{PP,\ FO} \quad [MJ] \tag{3.41}$$

Cielo D'Italia With a given fuel oil bunker volume of 3.020 m^3, the total effective energy ($E_{eff,\ total}$) is 49.470.258 MJ.

The total effective energy consists of the effective energy for the main engine(s) ($E_{eff,\ ME}$) and the effective energy for the auxiliary engine(s) ($E_{eff,\ AE}$) according to equation 3.42. The effective energy for the auxiliary engines is divided into the effective energy for the power plant ($E_{eff,\ AE\ PP}$) and the effective energy for non power plant consumers ($E_{eff,\ AE\ non-PP}$). It is necessary to distinguish the difference as the powering impact only effects the engine powers associated to the propulsion ($E_{eff,\ ME}$ and $E_{eff,\ AE\ PP}$). The effective energy share for the other energy users is not impacted by the powering impact and therefore it remains constant.

$$\begin{aligned} E_{eff,\ total} &= E_{eff,\ ME} + E_{eff,\ AE} \quad [MJ] \\ &= E_{eff,\ ME} + E_{eff,\ AE\ PP} + E_{eff,\ AE\ non-PP} \quad [MJ] \end{aligned} \tag{3.42}$$

The main engine effective energy and auxiliary engine effective energy are determined based on the specific fuel consumption (sfc) and brake power (P_B). The specific fuel consumption for the main engine according to Lamb is between 160 and 180 g/kWh for a slow speed two stroke diesel engine and between 165 and 250 g/kWh for a medium speed four stroke diesel engine [84]. The average of 170 g/kWh is selected for a two stoke diesel engine and the average of 207.5 g/kWh for a four stroke diesel engine. The main engine brake power ($P_{B,\ ME}$) is determined using the powering approximation method. The auxiliary engine brake power ($P_{B,\ AE}$) is equal to the given installed auxiliary engine power, plus the main engine shaft generator/PTO power (P_{PTO}) and minus the engine margin (EM). The main engine effective energy is calculated according to equation 3.43. The auxiliary engine effective energy is therefore the total effective energy minus the main engine effective energy and calculated according to equation 3.44.

$$E_{eff,\ ME} = \frac{sfc_{ME} \cdot P_{B,\ ME}}{sfc_{ME} \cdot P_{B,\ ME} + sfc_{AE} \cdot P_{B,\ AE}} \cdot E_{eff,\ total} \quad [MJ] \tag{3.43}$$

$$E_{eff,\ AE} = E_{eff,\ total} - E_{eff,\ ME} \quad [MJ] \tag{3.44}$$

Cielo D'Italia The main engine brake power ($P_{B,\ ME}$) is determined to be 10.964 kW according to the propulsion powering method. The given installed auxiliary engine power is 2.340 kW and there is no shaft generator or power take off (P_{PTO}). With the engine margin (EM) of 12.5%, the auxiliary engine brake power ($P_{B,\ AE}$) is 2.048 kW. Therefore the main engine effective energy ($E_{eff,\ ME}$) is 40.287.319 MJ at 81% and the auxiliary engine effective energy ($E_{eff,\ AE}$) is 9.182.938 MJ at 19%.

The auxiliary engine effective energy is split into power plant users ($E_{eff,\ AE\ PP}$) and non power plant users ($E_{eff,\ AE\ non-PP}$). In section 2.1.7 it was concluded that the auxiliary engine power for the power plant differs per power plant configuration and energy carrier. Therefore the effective energy content for the non power plant users must remain constant as it will not change due to changing the energy carrier and power plant. The shares calculated according to equation 3.45.

$$E_{eff,\ AE} = E_{eff,\ AE\ PP} + E_{eff,\ AE\ non-PP} \quad [MJ] \tag{3.45}$$

The auxiliary engine effective energy for the power plant users is calculated according to equation 3.46. With the minimum auxiliary brake power necessary for the fuel oil power plant ($P_{B,\ AE\ PP}$) is equal to 5% ($PP_{aux,\ FO}$) of the main engine brake power ($P_{B,\ ME}$) as per section 2.1.7.

$$E_{eff,\ AE\ PP} = \frac{PP_{aux,\ FO} \cdot P_{B,\ ME}}{P_{B,\ AE}} \cdot E_{eff,\ AE} \quad [MJ] \tag{3.46}$$

Cielo D'Italia The auxiliary engine power for the power plant ($P_{B,\ AE\ PP}$) with fuel oil is 5% of the main engine brake power ($P_{B,\ ME}$) and is equal to 548 kW. The auxiliary engine brake power ($P_{B,\ AE}$) is 2.048 kW and therefore 27% (548/2048) of the total auxiliary engine power is for the power plant. The auxiliary engine effective energy for the power plant ($E_{eff,\ AE\ PP}$) is therefore also 27% and equal to 2.458.711 MJ.

The auxiliary engine effective energy not for the power plant users ($E_{eff,\ AE\ non-PP}$) is therefore calculated according to equation 3.47.

$$E_{eff,\ AE\ non-PP} = E_{eff,\ AE} - E_{eff,\ AE\ PP} \quad [MJ] \tag{3.47}$$

Cielo D'Italia The remaining auxiliary effective energy by non-power plant users ($E_{eff,\ AE\ non-PP}$) is therefore 6.724.224 MJ at 73% of the total auxiliary power.

The powering impact only influences the effective energy for the propulsion which translates to the effective energy for the main engine ($E_{eff,\ ME}$). However, the effective auxiliary energy for the power plant ($E_{eff,\ AE\ PP}$) is based on a percentage of the main engine brake power which is impacted by the powering impact. Therefore this part of the effective auxiliary energy is also influenced.

Cielo D'Italia Overview of the effective energy of fuel oil in the Cielo D'Italia:

$E_{eff,\ total}$ = 49.470.258 MJ
$E_{eff,\ ME}$ = 40.287.319 MJ (81% of total)
$E_{eff,\ AE}$ = 9.182.938 MJ (19% of total)
$E_{eff,\ AE\ PP}$ = 2.458.711 MJ (27% of auxiliaries)
$E_{eff,\ AE\ non-PP}$ = 6.724.224 MJ (73% of auxiliaries)

Step one of the design impact is the energy carrier substitution where the fuel oil bunker space is replaced with the AMEC bunker space. The total effective energy is not exactly the same as the power plant auxiliary power differs. The effective energy for the main engine and for the auxiliary engines not for the power plant do not change. The total effective energy for an AMEC is calculated according to equation 3.48. The resulting total bunker volume by an AMEC ($V_{BUNK,\ AMEC}$) is calculated according to equation 3.49 and the total bunker weight by an AMEC ($m_{BUNK,\ AMEC}$) is calculated according to equation 3.50.

$$E_{eff,\ total\ AMEC} = E_{eff,\ ME} + E_{eff,\ AE\ PP} \cdot \frac{PP_{aux,\ AMEC}}{PP_{aux,\ FO}} + E_{eff,\ AE\ non-PP} \quad [MJ] \tag{3.48}$$

$$V_{BUNK,\ AMEC} = \frac{E_{eff,\ total\ AMEC}}{\rho_{V\ E\ con\ AMEC} \cdot \eta_{PP\ AMEC}} \quad [L] \tag{3.49}$$

$$m_{BUNK,\ AMEC} = V_{BUNK,\ AMEC} \cdot \rho_{con\ AMEC} \quad [kg] \tag{3.50}$$

The volume and weight of the fuel oil bunker space is substituted with that of the AMEC bunker space. Therefore the additional bunker volume of the AMEC ($\Delta V_{BUNK,\ AMEC}$) is the difference between the total AMEC bunker volume and that of the fuel oil. The same applies to the additional bunker weight of the AMEC ($\Delta m_{BUNK,\ AMEC}$). The additional volume and weight of the AMEC are calculated according to equation 3.51 and 3.52 respectively.

$$\Delta V_{BUNK,\ AMEC} = (V_{BUNK,\ AMEC} - V_{BUNK,\ FO}) \cdot 1000 \quad [m^3] \tag{3.51}$$

$$\Delta m_{BUNK,\ AMEC} = (m_{BUNK,\ AMEC} - m_{BUNK,\ FO}) \cdot 1000 \quad [t] \tag{3.52}$$

Cielo D'Italia The original contained fuel oil bunker volume ($V_{BUNK,\ FO}$) is 3020 m^3 and its contained weight ($m_{BUNK,\ FO}$) is equal to 3382 t. The bunker substitution results in the following necessary effective energy, contained volume addition and contained weight addition are displayed in the table below.

Effective energy, additional bunker volume and weight per energy carrier type

Energy carrier type	$E_{eff,\ total\ AMEC}$ [MJ]	$\Delta V_{BUNK,\ AMEC}$ [m^3]	$\Delta m_{BUNK,\ AMEC}$ [t]
Fuel oil (original)	49 470 258	0	0
Methanol	48 486 773	4 086	2 888
LNG	48 486 773	4 449	137
Liq. hydrogen	52 420 711	22 952	6830
Ammonia	54 422 102	7 787	5 347
Elec. + LIB	47 503 288	248 923	164 581

Additional AMEC bunker space application procedure
Both the bunker space substitution and scaling result in a new bunker volume and weight. The additional volume and weight affect the ship dimensions using the same design impact method. The method involves applying the additional bunker space to the ship dimensions. The additional bunker volume is added by lengthening the ship in the midship section to the maximum length-beam ratio and thereafter increasing the beam if necessary. The additional bunker weight is calculated to determine the new draft. First the midship area (A_{MID}) is calculated according to equation 3.53 to determine the maximum volume by lengthening the ship.

$$A_{MID} = B \cdot D \cdot C_M \quad [m^2] \tag{3.53}$$

Cielo D'Italia With an original beam (B) of 43 m, a depth (D) of 21.6 m and a midship section coefficient (C_M) of 0.998, the Cielo D'Italia has an original midship area (A_{MID}) of 927 m^2.

To find the new maximum length overall while keeping the beam constant, the maximum length-beam formula per ship type must intersect the length-beam ratio formula of the ship. The maximum length-beam formulas per ship type are established and presented in section 2.2 and has the form according to equation 3.54. The length-beam ratio formula for lengthening is equal to the directional coefficient of the current length-beam ratio. The length-beam ratio formula of the ship is according to equation 3.55 with directional coefficient (c) is equal to $1/B$. The intersection between the two formulas results in the maximum length overall for a specific ship according to equation 3.56

$$L_{OA}/B_{MAX,\ ship\ type} = a \cdot L_{OA} + b = a \cdot x + b \quad [-] \tag{3.54}$$

$$L_{OA}/B_{ship} = \frac{1}{B} \cdot L_{OA} = c \cdot x \quad [-] \tag{3.55}$$

$$a \cdot x + b = c \cdot x \quad \rightarrow \quad x = \frac{b}{c - a} = \frac{b}{\frac{1}{B} - a} = L_{OA,\ MAX} \quad [m] \tag{3.56}$$

In some cases the length-beam ratio exceeds the calculated maximum length-beam ratio ($L_{OA}/B_{ship} > L_{OA}/B_{MAX}$). In those cases the additional bunker volume of the AMEC ($\Delta V_{BUNK,\ AMEC}$) is immediately applied as the additional volume by increasing the beam (ΔV_B). This volume is reintroduced into the method from equation 3.69 onwards.

Cielo D'Italia With an original length overall (L_{OA}) of 245 m and an original beam (B) of 43 m, the length beam ratio (L_{OA}/B) is 5.698. The maximum length-beam ratio of a bulk carrier at this given length overall ($L_{OA}/B_{MAX,\ bulker}$) is 7.042. Therefore the maximum length overall for the Cielo D'Italia is 282.49 m.

The maximum lengthening (ΔL_{MAX}) of the ship is therefore the difference between the maximum length and the current length according to equation 3.57. The maximum volume available by lengthening the ship ($\Delta V_{L,\ MAX}$) is consequently the maximum lengthening multiplied by the midship area according to equation 3.58.

$$\Delta L_{MAX} = L_{OA,\ MAX} - L_{OA} \quad [m] \tag{3.57}$$

$$\Delta V_{L,\ MAX} = A_{MID} \cdot \Delta L_{MAX} \quad [m^3] \tag{3.58}$$

Cielo D'Italia With an original length overall (L_{OA}) of 245 m and the maximum length overall ($L_{OA,\ MAX}$) of 282.49 m, the maximum lengthening (ΔL_{MAX}) equals 37.49 m. With the midship area (A_{MID}) of 927 m^2, the maximum volume available by lengthening the ship ($\Delta V_{L,\ MAX}$) is 34 766 m^3.

The actual lengthening of the ship (ΔL) is based on the AMEC bunker volume change ($\Delta V_{BUNK,\ AMEC}$) and the maximum volume available by lengthening the ship ($\Delta V_{L,\ MAX}$). If the bunker volume change is less than the available volume by lengthening, the actual lengthening is calculated according to equation 3.59. Only 50% of the necessary additional AMEC bunker volume is applied, because the heightening in the next step is done for constant depth-length ratio. Therefore, the additional volume by heightening is practically the same volume. If the bunker volume change exceeds the available volume by lengthening, the actual lengthening is equal to the maximum lengthening according to equation 3.60. The resulting

new length overall ($L_{OA,\ new}$) and new waterline length ($L_{WL,\ new}$) are calculated according to equation 3.61 and 3.62 respectively.

$$\Delta L \quad (\Delta V_{BUNK,\ AMEC} < \Delta V_{L,\ MAX}) = \frac{50\% \cdot \Delta V_{BUNK,\ AMEC}}{A_{MID}} \quad [m] \tag{3.59}$$

$$\Delta L \quad (\Delta V_{BUNK,\ AMEC} > \Delta V_{L,\ MAX}) = \Delta L_{MAX} \quad [m] \tag{3.60}$$

$$L_{OA,\ new} = L_{OA} + \Delta L \quad [m] \tag{3.61}$$

$$L_{WL,\ new} = L_{WL} + \Delta L \quad [m] \tag{3.62}$$

Cielo D'Italia The additional bunker volumes ($\Delta V_{BUNK,\ AMEC}$) of methanol, LNG, hydrogen, and ammonia do not exceed the maximum volume available by lengthening the ship ($\Delta V_{L,\ MAX}$). Therefore the actual lengthening (ΔL) is less than the maximum lengthening (ΔL_{MAX}). The additional bunker volume for electricity in lithium ion batteries does exceed the maximum lengthening volume. The new lengths per energy carrier are displayed in the table below.

Additional length, new length overall and new waterline length per energy carrier type

Energy carrier type	$\Delta L\ [m]$	$L_{OA,\ new}\ [m]$	$L_{WL,\ new}\ [m]$
Fuel oil (original)	0.00	245.00	245.00
Methanol	2.20	247.20	247.20
LNG	2.40	247.40	247.40
Liq. Hydrogen	12.38	257.38	257.38
Ammonia	4.20	249.20	249.20
Elec. + LIB	*37.49	282.49	282.49

* equal to ΔL_{MAX}

The length overall and the waterline length are the same for the Cielo D'Italia and therefore their new length overall and new waterline length are identical.

The actual volume change by lengthening (ΔV_L) is calculated according to equation 3.63. The remaining volume after lengthening is calculated according to equation 3.64. For ships where the total necessary additional bunker volume was less than the maximum volume available by lengthening, there still is 50% additional bunker volume remaining after lengthening.

$$\Delta V_L = \Delta L \cdot A_{MID} \quad [m^3] \tag{3.63}$$

$$\Delta V_{BUNK,\ REMAIN\ L} = \Delta V_{BUNK,\ AMEC} - \Delta V_L \quad [m^3] \tag{3.64}$$

Cielo D'Italia With midship cross sectional area of 927.2 m^2 and the actual lengthening per energy carrier type. Only the additional bunker volume for the battery electric configuration requires more volume than maximum volume by lengthening. Therefore for the other AMECs, the remaining volume is 50% of the total additional bunker volume, which is equal to the additional volume by lengthening.

Additional bunker bunker volume, actual volume change by lengthening and remain bunker volume after lengthening per energy carrier type

Energy carrier type	$\Delta V_{BUNK,\ AMEC}\ [m^3]$	$\Delta V_L\ [m^3]$	$\Delta V_{BUNK,REMAIN\ L}\ [m^3]$
Fuel oil (original)	0	0	0
Methanol	4 086	2 043	2 043
LNG	4 449	2 225	2 225
Liq. Hydrogen	22 952	11 476	11 476
Ammonia	7 787	3 894	3 894
Elec. + LIB	248 923	*34 766	214 157

* equal to $\Delta V_{L,\ MAX}$

Lengthening a ship causes higher bending moments in the ship structure, therefore to prevent higher stresses and subsequently structural failures, the depth-length ratio ($D - L$) is kept constant. This also coincides with adhering to dimension trend of the ship type. In order to keep the depth-length ratio constant for a lengthened ship, the depth must increase as well. The additional depth (ΔD) is equal to the depth-length ratio multiplied by the actual lengthening (ΔL) according to equation 3.65. The new depth (D_{new}) is calculated accordingly to equation 3.66. The additional volume by increasing the depth (ΔV_D) is applied to the new waterplane area (A_{WP}) of the ship according to equation 3.67. The new waterplane area is equal to the original waterplane area plus the actual lengthening (ΔL) over the beam (B).

$$\Delta D = \frac{D}{L_{OA,\ original}} \cdot \Delta L \quad [m] \tag{3.65}$$

$$D_{new} = D + \Delta D \quad [m] \tag{3.66}$$

$$\Delta V_D \quad = \quad \Delta D \cdot A_{WP,\ new} \quad = \quad \Delta D \cdot (A_{WP,\ original} + \Delta L \cdot B) \quad [m^3] \tag{3.67}$$

Cielo D'Italia With a depth-length ratio ($D - L$) of 0.088, an original waterplane area (A_{WP}) of 9 403 m^2, and beam (B) of 43 m. The resulting additional depth (ΔD), new depth (D_{new}) and additional volume by increasing the depth (ΔV_D) are displayed in the table below.

Additional length, additional depth, new depth and additional volume by increasing the depth per energy carrier type

Energy carrier type	$\Delta L\ [m]$	$\Delta D\ [m]$	$D_{new}\ [m]$	$\Delta V_D\ [m^3]$
Fuel oil (original)	0	0	0	0
Methanol	2.20	0.19	21.79	1 845
LNG	2.40	0.21	21.81	2 011
Liq. Hydrogen	12.38	1.09	22.69	10 841
Ammonia	4.20	0.37	21.97	3 548
Elec. + LIB	*37.49	3.31	24.91	36 413

* equal to ΔL_{MAX}

The remaining volume after heightening ($\Delta V_{BUNK,\ REMAIN,\ D}$) is calculated according to equation 3.68. There are three scenarios for calculating the additional volume by widening (ΔV_B) according to equation 3.69. The first is if there is a positive remaining volume after heightening ($\Delta V_{BUNK,\ REMAIN,\ D}$). In general this is always the case unless the waterplane area coefficient is larger than the midship area coefficient ($C_{WP} > C_M$). The second scenario is for when the remaining volume after heightening is

negative. In this case, there is more volume applied to the ship design than required and therefore the excess volume is considered a surplus volume ($\Delta V_{SURPLUS}$) and calculated according to equation 3.70. Consequently, the additional volume by widening (ΔV_B) is zero and the surplus volume is deducted from the necessary AMEC bunker volume for the second revision design generation (AMEC upscaling) later on in equation 3.82. The third scenario is if the original length-beam ratio exceeds the maximum length-beam ratio line ($L/B > L/B_{MAX}$). In this case, the lengthening and heightening is skipped and the total additional AMEC bunker volume is immediately applied by widening. See for instance figure 2.9 where there is a single container ship above the maximum L/B-line line at $\sim$ 260 m.

$$\Delta V_{BUNK,\,REMAIN,\,D} = \Delta V_{BUNK,\,REMAIN\,L} - \Delta V_D \quad [m^3] \tag{3.68}$$

$$\begin{aligned} \Delta V_B \quad (\Delta V_{BUNK,\,REMAIN,\,D} > 0) &= \Delta V_{BUNK,\,REMAIN,\,D} \quad [m^3] \\ \Delta V_B \quad (\Delta V_{BUNK,\,REMAIN,\,D} < 0) &= 0 \quad [m^3] \\ \Delta V_B \quad (L/B_{original} > L/B_{MAX}) &= \Delta V_{BUNK,\,AMEC} \quad [m^3] \end{aligned} \tag{3.69}$$

$$\begin{aligned} \Delta V_{SURPLUS} \quad (\Delta V_{BUNK,\,REMAIN,\,D} > 0) &= 0 \quad [m^3] \\ \Delta V_{SURPLUS} \quad (\Delta V_{BUNK,\,REMAIN,\,D} < 0) &= -\Delta V_{BUNK,\,REMAIN,\,D} \quad [m^3] \end{aligned} \tag{3.70}$$

Cielo D'Italia The second scenario where the remaining volume after heightening is negative, is uncommon. It only occurs if the total additional bunker volume exceeds the maximum volume by lengthening, but is less sum of the additional volume by lengthening and heightening. In the case of the Cielo D'Italia, there is not an AMEC that results in this situation. Therefore the remaining volume after heightening is equal to the additional volume by widening and there is no surplus volume.

The additional bunker volume remaining after increasing the depth, additional volume by increasing the beam and the surplus volume per energy carrier type

Energy carrier type	$\Delta V_{BUNK,\,REMAIN\,D}$ $[m^3]$	ΔV_B $[m^3]$	$\Delta V_{SURPLUS}$ $[m^3]$
Fuel oil (original)	0	0	0
Methanol	198	198	0
LNG	214	214	0
Liq. Hydrogen	635	635	0
Ammonia	346	346	0
Elec. + LIB	177 744	177 744	0

The additional bunker volume by increasing the beam (ΔV_B) is applied in the centerline cross sectional area of the ship. The centerline cross sectional area is approximated to be 90% of the area of the new length overall ($L_{OA,\,new}$) by the new depth (D_{new}). Accordingly the beam increase (ΔB) is calculated according to equation 3.71 and results in the new beam (B_{new}) according to equation 3.72.

$$\Delta B = \frac{\Delta V_B}{0.90 \cdot L_{OA,\,new} \cdot D_{new}} \quad [m] \tag{3.71}$$

$$B_{new} = B + \Delta B \quad [m] \tag{3.72}$$

Cielo D'Italia As mentioned previously, the additional beam (ΔV_B) for the first scenario is relatively small due to the difference in midship area- and water plane area coefficient. However, the second scenario, which only occurs for the battery configuration is significantly large.

The additional bunker volume by increasing the beam and new beam per energy carrier type type

Energy carrier type	$\Delta V_B\ [m^3]$	$\Delta B\ [m]$	$B_{new}\ [m]$
Methanol	198	0.04	43.04
LNG	214	0.04	43.04
Liq. Hydrogen	635	0.12	43.12
Ammonia	346	0.07	43.07
Elec. + LIB	177744	28.07	71.07

The new overall internal volume ($V_{INT,\ new}$) is the sum of the original overall internal volume (V_{INT}), the additional volume change by lengthening (ΔV_L), the additional volume by increasing the depth (ΔV_D), and the additional volume by increasing the beam (ΔV_B). It is calculated according to equation 3.73.

$$V_{INT,\ new} = V_{INT} + \Delta V_L + \Delta V_D + \Delta V_B \quad [m^3] \tag{3.73}$$

Cielo D'Italia With an original overall internal volume of 172 955 m^3, the new overall internal volumes per energy carrier type are displayed in the table below.

Additional volumes and new internal volume per energy carrier type

Energy carrier type	$\Delta V_L\ [m^3]$	$\Delta V_D\ [m^3]$	$\Delta V_B\ [m^3]$	$V_{INT,\ new}\ [m^3]$
Fuel oil (original)	0	0	0	172 955
Methanol	2 043	1 845	198	177 041
LNG	2 225	2 011	214	177 405
Liq. Hydrogen	11 476	10 841	635	195 908
Ammonia	3 894	3 548	346	180 743
Elec. + LIB	34 766	36 413	177 744	421 879

The new draft (T_{new}) is calculated to be the original draft (T) plus the additional draft (ΔT) caused by the additional weight, additional waterplane area and sea water density (ρ_{sw}). The total additional weight is equal to the weight of the contained bunker volume ($\Delta m_{BUNK,\ AMEC}$) and the additional weight of the steel structure (W_S). The additional weight of the steel structure is calculated by the structural density (C_S) multiplied by the sum of the additional volumes ($\Delta V_L + \Delta V_D + \Delta V_B$). The structural density (C_S) is estimated at an average of 0.08 t/m^3 for ship with a gravimetric displacement (∇) ranging between 10 000 and 1 000 000 tons according to Friis et al. [40]. the sea water density is approximated at 1.025 t/m^3. The new waterplane area coefficient (C_{WP}) is calculated according to equation 3.9 from the resistance sub-model with the new ship dimensions. The new draft and new depth result in a new freeboard, calculated according to equation 3.75.

$$\begin{aligned}
T_{new} &= T + \Delta T \quad [m] \\
T_{new} &= T + \frac{\Delta m_{BUNK,\ AMEC} + W_S}{L_{WL,\ new} \cdot B_{new} \cdot C_{WP,\ new} \cdot \rho_{sw}} \quad [m] \\
T_{new} &= T + \frac{\Delta m_{BUNK,\ AMEC} + C_S \cdot (\Delta V_L + \Delta V_D + \Delta V_B)}{L_{WL,\ new} \cdot B_{new} \cdot C_{WP,\ new} \cdot \rho_{sw}} \quad [m]
\end{aligned} \tag{3.74}$$

$$f_{new} = D_{new} - T_{new} \quad [m] \tag{3.75}$$

Cielo D'Italia Due to the high amount batteries necessary to keep the operational conditions constant, the new freeboard (f) of this case is negative and therefore does not float. The AMECs that have a higher uncontained gravimetric energy density than fuel oil (LNG and Liq. hydrogen) cause the ship to have a higher freeboard even though the draft (T) has increased.

The additional draft, new draft and new freeboard per energy carrier type

Energy carrier type	ΔT $[m]$	T_{new} $[m]$	f_{new} $[m]$
Fuel oil (original)	0.00	15.60	6.00
Methanol	0.33	15.93	5.86
LNG	0.05	15.65	6.16
Liq. Hydrogen	0.85	16.45	6.24
Ammonia	0.61	16.21	5.76
Elec. + LIB	10.06	25.66	-0.75

A larger propeller diameter (D_P) generates a higher thrust and therefore the new propeller diameter ($D_{P,\ new}$) is determined by scaling the original propeller diameter by new draft (T_{new}) over the original according to equation 3.76.

$$D_{P,\ new} = \frac{T_{new}}{T} \cdot D_P \quad [m] \tag{3.76}$$

Cielo D'Italia Due to higher new drafts for all energy carriers, all designs have a larger propeller diameter.

The new draft and new propeller diameter per energy carrier type

Energy carrier type	T_{new} $[m]$	$D_{P,\ new}$ $[m]$
Fuel oil (original)	15.60	8.19
Methanol	15.93	8.36
LNG	15.65	8.22
Liq. Hydrogen	16.45	8.64
Ammonia	16.21	8.51
Elec. + LIB	25.66	13.47

The new deadweight tonnage (DWT_{new}) is calculated by subtracting the original uncontained fuel oil weight ($m_{FO\ uncon}$) from the original deadweight tonnage (DWT) and adding the uncontained AMEC weight ($m_{AMEC\ uncon}$). The contained densities include the weight of the tanks which are not free weights and therefore are not included in the deadweight tonnage. The new deadweight tonnage is calculated according to equation 3.77. The weights of the fuel oil and AMEC are calculated using the contained volumetric energy density ($\rho_{V\ E\ con}$) and the uncontained gravimetric density ($\rho_{G\ E\ uncon}$), also known as the lower heating value (LHV). Only in the case of the electrically charged lithium ion batteries is the new energy carrier not a free weight and therefore does not contribute to the deadweight tonnage. The new deadweight tonnage for the case of electrically charged lithium ion batteries is calculated according to equation 3.78. The new lightweight ship ($m_{LIGHT\ new}$) is calculated according to equation 3.79 by subtracting the new deadweight tonnage from the new gravimetric displacement (Δ_{new}). The new gravimetric displacement (Δ_{new}) is the sum of the original gravimetric displacement ($\Delta_{original}$), additional contained bunker weight ($\Delta m_{BUNK,\ AMEC}$) and the weight of the additional steel structure (W_S).

$$
\begin{aligned}
DWT_{new} &= DWT - m_{FO\ uncon} + m_{AMEC\ uncon} \quad [t] \\
DWT_{new} &= DWT - V_{BUNK,\ FO} \cdot \frac{\rho_{V\ E\ FO\ con}}{\rho_{G\ E\ FO\ uncon}} + V_{BUNK,\ AMEC} \cdot \frac{\rho_{V\ E\ AMEC\ con}}{\rho_{G\ E\ AMEC\ uncon}} \quad [t]
\end{aligned} \tag{3.77}
$$

$$
DWT_{new\ ELEC+LIB} = DWT - m_{FO\ uncon} \quad [t] \tag{3.78}
$$

$$
\begin{aligned}
m_{LIGHT,\ new} &= \Delta_{new} - DWT_{new} \quad [t] \\
m_{LIGHT,\ new} &= \Delta_{original} + \Delta m_{BUNK,\ AMEC} + W_S - DWT_{new} \quad [t] \\
m_{LIGHT,\ new} &= \Delta_{original} + \Delta m_{BUNK,\ AMEC} + C_S \cdot (\Delta V_L + \Delta V_D + \Delta V_B) - DWT_{new} \quad [t]
\end{aligned} \tag{3.79}
$$

Cielo D'Italia With a contained fuel oil bunker volume ($V_{BUNK,\ FO}$) of 3 020 m^3 and an original deadweight tonnage (DWT) of 117 438 t, the resulting new deadweight tonnages and lightweight ships are displayed in the table below.

The new deadweight tonnage and new lightweight ship per energy carrier type

Energy carrier type	DWT_{new} [t]	$m_{LIGHT,\ new}$ [t]
Fuel oil (original)	117 438	23 870
Methanol	119 937	24586
LNG	117 028	24 773
Liq. Hydrogen	115 994	33 980
Ammonia	119 641	27 638
Elec. + LIB	114 998	210 804

Step two: Upscaling AMEC bunker space

Step one of the powering impact accounted for the substitution of the fuel oil with an AMEC for constant operational requirements. This results in new ship dimensions and weights caused by the additional bunker and structural volume and weight. Therefore the total ship resistance after the energy carrier substitution ($R_{TOT\ 1}$) is calculated according to the same resistance sub-model in section 3.1.1. Consequently the propulsion power after the energy carrier substitution ($P_{B,\ ME\ AMEC\ 1}$) is calculated as well with the same propulsion power sub-model in section 3.1.2. The new engine brake power for the AMEC is used to scale the bunkering which is intended for the main engine and power plant components.

Cielo D'Italia The main engine brake power after the energy carrier substitution ($P_{B,\ ME\ AMEC\ 1}$) increases for all AMEC types for the Cielo D'Italia. The results are displayed in the table below.

The resistance and main engine brake power after the energy carrier substitution per energy carrier type

Energy carrier type	$R_{TOT\ 1}$ [kN]	$P_{B,\ ME\ AMEC\ 1}$ [kW]
Fuel oil (original)	1 351	10 964 (0.0%)
Methanol	1 372	11 158 (+1.8%)
LNG	1 359	11 057 (+0.8%)
Liq. Hydrogen	1 416	11 630 (+6.1%)
Ammonia	1 390	11 326 (+3.3%)
Elec. + LIB	2 854	22 254 (+103.0%)

The main engine power and the auxiliary engine power for power plant components are impacted by the propulsion power increase. Therefore the effective energy intended for these engines is scaled by the power increase. The additional effective energy necessary after the energy carrier substitution is calculated according to equation 3.80. The power increase is equal to the new main engine brake power ($P_{B,\ ME\ AMEC\ 1}$) divided by the original fuel oil main engine brake power ($P_{B,\ ME\ FO}$). The effective energy that is impacted is equal to the total AMEC effective energy ($E_{eff,\ total\ AMEC}$) minus the auxiliary non power plant effective energy ($E_{eff,\ AE\ non-PP}$).

$$\Delta E_{eff,\ total\ AMEC} = \left(\frac{P_{B,\ ME\ AMEC\ 1}}{P_{B,\ ME\ FO}} - 1 \right) \cdot (E_{eff,\ total\ AMEC} - E_{eff,\ AE\ non-PP}) \quad [MJ] \tag{3.80}$$

The gross additional AMEC bunker volume ($\Delta V_{BUNK,\ AMEC\ GROSS}$) and net weight ($\Delta m_{BUNK,\ AMEC\ NET}$) due to upscaling the bunker space is calculated according to equation 3.81 and 3.83 respectively. However, the surplus volume ($\Delta V_{SURPLUS}$) of the energy carrier substitution is subtracted from the necessary additional bunker volume to determine the net additional bunker volume ($\Delta V_{BUNK,\ AMEC\ NET}$) and calculated according to equation 3.82. If the net additional bunker volume is negative, there is no volume change applied to the design and therefore equals zero. The additional bunker weight ($\Delta m_{BUNK,\ AMEC}$) is not affected by the surplus volume.

$$\Delta V_{BUNK,\ AMEC\ GROSS} = \frac{\Delta E_{eff,\ total\ AMEC}}{\rho_{V\ E\ con\ AMEC} \cdot \eta_{PP\ AMEC} \cdot 1000} \quad [m^3] \tag{3.81}$$

$$\Delta V_{BUNK,\ AMEC\ NET} = \Delta V_{BUNK,\ AMEC\ GROSS} - \Delta V_{SURPLUS} \quad [m^3] \tag{3.82}$$

$$\Delta m_{BUNK,\ AMEC} = \Delta V_{BUNK,\ AMEC} \cdot \rho_{con\ AMEC} \quad [t] \tag{3.83}$$

Cielo D'Italia Due to there not being a surplus volume after the fuel oil substitution, the gross additional bunker volume is equal to the net additional bunker volume.

The gross additional bunker volume, net additional bunker volume and additional bunker weight per energy carrier type

Energy carrier type	$\Delta V_{BUNK,\ GROSS}\ [m^3]$	$\Delta V_{BUNK,\ NET}\ [m^3]$	$\Delta m_{BUNK,\ AMEC}\ [t]$
Fuel oil (original)	0	0	0
Methanol	108	108	96
LNG	63	63	30
Liq. Hydrogen	1 577	1 577	620
Ammonia	356	356	288
Elec. + LIB	259 429	259 429	172 952

The additional net bunker volume ($\Delta V_{BUNK,\ AMEC\ NET}$) and the additional bunker weight ($\Delta m_{BUNK,\ AMEC}$) is applied in the common ship design impact in the previous section at equations 3.51 and 3.52 respectively and results in the final ship dimensions.

Cielo D'Italia The final ship design dimensions, overall internal volume, deadweight tonnage, and lightweight ship per energy carrier type are displayed in the table below. Notice that the draft is higher than the depth in the electrically charged lithium ion batteries case and therefore it is not feasible.

The final ship design dimensions per energy carrier type

Energy carrier type	L_{OA} $[m]$	B $[m]$	D $[m]$	T $[m]$
Methanol	247.26	43.04	21.80	15.94
LNG	247.43	43.04	21.81	15.65
Liq. Hydrogen	258.18	43.14	22.76	16.53
Ammonia	249.39	43.07	21.99	16.24
Elec. + LIB	379.84	71.07	33.49	34.12

The final overall internal volume, lightweight ship, and deadweight tonnage

	ΔV_{INT}	ΔV_{INT}%	Δm_{LIGHT}	Δm_{LIGHT}%	ΔDWT	ΔDWT%
Fuel oil (original)	172 955	0.0%	23 870	0.0%	117 438	0.0%
Methanol	177 150	+2.4%	24 615	+3.1%	120 012	+2.2%
LNG	177 468	+2.6%	24 791	+3.9%	117 046	-0.3%
Liq. Hydrogen	197 485	+14.2%	34 666	+45.2%	116 055	-1.2%
Ammonia	181 099	+4.7%	27 801	+16.5%	119 794	+2.0%
Elec. + LIB	806 808	+366.5%	414 551	+1636.7%	114 998	-2.1%

Step one and two of the powering impact accounted for the substitution of the fuel oil and upscaling of the bunkering for constant operational requirements. This results in the final ship dimensions, volumes and weights caused by the additional bunker and structural volume and weight. Therefore the final total ship resistance after both steps ($R_{TOT\ 2}$) is calculated according to the same resistance sub-model in section 3.1.1. Consequently the propulsion power after both steps ($P_{B,\ ME\ AMEC\ 2}$) is calculated as well with the same propulsion power sub-model in section 3.1.2.

Cielo D'Italia The final total ship resistance and main engine brake power per energy carrier type are displayed in the table below. The main engine brake power percentage increase is with respect to the original power (10 964 kW).

The resistance and main engine brake power after both steps per energy carrier type

Energy carrier type	$R_{TOT\ 2}$ $[kN]$	$P_{B,\ ME\ AMEC\ 2}$ $[kW]$
Fuel oil (original)	1 351	10 964 (0.0%)
Methanol	1 373	11 164 (+1.8%)
LNG	1 360	11 060 (+0.9%)
Liq. Hydrogen	1 422	11 684 (+6.6%)
Ammonia	1 392	11 344 (+3.5%)
Elec. + LIB	3 672	33 189 (+202.7%)

3.1.4. Design impact results

The ship parameters after conducting the design impact assessments of the energy carrier substitution (step one) and the upscaling of the bunkering space (step two) are displayed in appendix C. The design impacts for all energy carriers on all the sampled ships are displayed in table C.1 for bulk carriers, table C.2 for tankers, table C.3 for container ships, and table C.4 for TSHDs. The impacted parameters included

in the tables are listed below.

- Length overall (L_{OA})
- Beam (B)
- Depth (D)
- Draft (T)
- Freeboard (f)
- Overall internal volume (V_{INT})
- Deadweight tonnage (DWT)
- Lightweight ship (m_{LIGHT})
- Length-beam ratio (L/B)

The average overall internal volume change (ΔV_{INT}), average lightweight ship change (Δm_{LIGHT}), and average deadweight tonnage change (ΔDWT) per (A)MEC type and ship type combination are displayed in tables below. These parameters are an effect of the design generation procedure whereas the main dimensions are an impact. The difference being that the main dimensions are a marked/targeted outcome and the effected parameters are a consequence of the marked/targeted outcome.

Table 3.4: The average result of the effected parameters for bulk carriers

	ΔV_{INT}	Δm_{LIGHT}	ΔDWT
Fuel oil (original)	0.0%	0.0%	0.0%
Methanol	+2.7%	+4.1%	+2.4%
LNG	+2.9%	+5.1%	-0.4%
Liq. hydrogen	+18.1%	+62.7%	-1.2%
Ammonia	+5.3%	+21.8%	+2.2%
Elec. + LIB	+509.9%	+2514.0%	-2.3%

Table 3.5: The average result of the effected parameters for tankers

	ΔV_{INT}	Δm_{LIGHT}	ΔDWT
Fuel oil (original)	0.0%	0.0%	0.0%
Methanol	+2.7%	+1.8%	+2.8%
LNG	+2.8%	+2.3%	-0.4%
Liq. hydrogen	+17.6%	+27.6%	-1.5%
Ammonia	+5.2%	+9.6%	+2.5%
Elec. + LIB	+552.0%	+1118.1%	-2.6%

Table 3.6: The average result of the effected parameters for container ships

	ΔV_{INT}	Δm_{LIGHT}	ΔDWT
Fuel oil (original)	0.0%	0.0%	0.0%
Methanol	+3.8%	+3.5%	+6.0%
LNG	+4.0%	+4.3%	-0.9%
Liq. hydrogen	+22.3%	+51.1%	-3.1%
Ammonia	+7.4%	+18.5%	+5.5%
Elec. + LIB	+490.5%	+1881.7%	-5.6%

Table 3.7: The average result of the effected parameters for TSHDs

	ΔV_{INT}	Δm_{LIGHT}	ΔDWT
Fuel oil (original)	0.0%	0.0%	0.0%
Methanol	+3.8%	+3.5%	+6.0%
LNG	+4.0%	+4.3%	-0.9%
Liq. hydrogen	+22.3%	+51.1%	-3.1%
Ammonia	+7.4%	+18.5%	+5.5%
Elec. + LIB	+490.5%	+1881.7%	-5.6%

3.2. Powering impact results

The auxiliary engine power for non power plant consumers ($P_{B,\ AE\ non-PP}$) is not effected by the design impact and therefore it remains constant. The design impact does impact the necessary propulsion power which is expressed as the main engine brake power ($P_{B,\ ME}$). The auxiliary engine power for the power plant consumers ($P_{B,\ AE\ PP}$) is also affected by the design impact as it is a percentage of the main engine brake power. The sum of all the engine powers is the total installed engine brake power ($P_{B,\ TOT}$). A detailed overview of the impacts on the total engine brake power and main engine brake power after the first step of the design impact (fuel oil substitution) and after the second step of the design impact (bunker upscaling) is presented in appendix D. The average final main engine power impact per energy carrier and ship type combination is displayed in table 3.8. The main engine power impact represents the additional propulsion power necessary to fulfill the ship type's operational requirements with its new design. The average total installed engine brake power impact per energy carrier and ship type combination is displayed in table 3.9. The total installed engine brake power impact takes into the account all the engine power and is necessary for the environmental impact assessment. Ships with a small design impact (small change in overall internal volume and lightweight ship) will result in a small main engine powering impact and similar total installed brake power impact. However, ships with a large design impact will result in a large main engine powering impact, but not similar and large total installed powering impact. In conclusion, the larger the design impact, the larger the difference in main engine and total installed engine power.

Table 3.8: The average final main engine brake power (propulsion power) impact per (A)MEC and ship type combination

	Bulk carriers	Tankers	Container ships	TSHDs	Average
Fuel oil (original)	0.0%	0.0%	0.0%	0.0%	0.0%
Methanol	+2.3%	+2.2%	+3.1%	+3.1%	+2.7%
LNG	+1.1%	+1.1%	+1.2%	+7.5%	+2.7%
Liq. hydrogen	+10.3%	+9.8%	+10.2%	+17.2%	+11.9%
Ammonia	+4.4%	+4.2%	+5.9%	+11.6%	+6.5%
Elec. + LIB	+280.8%	+309.7%	+229.7%	+502.2%	+330.6%

The total installed brake power of all engines for an AMEC ($P_{B,\ TOT\ AMEC}$) is therefore calculated according to equation 3.84.

$$\begin{aligned} P_{B,\ TOT\ AMEC} &= \frac{P_{B,\ ME\ AMEC\ 2}}{P_{B,\ ME\ FO}} \cdot P_{B,\ TOT} \quad [kW] \\ P_{B,\ TOT\ AMEC} &= \frac{P_{B,\ ME\ AMEC\ 2}}{P_{B,\ ME\ FO}} \cdot P_{B,\ ME} \cdot (1 + PP_{aux,\ AMEC}) + P_{B,\ AE\ non-PP} \quad [kW] \end{aligned} \tag{3.84}$$

The total installed brake power impact of an AMEC type on a ship is calculated according to 3.85.

$$\frac{P_{B\ TOT\ AMEC}}{P_{B\ TOT\ FO}} = \text{Total installed brake power impact of an AMEC} \tag{3.85}$$

Table 3.9: The average total installed brake power impact per (A)MEC and ship type combination

	Bulk carriers	Tankers	Container ships	TSHDs	Average
Fuel oil (original)	0.0%	0.0%	0.0%	0.0%	0.0%
Methanol	+1.9%	+1.6%	+2.6%	+1.5%	+1.9%
LNG	+0.9%	+0.8%	+1.0%	+3.4%	+1.6%
Liq. hydrogen	+8.6%	+7.4%	+8.4%	+8.4%	+8.2%
Ammonia	+3.7%	+3.2%	+4.9%	+5.5%	+4.3%
Elec. + LIB	+235.3%	+234.4%	+190.1%	+249.9%	+227.4%

3.3. Discussion and conclusion

The design impact method is modeled in accordance with historic ship dimension data and therefore it is based on fuel oil powered ships. It is possible that historic dimension data for fuel oil powered ships is not fully applicable for AMEC powered ships. For instance, the first LNG powered container ship, the Isla Bella (IMO: 9680841) has its tanks on top of its deck at the aft of the ship. However, the model generates a design for bunkering tanks to be inside the main hull. As a result, the generated dimensions of the main hull are larger than in reality in this design case. Consequently, it justifies that historical ship data for fuel oil powered ships might not coincide with AMEC powered ships. Nonetheless, the bunkering tanks on top of the deck on the Isla Bella occupy space for containers at an easily accessible part of the ship for container cranes. This is not a standard design aspect of container ships and therefore it changes the standard operational requirement of cargo handling. Furthermore, on the contrary, the largest LNG powered container ship, CMA CGM Jacques Saade (IMO: 9839179), does have its LNG tanks within the main hull. It is the first of its class of nine sister ships and thus it is considered that LNG tanks on the top deck is not the standard design principle.

The design impact model is constructed under the assumption that the original overall internal volume is designed to not have excess/redundant space. There might already be a surplus volume available for the AMEC bunker space requirements. Therefore the necessary additional AMEC bunker volume ($\Delta V_{BUNK,\ AMEC}$) calculated in the model results in the maximum overall internal volume increase (ΔV_{INT}) and thus the maximum overall internal volume (V_{INT}). Accordingly, this also generates the dimensions of the main hull to be larger than in reality. Moreover, the design impact model does not generate slender body designs if the maximum volume by lengthening ($\Delta V_{L,\ MAX}$) including the volume by increasing the depth (ΔV_D) is only a fraction of the total necessary additional AMEC bunker volume. In all ship types, the average length-beam ratio increases for all AMECs except for the battery electric configuration. This is however only true for ship designs of which their original length-beam ratio (L/B) did not exceed the determined maximum length-beam ratio (L/B_{MAX}). Nonetheless, the generated designs for the battery electric configurations do not coincide with the goal of the design impact model and therefore the designs are considered inaccurate. For the battery electric configuration, it was expected that the generated ship design would have a lower length-beam ratio after the first step of the design impact (energy carrier substitution), but that the ratio would increase again by the second step of the design impact (bunker upscaling). However, the main engine power impact after upscaling the bunkering ($P_{B\ ME\ AMEC\ 2}/P_{B\ ME\ AMEC\ 1}$) is practically non existent for all AMECs except the battery electric configuration compared to the main engine power impact after fuel oil substitution ($P_{B\ ME\ AMEC\ 1}/P_{B\ ME\ FO}$). As a result, the design does not become slender in the second design impact step after becoming considerably wide in the first step of the design impact.

The resistance approximation method by Holtrop and Mennen is based on a regressional statistical analysis from random model tests and full scale ship trials from shipping vessels. Therefore the method is not fully intended for TSHDs. However the results of the main engine brake power impact of the AMECs are not out of the ordinary compared to the shipping vessels. Additionally, there are four TSHDs of which their length-beam ratio exceeds the maximum length-beam ratio. These are: HAM 318, Prins der Nederlanden, Queen of the Netherlands, and Vox Maxima. As mentioned previously, the generated designs of these vessels do not result in a slender body. These four TSHDs had their beam increased first to accommodate the additional bunker volume. In table 3.10, the final main engine brake power impact

($P_{B,\ ME\ AMEC\ 2}/P_{B,\ ME\ FO}$) results are displayed for all TSHDs, lengthened TSHDs ($L/B < L/B_{MAX}$) and widened TSHDs ($L/B > L/B_{MAX}$). The final main engine brake power of the widened TSHDs is significantly higher than those that were lengthened and therefore validating the lower ship resistance for slender body ship design. Moreover, the main engine power impact due to upscaling the AMEC bunker capacity ($P_{B,\ ME\ AMEC\ 2}/P_{B,\ ME\ AMEC\ 1}$) is negligible in all ship types and (A)MEC combinations compared to the main engine power impact due to fuel oil substitution ($P_{B,\ ME\ AMEC\ 1}/P_{B,\ ME\ FO}$), except for two cases. The first case is when the maximum volume by lengthening ($\Delta V_{L,\ MAX}$) including the volume by increasing the depth (ΔV_D) is only a fraction of the total necessary additional AMEC bunker volume. Which is the case for the battery electric configuration in all ship types. The second case is when the length-beam ratio exceeds the maximum length-beam ratio (L/B_{MAX}). Which is the case for the four TSHDs and thus highly influence the average result.

Table 3.10: The final main engine brake power (propulsion power) impact for TSHDs

	All	$L/B < L/B_{MAX}$	$L/B > L/B_{MAX}$
Fuel oil (original)	0.0%	0.0%	0.0%
Methanol	+3.1%	+2.0%	+5.3%
LNG	+7.5%	+0.2%	+22.1%
Liq. hydrogen	+17.2%	+9.7%	+32.4%
Ammonia	+11.6%	+4.1%	+26.6%
Elec. + LIB	+502.2%	+403.7%	+699.0%

In many cases of energy carrier type and ship type combinations it is questionable if the resulting small additional overall internal volume (ΔV_{INT}) and additional lightweight ship (Δm_{LIGHT}) should be applied to the design to keep the operational requirements constant. For example, LNG in tankers results in an average 4.8% additional overall internal volume (ΔV_{INT}) and an average 0.4% reduction in lightweight ship (Δm_{LIGHT}). Consequently resulting in an 1.33% increase in main engine brake power compared to fuel oil. As mentioned previously, if there is already excess/redundant volume available it could be used to accommodate for this small volume increase without affecting the operational requirements or ship design.

Fixed ship dimensions were not taken into account as a design requirement, however it is possible that a ship dimension is limited due to lock-, (dry) dock-, bridge- or port infrastructure size restrictions. Therefore in the case of ships being subjected to these dimension restrictions, the higher the additional overall internal volume (ΔV_{INT}), the lower the feasibility of the design. In most cases where ships are subjected to these restriction, the ship dimensions are selected to be the maximum allowable dimensions to have the highest space utilization possible. As a result, the main dimensions are not optimized for propulsion power as done in the design impact model, but rather must commit to geometry shape aspects to reduce ship resistance. For example, Suezmax and Panamax vessels have dimensions that are slightly lower than the maximum requirement to pass through the Suez and Panamax canal. An example from the generated ship design that is probably not feasible is the container ship OOCL Hong Kong with an original length of 400 m. The new generated lengths overall are therefore higher than 400 m for all AMEC types, but currently there are not any shipping vessels longer than 400 m according to the Clarksons historic data.

Ships currently have a higher bunker capacity than necessary to purchase cheaper fuel oil on its route. According to Terün, Kana and Dekker, a container ship can sail 2.5 times its route to do this [118]. Given the data of the sampled ships, bulk carriers have an average range of 95% of the circumference of the earth (40 075 km), tankers at 75%, container ships at 67%, and TSHDs at 44%. For TSHDs, the range is the lowest as expected because it is not a shipping vessel and therefore does not have a route that passes ports with cheaper fuel. Given the original fuel oil bunker volumes ($V_{BUNK,\ FO}$), power plant efficiencies (η_{PP}) and contained volumetric energy densities ($\rho_{V\ E\ con}$) of the energy carrier types, the approximate ranges per energy carrier and ship type combination are displayed in table 3.11. These ranges are based on continuous service speed at loaded design draft and therefore the ranges are considered to be the minimum distances. The average fuel oil powered container ship can sail 26 914 km and with its bunker capacity of 2.5 its route, the average route is 10 766 km. Therefore the average container ship can still sail

its full route powered by methanol or LNG without altering the ship design. Ammonia powered container ships can sail approximately 70% of the route and thus only needs minor additional bunker capacity. For container ships powered by liquid hydrogen and electrically charged lithium ion batteries there is significant additional bunker capacity necessary to accommodate the full route, however considerably less than the 1.5x overcapacity.

Table 3.11: The average approximate ranges per energy carrier and ship type combination for equal contained bunker volume

	Range	Bulk carriers (km)	Tankers (km)	Container ships (km)	TSHDs (km)
Fuel oil (original)	100%	38163	30174	26914	13955
Methanol	42%	16206	12813	11429	5926
LNG	40%	15417	12190	10872	5637
Liq. hydrogen	12%	4448	3517	3137	1626
Ammonia	28%	10690	8452	7539	3909
Elec. + LIB	1%	457	361	322	167

To determine the design impact and powering impact of a reduced bunkering capacity to sail the range of its route, the original fuel oil bunker volume has been reduced to 40% (1/2.5). In the reduced bunkering capacity case, all shipping vessels and half of the TSHDs have a positive freeboard (f) in the battery electric case. For all ship types and energy carrier combinations, the additional overall internal volume (ΔV_{INT}) is reduced by a minimum of 59% and a maximum of 84%. Moreover, the additional lightweight ship (Δm_{LIGHT}) is reduced by a minimum of 61% and a maximum of 79%. Likewise for the deadweight tonnage (DWT), the reduction is consistently $\sim$60%.

On the contrary, it is also possible that future ship designs powered by AMECs need more than 2.5 times the effective energy to sail their current route due to lower supply distribution around the world. For example, if a certain AMEC is only available in a certain part of the world, there is a high dependency on that location. Therefore it would be wise to have an even higher bunker overcapacity to minimize the chances of running out of bunkering. In this case, ship designs will be even more voluminous and heavier than the current design generation model produces. Consequently, it also causes an even higher energy consumption.

In conclusion, the design impact method is modeled in accordance with historic ship dimension data for fuel oil powered ships. In fuel oil powered ships, the fuel tanks are located inside the main hull and therefore the design impact method is modeled in that manner as well. However, the location of the AMEC tanks are not necessarily located within the main hull and thus the model can generate unrealistic designs. Additionally, the model is constructed under the assumption that the original overall internal ship volume does not have excess/redundant volume to accommodate for additional AMEC bunker volume. Accordingly this results in overestimated necessary additional overall internal volume for the new generated ship designs. Nonetheless, the new designs are generated to have the least additional resistance and therefore not taking into account the applicability of the additional volume in the designs. For this same reasoning it is questionable if small necessary additional overall internal volumes should be applied to the design.

The design impact method first increases the length and thereafter the beam for ships with a lower length-beam ratio than the determined maximum length-beam ratio. For ships with a higher length-beam ratio than the determined maximum length-beam ratio, the beam was increased first to accommodate the additional volume. As a result, the model does not generate a slender body design. Consequently, the resulting final main engine brake power (propulsion power) of the ships with higher length-beam ratios than the determined maximum were significantly higher than the ships with lower length-beam ratios than the determined maximum. This validates that slender body ship designs have a lower total ship resistance which is applied in the model. There are four sampled TSHDs with significantly higher length-beam ratios than the determined maximum length-beam ratio which cause the powering impact results to be considerably higher for all AMEC types. As a result, the additional overall internal volume and additional lightweight ship are relatively higher than for other ship types in the second step of the design impact (upscaling bunkering).

It is also questionable if significantly large additional overall internal volumes and large additional lightweight ship should be designed according to the design generation model or even not even consider the AMEC type. In all designs for battery and ship type combinations it results in considerably large and heavy ship that the utilization of the ship's volume is remarkably low or does not even float. Moreover, the generated large and heavy ship designs are less feasible as dimension restrictions for locks, (dry) docks, bridges and port infrastructure exist, which were not taken into account for the operational requirements. One of the constant operational requirements is to maintain the original sailing range, however fuel oil powered shipping vessels have higher bunker capacities to purchase cheap on their route. Their sailing range is estimated to be 2.5 times their route distance and it results in a significant increase in overall internal volume, lightweight ship and necessary propulsion power. However, ships powered by methanol and LNG with equal fuel oil bunker volume can sail their full route distance. consequently the full powering impact assessment was conducted with a 40% (1/2.5) fuel oil bunker volume. As a result, for all energy carrier and ship type combinations the additional overall internal volume is reduced by a minimum of 59% and a maximum of 84%. Moreover, the additional lightweight ship is reduced by a minimum of 61% and a maximum of 79%. Likewise for the deadweight tonnage (DWT), the reduction is consistently $\sim$60%. However, due to possible uneven distribution of AMEC supply around the world the world, the the AMEC bunker supply in ships could also be higher in future ship designs. In this case, ship designs will be even more voluminous and heavier than the current design generation model produces. Consequently, it also causes an even higher energy consumption.

3.4. Sensitivity analysis powering impact assessment

The resistance approximation method, the powering approximation method and the design impact method of the total ship powering impact assessment generation contribute to the total powering impact. However, the decisions made in the resistance and powering approximation methods for efficiencies and factors barely have an impact on the total powering impact. The ship design impact assessment does contain highly sensitive parameters which influence the total powering impact.

Within the common ship design impact method, the chosen maximum length-beam ratio of a ship type ($L_{OA}/B_{MAX,\ ship\ type}$) significantly influences the total powering impact. As an example, a 0.01 decrease in the directional coefficient (a) of the maximum length-beam formula, results in an increase of propulsion power for all energy carrier and ship type combinations. On average the propulsion power increases with 0.3% for methanol, 8.5% for LNG, 8.0% for liquid hydrogen, 8.3% for ammonia, and 1.2% for battery electric. For a 0.01 increase, on average the propulsion power barely changes with a slight increase of <0.15% for methanol, LNG, liquid hydrogen, and ammonia. However, for battery electric the propulsion power decreases with 47.2%. By increasing the initial value (b) of the maximum length-beam formula by 1%, the propulsion power barely changes with <0.25%, except for battery electric which decreases with 4.0%. By decreasing the initial value (b) of the maximum length-beam formula by 1%, the propulsion power barely changes with <0.25%, except for battery electric which increases with 3.5%.

In the allocation of bunkering share based on the brake powers of the main and auxiliary engine in the most energy consuming operational mode influences the total powering impact significantly. For example, TSHDs do not spend most of their time in the most energy consuming mode. By increasing the bunker space share with 50% to the main engine, the total powering impact increases for all AMECs. The total powering impact increases by $\sim$1% for methanol, $\sim$1% for LNG, $\sim$6% for hydrogen, $\sim$2% for ammonia, and $\sim$128% for batteries.

In the common ship design impact, the power plant efficiency of an AMEC effects the total powering impact. For example, the determined efficiency of the hydrogen power plant is 43.88% with a lower value of 42.23% and a higher value of 45.32%. In bulk carriers, the total powering impact increases by $\sim$2% for the lower efficiency and decreases by $\sim$2% for the higher efficiency.

4

Environmental impact assessment resistance, powering and design sub-models

The main objective of the environmental impact assessment is to determine and quantify the net environmental effects the selected energy carriers for equal energy content. The environmental impact of an energy carrier is assessed as a conceptual life cycle assessment. A conceptual life cycle assessment (LCA) is only performing the assessment of a part of a life cycle (gate-to-gate). In this case it is the operational stage of a ship with various energy carriers.The outcome of an LCA is the life cycle impact assessment (LCIA) in which the environmental effects are quantified per category. In this chapter the LCA generation is explained concerning the model, method and setup. Thereafter the approach to the life cycle inventory (LCI) per energy carrier is established. It is followed up by the gross and net LCIA results from the ReCiPe LCA method and power plant efficiency for the two energy carriers per energy carrier type. The gross and net results of each of the twelve energy carriers are given in the midpoint and endpoint impact category. The gross and net environmental impact results are then compared to literature for verification. Finally, the powering impacts per energy carrier type and ship type combination are introduced to the net LCIA results for the final environmental impact.

4.1. Model description

The environmental impact assessment model is significantly less complex than the powering impact assessment model. The environmental impact assessment model uses the LCA results for the selected energy carriers from a database. Together with the uncontained energy density, the environmental effects are determined for equal energy content. Thereafter the power plant efficiency is taken into account which yields the net environmental impact of the selected energy carriers for equal energy content. The final step is incorporating the powering impact assessment results per energy carrier and ship type combination. The final result is the environmental impact per energy carrier and ship type combination with respect to conventional fuel oil powered ships.

4.1.1. LCA method description

The assessment is done with the software SimaPro 9 which incorporates the collecting, analyzing and monitoring of the environmental performance of a service or product. The life cycle assessment method performed is ReCiPe 2016 V1.05 and it is developed by PRé Sustainability. The ReCiPe 2016 method can display the results in the eighteen midpoint categories and in the three endpoint areas of protection. The level of accuracy for endpoint area of protection is lower due to the use of a conversion factor from midpoint to endpoint. However, with only three endpoints the results are easier to distinguish rather than eighteen. For the reason of accuracy and ease, both midpoint and endpoint results are generated.

Within ReCiPe 2016 there are three perspectives for the characterization factor values as each perspective has its own time frame and impact within it. The hierarchist (H) perspective is selected as it is based

on a scientific consensus and in agreement of the plausibility of the impact mechanisms in a 100 year time horizon. The other two are the individualist and egalitarian perspectives. The individualist perspective is established on the basis of short term interests with environmental impacts that are acknowledged and it includes an optimistic stance towards human adaptation and technological solution generation. The egalitarian perspective takes into account the longest time frame and therefore it is the most precautionary.

To perform the life cycle assessment a life cycle inventory analysis (LCI) is done. It consists of compiling the inventory process data sets for the in- and output materials, energy, resources and emissions. Major components of this phase include process identification, planning and collection of data, constructing and quality check of the data, uncertainty preparation, and reporting [50]. Luckily the whole production process of the energy carriers does not have to be studied as existing LCI entry data exist. In these LCI databases the final energy carrier can already be present with its accompanying inputs and outputs. In some cases the energy carrier does not exist and therefore it must be fabricated with materials and processes that are available.

The impact magnitude can differ for the same process based on its location in the world. Therefore the listed process entries in the database are assigned to the location of where the LCA study was conducted. However, shipping vessels travel across the globe and are thus not subjected to a specific area. Fortunately many process entries are listed as a weighted global average (GLO) or they are extrapolated from a local process entry to the rest of the world (RoW). To apply the global impact of the energy carriers, only GLO and RoW process entries are selected if available.

Carbon sequestration, the process of capturing and storing atmospheric carbon dioxide by biomass, cannot be generated in the LCA. Accordingly, it can be perceived that the captured carbon from the atmosphere is returned back when combusted and therefore the net CO_2 change to the atmosphere is zero. This net zero change principle can also be applied to other substances from the atmosphere and biosphere. To apply this principle in the LCA, the combustion of the biofuels is not modeled. This does not yield a fully accurate result as the combustion can produce other (harmful) substances than the original captured substance.

4.1.2. LCA comparison issues

The LCI database in SimaPro 9 is compromised of many different libraries. In general, each library has its own theme which contains a list of processes to support the common subject. The in- and outputs per process are already predetermined, however the LCIA results are generated based on the LCA method. All the listed processes originate from a unique LCA study where all the input and outputs of substances and energy are measured. Consequently it causes issues if the scope of an LCA study is different for the same process. Despite the fact that the process is the same, the LCIA results are different. This scope discrepancy issue can be mitigated by using the same library because the library is governed by a single organisation. In general, the organisation will have a consistent guideline and approach to performing the LCA study. Therefore, this research strives to use a single library if possible. As mentioned in section 1.6.3, the Ecoinvent 3 database/library is the most consistent and popular database with high quality data with varying themes. Accordingly, the Ecoinvent 3 database is the preferred library.

An additional comparison issue is the varying source and production of the alternative energy carrier within an energy carrier type. The first energy carrier of the six energy carrier types is considered the conventional kind which is fossil sourced. There is less variety in the extraction, production and processing method of fossil sourced energy carriers than the bio or renewable version. For example, conventional diesel originates from crude oil wells and it is produced through the distillation process at refinery plants. This simplified example is the norm globally. However, biodiesel can be produced from various sources through various production processes and procedures. Therefore, there are significantly more well-to-tank pathways for the alternative version than the conventional fossil version. As a result, the selected process in the LCI database will not yield a generalized outcome for bio fuels. Accordingly, the bio- and renewable version of the energy carrier type should rather be consider a case study. There is not any real mitigation strategy to this pathway discrepancy issue. However, it can be considered that selecting a bio/renewable process with the highest production volume has the highest contribution towards the

general outcome of an alternative energy carrier type. Unfortunately, it is not possible to sort processes by production volume, but the Ecoinvent 3 database primarily does not contain processes of low volumes.

4.2. Gross LCIA results per (A)MEC type

Some (alternative) marine energy carriers are listed in the LCI databases and some are not. For the energy carriers that are not listed in the databases, literature of the production process is used to fabricate the entry. In this section, the six energy carrier types are investigated for two different sources. The first source is the traditional source which is fully or predominantly from fossil origins. The second source is considered to be the natural source which originates from biomass or renewable energy. To compare their impact on the environment, all energy carriers are in the same unit of comparison in mega joules (MJ). The database entries are listed as environmental impact per volume (m^3) or per weight (kg). Together with the uncontained gravimetric and volumetric energy densities of the energy carriers, they are all adjusted to 1 MJ. The LCIA results are displayed per energy carrier type from two sources in midpoint impact categories and in endpoint areas of protection. The power plant efficiencies are not taken into account yet in the results and therefore the results are the gross impact per 1 MJ.

4.2.1. Fuel oil

Fuel oil is the conventional energy carrier of the maritime industry of which very low sulphur fuel oil (VLSFO) is the most sold kind in the port of Rotterdam [51]. However this fuel oil kind is not available in the LCI databases. Diesel is a comparable fuel oil which is produced in the same process, has a similar chemical composition and equal uncontained energy density. Both the production of diesel and biodiesel are available in the databases and thus these entries will be used. The regular diesel is listed as low sulfur diesel and it includes combustion. It is from the IDEMAT 2022 V2.1 database. The biodiesel is listed as vegetable oil methyl ester for the global market and it is from the Ecoinvent 3 database. 1 kg of each entry is added to the inventory and with the uncontained gravimetric energy density, it yields the impact for 1 MJ. The environmental impact of the production and combustion of 1 MJ fossil diesel and production of biodiesel at midpoint and endpoint are displayed in table 4.1.

Table 4.1: Fuel oil LCIA at midpoint and endpoint for 1 MJ - ReCiPe 2016 (H)

Midpoint impact category	Unit	Diesel	Bio diesel
Global warming	kg CO_2 eq	8.95E-02	6.52E-02
Stratospheric ozone depletion	kg CFC-11 eq	1.82E-08	4.23E-07
Ionizing radiation	kBq Co-60 eq	2.43E-05	1.00E-03
Ozone formation (human health)	kg NO_X eq	3.21E-05	1.00E-04
Fine particulate matter formation	kg $PM_{2.5}$ eq	1.96E-05	8.03E-05
Ozone formation (ecosystems)	kg NO_X eq	3.38E-05	1.05E-04
Terrestrial acidification	kg SO_2 eq	7.47E-05	3.04E-04
Freshwater eutrophication	kg P eq	7.62E-08	1.19E-05
Marine eutrophication	kg N eq	1.35E-06	1.32E-04
Terrestrial ecotoxicity	kg 1,4-DCB	4.87E-03	6.35E-02
Freshwater ecotoxicity	kg 1,4-DCB	5.13E-06	1.02E-03
Marine ecotoxicity	kg 1,4-DCB	6.69E-05	1.22E-03
Human carcinogenic toxicity	kg 1,4-DCB	7.23E-06	1.63E-03
Human non-carcinogenic toxicity	kg 1,4-DCB	1.10E-02	6.57E-02
Land use	m^2 a crop eq	8.20E-03	1.20E-01
Mineral resource scarcity	kg Cu eq	6.03E-06	1.07E-04
Fossil resource scarcity	kg oil eq	2.63E-02	6.96E-03
Water consumption	m^3	2.82E-07	1.00E-03
Endpoint area of protection	**Unit**	**Diesel**	**Bio diesel**
Human health	DALY	9.81E-08	1.32E-07
Natural environment	Species x yr	3.44E-10	1.35E-09
Resource scarcity	USD (2013)	1.18E-02	2.37E-03

1 MJ = 0.2778 kWh

4.2.2. Methanol

For the energy carrier type methanol, both the production process of fossil methanol and bio methanol are available in the databases. The production of fossil methanol is listed as methanol production for the global market and the production of the bio methanol is listed as methanol production from synthetic biomass. Both are form the Ecoinvent 3 database. 1 kg of each is added to each inventory. Methanol requires a pilot fuel to improve the combustion process of which 1% of fuel oil by weight is sufficient [20]. Consequently the inventory of both energy carriers are multiplied by 99% and 0.01 kg of fossil diesel is added to the fossil methanol inventory, and 0.01 kg of bio diesel is added to the bio methanol inventory.

The combustion of the fossil methanol is fabricated by using the fuel conversion factor by the IMO for natural gas which 1.375 kg CO2 / kg methanol [61]. Therefore 99% of 1.375 kg is added to the global warming midpoint impact category. The combustion of the bio methanol is not accounted for since carbon sequestration cannot be generated. Using the uncontained gravimetric energy density yields the environmental impact for 1 MJ. The environmental impact of the production and combustion of 1 MJ fossil methanol and production of bio methanol at midpoint and endpoint are displayed in table 4.2.

Table 4.2: Methanol LCIA at midpoint and endpoint for 1 MJ - ReCiPe 2016 (H)

Midpoint impact category	Unit	Methanol	Bio methanol
Global warming	kg CO_2 eq	1.03E-01	3.45E-02
Stratospheric ozone depletion	kg CFC-11 eq	1.76E-08	2.59E-08
Ionizing radiation	kBq Co-60 eq	5.08E-04	2.69E-03
Ozone formation (human health)	kg NO_X eq	5.64E-05	1.38E-04
Fine particulate matter formation	kg $PM_{2.5}$ eq	2.84E-05	7.48E-05
Ozone formation (ecosystems)	kg NO_X eq	6.09E-05	1.42E-04
Terrestrial acidification	kg SO_2 eq	7.82E-05	1.41E-04
Freshwater eutrophication	kg P eq	2.88E-06	1.50E-05
Marine eutrophication	kg N eq	3.00E-07	5.53E-06
Terrestrial ecotoxicity	kg 1,4-DCB	9.90E-03	9.93E-02
Freshwater ecotoxicity	kg 1,4-DCB	4.72E-04	1.68E-03
Marine ecotoxicity	kg 1,4-DCB	6.38E-04	2.25E-03
Human carcinogenic toxicity	kg 1,4-DCB	1.07E-03	3.31E-03
Human non-carcinogenic toxicity	kg 1,4-DCB	8.93E-03	8.10E-02
Land use	m^2 a crop eq	2.98E-04	1.23E-01
Mineral resource scarcity	kg Cu eq	4.18E-05	1.21E-04
Fossil resource scarcity	kg oil eq	3.76E-02	9.30E-03
Water consumption	m^3	2.18E-04	6.23E-04
Endpoint area of protection	**Unit**	**Methanol**	**Bio methanol**
Human health	DALY	6.50E-08	1.10E-07
Natural environment	Species x yr	1.97E-10	1.26E-09
Resource scarcity	USD (2013)	2.43E-04	2.43E-03

1 MJ = 0.2778 kWh

4.2.3. LNG

For the energy carrier type LNG, both LNG and bio LNG are not available in the databases (in a liquefied state). However, the production of vehicle grade natural gas for the global market and the production of vehicle grade bio methane for the rest of the world market are listed. Both production processes are listed in the Ecoinvent 3 database. 1 kg of each is added to each inventory. According to Mohkatab et al. about 8% of the feed gas to the LNG plants is used for the liquefaction process [100]. Therefore 0.08 kg of natural gas is added to each inventory to produce a net 1 kg of LNG. Like methanol, LNG also requires a pilot fuel to improve the combustion process of which 1% of fuel oil by weight is sufficient [20]. Consequently the inventory of both energy carriers are multiplied by 99% and 0.01 kg of fossil diesel is added to the fossil natural gas inventory, and 0.01 kg of bio diesel is added to the bio natural gas inventory.

The combustion of the fossil natural gas is fabricated by using the fuel conversion factor by the IMO

for natural gas which 2.75 kg CO2 / kg natural gas [61]. Therefore 99% of 2.75 kg is added to the global warming midpoint impact category. The combustion of the bio natural gas is not accounted for since carbon sequestration cannot be generated.

Lastly, approximately 1.6% of methane slips during the combustion process as described in section 2.1.3. 1.6% might not be much, however the global warming potential of methane is around 35 times more effective than CO2 in the hierarchist perspective of ReCiPe 2016. Therefore 1.6% of 1 kg of natural gas is equal to 35 times 0.016 kg of CO2 to global warming. Using the uncontained gravimetric energy density yields the environmental impact for 1 MJ. The environmental impact of the production, combustion and slip of 1 MJ fossil LNG and production and slip of bio LNG at midpoint and endpoint are displayed in table 4.3.

Table 4.3: LNG LCIA at midpoint and endpoint for 1 MJ - ReCiPe 2016 (H)

Midpoint impact category	Unit	LNG	Bio LNG
Global warming	kg CO_2 eq	8.28E-02	3.27E-02
Stratospheric ozone depletion	kg CFC-11 eq	1.16E-08	1.21E-08
Ionizing radiation	kBq Co-60 eq	7.99E-04	1.44E-03
Ozone formation (human health)	kg NO_X eq	3.49E-05	3.22E-05
Fine particulate matter formation	kg $PM_{2.5}$ eq	2.55E-05	3.17E-05
Ozone formation (ecosystems)	kg NO_X eq	3.75E-05	3.27E-05
Terrestrial acidification	kg SO_2 eq	5.98E-05	5.97E-05
Freshwater eutrophication	kg P eq	3.20E-06	6.28E-06
Marine eutrophication	kg N eq	3.17E-07	1.59E-06
Terrestrial ecotoxicity	kg 1,4-DCB	5.43E-03	1.26E-02
Freshwater ecotoxicity	kg 1,4-DCB	2.21E-04	6.52E-04
Marine ecotoxicity	kg 1,4-DCB	3.20E-04	8.41E-04
Human carcinogenic toxicity	kg 1,4-DCB	7.99E-04	9.51E-04
Human non-carcinogenic toxicity	kg 1,4-DCB	6.55E-03	1.30E-02
Land use	m^2 a crop eq	1.92E-04	2.37E-03
Mineral resource scarcity	kg Cu eq	1.45E-05	2.58E-05
Fossil resource scarcity	kg oil eq	2.70E-02	4.91E-03
Water consumption	m^3	5.05E-05	1.04E-04
Endpoint area of protection	**Unit**	**LNG**	**Bio LNG**
Human health	DALY	5.67E-08	5.33E-08
Natural environment	Species x yr	1.32E-10	1.25E-10
Resource scarcity	USD (2013)	9.42E-03	1.23E-03

1 MJ = 0.2778 kWh

4.2.4. Liquid hydrogen

For the energy carrier type hydrogen, only the production of liquid fossil hydrogen is available and thus the renewable liquid hydrogen is fabricated. The fossil liquid hydrogen is listed as liquid hydrogen for the rest of world market and it originates from the Ecoinvent 3 database. Hydrogen can be produced from pure water and electricity through the process of electrolysis. To fabricate renewable liquid hydrogen, 9 kg of ultrapure water is necessary to produce 1 kg of hydrogen based on its molar mass. According to Bossel and Eliasson, the energy cost of electrolysis, liquefaction, distribution, storage, and transfer is 2.12 times the higher heating value (HHV) of hydrogen [16]. Ultrapure water is listed in the Ecoinvent 3 database and 9 kg is added to the inventory. The electrical renewable energy originates from the Ecoinvent 3 database as well and is listed as high voltage electricity from wind power. Accordingly 2.12 times the higher heating value of 39.4 kWh/kg for 1 kg of hydrogen is added to the inventory from wind power. There is no combustion in the fuel cell power plant, but there is an electrochemical reaction which only emits pure water. Using the uncontained gravimetric energy density yields the environmental impact for 1 MJ. The environmental impact of the production and use of 1 MJ fossil and renewable hydrogen at midpoint and endpoint are displayed in table 4.4.

Table 4.4: Hydrogen LCIA at midpoint and endpoint for 1 MJ - ReCiPe 2016 (H)

Midpoint impact category	Unit	Hydrogen	Renew. hydrogen
Global warming	kg CO_2 eq	2.08E-02	1.23E-02
Stratospheric ozone depletion	kg CFC-11 eq	5.66E-09	5.37E-09
Ionizing radiation	kBq Co-60 eq	4.33E-04	6.77E-04
Ozone formation (human health)	kg NO_X eq	3.36E-05	3.73E-05
Fine particulate matter formation	kg $PM_{2.5}$ eq	1.97E-05	2.41E-05
Ozone formation (ecosystems)	kg NO_X eq	3.55E-05	3.90E-05
Terrestrial acidification	kg SO_2 eq	4.18E-05	4.25E-05
Freshwater eutrophication	kg P eq	2.62E-06	9.28E-06
Marine eutrophication	kg N eq	2.78E-07	1.48E-06
Terrestrial ecotoxicity	kg 1,4-DCB	8.18E-03	6.35E-02
Freshwater ecotoxicity	kg 1,4-DCB	3.17E-04	6.03E-03
Marine ecotoxicity	kg 1,4-DCB	4.12E-04	7.43E-03
Human carcinogenic toxicity	kg 1,4-DCB	5.79E-04	1.82E-02
Human non-carcinogenic toxicity	kg 1,4-DCB	6.67E-03	2.96E-02
Land use	m^2 a crop eq	1.15E-04	1.02E-03
Mineral resource scarcity	kg Cu eq	1.73E-05	3.00E-04
Fossil resource scarcity	kg oil eq	1.38E-02	3.45E-03
Water consumption	m^3	3.63E-04	2.34E-04
Endpoint area of protection	**Unit**	**Hydrogen**	**Renew. hydrogen**
Human health	DALY	1.93E-08	1.14E-08
Natural environment	Species x yr	5.81E-11	3.45E-11
Resource scarcity	USD (2013)	1.59E-15	9.42E-16

1 MJ = 0.2778 kWh

4.2.5. Ammonia

For the energy carrier type ammonia, only the production of liquid fossil ammonia is available and thus the renewable liquid ammonia is fabricated. The fossil liquid ammonia is listed as liquid anhydrous ammonia from steam reforming for the rest of world market and it originates from the Ecoinvent 3 database. Renewable ammonia can be produced from renewable hydrogen, nitrogen, and renewable electricity through the electrochemical synthesis process. To fabricate ammonia through this process, 0.178 kg of hydrogen and 0.822 kg of nitrogen is necessary to produce 1 kg of ammonia based on the molar masses. Renewable hydrogen was previously fabricated in section 4.2.4 and 0.178 kg is added to the inventory. Liquid nitrogen is available in the Ecoinvent 3 database and it is listed as liquid nitrogen from cryogenic air separation in Europe. 0.822 kg is added to the inventory. According to Soloveichik, the conventional Haber-Bosch process to produce 1 kg ammonia from natural gas uses 7.9 kWh of electricity [116]. A large portion of the energy is for the reforming of the natural gas to remove the carbon and produce nitrogen and hydrogen [44]. The other part of the process is to combine the nitrogen and hydrogen to form ammonia. Soloveichik states that 2.0 kWh/kg of the 7.9 kWh/kg electricity is used for pressurization, heating, pumping and so on. Therefore 5.9 kWh electricity is added to the inventory from the high voltage wind power. Using the uncontained gravimetric energy density yields the environmental impact for 1 MJ. The environmental impact of the production and use of 1 MJ fossil and renewable ammonia at midpoint and endpoint are displayed in table 4.5.

Table 4.5: Ammonia LCIA at midpoint and endpoint for 1 MJ - ReCiPe 2016 (H)

Midpoint impact category	Unit	Ammonia	Renew. ammonia
Global warming	kg CO_2 eq	1.16E-01	2.52E-02
Stratospheric ozone depletion	kg CFC-11 eq	1.44E-08	1.12E-08
Ionizing radiation	kBq Co-60 eq	1.10E-03	5.31E-03
Ozone formation (human health)	kg NO_X eq	1.27E-04	6.57E-05
Fine particulate matter formation	kg $PM_{2.5}$ eq	5.68E-05	4.51E-05
Ozone formation (ecosystems)	kg NO_X eq	1.33E-04	6.82E-05
Terrestrial acidification	kg SO_2 eq	1.63E-04	8.90E-05
Freshwater eutrophication	kg P eq	6.00E-06	1.97E-05
Marine eutrophication	kg N eq	6.82E-07	2.42E-06
Terrestrial ecotoxicity	kg 1,4-DCB	7.32E-02	9.21E-02
Freshwater ecotoxicity	kg 1,4-DCB	2.30E-03	8.52E-03
Marine ecotoxicity	kg 1,4-DCB	2.95E-03	1.05E-02
Human carcinogenic toxicity	kg 1,4-DCB	4.64E-03	2.53E-02
Human non-carcinogenic toxicity	kg 1,4-DCB	3.48E-02	5.09E-02
Land use	m^2 a crop eq	7.36E-04	1.58E-03
Mineral resource scarcity	kg Cu eq	2.74E-04	4.16E-04
Fossil resource scarcity	kg oil eq	4.00E-02	6.95E-03
Water consumption	m^3	2.60E-03	7.38E-04
Endpoint area of protection	**Unit**	**Ammonia**	**Renew. ammonia**
Human health	DALY	1.08E-07	2.34E-08
Natural environment	Species x yr	3.25E-10	7.05E-11
Resource scarcity	USD (2013)	8.88E-15	1.93E-15

1 MJ = 0.2778 kWh

4.2.6. Electrically charged lithium ion batteries

For the energy carrier type li-ion battery (LIB), the electrical charging energy from global mix and renewable energy are both available in the Ecoinvent 3 database. The global mix electricity is listed as high voltage electricity as a global average. The renewable electricity is listed as high voltage wind power imported from Germany to Switzerland. 1 MJ of both sources is added to the inventory. As explained in section 2.1.6, the production of li-ion batteries is extremely energy intensive and it involves extracting many minerals which are reactive and or toxic. Therefore the lithium battery is also included in the inventory. In the IDEMAT 2022 V2.1 database a lithium battery is available. It is listed as Lithium NMC 811 (241 Wh/kg cell). Consequently 1.153 kg is necessary for 1 MJ worth of charge. However, the assumption is made that the battery lasts a full ship service lifetime of approximately 25 years [27]. Moreover, it is assumed that the battery is charged every four weeks (28 days) and thus the battery goes through approximately 326 cycles in its lifetime. This is significantly less than the 50,000 cycle capability and 10 year life expectancy of an existing li-ion battery intended for maritime application by Echandia [33]. Lastly, presumably the battery is recycled for the extraction and recycling of the valuable minerals. According to Jacoby the recycling process is also energy intensive with similar processes as in the production of the batteries [73]. Therefore the battery is not fully allocated to the ship owner but at 75% and the remaining 25% is for the future battery owners. The total environmental impact of 1 MJ of lithium ion battery is thus 435 times less (326/0.75) than a single use charge. Thus 1/435 of the 1.153 kg of the lithium NMC 811 battery is added to the inventory. The environmental impact of 1 MJ charge from global electricity mix and renewable electricity including a single use equivalent of production for the LIB at midpoint and endpoint are displayed in table 4.6.

Table 4.6: Electrically charged li-ion battery LCIA at midpoint and endpoint for 1 MJ - ReCiPe 2016 (H)

Midpoint impact category	Unit	E mix + LIB	E renew + LIB
Global warming	kg CO_2 eq	3.08E-01	1.18E-01
Stratospheric ozone depletion	kg CFC-11 eq	8.42E-08	9.16E-09
Ionizing radiation	kBq Co-60 eq	2.38E-02	2.82E-04
Ozone formation (human health)	kg NO_X eq	5.03E-04	9.54E-05
Fine particulate matter formation	kg $PM_{2.5}$ eq	5.66E-04	1.50E-04
Ozone formation (ecosystems)	kg NO_X eq	5.09E-04	9.93E-05
Terrestrial acidification	kg SO_2 eq	1.12E-03	4.94E-04
Freshwater eutrophication	kg P eq	9.45E-05	2.30E-06
Marine eutrophication	kg N eq	6.62E-06	4.61E-07
Terrestrial ecotoxicity	kg 1,4-DCB	1.32E-01	4.53E-02
Freshwater ecotoxicity	kg 1,4-DCB	3.30E-03	2.40E-03
Marine ecotoxicity	kg 1,4-DCB	4.59E-03	2.99E-03
Human carcinogenic toxicity	kg 1,4-DCB	8.67E-03	7.28E-03
Human non-carcinogenic toxicity	kg 1,4-DCB	1.41E-01	1.25E-02
Land use	m^2 a crop eq	2.68E-03	4.26E-04
Mineral resource scarcity	kg Cu eq	1.62E-03	1.66E-03
Fossil resource scarcity	kg oil eq	8.39E-02	3.63E-02
Water consumption	m^3	1.45E-03	5.92E-05
Endpoint area of protection	**Unit**	**E mix + LIB**	**E renew + LIB**
Human health	DALY	7.04E-07	2.31E-07
Natural environment	Species x yr	1.26E-09	4.56E-10
Resource scarcity	USD (2013)	2.39E-02	1.53E-02

1 MJ = 0.2778 kWh

4.2.7. Compiled gross and net LCIA results all (A)MECs

The LCIA results of all the (alternative) marine energy carriers for 1 MJ ($LCIA_{\ MJ\ (A)MEC\ GROSS}$) are displayed in the appendix in table E.1. The results are displayed in midpoint impact categories and endpoint areas of protection according to the hierarchist perspective (H) of the ReCiPe 2016 method. The CII regulation will go into effect in 2023 and its purpose is to combat global warming by reducing green house gas emissions. However, the regulation only accounts for the direct green house gas emissions from the energy carrier use in ships, but not the emissions from production. If the total emissions from the AMEC production and use surpass that of conventional fuel oil, the purpose of the regulation will not be achieved. According to the midpoint impact category *Global warming* results in table E.1, fossil methanol, fossil ammonia, electricity mix + LIB, and electricity renew + LIB perform worse than conventional diesel in this category.

The LCIA results of all the (alternative) marine energy carriers for 1 MJ in table E.1 do not take into account the power plant efficiency of the energy carrier type ($\eta_{PP,\ EC}$). A more efficient power plant is better at converting the chemical energy (1 MJ) of the (A)MEC into mechanical or electrical energy. Therefore the LCIA results for 1 MJ are revised to include the power plant efficiency ($LCIA_{\ MJ\ (A)MEC\ NET}$) and are displayed in table E.2 in the appendix. By taking the power plant efficiency into account, the unit of comparison is per 1 MJ of engine/motor shaft output. According to the midpoint impact category *Global warming* results in table E.2, electricity renew + LIB now performs better than conventional diesel in this category. The other AMECs that performed worse than conventional diesel previously still perform worse. The results of the three endpoint areas of protection are visualized for the impact of 1 MJ of LHV ($LCIA_{\ MJ\ (A)MEC\ GROSS}$) and compared to 1 MJ shaft output ($LCIA_{\ MJ\ (A)MEC\ NET}$).

Human health

The LCIA results for human health area of protection with the characterization factor disability-adjusted loss of life years (DALY) are visualized in figures 4.1 and 4.2. The results are compared per 1 MJ excluding and including the power plant efficiency. The least damaging energy carrier to human health is renewable

hydrogen including the power plant efficiency with 3.59E-08 DALY. The most harmful energy carrier to human health is the electricity mix + LIB including the power plant efficiency with 8.53E-07 DALY. This is a factor of 24 times more harmful.

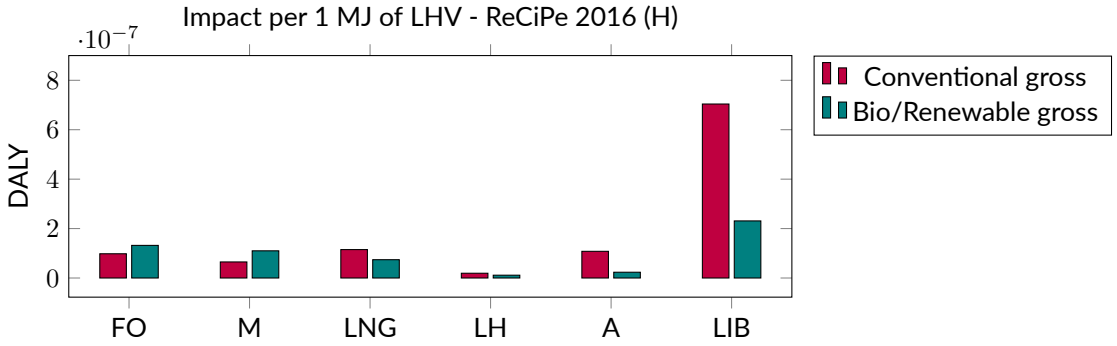

Figure 4.1: Gross human health impact by (A)MECs

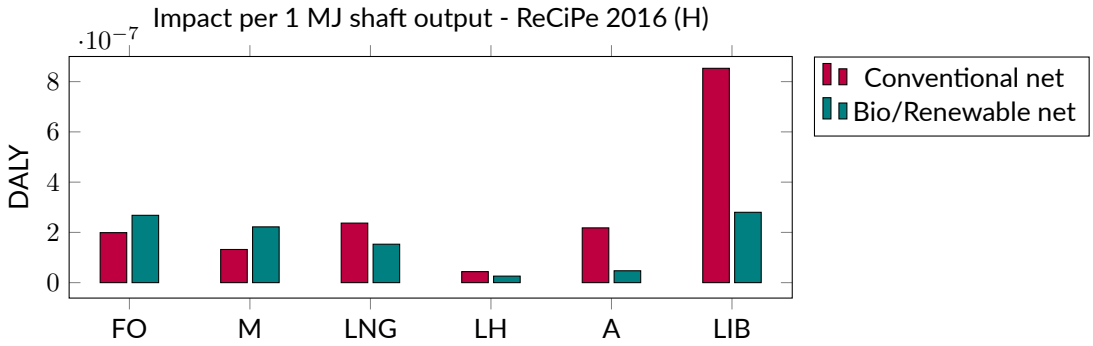

Figure 4.2: Net human health impact by (A)MECs

Natural environment

The LCIA results for natural environment area of protection with the characterization factor time-integrated species loss (Species x Year) are visualized in figures 4.3 and 4.4. The results are compared per 1 MJ excluding and including the power plant efficiency. The least damaging energy carrier to the natural environment is once again renewable hydrogen including the power plant efficiency with 1.08E-10 species x year. The most harmful energy carrier to the natural environment is bio diesel including the power plant efficiency with 2.73E-09 Species x Year. This is a factor of 25 times more harmful.

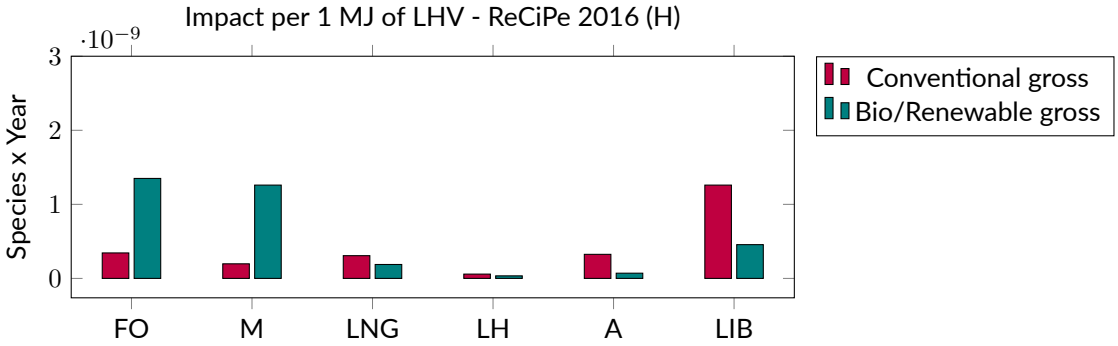

Figure 4.3: Gross natural environment impact by (A)MECs

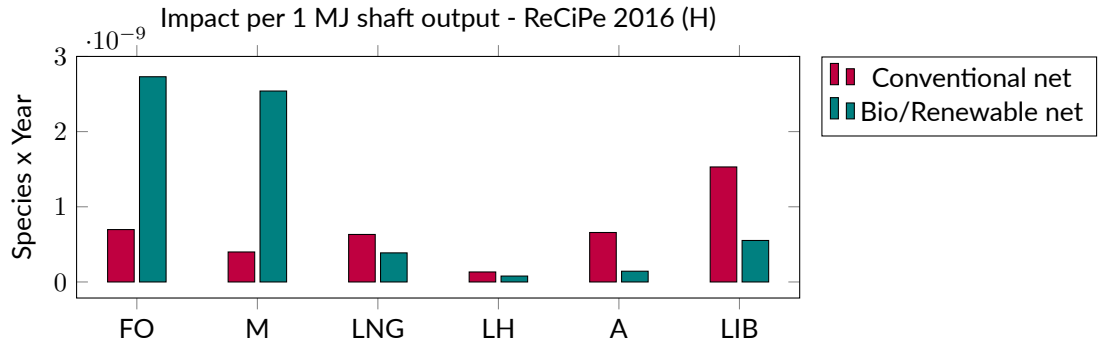

Figure 4.4: Net natural environment impact by (A)MECs

Resource scarcity

The LCIA results for the resource scarcity area of protection with characterization factor surplus cost of extraction (USD) are visualized in figures 4.5 and 4.6. The results are compared per 1 MJ excluding and including the power plant efficiency. The least damaging energy carrier to resource scarcity is the electricity mix + LIB including the power plant efficiency with 2.89E-02 USD. The most harmful energy carrier to resource scarcity is renewable hydrogen including the power plant efficiency with 2.96E-15 USD. This is a factor of 9.8 billion times more harmful.

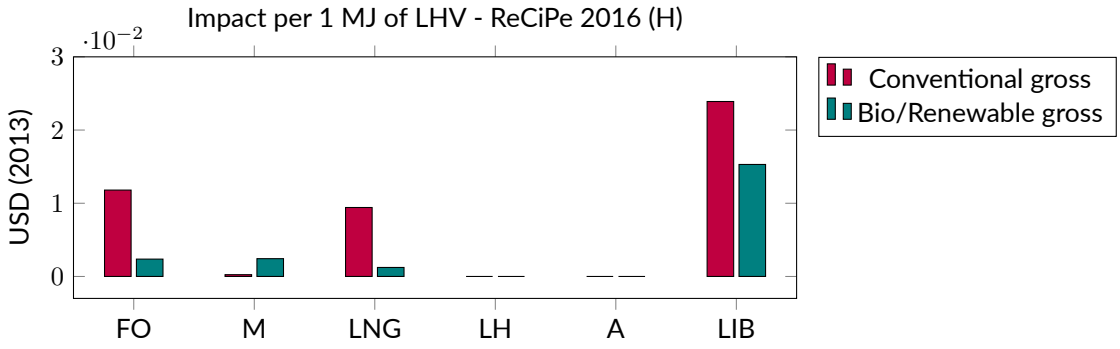

Figure 4.5: Gross resource scarcity impact by (A)MECs

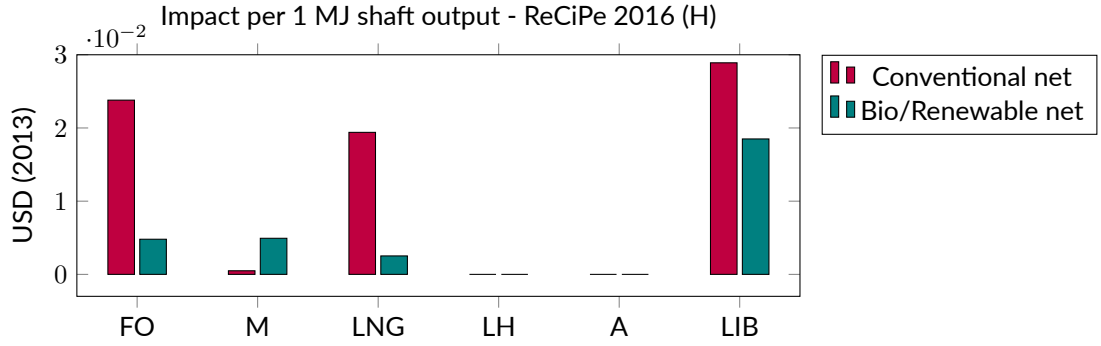

Figure 4.6: Net resource scarcity impact by (A)MECs

4.2.8. Verification

In order to verify the results, the net midpoint global warming impact per MJ shaft output value of the various energy carriers is used to compare to literature results. The 2019 report 'Comparison of Alternative Marine Fuels' by the classification organization DNV-GL [30] and the 2021 study titled 'Reduction of maritime GHG emissions and the potential role of E-fuels' by Lindstadt et al. [88] are used to conduct the verification. Both sources provide the well-to-wake (WTW) CO_2 equivalent emissions per energy carrier.

The energy densities of various energy carrier types and power plant efficiencies of various power plant types are taken into account. This is identical to the method in this research. The use of CO_2 equivalent emission data is different in the two sources. The report by DNV-GL does not mention using LCA results in their methodology, yet does use more than 100 sources to assess the GHG emissions. Many of these sources are LCA studies on energy carriers. The study by Lindstadt et al. does conduct an LCA in a 100 year time horizon which is also identical to the LCA method in this research. The report by DNV-GL does not specify a time horizon, but provides the emission data as an average and range. Both sources present their emission data as the global average, also identical to this research.

The global warming midpoint impact category in this research is the equivalent to the well-to-wake global warming potential in the two sources. The current unit of 'kg CO_2 eq/MJ shaft output' are adjusted to unit of 'g CO_2 eq/kWh shaft output' of the two sources. The global warming potential of the lithium ion batteries are excluded to coincide with the results exclusively for the electricity mix. The results of DNV-GL and Lindstadt et al. are displayed in figures 4.7 and 4.8 respectively. The resulting well-to-wake grams of CO_2 equivalent per kWh shaft output of this research are displayed in table 4.7. DNV-GL provides their results in a range and weighted average while Lindstadt et al. provide their results as a single value. Each source does not provide all the results for all the energy carrier and power plant combination in this research. Therefore both are necessary for verification. The calculated results are in agreement if they are within the given range by DNV-GL and/or within 10% range of the single value from Lindstadt et al.

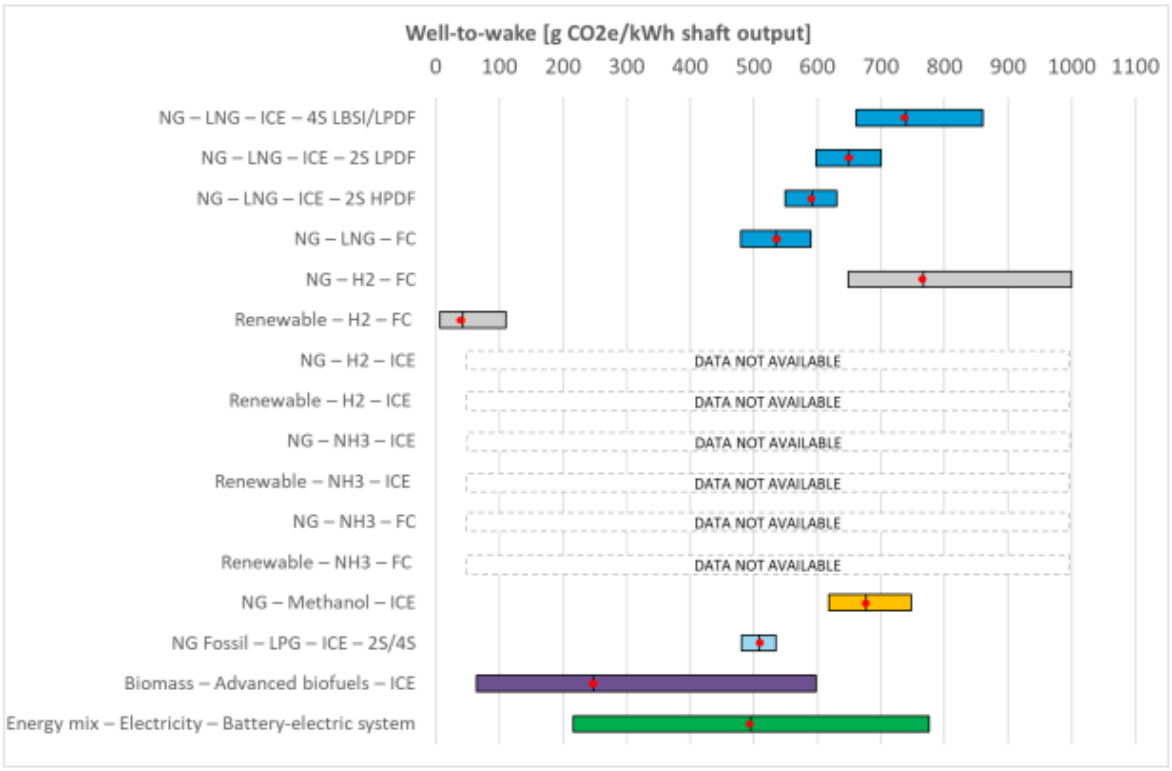

Figure 4.7: Well-to-wake CO_2e emissions for various energy carrier and power plant pathways [30]

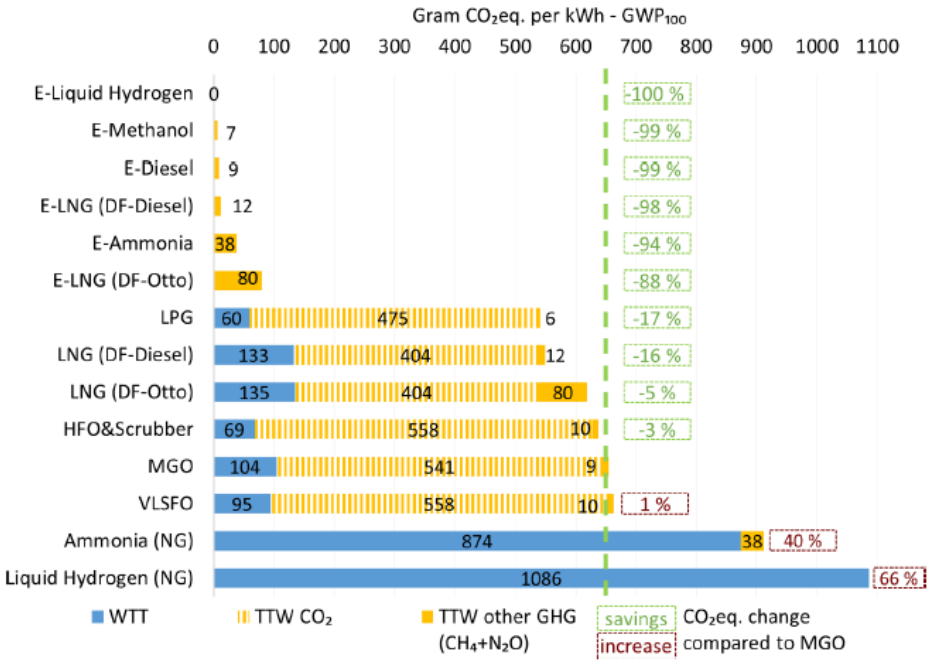

Figure 4.8: Well-to-wake CO_2e emissions for various energy carrier and power plant pathways [88]

Fuel oil Conventional and bio fuel oil result in 653 and 476 WTW g CO_2e/kWh shaft output respectively. Only the study by Lindstadt et al. provide a value for conventional fuel oil (HFO&Scrubbers, MGO, VLSFO), ranging from 637 to 663 WTW g CO_2e/kWh shaft output. Therefore the results for conventional fuel oil are in agreement with the literature. Only DNV-GL provides a value/range for advanced bio fuels which is approximately between 75 and 600 with a weighted average of 240 WTW g CO_2e/kWh shaft output. Therefore the results for bio fuel oil are in agreement with the literature. However, the range for advanced bio fuels is significantly larger compared to the conventional fossil fuels in the report. This is most likely due to the high susceptibility for the pathway discrepancy issue by bio fuels, explained in section 4.1.2.

Methanol Conventional and bio methanol result in 750 and 252 WTW g CO_2e/kWh shaft output respectively. Only the report by DNV-GL provides a value for conventional methanol, ranging approximately between 620 and 760 with a weighted average of 670 WTW g CO_2e/kWh shaft output. Therefore the results for conventional fuel oil are in agreement with the literature. Both sources do not specifically provide a value for bio methanol, however when comparing to the value/range by DNV-GL for advanced bio fuels, it is in agreement with the literature.

LNG Conventional and bio LNG result in 614 and 243 WTW g CO_2e/kWh shaft output respectively. Both sources provide a value/range for conventional LNG. DNV-GL provides two ranges for two stroke configuration with a combined approximate range between 550 and 700 with a combined weighted average of 625 WTW g CO_2e/kWh shaft output. Lindstadt et al. provide a value of 549 WTW g CO_2e/kWh shaft output for the conventional LNG diesel cycle, which is within a 10%. Therefore the results for conventional LNG are in agreement with the literature. Both sources do not specifically provide a value for bio LNG, however when comparing to the value/range by DNV-GL for advanced bio fuels, it is in agreement with the literature.

Liquid hydrogen Conventional and renewable liquid hydrogen result in 170 and 101 WTW g CO_2e/kWh shaft output respectively. Both sources provide a value/range for conventional and renewable liquid hydrogen. DNV-GL provides a value for conventional liquid hydrogen, ranging approximately between 650 and 1000 with a weighted average of 775 WTW g CO_2e/kWh shaft output. Lindstadt et al. provide a value of 1086 WTW g CO_2e/kWh shaft output for conventional liquid hydrogen. The values/ranges

by both sources are five to six times higher and therefore the results for conventional liquid hydrogen are conflicting with literature. DNV-GL provides a value for renewable liquid hydrogen, ranging approximately between 0 and 115 with a weighted average of 40 WTW g CO_2e/kWh shaft output. Lindstadt et al. also provide a value of 0 WTW g CO_2e/kWh shaft output for renewable liquid hydrogen. A value of 0 is not considered accurate as can be seen that the well-to-tank (WTT) emissions are not taken into account for the renewable energy carriers (E-fuels). Therefore the results for renewable liquid hydrogen are considered in agreement with the literature.

Ammonia Conventional and renewable ammonia result in 813 and 176 WTW g CO_2e/kWh shaft output respectively. Only Lindstadt et al. provide a value for these energy carriers, however it is calculated for an ICE configuration compared to a fuel cell configuration in this research. Therefore only the results for WTT are compared as the overall power plant efficiency is similar (51% vs 50%). Since the WTT emissions are not taken into account for the renewable energy carriers, it does not yield a conclusive result. The WTT value by Lindstadt et al. for conventional ammonia is 874 WTW g CO_2e/kWh shaft output. This is within the acceptable 10% range and therefore the conventional ammonia is in agreement with the literature.

Electricity (no LIB) Conventional and renewable electricity result in 819 and 20 WTW g CO_2e/kWh shaft output respectively. Only DNV-GL provides a value/range for the global electricity mix which is approximately between 210 and 775 with a weighted average of 500 WTW g CO_2e/kWh shaft output. Therefore the result for conventional electricity mix is considered in agreement with the literature, but on the higher end. The range is based regional averages where there can be significant differences within it. DNV-GL states that the minimal value of the range represents Europe as an average, but there are some countries with a near zero emission electricity production. Therefore the calculated result for renewable electricity is in agreement with the literature.

Table 4.7: Well-to-wake g CO_2e/kWh shaft output

Energy carrier type	Conventional	Bio/Renewable
Fuel oil	653	476
Methanol	750	252
LNG	614	243
Liq. hydrogen	170	101
Ammonia	813	176
Electricity (no LIB)	819	20

In agreement | Conflicting | No data/Inconclusive

4.3. Discussion

In all cases, the bio/renewable energy carrier version has a significant lower net global warming impact compared to its conventional fossil version. This is expected as the focus of bio/renewable versions is generally aimed to combat global warming. However, not every fossil energy carrier version of the alternative energy carrier types has a lower net global warming impact. In other words, not all the other fossil energy carriers have a lower net global warming impact than conventional diesel. Fossil methanol, fossil ammonia and electricity mix including LIB have a greater net global warming impact than conventional fossil diesel. The combustion of bio diesel, bio methanol and bio LNG have not been taken into account because carbon sequestration, the process of capturing and storing atmospheric carbon dioxide by biomass, cannot be modeled. Additionally other substances captured and stored by biomass also cannot be modeled. However, it is still not accurate to fully not include the combustion of these fuels. The outputs/emissions during the use of hydrogen, ammonia and batteries is harmless or non existent and thus this issue is only specific to fuels.

The bio fuel energy carriers (bio diesel, bio methanol and bio LNG) have a lower fossil resource scarcity and a higher mineral resource scarcity compared to its conventional fossil counterpart. This is expected as the bio version does not originate from fossil sources and the cultivation of the biomass requires minerals

to grow. However, only bio methanol results in a higher 'resource scarcity' endpoint impact compared to its conventional fossil counter part. The midpoint impact categories 'fossil resource scarcity' and 'mineral resource scarcity' units are measured in weight whereas the endpoint impact category 'resource scarcity' unit is measured in USD. Therefore it can only be concluded that the price of the extraction of minerals used to produce bio methanol are the significantly high and are specifically used to for the biomass production for methanol. It is however unlikely that the minerals for the cultivation of biomass for methanol highly differ from the minerals for the cultivation of biomass for bio diesel. This is probably due to the LCA scope and pathway discrepancy issue explained in section 4.1.2.

The bio LNG is sourced from bio waste and therefore the environmental impact from the biomass production is not allocated to the waste user. In LCA impact allocation, the user of waste materials does not carry the environmental consequences of the previously caused damages by the used waste material. The production of bio LNG from bio waste is limited by the bio waste production volume. It is not possible to intentionally manufacture bio waste as it would not be considered waste anymore. Therefore the environmental impact of bio LNG exclusively includes the production and distribution processes. It is expected that the supply of bio LNG cannot keep up with the demand of fossil LNG without having to manufacture biomass. Accordingly, the LCIA results for bio LNG from waste materials is less harmful compared to intentionally produced bio mass for bio diesel or bio methanol. This is a prime example of the scope discrepancy issue for comparative LCA studies.

The battery electric operational use in ships does not coincide with the operational use of ships. The lithium ion batteries are modeled to only be charged 326 while they can achieve up to 50 000 cycles. Additionally, the LIBs are modeled to reach the full service life of a ship at 25 years, but the life expectancy of LIBs for maritime application is only 10 years. Therefore the environmental impact of LIBs in shipping vessels is unrealistic from an operational perspective. This does not even incorporate the extreme powering impact results of the battery electric configuration.

The conflicting well-to-wake global warming potential result for conventional liquid hydrogen with literature is surprising as it was expected that there would be less discrepancy in the scope and pathway for conventional energy carriers. The calculated value is three to five lower than the values by DNV-GL and Lindstadt et al. and therefore not reasonably close either. The value calculated by Lindstadt et al. also does not fall between the range of DNV-GL, but it is slightly higher. Therefore, it seems that the global warming potential for conventional liquid hydrogen is inconsistent. Additionally, there is only a single process listed in Ecoinvent 3 for conventional liquid hydrogen, yet it is the most consistent and popular LCI database. Hence, it is questionable where the LCA data originates from or what is included in the scope of the LCA.

4.4. Total environmental impact all (A)MECs

The total environmental impact of an (A)MEC per ship type ($EI_{TOT\ (A)MEC,\ ST}$) is the LCIA result of an (A)MEC including power plant efficiency ($LCIA_{\ MJ\ (A)MEC\ NET}$) multiplied by the average total installed power impact factor per energy carrier type per ship type ($\left(\frac{P_{B\ TOT\ AMEC}}{P_{B\ TOT\ FO}}\right)_{ST}$) according to equation 4.1. The $LCIA_{\ MJ\ (A)MEC\ NET}$ results are displayed in table E.2 in the appendix and are compiled from the individual tables per (A)MEC type in the previous section 4.2. The $\left(\frac{P_{B\ TOT\ AMEC}}{P_{B\ TOT\ FO}}\right)_{ST}$ values are from table 3.9 in section 3.2 and are displayed in table 4.8 below once again. The total environmental impact of an (A)MEC per ship type:

$$EI_{TOT\ (A)MEC,\ ST} = LCIA_{\ MJ\ (A)MEC\ NET} \cdot \left(\frac{P_{B\ TOT\ AMEC}}{P_{B\ TOT\ FO}}\right)_{ST}$$
$$EI_{TOT\ (A)MEC,\ ST} = \frac{LCIA_{\ MJ\ (A)MEC\ GROSS}}{\eta_{PP,\ (A)MEC}} \cdot \left(\frac{P_{B\ TOT\ AMEC}}{P_{B\ TOT\ FO}}\right)_{ST} \tag{4.1}$$

In simple terms, the $LCIA_{\ MJ\ (A)MEC\ NET}$ table E.2 is multiplied by each column of table 4.8 and constructing four results tables per ship type. Table 4.8 is a duplicate of table 3.9 for easy retrieval.

Table 4.8: The average total installed power impact factor per energy carrier type per ship type

	Bulk carriers	Tankers	Container ships	TSHDs
Fuel oil (original)	0.0%	0.0%	0.0%	0.0%
Methanol	+1.9%	+1.6%	+2.6%	+1.5%
LNG	+0.9%	+0.8%	+1.0%	+3.4%
Liq. hydrogen	+8.6%	+7.4%	+8.4%	+8.4%
Ammonia	+3.7%	+3.2%	+4.9%	+5.5%
Elec. + LIB	+235.3%	+234.4%	+190.1%	+249.9%

$\left(\frac{P_{B\ TOT\ AMEC}}{P_{B\ TOT\ FO}}\right)_{ST}$ for fuel oil is 100% and therefore there is no powering impact

The results of the total environmental impact of an (A)MEC per ship type ($EI_{TOT\ (A)MEC,\ ST}$) are displayed in appendix F in table F.1 for bulk carriers, table F.2 for tankers, table F.3, and table F.4 for TSHDs. According to the midpoint impact category *Global warming* results for all ship types, electricity renew + LIB now performs worse again compared to conventional diesel in this category. The other AMECs that performed worse than conventional diesel including the power plant efficiency still perform worse.

4.5. Sensitivity analysis environmental impact assessment

The total environmental impact of an (A)MEC per ship type ($EI_{TOT\ (A)MEC,\ ST}$) is dependent on two intermediate results: $LCIA_{\ MJ\ (A)MEC\ NET}$ and $\left(\frac{P_{B\ TOT\ AMEC}}{P_{B\ TOT\ FO}}\right)_{ST}$. However, both are considerably influenced by the power plant efficiency (η_{PP}). The power plant efficiency parameter functions as a denominator in the powering impact model and especially in the net LCIA results. As a result, the lower the power plant efficiency, the higher the total powering impact and the higher net LCIA results. Nonetheless, as explained in the sensitivity analysis of the powering impact assessment, the power plant efficiency does strongly influence the powering impact results, but to a considerably lesser extent than in the net LCIA results. For example, the optimistic power plant efficiency of liquid hydrogen in bulk carriers results in a $\sim$2 decrease in net total powering impact. The results from the power plant efficiency sensitivity analysis in section 2.1.8 are used to determine the multiplier values for the net LCIA results and presented in table 4.9. The net LCIA results for electrically charged lithium ion batteries could be $\sim$11% higher or lower, depending on the chosen optimistic and pessimistic component efficiencies.

Table 4.9: Power plant efficiency sensitivity on net LCIA results

Energy carrier	Average multiplier	Pessimistic	Optimistic	Half range*	Effect
Fuel oil (original)	2.03	2.03	2.03	0.00	0.0%
Methanol	2.03	2.03	2.03	0.00	0.0%
LNG	2.06	2.09	2.03	0.03	1.5%
Liq. hydrogen	2.28	2.37	2.21	0.08	4.2%
Ammonia	1.95	2.02	1.88	0.07	3.6%
Elec. + LIB	1.17	1.31	1.05	0.14	11.1%

* Half range = (Pessimistic - Optimistic)/2

Within the LCI generation of LNG, the addition of 1.6% methane slip in the combustion engine causes a 16% increase in *Global warming* LCIA result. This is primarily due to the global warming potential of methane being 35 times more potent than CO_2 in the hierachist perspective. However, in the egalitarian perspective this is only $\sim$5 times more potent and causes a 2% increase in *Global warming* LCIA result. Moreover, within the LCI generation of electrically charged lithium ion batteries, the lithium ion battery contributes the most to the environmental impact. The allocation of environmental impact based on the amount of cycles causes this. The batteries are assumed to go through 326 cycles over the course of its life time, which is significantly less than the 50 000 cycle capability. Therefore the endpoint LCIA has been reassessed for 50 000 cycles and the reduction results are displayed in table 4.10. Extreme

reductions up to 97% (resource scarcity) can be achieved and consequently it can be concluded that the operational use of lithium ion batteries does not match the operational fueling frequency of ships.

Table 4.10: Electrically charged li-ion battery LCIA reduction for 50.000 vs 326 cycles at endpoint for 1 MJ - ReCiPe 2016 (H)

Endpoint area of protection	Unit	E mix + LIB	E renew + LIB
Human health	DALY	-27%	-83%
Natural environment	Species x yr	-34%	-94%
Resource scarcity	USD (2013)	-62%	-97%

1 MJ = 0.2778 kWh

5

Conclusion

The *External Requirements* for shipping vessels are actively changing through GHG emission regulations and therefore involuntarily impacting the *Available Technology* and *Commercial Aspect* while the *Operational Requirements* do not change. As a result, ship designs will change for different energy carrier types and cause the required propulsion power to change as well. However the *Environmental Consequences* relative to conventional fuel oil powered ships for equal operational requirements are unknown. Therefore, the goal of this research project is to determine the full environmental impact of AMECs in ships while taking the powering impact into account with regards to conventional fuel oil powered ships. This is necessary because the space requirements for AMECs cause significant additional volume and weight to the ship design for equal operational requirements. As a result, the ship resistance, propulsion powering and energy carrier consumption increase as well. Accordingly, if the total environmental impact including the increased consumption of an AMEC exceeds the total environmental impact of conventional fuel oil, the purpose of the AMEC is not achieved.

To support the research approach, six sub research questioned have been established to be answered before answering the main research question. In this chapter, the sub research questions are answered based on literature and assessment results, followed by the overall conclusion which answers the main research question. Lastly, the research approach and results are discussed including further recommendations.

In order to determine the full environmental impact of an AMEC, the powering impact and environmental impact need to be determined separately. The powering impact is performed on four ship types (bulk carriers, tankers, container ships, and trailing suction hopper dredgers) which are represented by twelve existing ships per ship type. Six selected energy carrier types (fuel oil, methanol, LNG, liquid hydrogen, ammonia, electrically charged lithium ion batteries) are applied to the designs of these sampled ships. The environmental impact is performed on the six energy carrier types originating from the conventional and a bio/renewable source through a life cycle assessment. Some of the answers to the sub research questions are necessary for both the powering- and environmental impact assessment. The first sub research states:

1. *What are the power plant efficiencies and energy densities of the current and future (A)MEC types?*

The total power plant efficiencies of fuel oil, methanol and LNG are primarily determined by the internal combustion efficiency. However, in the liquid hydrogen, ammonia and battery power plants, there are more components that cause energy losses. Besides the total power plant efficiency, the necessary auxiliary power to run the power plant differs per power plant type. This is caused by the necessary power to store, prepare and apply the energy carrier. Various energy carrier types require specialized tanks to contain it under specific conditions. These tanks therefore add extra volume and weight alongside the volume and weight of the energy carrier alone. The energy carrier contained in the tank characterizes the contained energy density, while the energy carrier alone characterizes the uncontained energy density. The total power plant efficiency, necessary auxiliary power, contained energy density and uncontained energy density are presented in the table below and are necessary to answer the forthcoming sub questions.

Table 5.1: Overview (A)MEC type densities and power plant efficiencies

	Contained			Uncontained			Power plant	
	$\rho_{V\ E\ con}$ MJ/L	$\rho_{G\ E\ con}$ MJ/kg	ρ_{con} kg/L	$\rho_{V\ E\ uncon}$ MJ/L	$\rho_{G\ E\ uncon}$ MJ/kg	ρ_{uncon} kg/L	η_{PP} -	PP_{aux} -
Fuel oil	33.20	29.65	1.12	35.70	41.00	0.87	49.34%*	5%**
Methanol	13.83	15.67	0.88	15.60	19.90	0.78	49.34%	3%
LNG	13.37	28.38	0.47	22.37	49.20	0.45	48.55%	3%
Liq. hydrogen	4.60	11.70	0.39	7.55	120.00	0.06	43.88%	11%
Ammonia	9.45	11.70	0.81	12.70	22.00	0.58	51.33%	11%
Elec. + LIB	0.22	0.33	0.67	2.98	0.50	5.96	85.70%	1%

* 41% for pure MDO in 4-stroke diesel engines
** 1% for pure MDO in 4-stroke diesel engines

2. *What are the historical design elements/dimension trends of ship types?*

According to the literature, slender body ships have a lower total resistance compared to ships with equal internal volume and weight. A lower resistance results in a lower propulsion powering and consequently a lower energy carrier consumption. Therefore the length-beam ratio is the governing dimension trend to be determined for a given ship type. As a consequence additional volume for existing ship designs should be applied to the length within the maximum boundaries of the historical length-beam ratio trend. The maximum boundaries of the length-beam ratio trend are determined by using the World Fleet Register by Clarksons. The determined maximum length-beam ratio trend is formulated according to equation 5.1 with the parameters for the selected ship types in table 5.2. A negative slope value (a) results in a lower maximum length-beam ratio at a greater length. Therefore only container ships increase in a maximum length-beam ratio at greater lengths, however they also have a lower starting maximum length-beam ratio (b) compared to the other ship types. Additionally, specific design elements related to the ship resistance such as a bulbous bow, bow thruster tunnels and propeller configurations are acquired and noted in the sampled ship data parameters.

$$L_{OA}/B_{MAX,\ ship\ type} = a \cdot L_{OA} + b \quad [-] \tag{5.1}$$

Table 5.2: Maximum length-beam ratio trend parameters per ship type

	a	b
Bulk carriers	-0.0125858	10.1251
Tankers	-0.0080163	8.3795
Container ships	0.0047341	5.862
TSHDs	-0.0068975	7.2756

3. *How can the resistance and propulsion power be calculated while taking the design elements per ship type into account?*

The resistance approximation method by Holtrop & Mennen is considered to be efficient and accurate for calculating the required propulsive power. It is applicable for this research project to determine the ship resistance, because it can be applied analytically on all the ships with the ship type design elements. The propulsion power can be approximated analytically as well using the results from the Holtrop & Mennen method together with the given sampled parameters. Both the resistance and propulsion power approximation method can be performed regardless if the value of the sampled parameters changes. Therefore the combination of the two approximation methods are highly suitable for the iterative ship design process.

4. *How can the total bunker volume and weight change by the AMEC types be determined while maintaining the same operational requirements?*

The total bunker volume and weight for an AMEC type is determined for equal and increased propulsion power. In order to maintain equal operational requirements for equal propulsion power, the effective energy of the original fuel oil must be the same when substituting for an AMEC type. However, the ship design requires additional volume and weight to accommodate for equal effective energy by an AMEC type without surrendering the original spaces to perform its tasks. As a result, the necessary propulsion power will increase and simultaneously the energy carrier consumption as well. Therefore, the effective energy associated to the propulsion power is proportionately scaled to the propulsion power increase. The bunker volume and weight for the AMEC types are calculated using the original total effective energy, the contained volumetric and gravimetric energy densities, power plant efficiencies and minimum auxiliary power plant power percentages. By subtracting the original fuel oil bunker volume and weight from the AMEC bunker volume and weight for equal and increased propulsion power, yields the total bunker volume and weight change. To summarize, the total additional AMEC bunker volume and weight is applied in two steps within the iterative process of ship design. In the first step the additional AMEC bunker volume and weight is applied by means of fuel oil substitution. In the second step the additional AMEC bunker volume and weight is applied by means of the propulsion power bunker scaling.

5. *How can the total bunker volume and weight change be applied to the ship design while striving for the lowest propulsion power as possible within a ship type?*

It was determined that slender body ships have a lower total resistance compared to ships with equal internal volume and weight. Therefore the additional AMEC bunker volume and weight is applied in a manner which takes this principle into account while also staying within the maximum dimension trend limits. The determination of the amount of additional AMEC bunker volume and weight is different, but the application is the same. The additional AMEC bunker volume and weight is applied by first lengthening, then deepening and finally widening the ship design. The lengthening is applied in the midship section until the additional AMEC volume is accommodated or until the maximum length-beam ratio trend is met of the ship type. Thereafter the depth is increased to keep the depth-length ratio of the original ship constant, regardless if the AMEC bunker volume was accommodated previously. This is to prevent structural failures from occurring due to increased bending moments by lengthening the ship. If there is additional bunker volume remaining after lengthening and deepening, the beam is increased in the longitudinal section.

6. *How can the magnitudes of the environmental impacts be determined of the operational stage of a ship for current and future (A)MECs?*

To determine the magnitudes of the environmental impacts of the operational stage of a ship, a conceptual life cycle assessment was conducted for the selected (A)MEC types. The (A)MEC types were selected based on their current and future predicted presence according to literature. For each (A)MEC type, a conventional fossil sourced well-to-wake pathway and a bio/renewable sourced pathway were selected. The LCA was performed using the ReCiPe 2016 method in a hierarchical perspective (100 year time horizon) as a global average. The gross LCIA results were determined in midpoint and endpoint impact categories for equal energy content based on the uncontained energy density. Lastly, the gross LCIA results were adjusted by implementing the previously determined total power plant efficiency, yielding the net LCIA results per shaft output.

What is the impact on the ship's propulsion powering and consequently the environment by alternative marine energy carriers?

The research approach is modeled by two main components which are performed separately: the powering impact per (A)MEC type on a ship type, and the net environmental impact per (A)MEC. All the considered AMEC type and ship type combinations result in a larger overall internal volume to accommodate the necessary additional AMEC tank volume for constant operational requirements. The average additional overall internal volume for methanol, LNG, liquid hydrogen, ammonia and batteries are +3.3%, +3.5%, +21.5%, +6.7%, and +771.3% respectively. As a result the lightweight ship increases for all AMEC

type and ship type combinations except LNG. The average additional lightweight ship by methanol, LNG, liquid hydrogen, ammonia and batteries are +3.3%, +4.1%, +53.8%, +18.6%, and 2 558.9% respectively. Battery electric propulsion is not considered feasible in many ship types as the generated ship design cannot withstand the additional weight by the batteries and therefore does not float. All the generated designs result in a higher required propulsion power for all AMEC types. The average additional main engine brake power increase for methanol, LNG, liquid hydrogen, ammonia and batteries are +2.3%, +1.1%, +8.6%, +3.7%, and +235.3% respectively. The additional propulsion power is significantly lower for ships which are lengthened rather than widened to accommodate for equal percentage additional volume. This concludes the lower total ship resistance for slender body ship designs. Currently, fuel oil powered shipping vessels have a higher bunker capacity than necessary to sail their shipping route 2.5 times to purchase cheap fuel elsewhere in the world. By reducing the capacity to equal the distance of a single route the additional overall internal volume is approximately reduced by a minimum of 59% and a maximum of 84%. Likewise, the additional lightweight ship is approximately reduced by a minimum of +61% and a maximum of 79% compared to the results of the full bunker capacity. Likewise for the deadweight tonnage (DWT), the reduction is consistently around $\sim$60%.

The net environmental impacts of the (A)MECs were compared and concluded that eight of the eleven AMECs result in a lower *global warming* impact per shaft output compared to conventional diesel. The AMECs with a higher *global warming* impact compared to conventional diesel are fossil methanol, fossil ammonia, and electricity mix including lithium ion batteries. When taking the powering impact into account, it only causes renewable electricity including LIBs to reverse from a lower to a higher *global warming* impact compared to conventional diesel. This is the case in all ship types. The net environmental impact at the three endpoint categories (human health, natural environment and resource scarcity), five of the eleven AMECs have a lower impact in all three endpoints compared to conventional diesel: fossil methanol, bio LNG, fossil liquid hydrogen, renewable liquid hydrogen, and renewable ammonia. Only electricity mix including LIBs performs worse in all three endpoints. When taking the powering impact into account, it does not cause an AMEC to reverse from better to worse performing on the *human health* endpoint in all ship types. Fossil ammonia in container ships reverses the performance from better to worse performing on the *natural environment* endpoint category. Renewable electricity including LIBs reverses the performance from better to worse performing on the *natural environment* and *resource scarcity* endpoint category in all ship types. There are four AMECs which perform better on *global warming* impact and all three endpoint categories: bio LNG, fossil liquid hydrogen, renewable liquid hydrogen, and renewable ammonia.

5.1. Discussion and recommendations

In this section, the research approach and results are discussed. Based on the limitations and interpretations of this discussion, further research recommendations are made. The main goal of this research project is to determine the total environmental impact of AMECs in ships in order to support the energy carrier selection of the future by the maritime industry. Therefore a recommendation is made on the preferred energy carrier based on environmental performance.

Research input data

Both the powering impact assessment and the environmental impact assessment use two mutual input data sets: the energy densities and total power plant efficiencies. These two data sets are in agreement with literature with slight variations. A lower technical readiness of the AMECs and their accompanying power plant result in higher contained energy density and power plant efficiency variations. However, this is not the case for the uncontained energy densities as they are considered scientific standards. The low technical readiness particularly varies the density of the tank system and power plant components. It is possible that contained energy densities and total power plant efficiencies will increase in the future due technical advancement. As a result, the powering impact and net LCIA results will decrease separately. Consequently, the total environmental impact results will decrease further due to double dependence.

The powering impact assessment uses two more data sets: detailed data of sampled ships and the dimension trends. In order for the powering impact results to be practical, the detailed sample data must coincide with the trend data. The length-beam ratio trendline of the sampled bulkers, tankers and container ships are similar to the dimension trend trendlines and therefore they are representative. However,

the length-beam ratio trendline of the sampled TSHDs is significantly different compared to the dimension trend data set. Seven of the twelve sampled TSHDs are the seven largest in the dimension trend data set out of 140 entries. Consequently, the powering impact results of the TSHD are less representative. It can also be questioned whether twelve sample ships are enough to represent a whole ship type.

The life cycle inventory phase of the LCA consists of gathering LCI information from a database. The listed processes in the database originate from LCA studies where all the in- and output materials, energy, resources and emissions are recorded of a a system, product, service or process over its full life time. Therefore if the scope of the LCA studies are not the same for a similar products such as energy carriers, the LCIA results will be less comparable. Moreover, this varying scope issue can be mitigated by using a single database. For most of the (A)MECs this is the case. The Ecoinvent 3 database was the primary LCI library used which according to literature is the most popular, transparent, consistent and high quality. However, just because an other database is used as well, does not mean that the LCIA is incorrect.

Powering impact assessment approach and results
The powering impact assessment approach is an iterative process of which the design impact sub model is the academic research novelty. The propulsion power was determined twice in the powering impact assessment model for a new generated ship design. The first time is after substituting the fuel oil bunker volume with the necessary AMEC bunker volume. The second time is after upscaling the bunker volume based on the first propulsion impact determination. Therefore if the first propulsion impact is minimal, the second propulsion impact is minimal as well. For methanol and LNG, the design impact is minimal where in almost all cases, the sample ship only needed to be lengthened. As a result, the propulsion impact is also minimal. Therefore, conducting a powering impact on AMEC types which have a relatively high combination of contained energy densities and total power plant efficiency is less necessary. On the contrary, batteries have a significantly low contained energy density that the design impact sequence does not result in slender body ship design. Consequently, the resulting propulsion power is higher than necessary for a slender body ship design with equal overall internal volume. Additionally, many of the battery powered ship designs do not float due to the weight of the batteries. Accordingly, it could be concluded that battery powered shipping vessels are not feasible and/or the design impact model is not suitable for relatively low combination of contained energy density and total power plant efficiency.

Currently merchant shipping vessels have enough fuel oil bunker volume to travel 2.5 times their shipping route. This is done to purchase cheap fuel oil along their route and use fuel price outlooks to determine when to refuel. However, this overcapacity causes significant additional AMEC bunker volume and weight for various AMEC types. Therefore it is expected that the bunker capacity to be reduced to at least a single route. This results in the total additional AMEC bunker volume and weight to be significantly reduced, and consequently also the propulsion power impact. Additionally, it also is not certain if AMECs will have the same global price variations comparable to fuel oil in the future that it is profitable to have the bunker overcapacity. On the contrary, uneven global distribution of AMECs could potentially cause an even higher overcapacity to decrease the consequences of this dependence.

Environmental impact assessment approach and results
The environmental impact assessment approach is conducted through a life cycle assessment. The LCI phase consisted of selecting processes from the database to construct the well-to-wake life cycle of the (A)MECs. In order to produce LCIA results as a global average, the geography of the process listings was set to global or rest-of-world market processes. However, the approach of selecting processes in the LCI database was on the basis of what was available. Accordingly, it was not always possible to select a global market process. Moreover, this availability issue is also prevalent in the bio/renewable AMECs selection. The chance that conventional versions of the marine energy carriers are available in the LCI database is considerably higher than the bio/renewable version. Therefore the bio/renewable versions consist of more LCI process entries and does not encompass the full well-to-wake pathway as in a true LCA study. Additionally, the bio/renewable versions have many more possible well-to-wake pathways and therefore the LCIA results vary significantly. In conclusion, the selection method of LCI processes on the basis of availability causes variations in the LCIA results, especially for bio/renewable AMECs. Consequently, the LCIA results should not be interpreted as factual, but rather as a generalized case study.

The combustion of bio diesel, bio methanol and bio LNG have not been taken into account because car-

bon sequestration, the process of capturing and storing atmospheric carbon dioxide by biomass, cannot be modeled. Additionally other substances captured and stored by biomass also cannot be modeled. In the case of carbon dioxide, it is captured and emitted again into the atmosphere in the same form. However, this not necessarily the case for the other substances which are captured. Therefore it is not fully accurate to not include the combustion of bio fuels and thus the LCIA results are not fully accurate as well.

The energy carrier market for the maritime industry will not voluntarily switch to an AMEC if fuel oil can still be used under the emission regulation. Due to the emission regulations becoming stricter, the AMECs and accompanying technologies become more attractive to use. According to the future outlook of AMEC will increase in ships and therefore the production and distribution will increase as well. Therefore it is expected that use, production and distribution of AMECs with a low technical readiness will become more efficient and durable. Additionally, as the purpose of AMECs is to become more environmentally friendly (specifically global warming), it is also expected that the production and distribution will be become more environmentally friendly. Consequently, the obtained AMEC environmental impacts will probably decrease in the future.

Recommendations
The design impact assessment does not take into account the stability or manoeuvrability of the newly generated ships with AMECs. Therefore it is unknown how the newly generated ships will behave in sea state. A possible consequence of liquid hydrogen is that the sloshing of the liquid hydrogen in the relatively large tanks can cause the ship to capsize. A possible consequence of, for instance batteries, is that the generated ship is remarkably heavy that it will 'plow' through the waves and cause structural damages. This uncertainty in stability and manoeuvrability needs to be researched further to determine the feasibility of the generated ship designs.

The constant operational requirements are based on fuel oil powered ships. However it is possible that these might change due to using an AMEC and its accompanying technology. It could also be possible that the used dimension trends for the considered ship types, that are based on fuel oil powered ships, are not relevant for AMEC powered ships. Moreover, the generated designs for constant operational operational requirements are based on existing ships with a multi purpose objective to have the least amount of added resistance with the additional AMEC bunker volume and weight. Nonetheless, this does not have to be the case when considering a completely new design where it does not have to be related to an existing ship design.

Climate change due to global warming is currently the main environmental concern around the world. The maritime industry is responsible for 3% of the global GHG emissions which originate from fossil sources. Therefore the preferred AMEC is not from a fossil source and has a lower well-to-wake global warming impact than conventional fuel oil. Additionally, the preferred AMEC also has a lower impact on all three net endpoint areas of protection. Renewable liquid hydrogen and ammonia are most environmentally friendly energy carrier including the powering impact on the criteria of global warming impact and all three endpoint areas of protection. Bio fuels offer a solution to lower the global warming impact in current marine power plants with minor alterations, however the renewable energy carriers significantly better. Therefore it is recommended to research the application of these AMECs in the internal combustion engine as it plays an important role in the maritime powering industry.

References

[1] Faig Abbasov. “Statistical analysis of the energy efficiency performance (EEDI) of new ships”. In: *Transport & Environment* (Sept. 2017).

[2] Pauzi Abdul Ghani and Philip Wilson. “Experimental analysis of the seakeeping performance of catamaran forms with bulbous bows”. In: *International Shipbuilding Progress* 65.1 (2018), pp. 1–28.

[3] Airgas. *Safety Data Sheet - Ammonia*. Jan. 2019, p. 6.

[4] Airgas. *Safety data sheet - Hydrogen*. Nov. 2020, p. 5.

[5] Airgas. *Safety data sheet - Methane*. Oct. 2020, pp. 5–6.

[6] Airgas. *Safety data sheet - Methanol*. June 2018, p. 6.

[7] DJ Andrews and C Dicks. “The building block design methodology applied to advanced naval ship design”. In: 1997.

[8] MI Arbab et al. “Fuel properties, engine performance and emission characteristic of common biodiesels as a renewable and sustainable source of fuel”. In: *Renewable and Sustainable Energy Reviews* 22 (2013), pp. 133–147.

[9] Charlotte Banks et al. “Understanding ship operating profiles with an aim to improve energy efficient ship operations”. In: *Proceedings of the low carbon shipping conference, London*. Vol. 9. 2013.

[10] Z Bazari. *National Workshop (virtual) on Ratification and Effective Implementation of MARPOL Annex VI for Algeria*. Nov. 2020. URL: https://www.rempec.org/en/knowledge-centre/online-catalogue/3-zb-l01-marpol-annex-vi-regulations-final.pdf.

[11] Lindert van Biert et al. “A review of fuel cell systems for maritime applications”. In: *Journal of Power Sources* 327 (2016), pp. 345–364.

[12] Levent Bilgili. “Comparative assessment of alternative marine fuels in life cycle perspective”. In: *Renewable and Sustainable Energy Reviews* 144 (2021), p. 110985.

[13] Lothar Birk. *Holtrop and Mennen’s Method*. John Wiley & Sons, Ltd, Apr. 2019, pp. 611–627. ISBN: 9781118855485. DOI: 10.1002/9781119191575.ch50. URL: https://onlinelibrary.wiley.com/doi/10.1002/9781119191575.ch50.

[14] Wijnand Bodewes. “A conceptual design study to prepare a general cargo ship for a refit towards alternative fuels”. MA thesis. Delft, The Netherlands: Delft University of Technology, 2020.

[15] Alberto Boretti. “Hydrogen internal combustion engines to 2030”. In: *International Journal of Hydrogen Energy* 45.43 (2020), pp. 23692–23703.

[16] Ulf Bossel and Baldur Eliasson. *Energy and the hydrogen economy*. Methanol Institute, Arlington, VA, 2003.

[17] AJTH Bot. *Verschuiving van hulpvermogen van FO naar LNG of methanol*. (Private email). Oct. 2022.

[18] Rafael Castelo Branco. *Basics of-ship-resistance*. 2011. URL: https://www.slideshare.net/adsokant/basics-ofshipresistance (visited on 10/31/2022).

[19] Hannah Brown. “Infrared footage shows ’green’ ships leaking methane into the atmosphere”. In: *Euronews* (Apr. 2020). URL: https://www.euronews.com/green/2022/04/13/infrared-footage-shows-green-ships-leaking-methane-into-the-atmosph (visited on 09/08/2022).

[20] Selma Brynolf, Erik Fridell, and Karin Andersson. “Environmental assessment of marine fuels: liquefied natural gas, liquefied biogas, methanol and bio-methanol”. In: *Journal of cleaner production* 74 (2014), pp. 86–95.

[21] Bureau Veritas. *EEXI and CII: Dual regulations reducing ship’s carbon impact*. May 2021.

[22] MBG Castro, BTW Mestemaker, and HN van den Heuvel. “Towards zero emission work vessels: The case of a dredging vessel”. In: *Proceedings of the 2nd International Conference on Modelling and Optimisation of Ship Energy Systems (MOSES2019)*. 2019, pp. 8–10.

[23] Ricardo Alvariño Castro, Juan José Azpíroz Azpíroz, and Manuel Meizoso Fernández. *El proyecto básico del buque mercante*. Fondo Editorial de Ingeniería Naval, 1997.

[24] Clarksons Research. *World fleet register*. 2022.

[25] ClassNK. *Outlines of EEXI regulation*. Dec. 2021.

[26] Jeremy Crossman. *Wärtsilä 32 methanol - The power to reach carbon-neutral (Webinar)*. 2022.

[27] O Dinu and AM Ilie. "Maritime vessel obsolescence, life cycle cost and design service life". In: *IOP conference series: materials science and engineering*. Vol. 95. 1. IOP Publishing. 2015, p. 012067.

[28] DNV. *CII – Carbon Intensity Indicators*. URL: https://www.dnv.com/maritime/insights/topics/CII-carbon-intensity-indicator/implementation.html (visited on 04/26/2022).

[29] DNV GL SE. "Section 14: Rudder and Manoeuvring Arrangement". In: *Rules for Classification and Construction*. Hamburg, DE: DNV GL SE, 2016, pp. 14-3–14-4.

[30] DNV-GL. *Comparison of Alternative Marine Fuels*. July 2019, p. 7.

[31] DNV-GL. *Maritime Forecast To 2050: Energy Transition Outlook 2019*. 2019.

[32] Jill Dunbar. *The Ozone Layer*. 2001. URL: https://www.nas.nasa.gov/About/Education/Ozone/ozonelayer.html (visited on 05/24/2022).

[33] Echandia. *Technical Data Sheet V 03.100 - 20220610*. Jan. 2022.

[34] Echandia. *Technical Specification sheet - full electric ferry*. Apr. 2022.

[35] ecoinvent. *About ecoinvent*. 2022. URL: https://ecoinvent.org/the-ecoinvent-association/ (visited on 05/25/2022).

[36] JH Evans. "Ship Design Spiral". In: *TKI Maritiem* (1959).

[37] Shahjadi Hisan Farjana, M. A. Parvez Mahmud, and Nazmul Huda. "Chapter 1 - Introduction to Life Cycle Assessment". In: *Life Cycle Assessment for Sustainable Mining*. Ed. by Shahjadi Hisan Farjana, M. A. Parvez Mahmud, and Nazmul Huda. Elsevier, 2021, pp. 1–13. ISBN: 978-0-323-85451-1. DOI: https://doi.org/10.1016/B978-0-323-85451-1.00001-9.

[38] A Fet. "Environmental reporting in marine transport." In: *Journal of Marine Design and Operations* (2002), pp. 17–25.

[39] MA Fet. "Environmental management tools and their application: A review with references to case studies". In: *Knowledge for Inclusive Development: International Series on Technology Policy and Innovation; Conceição, P., Gibson, DV, Heitor, MV, Sirilli, G., Veloso, F., Eds* (1999), pp. 449–464.

[40] AM Friis, P Anderson, and JJ Jensen. "Ship design (Part 1 & II)". In: *Section of Maritime Engineering, Dept. of Mechanical Engineering, Technical University of Denmark, Denmark* (2002).

[41] FuelCellWorks. *Norse Group announces launch of MF Hydra, world's first LH2 driven ferry boat*. 2020. URL: https://fuelcellsworks.com/news/norse-group-announces-launch-of-mf-hydra-worlds-first-lh2-driven-ferry-boat/ (visited on 11/04/2022).

[42] Jaap Gelling. "Lecture 1: "Introduction", "Human power" and "Wind power", Design of Advanced Marine Vehicle MT44095". In: *Delft University of Technology* (Apr. 2021). (Attended 2021-04-21).

[43] SE Germanischer Lloyd. *Rules for Classification and Construction, VI Additional Rules and Guidelines, 13 Energy efficiency*. 2013.

[44] Seyedehhoma Ghavam et al. "Sustainable ammonia production processes". In: *Frontiers in Energy Research* (2021), p. 34.

[45] GreenDelta. *openLCA Nexus - Databases*. 2022. URL: https://nexus.openlca.org/databases (visited on 05/25/2022).

[46] Suzanne Greene, Haiying Jia, and Gabriela Rubio-Domingo. "Well-to-tank carbon emissions from crude oil maritime transportation". In: *Transportation Research Part D: Transport and Environment* 88 (2020), p. 102587.

[47] HE Guldhammer and Sv Aa Harvald. "SHIP RESISTANCE-Effect of form and principal dimensions.(Revised)". In: *Danish Technical Press, Danmark, Danmarks Tekniske Hojskole, kademisk Forlag, St. kannikestrade 8, DK 1169 Copenhagen* (1974).

[48] Susan Guthrie et al. “The impact of ammonia emissions from agriculture on biodiversity”. In: *RAND Corporation and The Royal Society, Cambridge, UK* (2018).

[49] Matias Halinen et al. “Performance of a 10 kW SOFC demonstration unit”. In: *ECS Transactions* 35.1 (2011), p. 113.

[50] Michael Z Hauschild, Ralph K Rosenbaum, and Stig Irvin Olsen. *Life cycle assessment*. Springer, 2018.

[51] Havenbedrijf Rotterdam. *Bunker Sales Port of Rotterdam 2020-2021*. 2021.

[52] Havenbedrijf Rotterdam. *Port of Rotterdam bunker sales 2018-2021*. 2021.

[53] J Holtrop. “A statistical re-analysis of resistance and propulsion data”. In: *International Shipbuilding Progress* 28 (363 1984), p. 272.

[54] J Holtrop. “A statistical resistance prediction method with a speed dependent form factor”. In: *Proceedings of the 17th Session BSHC, Varna* 1 (1988), pp. 3–1.

[55] J Holtrop. “Statistical analysis of performance test results”. In: *International Shipbuilding Progress* 24.270 (1977).

[56] J Holtrop and GGJ Mennen. “A statistical power prediction method”. In: *International shipbuilding progress* 25.290 (1978).

[57] J Holtrop and GGJ Mennen. “An approximate power prediction method”. In: *International Shipbuilding Progress 29* (335 1982), pp. 166–170.

[58] MAJ Huijbregts et al. *ReCiPe 2016 v1.1 A harmonized life cycle impact assessment method at midpoint and endpoint level Report I: Characterization*. 2017.

[59] MAJ Huijbregts et al. *ReCiPe 2016 v1.1 A harmonized life cycle impact assessment method at midpoint and endpoint level Report I: Characterization*. 2017. URL: www.rivm.nl/en.

[60] Christine Roxanne Hung, Linda Ager-Wick Ellingsen, and Guillaume Majeau-Bettez. “LiSET: A Framework for Early-Stage Life Cycle Screening of Emerging Technologies”. In: *Journal of Industrial Ecology* 24 (1 Feb. 2020), pp. 26–37. ISSN: 1088-1980. DOI: 10.1111/jiec.12807. URL: https://onlinelibrary.wiley.com/doi/10.1111/jiec.12807.

[61] IMO. “Draft life cycle GHG and carbon intensity guidelines for maritime fuels”. In: *INTERSESSIONAL MEETING OF THE WORKING GROUP ON REDUCTION OF GHG EMISSIONS FROM SHIPS 7th session*. 2020.

[62] IMO. *Energy Efficiency Measures*. URL: https://www.imo.org/en/OurWork/Environment/Pages/Technical-and-Operational-Measures.aspx (visited on 08/02/2022).

[63] IMO. *Greenhouse Gas Emissions*. URL: https://www.imo.org/en/OurWork/Environment/Pages/GHG-Emissions.aspx (visited on 07/29/2022).

[64] IMO. *Initial IMO GHG Strategy*. URL: https://www.imo.org/en/MediaCentre/HotTopics/Pages/Reducing-greenhouse-gas-emissions-from-ships.aspx (visited on 07/29/2022).

[65] IMO. *International Convention for the Prevention of Pollution from Ships (MARPOL)*. URL: https://www.imo.org/en/About/Conventions/Pages/International-Convention-for-the-Prevention-of-Pollution-from-Ships-(MARPOL).aspx (visited on 08/01/2022).

[66] IMO. *International Convention on Tonnage Measurement of Ships*. 1969.

[67] IMO. “ Module 2: ship energy efficiency regulations and related guidelines”. In: *TTT course on energy efficient ship operation*. 2015.

[68] IMO. “Resolution A.708(17) Navigation bridge visibility and functions”. In: *SOLAS* (1991).

[69] IMO. *The International Convention for the Prevention of Pollution from Ships (MARPOL): Prevention of Air Pollution from Ships (Annex VI)*. London, 1997.

[70] IPCC. *Climate Change 2022: Mitigation of Climate Change. Contribution of Working Group III to the Sixth Assessment Report of the Intergovernmental Panel on Climate Change*. 2021.

[71] ISO. *Environmental management — Life cycle assessment — Principles and framework*. Geneva, CH: International Organization for Standardization, July 2006.

[72] ITTC. “Fresh water and seawater properties”. In: *ITTC procedure 7.5-02-01-03* (2011).

[73] Mitch Jacoby. “It’s time to get serious about recycling lithium-ion batteries”. In: *C&EN* (2019).

[74] G Jensen. “Moderne Schiffslinien”. In: *Handbuch der Werften* XXII (1994).

[75] Per Johannesen and Uwe Heine. *Dispelling the myth of high losses in modern electrically enhanced propulsion systems*. Nov. 2021. URL: https://www.wartsila.com/insights/article/dispelling-the-myth-of-high-losses-in-modern-electrically-enhanced-propulsion-systems (visited on 09/06/2022).

[76] Tae-Hwan Joung et al. “The IMO initial strategy for reducing Greenhouse Gas(GHG) emissions, and its follow-up actions towards 2050”. In: *Journal of International Maritime Safety, Environmental Affairs, and Shipping* 4 (1 Jan. 2020), pp. 1–7. ISSN: 2572-5084. DOI: 10.1080/25725084.2019.1707938. URL: https://www.tandfonline.com/doi/full/10.1080/25725084.2019.1707938.

[77] Michihiro Kameyama, Katsuhide Hiraoka, Hiroaki Tauchi, et al. “Study on life cycle impact assessment for ships”. In: *NMRI* (2007).

[78] Kawasaki. *Kawasaki Receives First Order for Coastal Ship Large-capacity-battery Propulsion Systems*. Oct. 2020. URL: https://global.kawasaki.com/en/corp/newsroom/news/detail/?f=20201008_6641 (visited on 09/08/2022).

[79] Kyunghwa Kim et al. “A preliminary study on an alternative ship propulsion system fueled by ammonia: Environmental and economic assessments”. In: *Journal of marine science and engineering* 8.3 (2020), p. 183.

[80] Yoo-Chul Kim et al. “Analysis of added resistance and seakeeping responses in head sea conditions for low-speed full ships using URANS approach”. In: *International Journal of Naval Architecture and Ocean Engineering* 9.6 (2017), pp. 641–654.

[81] J Klein Woud and Douwe Stapersma. *Design of Propulsion and Electric Power Generation Systems*. IMarEST, 2002, p. 64.

[82] AM Kracht. “A Theoretical Contribution to the Wave-Resistance Problem of Ship-Bulb Combinations: Verification of the Negativeness of the Interaction Term”. In: *Journal of Ship Research* 14.01 (1970), pp. 1–7.

[83] Brian Kushner. *MarineTraffic: True Love*. 2020. URL: https://www.marinetraffic.com/en/ais/details/ships/shipid:2892026/mmsi:538005651/imo:9697143/vessel:TRUE_LOVE (visited on 08/24/2022).

[84] Thomas Lamb. *Ship Design and Construction*. SNAME, 2003. ISBN: 0-939773-40-6.

[85] Kai Levander. “Innovative Ship Design–Can innovative ships be designed in a methodological way”. In: *Proc. 8th Int. Marine Design Conference–IMDC03, Athens*. 2003.

[86] LGM Engineering. *LNG LP FGSS*. URL: http://en.gh-lgm.com/product_detail.php?id=7 (visited on 09/08/2022).

[87] Anders Lindblad. “On the design of lines for merchant ships”. In: *Chalmers University of Technology, Gothenburg, Sweden, Report 240* (1961).

[88] Elizabeth Lindstad et al. “Reduction of maritime GHG emissions and the potential role of E-fuels”. In: *Transportation Research Part D: Transport and Environment* 101 (2021), p. 103075.

[89] Haakon Lindstad, Egil Jullumstrø, and Inge Sandaas. “Reductions in cost and greenhouse gas emissions with new bulk ship designs enabled by the Panama Canal expansion”. In: *Energy Policy* 59 (2013), pp. 341–349.

[90] Haakon Lindstad, Inge Sandaas, and Sverre Steen. “Assessment of profit, cost, and emissions for slender bulk vessel designs”. In: *Transportation Research Part D: Transport and Environment* 29 (2014), pp. 32–39.

[91] Jiahui Liu and Okan Duru. “Future of marine fuel: Five projections of marine fuels from 2020 to 2050”. In: *Okan Duru, Shipping Economics and Research* (2019).

[92] Shukui Liu and Apostolos Papanikolaou. “Approximation of the added resistance of ships with small draft or in ballast condition by empirical formula”. In: *Proceedings of the Institution of Mechanical Engineers, Part M: Journal of Engineering for the Maritime Environment* 233.1 (2019), pp. 27–40.

[93] Machinery Spaces. *Fuel Oil System for Marine Diesel Engine*. URL: http://www.machineryspaces.com/fuel-oil-system.html (visited on 09/02/2022).

[94] MAN Energy Solutions. *Basic principles of ship propulsion*. 2018.

[95] MAN Energy Solutions. *The Methanol-fuelled MAN B&W LGIM Engine*. Jan. 2021.

[96] MARIN. "Holtrop-Mennen founders reveal the secret of method's long-lasting success". In: *MARIN Report 100*. Aug. 2010.

[97] McKinsey. *DWT - Energy Insights*. URL: https://www.mckinseyenergyinsights.com/resources/refinery-reference-desk/dwt/ (visited on 08/02/2022).

[98] Mercuria. *Safety data sheet - Fuel oil, residual, heavy fuel oil*. Jan. 2015, p. 2.

[99] Mermaid Consultants. *Bridge Visibility of Ship*. URL: https://www.mermaid-consultants.com/ship-bridge-visibility.html (visited on 05/10/2022).

[100] Saeid Mokhatab et al. "Chapter 5 - Natural Gas Liquefaction Cycle Enhancements and Optimization". In: *Handbook of Liquefied Natural Gas*. Gulf Professional Publishing, 2014, pp. 229–257. ISBN: 978-0-12-404585-9. DOI: https://doi.org/10.1016/B978-0-12-404585-9.00005-2. URL: https://www.sciencedirect.com/science/article/pii/B9780124045859000052.

[101] Anthony F Molland, Stephen R Turnock, and Dominic A Hudson. *Ship resistance and propulsion*. Cambridge university press, 2017.

[102] V Mrzljak, B Žarković, and J Prpić-Oršić. "MARINE SLOW SPEED TWO-STROKE DIESEL ENGINE–NUMERICAL ANALYSIS OF EFFICIENCIES AND IMPORTANT OPERATING PARAMETERS". In: *Machines. Technologies. Materials.* 11.10 (2017), pp. 481–484.

[103] Lampros Nikolopoulos and Evangelos Boulougouris. "A Study on the Statistical Calibration of the Holtrop and Mennen Approximate Power Prediction Method for Full Hull Form, Low Froude Number Vessels". In: *Journal of Ship Production and Design* 35 (01 Feb. 2019), pp. 41–68. ISSN: 2158-2866. DOI: 10.5957/JSPD.170034. URL: https://onepetro.org/JSPD/article/35/01/41/173670/A-Study-on-the-Statistical-Calibration-of-the.

[104] Nils Lindstrand. *Unlocking ammonia's potential for shipping*. 2021. URL: https://www.man-es.com/discover/two-stroke-ammonia-engine (visited on 05/24/2022).

[105] Paints For Life. *Consider the full life cycle of the product*. 2021. URL: https://www.paintsforlife.eu/en/product-development/consider-life-cycle (visited on 03/16/2022).

[106] Dominique Paulet, Dominique Presles, and Frédéric Neuman. *Architecture navale: connaissance et pratique*. Dunod, 2020.

[107] Maria Polakis, Panos Zachariadis, and Jan Otto de Kat. "The Energy Efficiency Design Index (EEDI)". In: Springer International Publishing, Jan. 2019, pp. 93–135. ISBN: 9783030043308. DOI: 10.1007/978-3-030-04330-8_3. URL: http://link.springer.com/10.1007/978-3-030-04330-8_3.

[108] Md Mustafizur Rahman, Christina Canter, and Amit Kumar. "Well-to-wheel life cycle assessment of transportation fuels derived from different North American conventional crudes". In: *Applied Energy* 156 (2015), pp. 159–173.

[109] John Raven et al. *Ocean acidification due to increasing atmospheric carbon dioxide*. The Royal Society, 2005.

[110] Mara Repele and Gatis Bazbauers. "Life cycle assessment of renewable energy alternatives for replacement of natural gas in building material industry". In: *Energy Procedia* 72 (2015), pp. 127–134.

[111] Royal Boskalis. *Equipment sheet - Queen of the Netherlands*. 2012.

[112] Dan Rutherford, Xiaoli Mao, and Bryan Comer. *Potential CO2 reductions under the Energy Efficiency Existing Ship Index*. ICCT, 2020.

[113] Herbert Schneekluth and Volker Bertram. *Ship design for efficiency and economy*. Vol. 218. Butterworth-Heinemann Oxford, 1998, p. 31.

[114] David J Singer, Norbert Doerry, and Michael E Buckley. "What is set-based design?" In: *Naval Engineers Journal* 121.4 (2009), pp. 31–43.

[115] Susan Solomon et al. "Emergence of healing in the Antarctic ozone layer". In: *Science* 353.6296 (2016), pp. 269–274.

[116] Grigorii Soloveichik. “Electrochemical synthesis of ammonia as a potential alternative to the Haber–Bosch process”. In: *Nature Catalysis* 2.5 (2019), pp. 377–380.

[117] Martin Stopford. *Maritime economics 3e*. Routledge, 2008.

[118] Kaan Terün, Austin A Kana, and Rommert Dekker. “Assessing Alternative Fuel Types for Ultra Large Container Vessels in Face of Uncertainty”. In: *21st Conference on Computer and IT Applications in the Maritime Industries (COMPIT'22)*. 2022.

[119] The Royal Institution of Naval Architects. *Significant Ships of 2015*. 2016.

[120] The Royal Institution of Naval Architects. *Significant Ships of 2016*. 2017.

[121] The Royal Institution of Naval Architects. *Significant Ships of 2017*. 2018.

[122] The Royal Institution of Naval Architects. *Significant Ships of 2018*. 2019.

[123] The Royal Institution of Naval Architects. *Significant Ships of 2019*. 2020.

[124] The Royal Institution of Naval Architects. *Significant Ships of 2020*. 2021.

[125] FH Todd. “Skin Friction Resistance of Ships”. In: *Journal of Ship Research* 1.03 (1957), pp. 3–12.

[126] José J de-Troya et al. “Analysing the possibilities of using fuel cells in ships”. In: *International Journal of Hydrogen Energy* 41.4 (2016), pp. 2853–2866.

[127] Edward A Turpin. *Merchant marine officers' handbook*. Cornell Maritime Press, 1944, pp. 330–331.

[128] UN. *Take urgent action to combat climate change and its impacts*. URL: https://sdgs.un.org/goals/goal13 (visited on 08/01/2022).

[129] UNCTAD. *Review of Maritime Transport 2021*. United Nations, Dec. 2021. ISBN: 9789210000970. DOI: 10.18356/9789210000970. URL: https://www.un-ilibrary.org/content/books/9789210000970.

[130] United States Naval Society (USNA). *Chapter 7 - Resistance and powering of ships*. URL: https://www.usna.edu/NAOE/_files/documents/Courses/EN400/02.07%20Chapter%207.pdf.

[131] Thuy Chu Van et al. “Global impacts of recent IMO regulations on marine fuel oil refining processes and ship emissions”. In: *Transportation Research Part D: Transport and Environment* 70 (May 2019), pp. 123–134. ISSN: 13619209. DOI: 10.1016/j.trd.2019.04.001. URL: https://linkinghub.elsevier.com/retrieve/pii/S1361920918309155.

[132] Guus JM Velders et al. “Preserving Montreal Protocol climate benefits by limiting HFCs”. In: *Science* 335.6071 (2012), pp. 922–923.

[133] Berend Veldhuizen et al. “Comparative thermodynamic analysis of marine SOFC system for alternative fuels”. In: *European SOFC & SOE Forum*. July 2022.

[134] Philip J Vergragt, Nils Markusson, and Henrik Karlsson. “Carbon capture and storage, bio-energy with carbon capture and storage, and the escape from the fossil-fuel lock-in”. In: *Global Environmental Change* 21.2 (2011), pp. 282–292.

[135] WJ Vlasblom. “Chapter 2: Trailing suction hopper dredger”. In: *Lecture notes - Design of dredging equipment WB3408*. TU Delft, 2005.

[136] Christina Vossen, Robert Kleppe, and S Randi. “Ship design and system integration”. In: *DMK Conference*. 2013.

[137] Vuyk Engineering. *Alternative Marine Fuels - Application Notes*. May 2019, p. 5.

[138] Vuyk Engineering. *Pugh Matrix - Energy Sources*. Dec. 2021.

[139] Shuaian Wang, Harilaos N Psaraftis, and Jingwen Qi. “Paradox of international maritime organization's carbon intensity indicator”. In: *Communications in Transportation Research* 1 (2021), p. 100005.

[140] Wärtsilä. *Encyclopedia of ship technology*. 2015.

[141] Wärtsila. *Wärtsila 32 methanol engine - brochure*. 2021.

[142] David GM Watson. *Practical ship design*. Vol. 1. Elsevier, 1998, p. 141.

[143] WCS Wigley. *The theory of the bulbous bow and its practical application*. North East Coast Institution of Engineers and Shipbuilders, 1936.

[144] Wesley Wilson, Dane Hendrix, and Joseph Gorski. “Hull form optimization for early stage ship design”. In: *Naval Engineers Journal* 122.2 (2010), pp. 53–65.

[145] Behnam Zakeri and Sanna Syri. “Electrical energy storage systems: A comparative life cycle cost analysis”. In: *Renewable and sustainable energy reviews* 42 (2015), pp. 569–596.

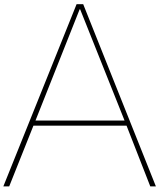

Sampled ship parameter data

Table A.1: Ship parameter data of sampled bulk carriers

BULK CARRIER			CIELO D'ITALIA	TRUE LOVE	VENTURE GOAL	RB JORDANA	GREAT INTELLIGENCE	YUAN HE HAI	SAO DIANA	ADMIRAL SCHMIDT	CHINA STEEL LIBERTY	DIETRICH OLDENDORFF	SARA	BEATE OLDENDORFF
IMO number	IMO	-	9539274	9697143	9670731	9730816	9800623	9806873	9822255	9838838	9832975	9860350	9837119	9853022
Length overall	L_{OA}	m	245.00	179.95	189.90	229.00	179.95	361.90	333.00	250.00	299.70	234.96	229.00	200.00
Length between perpendiculars	L_{PP}	m	241.60	177.00	187.05	225.00	177.00	355.00	323.10	241.79	295.20	231.00	222.00	196.00
Beam moulded	B	m	43.00	32.00	30.00	32.26	32.00	65.00	60.00	43.00	50.00	38.00	32.26	32.26
Depth moulded	D	m	21.60	15.00	15.00	20.20	15.00	30.40	29.80	21.80	25.00	20.62	20.05	18.97
Draft	T	m	15.60	10.50	10.70	14.55	10.50	23.00	22.72	14.50	18.50	15.00	14.45	13.35
Gross tonnage	GT	gt	63087	25515	26411	43600	25561	203403	160290	66291	105964	53219	43735	34909
Deadweight tonnage	DWT	t	117438	38800	43500	81500	38797	398595	326107	104553	208600	100449	80700	62623
Ship speed	V_S	kt	14.50	13.85	14.00	14.00	13.90	14.50	14.50	14.08	14.50	14.00	14.20	14.50
Diameter propeller	D_P	m	8.19	6.20	5.62	7.60	6.40	11.20	10.40	7.90	9.10	7.88	7.20	7.01
Fuel oil bunker volume	V_{BUNK}	m^3	3020	1600	1440	2700	1350	9983	7600	4031	5160	2981	2880	2019
TEU capacity	n_{TEU}	-	0	0	0	0	0	0	0	0	0	0	0	0
Cargo capacity volume	V_{CC}	m^3	135000	50873	54000	95000	50906	212628	182235	130468	210500	115356	95570	79506
Total main engine power (MCR)	P_{ME}	kW	11010	6050	6100	8610	6408	24200	23390	9960	14900	9000	9665	7220
Number of main engines	k_{ME}	-	1	1	1	1	1	1	1	1	1	1	1	1
Total auxiliary engine power (MCR)	P_{AE}	kW	2340	1980	2400	1950	1980	4035	4500	2880	2850	2580	3210	2580
Total shaft/ME PTO	P_{PTO}	kW	0	0	0	0	0	0	0	0	0	0	0	0
Bulbous bow presence	BB	-	No	No	No	No	No	No	No	No	No	No	Yes	No
Number of propellers	k_p	-	Single	Single	Single	Single	Single	Single	Single	Single	Single	Single	Single	Single
Number of bow thruster tunnels	n_{TH}	-	0	0	0	0	0	0	0	0	0	0	0	0

Sourced from Significant Ships edition 2015 to 2020 [119] [120] [121] [122] [123] [124] and Clarksons World Fleet Register

Table A.2: Ship parameter data of sampled tankers

TANKER			ASPHALT SPLENDOR	D&K ABDUL RAZZAK KHALID ZAID AL-KHALID	KMARIN RESPECT	HERON	WHITE STAR	CABO VICTORIA	IBERIAN SEA	NAUTICAL DEBORAH	HILI	BOW ORION	SOLAR SHARNA	TOVE KNUTSEN
IMO number	IMO	-	9763332	9700213	9683001	9730086	9799109	9778674	9815604	9794836	9851830	9818515	9877614	9868376
Length overall	L_{OA}	m	179.90	182.90	249.85	333.00	119.00	244.00	249.80	227.98	336.00	182.88	169.06	278.95
Length between perpendiculars	L_{PP}	m	176.90	173.90	239.00	321.90	112.00	234.00	239.00	224.00	330.00	179.43	161.00	268.70
Beam moulded	B	m	30.60	32.20	44.00	60.00	20.40	43.00	44.00	38.00	60.00	32.20	25.60	48.00
Depth moulded	D	m	16.80	19.10	21.30	29.50	10.65	21.80	21.35	19.80	29.50	19.80	15.60	23.60
Draft	T	m	10.40	13.30	15.50	21.60	6.70	15.20	15.10	13.20	21.60	13.20	10.00	17.15
Gross tonnage	GT	gt	26119	29554	64309	156517	7538	61888	63416	46372	156452	34646	17915	84666
Deadweight tonnage	DWT	t	36962	50104	109584	298439	7895	113000	114218	75343	128800	49042	25039	152868
Ship speed	V_S	kts	14.15	14.50	14.50	14.80	13.24	14.50	14.50	14.00	14.80	14.00	14.50	14.50
Diameter propeller	D_P	m	6.05	6.80	8.40	10.70	4.50	8.00	8.00	7.20	10.60	7.00	5.80	8.70
Fuel oil bunker volume	V_{BUNK}	m^3	1251	1874	3175	6609	769	3200	3530	2770	7085	2686	1370	3513
TEU capacity	n_{TEU}	-	0	0	0	0	0	0	0	0	0	0	0	0
Cargo capacity volume	V_{CC}	m^3	35660	54012	124952	344826	8073	126000	130200	86716	341870	54600	30200	170028
Total main engine power (MCR)	P_{ME}	kW	6400	7020	11890	17200	3400	12420	13500	10850	24510	7820	7000	16190
Number of main engines	k_{ME}	-	1	1	1	1	1	1	1	1	1	1	1	1
Total auxiliary engine power (MCR)	P_{AE}	kW	2700	3150	3960	3789	1680	3060	2700	2880	4620	4240	3150	18720
Total shaft gen./ME PTO power	P_{PTO}	kW	0	0	0	0	0	0	0	0	0	0	0	0
Bulbous bow presence	BB	-	Yes	Yes	Yes	Yes	Yes	Yes	Yes	No	No	No	Yes	No
Number of propellers	k_p	-	Single	Single	Single	Single	Single	Single	Single	Single	Single	Single	Single	Single
Number of bow thruster tunnels	n_{TH}	-	1	0	0	0	1	0	0	0	0	1	0	3

Sourced from Significant Ships edition 2015 to 2020 [119] [120] [121] [122] [123] [124] and Clarksons World Fleet Register

Table A.3: Ship parameter data of sampled container ships

CONTAINER SHIP			AL MURABBA	CMA CGM ARKANSAS	CAPE AKRITAS	MAERSK BERMUDA	EVER BLISS	OOCL HONG KONG	DANIEL K INOUYE	SABRE TRADER	MSC JOSSELINE	SEATRADE GREEN	KMTC SEOUL	YM CELEBRITY
IMO number	IMO	-	9708837	9722651	9706190	9697014	9786932	9776171	9719056	9817884	9842061	9810915	9882205	9864502
Length overall	L_{OA}	m	368.52	299.99	330.00	194.93	211.90	399.87	260.30	172.00	365.84	185.00	197.40	209.75
Length between perpendiculars	L_{PP}	m	352.00	286.00	316.40	184.93	206.90	383.00	248.50	164.00	347.00	176.00	185.00	206.20
Beam moulded	B	m	51.00	48.20	48.20	32.20	32.80	58.80	35.00	28.40	48.20	30.00	32.50	32.80
Depth moulded	D	m	30.35	25.00	27.20	17.00	16.80	32.50	21.00	14.20	29.85	16.50	16.80	16.80
Draft	T	m	15.50	14.50	16.00	11.50	11.20	16.00	12.20	9.50	16.00	10.00	11.70	11.20
Gross tonnage	GT	gt	153148	94440	112836	28316	32659	210890	48409	19035	140976	24876	27997	32720
Deadweight tonnage	DWT	t	149360	104236	134869	35157	37546	191400	51400	23439	150893	26868	37200	37435
Ship speed	V_S	kts	21.00	22.00	22.16	19.00	21.80	23.00	23.50	18.50	22.00	18.90	18.60	21.00
Diameter propeller	D_P	m	10.00	9.00	8.70	6.80	6.09	10.50	8.70	6.60	10.00	6.70	7.20	7.80
Fuel oil bunker volume	V_{BUNK}	m^3	8834	8500	8307	2725	2970	14850	4594	1590	8700	2111	1480	2900
TEU capacity	n_{TEU}	-	14990	9896	11037	2508	2926	21413	3652	1774	14300	2266	2540	2940
Cargo capacity volume	V_{CC}	m^3	0	0	0	0	0	0	0	0	0	0	0	0
Total main engine power (MCR)	P_{ME}	kW	54900	45300	54960	13400	24260	61530	38000	11150	46422	13100	16700	20500
Number of main engines	k_{ME}	-	1	1	1	1	1	1	1	1	1	1	1	1
Total auxiliary engine power (MCR)	P_{AE}	kW	17280	16000	17000	9240	6000	18000	8550	5480	13416	7360	5100	5700
Total shaft gen./ME PTO power	P_{PTO}	kW	4140	0	0	0	0	4000	0	0	0	0	0	0
Bulbous bow presence	BB	-	Yes	Yes	Yes	Yes	No	Yes	Yes	Yes	Yes	Yes	Yes	No
Number of propellers	k_p	-	Single	Single	Single	Single	Single	Single	Single	Single	Single	Single	Single	Single
Number of bow thruster tunnels	n_{TH}	-	2	1	1	1	0	2	1	1	2	1	1	1

Sourced from Significant Ships edition 2015 to 2020 [119] [120] [121] [122] [123] [124] and Clarksons World Fleet Register

Table A.4: Ship parameter data of sampled TSHDs **[CONFIDENTIAL]**

TSHD			BONNY RIVER	CHARLES DARWIN	CONGO RIVER	GALILEO GALILEI	HAM 318	INAI KENANGA	LEIV EIRIKSSON	PRINS DER NEDERLANDEN	QUEEN OF THE NETHERLANDS	VASCO DA GAMA	VOX MAXIMA	WILLEM VAN ORANJE
IMO number	IMO	-	9810939	9538079	9574523	9872365	9229556	9568782	9429584	9263899	9164031	9187473	9454096	9449065

Sourced from Vuyk Engineering and Clarksons World Fleet Register
CONFIDENTIAL INFORMATION

B

Holtrop & Mennen resistance approximation procedure

The frictional resistance as of a flat plate is calculated according to equation B.1. The correlation line factor (C_F) is calculated according to equation B.2 [125].

$$R_F = \frac{1}{2} \cdot \rho \cdot V_S^2 \cdot S \cdot C_F \quad [kN] \tag{B.1}$$

$$C_F = \frac{0.075}{(log_{10}(R_e) - 2)^2} \quad [-] \tag{B.2}$$

With the Reynolds number (R_e) according to equation B.3 with the kinematic viscosity (ν) of seawater at 15° Celsius equal to 1.1892E-06 m^2/s [72].

$$R_e = \frac{V_s \cdot L_{WL}}{\nu} \tag{B.3}$$

The frictional resistance is calculated as a flat plate and therefore does not represent the underwater shape of a ship. The flat plate frictional resistance is multiplied by a form factor $1 + k$ to embody the underwater ship shape. The form factor is calculated according to equation B.4 [53].

$$k = 0.07 + 0.487118 \cdot c_{14} \cdot \left[\left(\frac{B}{L_{WL}} \right)^{1.06806} \cdot \left(\frac{T}{L_{WL}} \right)^{0.46106} \cdot \left(\frac{L_{WL}}{L_R} \right)^{0.121563} \cdot \left(\frac{L_{WL}^3}{\nabla} \right)^{0.36486} \cdot (1 - C_P)^{-0.604247} \right] \quad [-] \tag{B.4}$$

With the only unknown parameter being the constant c_{14} which is calculated according to equation B.5.

$$c_{14} = 1.0 + 0.011 \cdot C_{stern} \quad [-] \tag{B.5}$$

The next resistance component is the appendage resistance (R_{APP}) and is calculated according to equation B.6. The resistance component is compiled of the sum of the resistances from all the appendages. The resistance of the bow thruster tunnels (R_{TH}) is calculated separately. For simplicity, all merchant ships have a rudder behind skeg, bilge keels and a skeg. The TSHD have twin screw rudder (slender), two skegs and bilge keels. The appendages have their own form factor (k_{2i}) and are presented in table B.1. The rudder surface area for all ships is calculated according to equation 3.25. The skeg(s) surface area for all ships is calculated according to equation 3.29. The bilge keel surface area for all ships is calculated according to equation 3.26.

$$R_{APP} = \frac{1}{2} \cdot \rho \cdot V_S^2 \cdot (1 + k_2)_{\text{eq}} \cdot C_F \cdot \sum_i S_{APP_i} + \sum R_{TH} \quad [kN] \tag{B.6}$$

Table B.1: Approximate values for appendage form factor k_{2i} [54]

Appendage	k_{2i} value	Remark
Rudder behind skeg	0.2-0.5	
Rudder behind stern	0.5	
Twin screw rudder (slender)	1.5	
Twin screw rudder (thick)	2.5	
Shaft brackets	2.0-4.0	
Skeg	0.5-1.0	
Strut bossing	2.0-3.0	
Hull bossing	1.0	
Exposed shafts	1.0	Angle with buttocks 10 degrees
Exposed shafts	4.0	Angle with buttocks 20 degrees
Stabilizer fins	1.8	
Dome	1.7	
Bilge keels	0.4	

Just like the frictional resistance form factor $(1 + k)$, the resistance of all the appendages is compiled to a single equivalent form factor $(1+k_2)$. The appendage single equivalent form factor is calculated according to equation B.7.

$$(1 + k_2)_{\text{eq}} = \frac{\sum_i (1 + k_{2i})\, S_{APP_i}}{\sum_i S_{APP_i}} \quad [-] \tag{B.7}$$

The resistance of the bow thruster tunnels is added to the total appendage resistance according to equation B.8. The value for the drag coefficient for the thruster tunnel $C_{D_{TH}}$ is between 0.003 and 0.012 [13]. The average of the two is taken for simplicity.

$$R_{TH} = n_{TH} \cdot \rho \cdot V_S^2 \cdot \pi \cdot d_{TH}^2 \cdot C_{D_{TH}} \quad [kN] \tag{B.8}$$

The wave making resistance (R_W) equation for ships that have a Froude number below 0.4, this is the equation, however different for $F_n \geq 0.4$

$$R_W = c_1 \cdot c_2 \cdot c_5 \cdot \rho \cdot g \cdot \nabla \cdot e^{[m_1 \cdot F_n^{-0.9} + m_4 \cdot \cos(\lambda \cdot F_n^{-2})]} \quad [kN] \tag{B.9}$$

With the following coefficients also for the condition $F_n \leq 0.4$. All ships have a Froude number below 0.4, however different for Fn ≥ 0.4.

$$c_1 = 2223105 \cdot c_7^{3.78613} \cdot \left(\frac{T}{B}\right)^{1.07961} \cdot (90 - i_E)^{-1.37565} \quad [-] \tag{B.10}$$

With

$$c_7 \quad (B/L_{WL} \leq 0.11) \quad = 0.229577 \cdot \left(\frac{B}{L_{WL}}\right)^{1/3} \quad [-] \tag{B.11}$$

Or

$$c_7 \quad (0.11 < B/L_{WL}) \leq 0.25 \quad = \frac{B}{L_{WL}} \quad [-] \tag{B.12}$$

Or

$$c_7 \quad (B/L_{WL} > 0.25) \quad = 0.5 - 0.0625 \cdot \frac{L_{WL}}{B} \quad [-] \tag{B.13}$$

With

$$c_2 = e^{-1.89 \cdot \sqrt{c_3}} \quad [-] \tag{B.14}$$

With

$$c_3 = 0.56 \cdot \frac{A_{BT}^{1.5}}{B \cdot T \cdot \left(0.31 \cdot \sqrt{A_{BT}} + T_F - h_B\right)} \quad [-] \tag{B.15}$$

With

$$c_5 = 1 - 0.8 \cdot \frac{A_T}{B \cdot T \cdot C_M} \quad [-] \tag{B.16}$$

With

$$m_1 = 0.0140407 \cdot \frac{L_{WL}}{T} - 1.75254 \cdot \frac{\nabla^{1/3}}{L_{WL}} - 4.79323 \cdot \frac{B}{L_{WL}} - c_{16} \quad [-] \tag{B.17}$$

With

$$c_{16} \quad (C_P \leq 0.8) = 8.07981 \cdot C_P - 13.8673 \cdot C_P^2 + 6.984388 \cdot C_P^3 \quad [-] \tag{B.18}$$

Or

$$c_{16} \quad (C_P > 0.8) = 1.73014 - 0.7067 \cdot C_P \quad [-] \tag{B.19}$$

With

$$m_4 = 0.4 \cdot c_{15} \cdot e^{-0.034 \cdot F_n^{-3.29}} \quad [-] \tag{B.20}$$

With

$$c_{15} \quad (\frac{L_{WL}^3}{\nabla} \leq 512) = -1.69385 \quad [-] \tag{B.21}$$

Or

$$c_{15} \quad (512 \leq \frac{L_{WL}^3}{\nabla} \leq 1726.91) = -1.69385 + \frac{\frac{LWL}{\nabla^{1/3}} - 8}{2.36} \quad [-] \tag{B.22}$$

Or

$$c_{15} \quad (\frac{L_{WL}^3}{\nabla} > 1726.91) = 0 \quad [-] \tag{B.23}$$

With

$$\lambda \quad (\frac{L_{WL}}{B} \leq 12) = 1.446 \cdot C_P - 0.03 \cdot \frac{L_{WL}}{B} \quad [-] \tag{B.24}$$

Or

$$\lambda \quad (\frac{L_{WL}}{B} > 12) = 1.44 \cdot C_P - 0.36 \quad [-] \tag{B.25}$$

The pressure resistance due to the bulbous bow near the water surface (R_B) is calculated according to equation B.26.

$$R_B = 0.11 \cdot \rho \cdot g \cdot (\sqrt{A_{BT}})^3 \cdot \frac{F_{n_B}^3}{1 + F_{n_B}^2} \cdot e^{-3.0 \cdot P_B^{-2}} \quad [-] \tag{B.26}$$

$$F_{n_B} = \frac{V_S}{\sqrt{g(T_F - h_B - 0.25 \cdot \sqrt{A_{BT}} + h_F + h_W)}} \quad [-] \tag{B.27}$$

h_F must be $\geq$ -0.01$\cdot L_{WL}$

$$h_F = C_P \cdot C_M \cdot \frac{B \cdot T}{L_{WL}}(136 - 316.3 \cdot F_n) \cdot F_n^3 \quad [m] \tag{B.28}$$

h_W must be $\leq$ 0.01$\cdot L_{WL}$

$$h_W = \frac{i_E \cdot V_S^2}{400 \cdot g} \quad [m] \tag{B.29}$$

$$P_B = 0.56 \cdot \frac{\sqrt{A_{BT}}}{T_F - 1.5 \cdot h_B + h_F} \quad [-] \tag{B.30}$$

The pressure resistance due to immersed transom (R_{TR}) is calculated according to equation B.31.

$$R_{TR} = \frac{1}{2} \cdot \rho \cdot V_S^2 \cdot A_T \cdot c_6 \quad [-] \tag{B.31}$$

With

$$c_6 \quad (F_{n_T} < 5) = 0.2 \cdot (1 - 0.2 \cdot F_{n_T}) \quad [-] \tag{B.32}$$

Or

$$c_6 \quad (F_{n_T} > 5) = 0 \quad [-] \tag{B.33}$$

$$F_{n_T} = \frac{V_S}{\sqrt{\frac{2 \cdot g \cdot A_T}{B + B \cdot C_{WP}}}} \quad [-] \tag{B.34}$$

The model-ship correlation resistance (R_A) is calculated according to equation B.35.

$$R_A = \frac{1}{2} \cdot \rho \cdot v_S^2 \cdot (C_A + \Delta C_A) \left[S + \sum S_{APP} \right] \quad [kN] \tag{B.35}$$

With

$$C_A = 0.00546 \cdot (L_{WL} + 100)^{-0.16} - 0.002 + 0.003 \cdot \sqrt{\frac{L_{WL}}{7.5}} \cdot C_B^4 \cdot c_2 \cdot (0.04 - c_4) + \Delta C_A \quad [-] \tag{B.36}$$

With

$$c_4 \quad (\frac{T_F}{L_{WL}} \leq 0.04) = \frac{T_F}{L_W L} \quad [-] \tag{B.37}$$

Or

$$c_4 \quad (\frac{T_F}{L_{WL}} > 0.04) = 0.04 \quad [-] \tag{B.38}$$

With standard surface roughness of k_S = 150 μm, the ΔC_A is equal to 0.

$$\Delta C_A = 0 \quad [-] \tag{B.39}$$

The air (above water plane) resistance (R_{AA}) with default drag coefficient C_{DA} is equal to 0.8 and the standard air density ρ_A is equal to 1.225 kg/m^3.

$$R_{AA} = \frac{1}{2} \cdot \rho_A \cdot V_S^2 \cdot C_{DA} \cdot A_V \quad [kN] \tag{B.40}$$

The total ship resistance is the sum of the resistance components according to equation B.41

$$R_{TOT} = R_F + R_{app} + R_W + R_B + R_{TR} + R_A + R_{AA} \quad [kN] \tag{B.41}$$

The following formulas calculate the wake fraction factor (w) and the thrust deduction factor (t) for a single or twin screw ship which are necessary for the propulsion chain method.

$$\begin{aligned} w_{single} = c_9 \cdot c_{20} \cdot C_V \cdot \frac{L_{WL}}{T_A} \cdot \left[0.050776 + 0.93405 \cdot \frac{c_{11} \cdot C_V}{1 - C_{P1}} \right] \\ + 0.27915 \cdot c_{20} \cdot \sqrt{\frac{B}{L_{WL} \cdot (1 - C_{P1})}} + c_{19} \cdot c_{20} \quad [-] \end{aligned} \tag{B.42}$$

Or

$$w_{twin} = 0.3095 \cdot C_B + 10 \cdot C_V \cdot C_B - 0.23 \frac{D}{\sqrt{B \cdot T}} \quad [-] \tag{B.43}$$

$$t_{single} = \frac{0.25014 \cdot \left(\frac{B}{L_{WL}}\right)^{0.28956} \cdot \left(\frac{\sqrt{B \cdot T}}{D}\right)^{0.2624}}{\left(1 - C_P + 0.0225 \cdot \ell_{CB}\right)^{0.01762}} + 0.0015 \cdot C_{\text{stern}} \quad [-] \tag{B.44}$$

Or

$$t_{twin} = 0.325 \cdot C_B - 0.1885 \cdot \frac{D}{\sqrt{B \cdot T}} \quad [-] \tag{B.45}$$

$$\eta_{R\,single} = 0.9922 - 0.05908 \cdot \frac{A_E}{A_0} + 0.07424 \cdot (C_P - 0.0225 \cdot l_{CB}) \quad [-] \tag{B.46}$$

Or

$$\eta_{R\,twin} = 0.9737 + 0.111 \cdot (C_P - 0.0225 \cdot l_{CB}) - 0.06325 \cdot \frac{P}{D} \quad [-] \tag{B.47}$$

With

$$\frac{A_E}{A_O} = K \cdot \frac{(1.3 + 0.3 \cdot Z) \cdot T}{D_p^2 \cdot (p_o - p_v + \rho_{sw} \cdot g \cdot h_p)} \quad [-] \tag{B.48}$$

Chosen five blade on the propeller (Z=5), K=0.05 for twin screw, K=0.2 for single screw, T is thrust, $p_o - p_v$ = 99047, h_p=$T_a - 0.5 \cdot D_p$.

$$C_V = \frac{(1+k) \cdot R_F + R_{APP} + R_A}{\frac{1}{2} \cdot \rho \cdot V_S^2 \cdot (S + \sum S_{APPi})} \quad [-] \tag{B.49}$$

$$c_9 \quad (c_8 \leq 28) = c_8 \quad [-] \tag{B.50}$$

Or

$$c_9 \quad (c_8 > 28) = 32 - \frac{16}{c_8 - 24} \quad [-] \tag{B.51}$$

With

$$c_8 \quad (B/T_A \leq 5) = \frac{S}{L_{WL} \cdot D} \cdot \frac{B}{T_A} \quad [-] \tag{B.52}$$

Or

$$c_8 \quad (B/T_A > 5) = \frac{S \cdot \left(7 \cdot \frac{B}{T_A} - 25\right)}{L_{WL} \cdot D \cdot \left(\frac{B}{T_A} - 3\right)} \quad [-] \tag{B.53}$$

$$c_{11} \quad (T_A/D \leq 2) = \frac{T_A}{D} \quad [-] \tag{B.54}$$

Or

$$c_{11} \quad (T_A/D > 2) = 0.0833333 \cdot \left(\frac{T_A}{D}\right)^3 + 1.33333 \quad [-] \tag{B.55}$$

$$c_{20} = 1 + 0.015 \cdot C_{stern} \quad [-] \tag{B.56}$$

$$C_{P1} = 1.45 \cdot C_P - 0.315 - 0.0225 \cdot l_{CB} \quad [-] \tag{B.57}$$

B.1. Resistance approximation example

Cielo D'Italia The detailed procedure results for the Holtrop & Mennen method for the original resistance of the Cielo D'Italia

Table B.2: Resistance approximation of the Cielo D'Italia

Parameter	Symbol	Unit	Value
Prismatic coefficient	C_P	-	0.840
Midship section coefficient	C_M	-	0.998
Waterplane area coefficient	C_{WP}	-	0.893
Longitudinal center of buoyancy	lcb	% midship	2.71
Height deck house	h_{dh}	m	16.86
Projected frontal area above waterline	A_V	m^2	801.9
Immersed transom area	A_T	m^2	65.9
Bulbous bow presence	BB	-	No
Transverse area bulbous bow	A_{BT}	m^2	0.0
Height bulbous bow	h_B	m	7.8
Stern shape parameter	C_{STERN}	-	0
Diameter bow thruster tunnel	d_{TH}	m	0.00
23 coefficient	c_{23}	-	0.859
Wetted surface area	S	m^2	15684.3
Displacement volumetric	V	m^3	137862
Half angle waterline entrance	i_E	deg	59.61
a coefficient	a	-	-0.42
Length of run	L_R	m	30.73
Length of entrance	L_E	m	17.35
Frictional coefficient ITTC 1957	C_F	-	0.00145
Reynolds number	R_n	-	1577647215
14 coefficient	c_{14}	-	1.00
Form factor	$(1+k_1)$	-	1.39
Rudder surface area	A_R	m^2	60.2
Rudder behind skeg form factor	$(1+k_2)_R$	-	1.35
Rudder appendage single screw (behind skeg)	$A_R(1+k_2)_R$		81.27
Bilge keel surface area	A_B	m^2	78.8
Bilge keel form factor	$(1+k_2)_B$	-	1.40
Bilge keel appendage	$A_B(1+k_2)_B$	-	110.28
Skeg surface area single screw	A_S	m^2	156.7
Skeg form factor	$(1+k_2)_S$	-	1.75
Skeg appendage	$A_S(1+k_2)_S$	-	274.29
Appendages form factor	$(1+k_2)$	-	1.58
Total appendage surface area	S_{APP}	m^2	295.7
Total surface area (ship app)	S_{TOT}	m^2	15980.0
Total resistance bow thruster tunnels	R_{TH}	kN	0.0
7 coefficient	c_7	-	0.176
1 coefficient	c_1	-	9.349
3 coefficient	c_3	-	0.000
2 coefficient	c_2	-	1.000
5 coefficient	c_5	-	0.921
15 coefficient	c_{15}	-	-1.694
16 coefficient	c_{16}	-	1.136
Lambda coefficient	λ	-	1.044
1 m coefficient	m_1	-	-2.127
4 m coefficient	m_4	-	-3.93E-08
Forward sinkage at bulbous bow	h_F	m	0.71
Local wave height at bow	h_W	m	0.85
Froude number immersed bulbous bow	$F_{n\,i-B}$	-	0.78
Bulb emergence parameter	P_B	-	0.00
Froude number immersed transom stern	$F_{n\,i-T}$	-	1.87
6 coefficient	c_6	-	0.125
4 coefficient	c_4	-	0.04
Correlation allowance coefficient	C_A	-	0.000144
Total resistance	$\mathbf{R_{TOT}}$	**kN**	**1350.8**
Frictional resistance including form factor	$\mathbf{R_F(1+k_1)}$	**kN**	**898.0**
Resistance of appendages	$\mathbf{R_{APP}}$	**kN**	**19.2**
Model-ship correlation resistance	$\mathbf{R_A}$	**kN**	**64.8**
Wave-making and wave-breaking resistance	$\mathbf{R_W}$	**kN**	**111.9**
Additional pressure resistance of bulbous bow	$\mathbf{R_B}$	**kN**	**0.0**
Additional pressure resistance of transom stern	$\mathbf{R_{TR}}$	**kN**	**235.0**
Air resistance	$\mathbf{R_{AA}}$	**kN**	**21.9**

Propulsion approximation example

Cielo D'Italia The detailed procedure results for the propulsion chain method for the original main engine brake power of the Cielo D'Italia

Table B.3: Engine/propulsion power approximation for the Cielo D'Italia

Parameter	Symbol	Unit	Value
Viscous resistance coefficient	C_V	-	0.000040
8 coefficient	c_8	-	71.81
9 coefficient	c_9	-	31.67
11 coefficient	c_{11}	-	0.72
19 coefficient	c_{19}	-	0.13
20 coefficient	c_{20}	-	1.00
CP1 coefficient	C_{P1}	-	0.843
Wake fraction factor	w	-	0.425
Thrust deduction factor	t	-	0.163
Thrust	T	kN	1613.4
Hull efficiency	η_H	-	1.457
Propeller expanded area ratio	A_E/A_O	-	0.514
Propeller open water efficiency	η_O	-	0.625
Relative rotative efficiency	η_R	-	1.020
Advance speed of the propeller	V_A	m/s	4.29
Shaft efficiency	η_S	-	0.990
Gearbox efficiency	η_{GB}	-	1.00
Effective towing power	**P_E**	**kW**	**10076.2**
Thrust power	**P_T**	**kW**	**6917.9**
Open water propeller power	**P_O**	**kW**	**11068.6**
Propeller power	**P_P**	**kW**	**10854.6**
Delivered power	**P_P**	**kW**	**10854.6**
Shaft power	**P_S**	**kW**	**10964.3**
Brake power main engine	**P_B**	**kW**	**10964.3**
Maximum continuous rating engine power	**P_{MCR}**	**kW**	**12530.6**

C

Design impact results

BULK CARRIERS			CIELO D'ITALIA	TRUE LOVE	VENTURE GOAL	RB JORDANA	GREAT INTELLIGENCE	YUAN HE HAI	SAO DIANA	ADMIRAL SCHMIDT	CHINA STEEL LIBERTY	DIETRICH OLDENDORFF	SARA	BEATE OLDENDORFF	
FUEL OIL (original)	L_{OA}	m	245.00	179.95	189.90	229.00	179.95	361.90	333.00	250.00	299.70	234.96	229.00	200.00	
	B	m	43.00	32.00	30.00	32.26	32.00	65.00	60.00	43.00	50.00	38.00	32.26	32.26	
	D	m	21.60	15.00	15.00	20.20	15.00	30.40	29.80	21.80	25.00	20.62	20.05	18.97	
	T	m	15.60	10.50	10.70	14.55	10.50	23.00	22.72	14.50	18.50	15.00	14.45	13.35	
	f	m	6.00	4.50	4.30	5.65	4.50	7.40	7.08	7.30	6.50	5.62	5.60	5.62	
	V_{INT}	m^3	172955	71454	73903	120567	71580	542852	430111	181530	287042	146481	120932	97040	
	DWT	t	117438	38800	43500	81500	38797	398595	326107	104553	208600	100449	80700	62623	
	m_{LIGHT}	t	23870	12313	8244	10926	12265	52134	57168	29473	28236	14748	10965	10326	
	L/B	-	5.70	5.62	6.33	7.10	5.62	5.57	5.55	5.81	5.99	6.18	7.10	6.20	
METHANOL	L_{OA}	m	247.26	182.29	192.13	232.31	181.91	362.14	335.96	253.02	302.58	237.62	232.31	202.31	+1.01%
	B	m	43.04	32.05	30.04	32.26	32.04	66.33	60.06	43.05	50.05	38.04	32.26	32.30	+0.36%
	D	m	21.80	15.19	15.18	20.49	15.16	30.42	30.07	22.06	25.24	20.85	20.34	19.19	+1.01%
	T	m	15.94	10.84	11.00	14.99	10.78	23.52	23.18	14.95	18.91	15.40	14.92	13.73	+2.61%
	f	m	5.86	4.36	4.17	5.50	4.38	6.90	6.89	7.11	6.33	5.45	5.42	5.46	-3.18%
	V_{INT}	m^3	177150	73692	75911	124679	73460	556948	440685	187182	294225	150646	125011	99858	+2.72%
	DWT	t	120012	40175	44733	83827	39951	407265	332598	108026	213010	103007	83181	64353	+2.40%
	m_{LIGHT}	t	24615	12712	8601	11628	12600	54659	59049	30481	29514	15490	11690	10827	+4.14%
	L/B	-	5.74	5.69	6.40	7.20	5.68	5.46	5.59	5.88	6.05	6.25	7.20	6.26	+0.84%
LNG	L_{OA}	m	247.43	182.46	192.31	232.31	182.06	362.11	336.19	253.24	302.79	237.82	232.38	202.48	+1.07%
	B	m	43.04	32.05	30.04	32.26	32.04	66.45	60.07	43.06	50.06	38.05	32.30	32.30	+0.40%
	D	m	21.81	15.21	15.19	20.49	15.18	30.42	30.09	22.08	25.26	20.87	20.35	19.20	+1.07%
	T	m	15.65	10.55	10.75	14.62	10.55	23.09	22.79	14.57	18.57	15.06	14.53	13.41	+0.42%
	f	m	6.16	4.65	4.44	5.87	4.63	7.33	7.29	7.51	6.69	5.81	5.82	5.79	+2.76%
	V_{INT}	m^3	177468	73861	76067	124679	73605	558026	441490	187601	294762	150959	125285	100066	+2.91%
	DWT	t	117046	38596	43316	81153	38624	397368	325126	104042	207932	100068	80339	62363	-0.36%
	m_{LIGHT}	t	24791	12805	8686	11758	12679	55248	59491	30714	29811	15663	11857	10943	+5.09%
	L/B	-	5.75	5.69	6.40	7.20	5.68	5.45	5.60	5.88	6.05	6.25	7.19	6.27	+0.87%
LIQ. HYDROGEN	L_{OA}	m	258.18	193.56	202.82	234.28	191.32	364.45	347.45	282.49	312.10	260.27	234.80	213.39	+5.55%
	B	m	43.14	32.12	30.11	36.11	32.12	72.70	61.34	43.00	51.79	38.00	36.44	32.38	+3.97%
	D	m	22.76	16.13	16.02	20.67	15.95	30.61	31.09	24.63	26.03	22.84	20.56	20.24	+5.57%
	T	m	16.53	11.40	11.51	15.74	11.25	24.43	23.98	15.93	19.63	16.21	15.73	14.36	+7.26%
	f	m	6.24	4.74	4.51	4.93	4.69	6.18	7.11	8.71	6.40	6.63	4.83	5.88	+1.12%
	V_{INT}	m^3	197485	84564	85555	143948	82512	629701	492857	243087	330004	186128	146310	113464	+18.10%
	DWT	t	116055	38071	42839	80319	38177	394243	322664	102798	206277	99122	79457	61699	-1.25%
	m_{LIGHT}	t	34666	18082	13372	21209	17077	90326	84778	47035	47139	26993	22124	17554	+62.69%
	L/B	-	5.99	6.03	6.74	6.49	5.96	5.01	5.66	6.57	6.03	6.85	6.44	6.59	+2.16%
AMMONIA	L_{OA}	m	249.39	184.46	194.19	232.68	183.72	362.47	338.75	255.86	305.30	240.11	232.73	204.45	+1.77%
	B	m	43.07	32.08	30.07	32.93	32.07	67.58	60.11	43.09	50.09	38.08	33.04	32.33	+0.97%
	D	m	21.99	15.38	15.34	20.52	15.31	30.45	30.31	22.31	25.47	21.07	20.38	19.39	+1.77%
	T	m	16.24	11.12	11.26	15.37	11.02	23.98	23.58	15.34	19.28	15.75	15.32	14.05	+4.88%
	f	m	5.75	4.25	4.08	5.15	4.29	6.47	6.73	6.97	6.19	5.33	5.05	5.34	-6.38%
	V_{INT}	m^3	181099	75778	77756	128006	75199	570622	450653	192514	301037	154553	128848	102482	+5.27%
	DWT	t	119794	40052	44610	83674	39841	406748	332056	107746	212660	102789	83011	64197	+2.22%
	m_{LIGHT}	t	27801	14400	10104	14513	14012	65518	67083	34771	34990	18643	14783	12953	+21.76%
	L/B	-	5.79	5.75	6.46	7.07	5.73	5.36	5.64	5.94	6.09	6.31	7.04	6.32	+0.99%
ELEC. + LIB	L_{OA}	m	379.84	317.71	334.02	411.78	297.75	523.36	484.45	419.03	457.90	394.99	421.47	345.31	+63.27%
	B	m	71.07	51.86	56.41	83.32	46.69	147.92	120.28	86.38	104.97	76.64	87.43	59.75	+102.68%
	D	m	33.49	26.48	26.38	36.32	24.82	43.96	43.35	36.54	38.20	34.66	36.90	32.75	+63.30%
	T	m	34.12	27.43	25.08	33.29	25.59	50.76	48.02	37.62	39.93	34.72	35.28	31.41	+130.82%
	f	m	-0.63	-0.94	1.31	3.03	-0.77	-6.80	-4.67	-1.08	-1.73	-0.06	1.63	1.35	-113.39%
	V_{INT}	m^3	806808	400237	461608	1159608	314214	3046999	2229866	1203372	1656609	960647	1269401	617624	+509.86%
	DWT	t	114998	37508	42337	79319	37706	390531	319968	101297	204432	98041	78374	60992	-2.26%
	m_{LIGHT}	t	414551	230068	209483	459774	180593	1652079	1172299	658306	797110	457679	553255	290086	+2514.01%
	L/B	-	5.34	6.13	5.92	4.94	6.38	3.54	4.03	4.85	4.36	5.15	4.82	5.78	-15.85%

Figure C.1: Design impact results bulk carriers

TANKERS			ASPHALT SPLENDOR	D&K ABDUL RAZZAK KHALID ZAID AL-KHALID	KMARIN RESPECT	HERON	WHITE STAR	CABO VICTORIA	IBERIAN SEA	NAUTICAL DEBORAH	HILI	BOW ORION	SOLAR SHARNA	TOVE KNUTSEN	
FUEL OIL (original)	L_{OA}	m	179.90	182.90	249.85	333.00	119.00	244.00	249.80	227.98	336.00	182.88	169.06	278.95	
	B	m	30.60	32.20	44.00	60.00	20.40	43.00	44.00	38.00	60.00	32.20	25.60	48.00	
	D	m	16.80	19.10	21.30	29.50	10.65	21.80	21.35	19.80	29.50	19.80	15.60	23.60	
	T	m	10.40	13.30	15.50	21.60	6.70	15.20	15.10	13.20	21.60	13.20	10.00	17.15	
	f	m	6.40	5.80	5.80	7.90	3.95	6.60	6.25	6.60	7.90	6.60	5.60	6.45	
	V_{INT}	m^3	73105	82478	176227	420214	21739	169744	173836	128047	420044	96326	50596	230537	
	DWT	t	36962	50104	109584	298439	7895	113000	114218	75343	128800	49042	25039	152868	
	m_{LIGHT}	t	11892	13803	34916	66754	4391	22518	26553	22978	240406	16620	9763	44237	
	L/B	-	5.88	5.68	5.68	5.55	5.83	5.67	5.68	6.00	5.60	5.68	6.60	5.81	
METHANOL	L_{OA}	m	181.59	185.03	252.20	335.58	121.54	246.37	252.41	230.56	339.49	185.86	171.48	281.11	+1.09%
	B	m	30.63	32.25	44.05	60.05	20.47	43.05	44.05	38.04	60.00	32.26	25.65	48.04	+0.12%
	D	m	16.96	19.32	21.50	29.73	10.88	22.01	21.57	20.02	29.81	20.12	15.82	23.78	+1.10%
	T	m	10.67	13.70	15.85	22.00	7.12	15.57	15.49	13.58	22.03	13.76	10.40	17.46	+2.69%
	f	m	6.29	5.63	5.65	7.73	3.76	6.45	6.09	6.44	7.78	6.37	5.43	6.32	-2.54%
	V_{INT}	m^3	74843	85096	180621	429341	22835	174190	178729	131918	431726	100122	52520	235434	+2.67%
	DWT	t	38028	51712	112279	304036	8570	115729	117220	77721	134851	51377	26222	155874	+2.78%
	m_{LIGHT}	t	12201	14270	35695	68370	4588	23308	27421	23668	242305	17300	10107	45108	+1.85%
	L/B	-	5.93	5.74	5.73	5.59	5.94	5.72	5.73	6.06	5.66	5.76	6.68	5.85	+1.03%
LNG	L_{OA}	m	181.73	185.20	252.39	335.79	121.73	246.57	252.61	230.75	339.49	186.08	171.67	281.31	+1.16%
	B	m	30.63	32.26	44.05	60.06	20.48	43.05	44.06	38.05	60.00	32.26	25.66	48.04	+0.12%
	D	m	16.97	19.34	21.52	29.75	10.89	22.03	21.59	20.04	29.81	20.15	15.84	23.80	+1.17%
	T	m	10.44	13.36	15.56	21.66	6.77	15.26	15.16	13.26	21.67	13.29	10.07	17.20	+0.44%
	f	m	6.53	5.98	5.96	8.08	4.12	6.77	6.43	6.78	8.13	6.85	5.77	6.60	+2.84%
	V_{INT}	m^3	74985	85300	180980	430084	22919	174548	179116	132215	431726	100402	52671	235871	+2.84%
	DWT	t	36802	49866	109174	297578	7803	112590	113761	74991	127884	48710	24869	152434	-0.42%
	m_{LIGHT}	t	12276	14381	35886	68766	4634	23500	27630	23830	242657	17456	10188	45331	+2.27%
	L/B	-	5.93	5.74	5.73	5.59	5.94	5.73	5.73	6.06	5.66	5.77	6.69	5.86	+1.11%
LIQ. HYDROGEN	L_{OA}	m	189.65	195.29	272.56	340.80	133.98	267.96	272.56	244.07	340.98	200.29	179.45	290.92	+6.36%
	B	m	30.69	32.37	44.00	63.14	20.58	43.00	44.00	38.00	64.66	32.30	26.95	48.20	+2.07%
	D	m	17.71	20.39	23.24	30.19	11.99	23.94	23.30	21.20	29.94	21.68	16.56	24.61	+6.41%
	T	m	11.12	14.35	16.56	22.70	7.79	16.34	16.25	14.24	22.76	14.67	11.06	17.97	+7.44%
	f	m	6.59	6.04	6.68	7.49	4.20	7.60	7.04	6.95	7.18	7.01	5.50	6.64	+4.05%
	V_{INT}	m^3	83137	97752	218149	475556	28292	214178	215958	151797	479596	118657	62130	258056	+17.64%
	DWT	t	36384	49248	108159	295475	7554	111574	112642	74086	125631	47831	24427	151220	-1.47%
	m_{LIGHT}	t	16308	20525	47829	91101	7273	35802	40631	33092	266605	26445	14837	56354	+27.58%
	L/B	-	6.18	6.03	6.19	5.40	6.51	6.23	6.19	6.42	5.27	6.20	6.66	6.04	+5.26%
AMMONIA	L_{OA}	m	183.13	187.00	254.36	339.49	123.92	248.59	254.86	232.95	339.75	188.62	173.69	282.96	+2.03%
	B	m	30.65	32.29	44.09	60.00	20.53	43.09	44.09	38.08	60.73	32.29	25.69	48.07	+0.33%
	D	m	17.10	19.53	21.68	30.07	11.09	22.21	21.78	20.23	29.83	20.42	16.03	23.94	+2.06%
	T	m	10.90	14.03	16.14	22.36	7.47	15.89	15.82	13.91	22.39	14.23	10.73	17.71	+5.00%
	f	m	6.20	5.50	5.54	7.71	3.62	6.32	5.96	6.32	7.44	6.19	5.30	6.23	-4.64%
	V_{INT}	m^3	76423	87512	184680	442028	23871	178342	183339	135521	439241	103650	54287	239603	+5.17%
	DWT	t	37914	51558	112014	303590	8520	115483	116965	77506	134366	51172	26106	155433	+2.53%
	m_{LIGHT}	t	13495	16234	38999	75671	5418	26669	31140	26585	249670	20153	11545	48623	+9.59%
	L/B	-	5.97	5.79	5.77	5.66	6.04	5.77	5.78	6.12	5.59	5.84	6.76	5.89	+1.89%
ELEC. + LIB	L_{OA}	m	308.00	335.89	416.83	505.45	299.94	411.76	431.15	415.10	518.68	385.66	266.64	361.70	+69.13%
	B	m	52.11	59.06	82.74	116.79	50.20	81.07	87.57	82.16	122.86	72.93	66.40	90.10	+101.67%
	D	m	28.76	35.08	35.54	44.78	26.84	36.79	36.85	36.05	45.54	41.75	24.60	30.60	+70.09%
	T	m	24.69	32.50	34.20	44.57	22.21	34.75	35.38	31.37	44.43	36.53	27.31	34.43	+132.65%
	f	m	4.08	2.58	1.33	0.21	4.63	2.04	1.47	4.68	1.10	5.22	-2.70	-3.83	-72.57%
	V_{INT}	m^3	421853	629360	1107018	2344274	377586	1108970	1261242	1129447	2585509	1099413	392065	862703	+551.99%
	DWT	t	35951	48590	107019	293100	7274	110415	111367	73105	123077	46872	23932	150030	-2.63%
	m_{LIGHT}	t	185311	290813	507662	1066017	160957	501733	582375	459455	1296393	475150	242132	503051	+1118.08%
	L/B	-	5.91	5.69	5.04	4.33	5.98	5.08	4.92	5.05	4.22	5.29	4.02	4.01	-14.55%

Figure C.2: Design impact results tankers

CONTAINER SHIPS			AL MURABBA	CMA CGM ARKANSAS	CAPE AKRITAS	MAERSK BERMUDA	EVER BLISS	OOCL HONG KONG	DANIEL K INOUYE	SABRE TRADER	MSC JOSSELINE	SEATRADE GREEN	KMTC SEOUL	YM CELEBRITY	
FUEL OIL (original)	L_{OA}	m	368.52	299.99	330.00	194.93	211.90	399.87	260.30	172.00	365.84	185.00	197.40	209.75	
	B	m	51.00	48.20	48.20	32.20	32.80	58.80	35.00	28.40	48.20	30.00	32.50	32.80	
	D	m	30.35	25.00	27.20	17.00	16.80	32.50	21.00	14.20	29.85	16.50	16.80	16.80	
	T	m	15.50	14.50	16.00	11.50	11.20	16.00	12.20	9.50	16.00	10.00	11.70	11.20	
	f	m	14.85	10.50	11.20	5.50	5.60	16.50	8.80	4.70	13.85	6.50	5.10	5.60	
	V_{INT}	m^3	411373	256504	305216	79103	90928	562373	133538	53681	379394	69707	78233	91094	
	DWT	t	149360	104236	134869	35157	37546	191400	51400	23439	150893	26868	37200	37435	
	m_{LIGHT}	t	87737	51850	61504	15297	13802	108682	22186	8185	71394	11359	15598	15031	
	L/B	-	7.23	6.22	6.85	6.05	6.46	6.80	7.44	6.06	7.59	6.17	6.07	6.39	
METHANOL	L_{OA}	m	372.51	305.01	334.46	198.51	215.85	405.33	264.88	174.85	370.08	188.08	199.31	213.59	+1.47%
	B	m	51.08	48.34	48.31	32.32	32.93	58.92	35.13	28.50	48.29	30.10	32.57	32.92	+0.27%
	D	m	30.68	25.42	27.57	17.31	17.11	32.94	21.37	14.44	30.20	16.77	16.96	17.11	+1.47%
	T	m	16.08	15.28	16.67	12.10	11.81	16.79	12.92	9.95	16.63	10.53	12.01	11.79	+4.67%
	f	m	14.60	10.14	10.90	5.22	5.31	16.15	8.45	4.48	13.57	6.25	4.95	5.32	-3.10%
	V_{INT}	m^3	423678	268513	316845	82969	95171	583144	140125	55937	391540	72704	80293	95242	+3.78%
	DWT	t	156915	111623	142013	37537	40159	204160	55459	24828	158352	28713	38464	39991	+5.96%
	m_{LIGHT}	t	89927	54002	63578	15991	14566	112385	23375	8590	73558	11897	15964	15779	+3.52%
	L/B	-	7.29	6.31	6.92	6.14	6.56	6.88	7.54	6.14	7.66	6.25	6.12	6.49	+1.22%
LNG	L_{OA}	m	372.82	305.36	334.79	198.76	216.06	405.73	265.14	175.05	370.38	188.29	199.45	213.79	+1.57%
	B	m	51.08	48.35	48.31	32.33	32.93	58.92	35.14	28.50	48.29	30.11	32.57	32.92	+0.29%
	D	m	30.70	25.45	27.59	17.33	17.13	32.98	21.39	14.45	30.22	16.79	16.97	17.12	+1.57%
	T	m	15.59	14.63	16.11	11.60	11.30	16.13	12.32	9.58	16.10	10.09	11.75	11.29	+0.75%
	f	m	15.11	10.82	11.49	5.74	5.83	16.85	9.07	4.88	14.12	6.71	5.22	5.83	+2.73%
	V_{INT}	m^3	424646	269339	317689	83235	95392	584681	140489	56094	392412	72910	80446	95457	+4.05%
	DWT	t	148232	103168	133806	34819	37167	189502	50827	23243	149767	26607	37008	37066	-0.88%
	m_{LIGHT}	t	90449	54478	64052	16144	14714	113240	23610	8680	74050	12016	16049	15923	+4.31%
	L/B	-	7.30	6.32	6.93	6.15	6.56	6.89	7.55	6.14	7.67	6.25	6.12	6.49	+1.30%
LIQ. HYDROGEN	L_{OA}	m	391.59	329.56	356.04	215.87	235.26	431.86	287.71	188.68	390.62	202.98	208.46	232.35	+8.62%
	B	m	51.27	48.63	48.54	32.57	33.20	59.16	35.46	28.74	48.51	30.35	32.79	33.17	+0.90%
	D	m	32.25	27.46	29.35	18.83	18.65	35.10	23.21	15.58	31.87	18.10	17.74	18.61	+8.62%
	T	m	17.05	16.54	17.77	13.04	12.79	18.11	14.13	10.68	17.67	11.37	12.53	12.73	+12.31%
	f	m	15.20	10.92	11.58	5.78	5.87	16.99	9.09	4.89	14.20	6.73	5.21	5.88	+3.34%
	V_{INT}	m^3	482850	327760	373460	101920	116293	684838	173393	67006	450730	87374	90195	115734	+22.32%
	DWT	t	145303	100427	131093	33935	36233	184668	49393	22726	146933	25921	36520	36148	-3.11%
	m_{LIGHT}	t	119196	83198	91535	25335	24959	162570	39713	14048	102786	19132	20862	25869	+51.09%
	L/B	-	7.64	6.78	7.33	6.63	7.09	7.30	8.11	6.57	8.05	6.69	6.36	7.00	+7.84%
AMMONIA	L_{OA}	m	376.17	309.79	338.66	201.88	219.69	410.47	269.36	177.54	374.09	190.97	201.09	217.33	+2.86%
	B	m	51.14	48.45	48.39	32.41	33.03	59.00	35.24	28.58	48.36	30.18	32.62	33.01	+0.48%
	D	m	30.98	25.82	27.91	17.61	17.42	33.36	21.73	14.66	30.52	17.03	17.11	17.41	+2.86%
	T	m	16.58	15.95	17.25	12.60	12.34	17.48	13.57	10.35	17.17	10.98	12.28	12.31	+8.73%
	f	m	14.40	9.87	10.67	5.00	5.07	15.88	8.16	4.31	13.35	6.05	4.83	5.10	-5.52%
	V_{INT}	m^3	435010	279963	327797	86616	99321	602788	146597	58078	403043	75532	82210	99297	+7.37%
	DWT	t	156172	111098	141427	37353	40028	203143	55272	24727	157760	28572	38348	39862	+5.51%
	m_{LIGHT}	t	99151	63160	72399	18919	17844	128181	28474	10305	82805	14167	17518	18981	+18.50%
	L/B	-	7.36	6.39	7.00	6.23	6.65	6.96	7.64	6.21	7.74	6.33	6.16	6.58	+2.43%
ELEC. + LIB	L_{OA}	m	715.71	716.64	702.72	491.39	535.82	867.49	669.58	406.54	737.38	446.00	349.66	524.56	+124.17%
	B	m	51.00	48.20	48.20	32.20	32.80	58.80	35.00	28.40	48.20	30.00	32.55	32.80	+0.01%
	D	m	58.94	59.72	57.92	42.85	42.48	70.51	54.02	33.56	60.16	39.78	29.76	42.01	+124.14%
	T	m	52.02	55.53	53.57	41.37	40.50	62.77	49.98	32.19	54.13	37.21	28.49	40.10	+252.77%
	f	m	6.93	4.19	4.36	1.49	1.98	7.73	4.04	1.37	6.04	2.57	1.27	1.91	-59.64%
	V_{INT}	m^3	1905676	1853933	1744385	611785	674420	3239613	1129800	348497	1896072	479077	289837	656193	+490.54%
	DWT	t	142224	97370	128159	32956	35147	179404	47689	22155	143865	25163	36004	35092	-5.57%
	m_{LIGHT}	t	1194362	1229541	1126540	407638	443033	2083456	745185	225978	1191449	312390	174121	430671	+1881.74%
	L/B	-	14.03	14.87	14.58	15.26	16.34	14.75	19.13	14.31	15.30	14.87	10.74	15.99	+127.12%

Figure C.3: Design impact results container ships

	TSHDs		BONNY RIVER	CHARLES DARWIN	CONGO RIVER	GALILEO GALILEI	HAM 318	INAI KENANGA	LEIV EIRIKSSON	PRINS DER NEDERLANDEN	QUEEN OF THE NETHERLANDS	VASCO DA GAMA	VOX MAXIMA	WILLEM VAN ORANJE	
FUEL OIL (original)	L_{OA}	m	158.20	183.20	168.00	166.55	227.20	197.70	223.00	201.00	230.71	207.32	203.40	143.53	
	B	m	30.00	40.00	38.00	36.00	32.00	36.40	41.00	28.00	32.00	36.20	31.00	28.00	
	D	m	13.70	17.50	13.30	13.60	15.50	14.90	20.00	15.00	15.90	19.00	17.50	13.50	
	T	m	8.00	13.00	12.15	9.75	13.55	12.30	15.15	12.10	11.03	13.45	12.25	10.00	
	f	m	5.70	4.50	1.15	3.85	1.95	2.60	4.85	2.90	4.87	5.55	5.25	3.50	
	V_{INT}	m^3	50516	90208	79970	79711	93254	83420	128050	66537	93029	101538	83475	39544	
	DWT	t	25320	54140	46946	30734	61280	51312	77148	39335	59168	58299	55546	22445	
	m_{LIGHT}	t	3369	18185	14009	12795	17176	20715	27701	13462	5147	16339	4957	7697	
	L/B	-	5.27	4.58	4.42	4.63	7.10	5.43	5.44	7.18	7.21	5.73	6.56	5.13	
METHANOL	L_{OA}	m	160.30	185.22	169.81	168.61	227.20	201.65	226.12	201.00	230.71	210.84	203.40	145.72	+0.90%
	B	m	30.08	40.09	38.07	36.10	33.03	36.50	41.12	28.69	33.70	36.27	32.33	28.09	+1.34%
	D	m	13.88	17.69	13.44	13.77	15.50	15.20	20.28	15.00	15.90	19.32	17.50	13.71	+0.95%
	T	m	8.32	13.34	12.39	10.05	13.92	12.79	15.64	12.38	11.66	14.00	12.82	10.37	+3.48%
	f	m	5.56	4.35	1.05	3.72	1.58	2.41	4.64	2.62	4.24	5.32	4.68	3.34	-6.81%
	V_{INT}	m^3	52241	93030	81791	81727	96508	87697	133149	68400	98657	106116	87735	41198	+3.94%
	DWT	t	26330	55797	48014	31914	63195	53822	80138	40426	62493	60984	58053	23414	+3.94%
	m_{LIGHT}	t	3621	18603	14278	13090	17663	21347	28452	13736	6004	17015	5595	7940	+3.59%
	L/B	-	5.33	4.62	4.46	4.67	6.88	5.53	5.50	7.01	6.85	5.81	6.29	5.19	-0.79%
LNG	L_{OA}	m	160.48	185.39	169.96	168.81	195.98	201.95	226.36	174.50	199.23	210.83	192.67	145.90	-3.37%
	B	m	30.09	40.10	38.08	36.11	44.67	36.50	41.13	38.16	45.57	36.39	36.24	28.10	+10.41%
	D	m	13.90	17.71	13.46	13.78	13.37	15.22	20.30	13.02	13.73	19.32	16.58	13.72	-2.79%
	T	m	7.99	12.99	12.14	9.74	13.55	12.28	15.13	12.09	11.04	13.43	12.25	9.98	-0.08%
	f	m	5.91	4.72	1.31	4.05	-0.18	2.94	5.17	0.93	2.69	5.89	4.32	3.74	-11.09%
	V_{INT}	m^3	52384	93270	81944	81915	96874	88022	133549	68622	99372	106550	88256	41331	+4.33%
	DWT	t	24930	53525	46544	30285	60618	50357	76009	38937	58104	57303	54688	22071	-1.43%
	m_{LIGHT}	t	3702	18736	14364	13190	17841	21532	28682	13842	6333	17244	5839	8015	+4.81%
	L/B	-	5.33	4.62	4.46	4.68	4.39	5.53	5.50	4.57	4.37	5.79	5.32	5.19	-12.97%
LIQ. HYDROGEN	L_{OA}	m	180.85	195.99	179.23	179.56	218.65	214.41	234.54	190.62	235.00	214.62	208.71	157.08	+4.30%
	B	m	30.00	40.38	38.28	36.40	42.44	39.98	44.68	36.35	43.60	42.48	38.71	28.31	+12.97%
	D	m	15.66	18.72	14.19	14.66	14.92	16.16	21.03	14.23	16.20	19.67	17.96	14.77	+4.63%
	T	m	8.99	14.01	12.86	10.63	14.70	13.73	16.61	12.97	13.06	15.18	14.04	11.02	+10.56%
	f	m	6.67	4.71	1.33	4.03	0.21	2.43	4.42	1.26	3.13	4.49	3.92	3.75	-13.51%
	V_{INT}	m^3	68510	108151	91321	92487	116260	112111	161814	79236	136798	134458	114824	49806	+27.95%
	DWT	t	24442	52750	46035	29719	59800	49257	74666	38437	56845	56175	53651	21607	-3.14%
	m_{LIGHT}	t	8681	26102	19020	18434	27311	33366	42593	19061	24402	30842	18761	12229	+73.82%
	L/B	-	6.03	4.85	4.68	4.93	5.15	5.36	5.25	5.24	5.39	5.05	5.39	5.55	-8.43%
AMMONIA	L_{OA}	m	162.35	187.25	171.60	170.63	199.87	211.68	232.54	177.17	205.40	211.41	197.55	147.88	-1.49%
	B	m	30.15	40.17	38.13	36.18	44.20	36.40	41.00	37.82	45.08	37.40	35.86	28.16	+10.27%
	D	m	14.06	17.89	13.58	13.93	13.64	15.95	20.86	13.22	14.16	19.37	17.00	13.91	-0.97%
	T	m	8.63	13.68	12.63	10.34	14.29	13.30	16.15	12.66	12.33	14.57	13.42	10.72	+6.99%
	f	m	5.43	4.21	0.95	3.59	-0.66	2.66	4.71	0.56	1.83	4.81	3.58	3.19	-25.31%
	V_{INT}	m^3	53926	95864	83598	83702	99955	97996	142395	70296	105129	110988	92477	42829	+9.09%
	DWT	t	26151	55548	47843	31709	62997	53400	79629	40269	62399	60694	57890	23251	+3.46%
	m_{LIGHT}	t	5042	20954	15787	14753	20449	25355	32992	15304	11035	20960	9348	9309	+24.60%
	L/B	-	5.38	4.66	4.50	4.72	4.52	5.82	5.67	4.69	4.56	5.65	5.51	5.25	-11.28%
ELEC. + LIB	L_{OA}	m	342.54	338.97	302.87	328.86	433.01	493.86	472.79	360.34	525.86	478.89	478.66	329.74	+111.55%
	B	m	69.72	68.65	58.40	65.68	100.96	127.64	117.77	75.23	144.13	120.55	120.45	65.93	+177.81%
	D	m	29.66	32.38	23.98	26.85	29.54	37.22	42.40	26.89	36.24	43.89	41.18	31.01	+111.86%
	T	m	24.53	34.01	26.64	27.67	33.98	32.94	39.21	28.42	41.07	41.79	37.51	27.74	+177.11%
	f	m	5.13	-1.63	-2.67	-0.81	-4.44	4.28	3.19	-1.52	-4.83	2.09	3.68	3.27	-87.69%
	V_{INT}	m^3	645577	663183	392718	535820	1193914	2205873	2146434	662826	2563803	2317214	2210830	613024	+1532.67%
	DWT	t	23967	51959	45532	29155	58800	48000	73183	37881	54968	54745	52295	21153	-5.16%
	m_{LIGHT}	t	257689	363485	201218	279029	648668	885619	888698	315349	1635368	1084539	975852	254320	+4721.89%
	L/B	-	4.91	4.94	5.19	5.01	4.29	3.87	4.01	4.79	3.65	3.97	3.97	5.00	-21.95%

Figure C.4: Design impact results TSHD

D

Detailed powering impact results

The powering impact is the result of the changed ship ship design to accommodate for the additional bunker volume and weight. The powering impact results are displayed per ship type in table D.1 for bulk carriers, in table D.2 for tankers, in table D.3 for container ships, and in table D.4 for TSHD's. The brake power impact only applies to the main engine ($P_{B\ ME}$) and the auxiliary engine power for the power plant systems ($P_{B\ AE\ PP}$). The auxiliary engine power for the power plant systems ($P_{B\ AE\ PP}$) is calculated as a percentage of the main engine brake power per energy carrier type (PP_{aux}). The auxiliary engine power for non power plant users ($P_{B,\ AE\ non-PP}$) remains constant as it is not influenced by the necessary propulsion power. The general total installed brake power of all engines ($P_{B,\ TOT}$) is therefore calculated according to equation D.1. An overview of the total installed brake power impact per energy carrier and ship type combination is displayed in tabled 3.9.

$$\begin{aligned} P_{B,\ TOT} &= P_{B\ ME} + P_{B\ AE\ PP} + P_{B\ AE\ non-PP} \quad [kW] \\ P_{B,\ TOT} &= P_{B\ ME} + P_{B\ ME} \cdot PP_{aux} + P_{B\ AE\ non-PP} \quad [kW] \\ P_{B,\ TOT} &= P_{B\ ME} \cdot (1 + PP_{aux}) + P_{B\ AE\ non-PP} \quad [kW] \end{aligned} \tag{D.1}$$

The total installed brake power of all engines for an AMEC ($P_{B,\ TOT\ AMEC}$) is therefore calculated according to equation D.2.

$$\begin{aligned} P_{B,\ TOT\ AMEC} &= \frac{P_{B,\ ME\ AMEC\ 2}}{P_{B,\ ME\ FO}} \cdot P_{B,\ TOT} \quad [kW] \\ P_{B,\ TOT\ AMEC} &= \frac{P_{B,\ ME\ AMEC\ 2}}{P_{B,\ ME\ FO}} \cdot P_{B,\ ME} \cdot (1 + PP_{aux,\ AMEC}) + P_{B,\ AE\ non-PP} \quad [kW] \end{aligned} \tag{D.2}$$

The following notations are used for the brake power definitions within the powering impact assessment results:

$P_{B,\ TOT\ AMEC}$ = The total installed brake power for an AMEC after the full powering impact assessment
$P_{B,\ TOT\ FO}$ = The original total installed brake power (fuel oil)
$P_{B,\ ME\ AMEC\ 2}$ = The main engine brake power after the full powering impact assessment for an AMEC
$P_{B,\ ME\ AMEC\ 1}$ = The main engine brake power after the energy carrier substitution for an AMEC
$P_{B,\ ME\ FO}$ = The original main engine brake power (fuel oil)

The results are displayed in columns two to five of the result table according to equations D.3 to D.6 respectively:

$$\frac{P_{B\ TOT\ AMEC}}{P_{B\ TOT\ FO}} = \text{Total installed brake power impact of an AMEC after fuel oil substitution and upscaling the bunkering} \tag{D.3}$$

$\frac{P_{B\ ME\ AMEC\ 2}}{P_{B\ ME\ FO}}$ = Main engine brake power (propulsion power) impact of an AMEC after fuel oil substitution and upscaling the bunkering (D.4)

$\frac{P_{B\ ME\ AMEC\ 1}}{P_{B\ ME\ FO}}$ = Main engine brake power impact of an AMEC after fuel oil substitution (D.5)

$\frac{P_{B\ ME\ AMEC\ 2}}{P_{B\ ME\ AMEC\ 1}}$ = Main engine brake power impact of an AMEC after upscaling the bunkering (D.6)

Table D.1: The average powering impact per energy carrier type in bulk carriers

BULK CARRIERS	$\frac{P_{B\ TOT\ AMEC}}{P_{B\ TOT\ FO}}$	$\frac{P_{B\ ME\ AMEC\ 2}}{P_{B\ ME\ FO}}$	$\frac{P_{B\ ME\ AMEC\ 1}}{P_{B\ ME\ FO}}$	$\frac{P_{B\ ME\ AMEC\ 2}}{P_{B\ ME\ AMEC\ 1}}$
Fuel oil (original)	0.0%	0.0%	0.0%	0.0%
Methanol	+1.9%	+2.3%	+2.2%	+0.1%
LNG	+0.9%	+1.1%	+1.1%	+0.0%
Liq. hydrogen	+8.6%	+10.3%	+9.4%	+0.7%
Ammonia	+3.7%	+4.4%	+4.2%	+0.2%
Elec. + LIB	+235.3%	+280.8%	+129.1%	+66.2%

Table D.2: The average powering impact per energy carrier type in tankers

TANKERS	$\frac{P_{B\ TOT\ AMEC}}{P_{B\ TOT\ FO}}$	$\frac{P_{B\ ME\ AMEC\ 2}}{P_{B\ ME\ FO}}$	$\frac{P_{B\ ME\ AMEC\ 1}}{P_{B\ ME\ FO}}$	$\frac{P_{B\ ME\ AMEC\ 2}}{P_{B\ ME\ AMEC\ 1}}$
Fuel oil (original)	0.0%	0.0%	0.0%	0.0%
Methanol	+1.6%	+2.2%	+2.1%	+0.1%
LNG	+0.8%	+1.1%	+1.0%	+0.0%
Liq. hydrogen	+7.4%	+9.8%	+9.0%	+0.7%
Ammonia	+3.2%	+4.2%	+4.0%	+0.3%
Elec. + LIB	+234.4%	+309.7%	+135.7%	+73.8%

Table D.3: The average powering impact per energy carrier type in container ships

CONTAINER SHIPS	$\frac{P_{B\ TOT\ AMEC}}{P_{B\ TOT\ FO}}$	$\frac{P_{B\ ME\ AMEC\ 2}}{P_{B\ ME\ FO}}$	$\frac{P_{B\ ME\ AMEC\ 1}}{P_{B\ ME\ FO}}$	$\frac{P_{B\ ME\ AMEC\ 2}}{P_{B\ ME\ AMEC\ 1}}$
Fuel oil (original)	0.0%	0.0%	0.0%	0.0%
Methanol	+2.6%	+3.1%	+3.0%	+0.1%
LNG	+1.0%	+1.2%	+1.2%	+0.1%
Liq. hydrogen	+8.4%	+10.2%	+9.0%	+1.0%
Ammonia	+4.9%	+5.9%	+5.4%	+0.5%
Elec. + LIB	+190.1%	+229.7%	+117.6%	+51.5%

Table D.4: The average powering impact per energy carrier type in TSHDs

TSHDs	$\frac{P_{B\ TOT\ AMEC}}{P_{B\ TOT\ FO}}$	$\frac{P_{B\ ME\ AMEC\ 2}}{P_{B\ ME\ FO}}$	$\frac{P_{B\ ME\ AMEC\ 1}}{P_{B\ ME\ FO}}$	$\frac{P_{B\ ME\ AMEC\ 2}}{P_{B\ ME\ AMEC\ 1}}$
Fuel oil (original)	0.0%	0.0%	0.0%	0.0%
Methanol	+1.5%	+3.1%	+3.0%	+0.1%
LNG	+3.4%	+7.5%	+1.2%	+6.2%
Liq. hydrogen	+8.4%	+17.2%	+13.6%	+3.2%
Ammonia	+5.5%	+11.6%	+5.7%	+5.6%
Elec. + LIB	+249.9%	+502.2%	+225.7%	+84.9%

E

LCIA results (A)MECs

Table E.1: Compiled gross LCIA results (A)MECs - ReCiPe 2016 (H)

		Fuel oil		Methanol		LNG		Liq. hydrogen		Ammonia		Elec. + LIB	
Midpoint impact category	Unit	Diesel	Bio diesel	Methanol	Bio meth.	LNG	Bio LNG	LH_2	eLH_2	NH_3	eNH_3	E.mix + LIB	E.ren + LIB
Global warming	kg CO_2 eq	8.95E-02	6.52E-02	1.03E-01	3.45E-02	8.28E-02	3.27E-02	2.08E-02	1.23E-02	1.16E-01	2.52E-02	3.08E-01	1.18E-01
Stratospheric ozone depletion	kg CFC11 eq	1.82E-08	4.23E-07	1.76E-08	2.59E-08	1.16E-08	1.21E-08	5.66E-09	5.37E-09	1.44E-08	1.12E-08	8.42E-08	9.16E-09
Ionizing radiation	kBq Co-60 eq	2.43E-05	1.00E-03	5.08E-04	2.69E-03	7.99E-04	1.44E-03	4.33E-04	6.77E-04	1.10E-03	5.31E-03	2.38E-02	2.82E-04
Ozone formation (human health)	kg NO_X eq	3.21E-05	1.00E-04	5.64E-05	1.38E-04	3.49E-05	3.22E-05	3.36E-05	3.73E-05	1.27E-04	6.57E-05	5.03E-04	9.54E-05
Fine particulate matter formation	kg $PM_{2.5}$ eq	1.96E-05	8.03E-05	2.84E-05	7.48E-05	2.55E-05	3.17E-05	1.97E-05	2.41E-05	5.68E-05	4.51E-05	5.66E-04	1.50E-04
Ozone formation (ecosystems)	kg NO_X eq	3.38E-05	1.05E-04	6.09E-05	1.42E-04	3.75E-05	3.27E-05	3.55E-05	3.90E-05	1.33E-04	6.82E-05	5.09E-04	9.93E-05
Terrestrial acidification	kg SO_2 eq	7.47E-05	3.04E-04	7.82E-05	1.41E-04	5.98E-05	5.97E-05	4.18E-05	4.25E-05	1.63E-04	8.90E-05	1.12E-03	4.94E-04
Freshwater eutrophication	kg P eq	7.62E-08	1.19E-05	2.88E-06	1.50E-05	3.20E-06	6.28E-06	2.62E-06	9.28E-06	6.00E-06	1.97E-05	9.45E-05	2.30E-06
Marine eutrophication	kg N eq	1.35E-06	1.32E-04	3.00E-07	5.53E-06	3.17E-07	1.59E-06	2.78E-07	1.48E-06	6.82E-07	2.42E-06	6.62E-06	4.61E-07
Terrestrial ecotoxicity	kg 1,4-DCB	4.87E-03	6.35E-02	9.90E-03	9.93E-02	5.43E-03	1.26E-02	8.18E-03	6.35E-02	7.32E-02	9.21E-02	1.32E-01	4.53E-02
Freshwater ecotoxicity	kg 1,4-DCB	5.13E-06	1.02E-03	4.72E-04	1.68E-03	2.21E-04	6.52E-04	3.17E-04	6.03E-03	2.30E-03	8.52E-03	3.30E-03	2.40E-03
Marine ecotoxicity	kg 1,4-DCB	6.69E-05	1.22E-03	6.38E-04	2.25E-03	3.20E-04	8.41E-04	4.12E-04	7.43E-03	2.95E-03	1.05E-02	4.59E-03	2.99E-03
Human carcinogenic toxicity	kg 1,4-DCB	7.23E-06	1.63E-03	1.07E-03	3.31E-03	7.99E-04	9.51E-04	5.79E-04	1.82E-02	4.64E-03	2.53E-02	8.67E-03	7.28E-03
Human non-carcinogenic toxicity	kg 1,4-DCB	1.10E-02	6.57E-02	8.93E-03	8.10E-02	6.55E-03	1.30E-02	6.67E-03	2.96E-02	3.48E-02	5.09E-02	1.41E-01	1.25E-02
Land use	m^2 a crop eq	8.20E-03	1.20E-01	2.98E-04	1.23E-01	1.92E-04	2.37E-03	1.15E-04	1.02E-03	7.36E-04	1.58E-03	2.68E-03	4.26E-04
Mineral resource scarcity	kg Cu eq	6.03E-06	1.07E-04	4.18E-05	1.21E-04	1.45E-05	2.58E-05	1.73E-05	3.00E-04	2.74E-04	4.16E-04	1.62E-03	1.66E-03
Fossil resource scarcity	kg oil eq	2.63E-02	6.96E-03	3.76E-02	9.30E-03	2.70E-02	4.91E-03	1.38E-02	3.45E-03	4.00E-02	6.95E-03	8.39E-02	3.63E-02
Water consumption	m^3	2.82E-07	1.00E-03	2.18E-04	6.23E-04	5.05E-05	1.04E-04	3.63E-04	2.34E-04	2.60E-03	7.38E-04	1.45E-03	5.92E-05
		Fuel oil		**Methanol**		**LNG**		**Liq. hydrogen**		**Ammonia**		**Elec. + LIB**	
Endpoint area of protection	Unit	Diesel	Bio diesel	Methanol	Bio meth.	LNG	Bio LNG	LH_2	eLH_2	NH_3	eNH_3	E.mix + LIB	E.ren + LIB
Human health	DALY	9.81E-08	1.32E-07	6.50E-08	1.10E-07	1.15E-07	7.41E-08	1.93E-08	1.14E-08	1.08E-07	2.34E-08	7.04E-07	2.31E-07
Natural environment	Species x yr	3.44E-10	1.35E-09	1.97E-10	1.26E-09	3.07E-10	1.88E-10	5.81E-11	3.45E-11	3.25E-10	7.05E-11	1.26E-09	4.56E-10
Resource scarcity	USD (2013)	1.18E-02	2.37E-03	2.43E-04	2.43E-03	9.42E-03	1.23E-03	1.59E-15	9.42E-16	8.88E-15	1.93E-15	2.39E-02	1.53E-02

1 MJ = 0.2778 kWh

Table E.2: Compiled LCIA results (A)MECs per MJ shaft output - ReCiPe 2016 (H)

		Fuel oil		Methanol		LNG		Liq. hydrogen		Ammonia		Elec. + LIB	
Midpoint impact category	Unit	Diesel	Bio diesel	Methanol	Bio meth.	LNG	Bio LNG	LH_2	eLH_2	NH_3	eNH_3	E.mix + LIB	E.ren + LIB
Global warming	kg CO_2 eq	1.81E-01	1.32E-01	2.09E-01	6.99E-02	1.71E-01	6.74E-02	4.73E-02	2.80E-02	2.26E-01	4.90E-02	3.59E-01	1.37E-01
Stratospheric ozone depletion	kg CFC11 eq	3.70E-08	8.58E-07	3.57E-08	5.24E-08	2.39E-08	2.50E-08	1.29E-08	1.22E-08	2.80E-08	2.19E-08	9.82E-08	1.07E-08
Ionizing radiation	kBq Co-60 eq	4.93E-05	2.04E-03	1.03E-03	5.46E-03	1.65E-03	2.96E-03	9.86E-04	1.54E-03	2.13E-03	1.03E-02	2.78E-02	3.29E-04
Ozone formation (human health)	kg NO_X eq	6.51E-05	2.03E-04	1.14E-04	2.80E-04	7.18E-05	6.64E-05	7.65E-05	8.49E-05	2.48E-04	1.28E-04	5.87E-04	1.11E-04
Fine particulate matter formation	kg $PM_{2.5}$ eq	3.97E-05	1.63E-04	5.75E-05	1.52E-04	5.26E-05	6.52E-05	4.48E-05	5.49E-05	1.11E-04	8.78E-05	6.61E-04	1.75E-04
Ozone formation (ecosystems)	kg NO_X eq	6.85E-05	2.13E-04	1.23E-04	2.89E-04	7.73E-05	6.73E-05	8.09E-05	8.90E-05	2.59E-04	1.33E-04	5.94E-04	1.16E-04
Terrestrial acidification	kg SO_2 eq	1.51E-04	6.16E-04	1.58E-04	2.86E-04	1.23E-04	1.23E-04	9.53E-05	9.68E-05	3.17E-04	1.73E-04	1.31E-03	5.76E-04
Freshwater eutrophication	kg P eq	1.54E-07	2.42E-05	5.84E-06	3.04E-05	6.59E-06	1.29E-05	5.96E-06	2.11E-05	1.17E-05	3.84E-05	1.10E-04	2.68E-06
Marine eutrophication	kg N eq	2.74E-06	2.67E-04	6.07E-07	1.12E-05	6.53E-07	3.28E-06	6.32E-07	3.36E-06	1.33E-06	4.71E-06	7.73E-06	5.38E-07
Terrestrial ecotoxicity	kg 1,4-DCB	9.86E-03	1.29E-01	2.01E-02	2.01E-01	1.12E-02	2.60E-02	1.87E-02	1.45E-01	1.43E-01	1.79E-01	1.54E-01	5.29E-02
Freshwater ecotoxicity	kg 1,4-DCB	1.04E-05	2.07E-03	9.57E-04	3.41E-03	4.56E-04	1.34E-03	7.22E-04	1.37E-02	4.48E-03	1.66E-02	3.85E-03	2.80E-03
Marine ecotoxicity	kg 1,4-DCB	1.36E-04	2.47E-03	1.29E-03	4.57E-03	6.60E-04	1.73E-03	9.38E-04	1.69E-02	5.74E-03	2.05E-02	5.36E-03	3.49E-03
Human carcinogenic toxicity	kg 1,4-DCB	1.46E-05	3.30E-03	2.17E-03	6.71E-03	1.65E-03	1.96E-03	1.32E-03	4.16E-02	9.03E-03	4.93E-02	1.01E-02	8.49E-03
Human non-carcinogenic toxicity	kg 1,4-DCB	2.23E-02	1.33E-01	1.81E-02	1.64E-01	1.35E-02	2.67E-02	1.52E-02	6.75E-02	6.78E-02	9.91E-02	1.64E-01	1.46E-02
Land use	m^2a crop eq	1.66E-02	2.44E-01	6.03E-04	2.49E-01	3.96E-04	4.88E-03	2.62E-04	2.31E-03	1.43E-03	3.07E-03	3.12E-03	4.97E-04
Mineral resource scarcity	kg Cu eq	1.22E-05	2.16E-04	8.47E-05	2.44E-04	2.98E-05	5.32E-05	3.93E-05	6.85E-04	5.33E-04	8.10E-04	1.89E-03	1.94E-03
Fossil resource scarcity	kg oil eq	5.33E-02	1.41E-02	7.62E-02	1.88E-02	5.56E-02	1.01E-02	3.15E-02	7.86E-03	7.78E-02	1.35E-02	9.79E-02	4.24E-02
Water consumption	m^3	5.72E-07	2.03E-03	4.42E-04	1.26E-03	1.04E-04	2.14E-04	8.28E-04	5.34E-04	5.07E-03	1.44E-03	1.69E-03	6.91E-05
		Fuel oil		**Methanol**		**LNG**		**Liq. hydrogen**		**Ammonia**		**Elec. + LIB**	
Endpoint area of protection	Unit	Diesel	Bio diesel	Methanol	Bio meth.	LNG	Bio LNG	LH_2	eLH_2	NH_3	eNH_3	E.mix + LIB	E.ren + LIB
Human health	DALY	1.99E-07	2.68E-07	1.32E-07	2.22E-07	2.37E-07	1.53E-07	4.39E-08	2.60E-08	2.10E-07	4.55E-08	8.21E-07	2.69E-07
Natural environment	Species x yr	6.97E-10	2.73E-09	3.99E-10	2.54E-09	6.32E-10	3.87E-10	1.33E-10	7.86E-11	6.33E-10	1.37E-10	1.48E-09	5.32E-10
Resource scarcity	USD (2013)	2.38E-02	4.80E-03	4.92E-04	4.93E-03	1.94E-02	2.52E-03	3.62E-15	2.15E-15	1.73E-14	3.75E-15	2.79E-02	1.79E-02
Power plant efficiency	-	49.34%		49.34%		48.55%		43.88%		51.33%		85.70%	

1 MJ = 0.2778 kWh

Table E.3: Compiled LCIA results (A)MECs per MJ shaft output w.r.t. to diesel - ReCiPe 2016 (H)

		Fuel oil		Methanol		LNG		Liq. hydrogen		Ammonia		Elec. + LIB	
Midpoint impact category	Unit	Diesel	Bio diesel	Methanol	Bio meth.	LNG	Bio LNG	LH_2	eLH_2	NH_3	eNH_3	E.mix+LIB	E.ren+LIB
Global warming	kg CO_2 eq	1.81E-01	-27%	+15%	-61%	-6%	-63%	-74%	-85%	+24%	-73%	+98%	-24%
Stratospheric ozone depl	kg CFC11 eq	3.70E-08	+2220%	-4%	+42%	-36%	-32%	-65%	-67%	-24%	-41%	+166%	-71%
Ionizing radiation	kBq Co-60 eq	4.93E-05	+4030%	+1988%	+10965%	+3237%	+5911%	+1899%	+3029%	+4228%	+20882%	+56279%	+568%
Ozone formation (human)	kg NO_X eq	6.51E-05	+211%	+76%	+331%	+10%	+2%	+18%	+30%	+281%	+97%	+801%	+71%
Fine particulate matter form.	kg $PM_{2.5}$ eq	3.97E-05	+310%	+45%	+282%	+32%	+64%	+13%	+38%	+179%	+121%	+1564%	+342%
Ozone formation (eco)	kg NO_X eq	6.85E-05	+211%	+80%	+321%	+13%	-2%	+18%	+30%	+277%	+94%	+767%	+69%
Terrestrial acidification	kg SO_2 eq	1.51E-04	+307%	+5%	+89%	-19%	-19%	-37%	-36%	+109%	+15%	+766%	+281%
Freshwater eutrophication	kg P eq	1.54E-07	+15555%	+3684%	+19625%	+4170%	+8276%	+3764%	+13596%	+7473%	+24802%	+71352%	+1637%
Marine eutrophication	kg N eq	2.74E-06	+9648%	-78%	+309%	-76%	+20%	-77%	+23%	-51%	+72%	+182%	-80%
Terrestrial ecotoxicity	kg 1,4-DCB	9.86E-03	+1205%	+103%	+1941%	+13%	+163%	+89%	+1368%	+1346%	+1720%	+1463%	+436%
Freshwater ecotoxicity	kg 1,4-DCB	1.04E-05	+19758%	+9098%	+32676%	+4282%	+12815%	+6836%	+131975%	+42965%	+159433%	+36939%	+26846%
Marine ecotoxicity	kg 1,4-DCB	1.36E-04	+1722%	+854%	+3269%	+387%	+1178%	+592%	+12394%	+4132%	+15047%	+3852%	+2476%
Human carcinogenic toxicity	kg 1,4-DCB	1.46E-05	+22459%	+14704%	+45734%	+11135%	+13279%	+8913%	+283827%	+61574%	+336506%	+68972%	+57898%
Human non-carcinogenic tox.	kg 1,4-DCB	2.23E-02	+496%	-19%	+634%	-40%	+20%	-32%	+202%	+204%	+344%	+636%	-35%
Land use	m^2a crop eq	1.66E-02	+1369%	-96%	+1399%	-98%	-71%	-98%	-86%	-91%	-82%	-81%	-97%
Mineral resource scarcity	kg Cu eq	1.22E-05	+1670%	+593%	+1899%	+144%	+335%	+221%	+5499%	+4259%	+6525%	+15357%	+15739%
Fossil resource scarcity	kg oil eq	5.33E-02	-74%	+43%	-65%	+4%	-81%	-41%	-85%	+46%	-75%	+84%	-20%
Water consumption	m^3	5.72E-07	+354210%	+77106%	+220498%	+18087%	+37251%	+144663%	+93199%	+886960%	+251375%	+295694%	+11980%
		Fuel oil		**Methanol**		**LNG**		**Liq. hydrogen**		**Ammonia**		**Elec. + LIB**	
Endpoint area of protection	Unit	Diesel	Bio diesel	Methanol	Bio meth.	LNG	Bio LNG	LH_2	eLH_2	NH_3	eNH_3	E.mix+LIB	E.ren+LIB
Human health	DALY	1.99E-07	+35%	-34%	+12%	+19%	-23%	-78%	-87%	+6%	-77%	+313%	+36%
Natural environment	Species x yr	6.97E-10	+291%	-43%	+265%	-9%	-44%	-81%	-89%	-9%	-80%	+112%	-24%
Resource scarcity	USD (2013)	2.38E-02	-80%	-98%	-79%	-19%	-89%	-100%	-100%	-100%	-100%	+17%	-25%
Power plant efficiency	-	49.34%		49.34%		48.55%		43.88%		51.33%		85.70%	

1 MJ = 0.2778 kWh

F

Total environmental impact (A)MECs per ship type

Table F.1: Total environmental impact bulk carriers [LCIA/MJ shaft output]

		Fuel oil		Methanol		LNG		Liq. hydrogen		Ammonia		Elec. + LIB	
Midpoint impact category	Unit	Diesel	Bio diesel	Methanol	Bio meth.	LNG	Bio LNG	LH_2	eLH_2	NH_3	eNH_3	E.mix + LIB	E.renew + LIB
Global warming	kg CO_2 eq	1.81E-01	1.32E-01	2.12E-01	7.12E-02	1.72E-01	6.81E-02	5.14E-02	3.04E-02	2.34E-01	5.08E-02	1.21E+00	4.61E-01
Stratospheric ozone depletion	kg CFC11 eq	3.70E-08	8.58E-07	3.63E-08	5.34E-08	2.41E-08	2.52E-08	1.40E-08	1.33E-08	2.90E-08	2.27E-08	3.29E-07	3.58E-08
Ionizing radiation	kBq Co-60 eq	4.93E-05	2.04E-03	1.05E-03	5.56E-03	1.66E-03	2.99E-03	1.07E-03	1.68E-03	2.21E-03	1.07E-02	9.32E-02	1.10E-03
Ozone formation (human health)	kg NO_X eq	6.51E-05	2.03E-04	1.16E-04	2.86E-04	7.25E-05	6.70E-05	8.31E-05	9.23E-05	2.57E-04	1.33E-04	1.97E-03	3.73E-04
Fine particulate matter formation	kg $PM_{2.5}$ eq	3.97E-05	1.63E-04	5.86E-05	1.54E-04	5.30E-05	6.58E-05	4.87E-05	5.96E-05	1.15E-04	9.11E-05	2.22E-03	5.88E-04
Ozone formation (ecosystems)	kg NO_X eq	6.85E-05	2.13E-04	1.26E-04	2.94E-04	7.80E-05	6.79E-05	8.79E-05	9.66E-05	2.68E-04	1.38E-04	1.99E-03	3.88E-04
Terrestrial acidification	kg SO_2 eq	1.51E-04	6.16E-04	1.61E-04	2.91E-04	1.24E-04	1.24E-04	1.04E-04	1.05E-04	3.29E-04	1.80E-04	4.40E-03	1.93E-03
Freshwater eutrophication	kg P eq	1.54E-07	2.42E-05	5.95E-06	3.10E-05	6.65E-06	1.30E-05	6.48E-06	2.30E-05	1.21E-05	3.99E-05	3.70E-04	8.99E-06
Marine eutrophication	kg N eq	2.74E-06	2.67E-04	6.19E-07	1.14E-05	6.59E-07	3.31E-06	6.87E-07	3.65E-06	1.38E-06	4.88E-06	2.59E-05	1.80E-06
Terrestrial ecotoxicity	kg 1,4-DCB	9.86E-03	1.29E-01	2.04E-02	2.05E-01	1.13E-02	2.62E-02	2.03E-02	1.57E-01	1.48E-01	1.86E-01	5.17E-01	1.77E-01
Freshwater ecotoxicity	kg 1,4-DCB	1.04E-05	2.07E-03	9.75E-04	3.47E-03	4.60E-04	1.36E-03	7.84E-04	1.49E-02	4.65E-03	1.72E-02	1.29E-02	9.40E-03
Marine ecotoxicity	kg 1,4-DCB	1.36E-04	2.47E-03	1.32E-03	4.65E-03	6.66E-04	1.75E-03	1.02E-03	1.84E-02	5.95E-03	2.13E-02	1.80E-02	1.17E-02
Human carcinogenic toxicity	kg 1,4-DCB	1.46E-05	3.30E-03	2.21E-03	6.84E-03	1.66E-03	1.98E-03	1.43E-03	4.52E-02	9.37E-03	5.11E-02	3.39E-02	2.85E-02
Human non-carcinogenic toxicity	kg 1,4-DCB	2.23E-02	1.33E-01	1.84E-02	1.67E-01	1.36E-02	2.70E-02	1.65E-02	7.33E-02	7.04E-02	1.03E-01	5.51E-01	4.90E-02
Land use	m^2a crop eq	1.66E-02	2.44E-01	6.15E-04	2.54E-01	4.00E-04	4.92E-03	2.85E-04	2.51E-03	1.49E-03	3.19E-03	1.05E-02	1.67E-03
Mineral resource scarcity	kg Cu eq	1.22E-05	2.16E-04	8.63E-05	2.49E-04	3.01E-05	5.37E-05	4.27E-05	7.44E-04	5.53E-04	8.40E-04	6.34E-03	6.50E-03
Fossil resource scarcity	kg oil eq	5.33E-02	1.41E-02	7.77E-02	1.92E-02	5.61E-02	1.02E-02	3.42E-02	8.53E-03	8.07E-02	1.40E-02	3.28E-01	1.42E-01
Water consumption	m^3	5.72E-07	2.03E-03	4.50E-04	1.29E-03	1.05E-04	2.16E-04	8.99E-04	5.80E-04	5.26E-03	1.49E-03	5.67E-03	2.32E-04
		Fuel oil		**Methanol**		**LNG**		**Liq. hydrogen**		**Ammonia**		**Elec. + LIB**	
Endpoint area of protection	Unit	Diesel	Bio diesel	Methanol	Bio meth.	LNG	Bio LNG	LH_2	eLH_2	NH_3	eNH_3	E.mix + LIB	E.renew + LIB
Human health	DALY	1.99E-07	2.68E-07	1.34E-07	2.27E-07	2.39E-07	1.54E-07	4.77E-08	2.83E-08	2.18E-07	4.72E-08	2.75E-06	9.04E-07
Natural environment	Species x yr	6.97E-10	2.73E-09	4.06E-10	2.59E-09	6.38E-10	3.91E-10	1.44E-10	8.54E-11	6.57E-10	1.42E-10	4.95E-09	1.78E-09
Resource scarcity	USD (2013)	2.38E-02	4.80E-03	5.01E-04	5.03E-03	1.96E-02	2.55E-03	3.93E-15	2.33E-15	1.79E-14	3.89E-15	9.34E-02	5.99E-02
Power plant efficiency	-	49.34%		49.34%		48.55%		43.88%		51.33%		85.70%	
Total powering impact	-	0.0%		+1.9%		+0.9%		+8.6%		+3.7%		+235.3%	

1 MJ = 0.2778 kWh

Table F.2: Total environmental impact tankers [LCIA/MJ shaft output]

		Fuel oil		Methanol		LNG		Liq. hydrogen		Ammonia		Elec. + LIB	
Midpoint impact category	Unit	Diesel	Bio diesel	Methanol	Bio meth.	LNG	Bio LNG	LH_2	eLH_2	NH_3	eNH_3	E.mix + LIB	E.renew + LIB
Global warming	kg CO_2 eq	1.81E-01	1.32E-01	2.12E-01	7.10E-02	1.72E-01	6.80E-02	5.08E-02	3.01E-02	2.33E-01	5.06E-02	1.20E+00	4.59E-01
Stratospheric ozone depletion	kg CFC11 eq	3.70E-08	8.58E-07	3.62E-08	5.33E-08	2.40E-08	2.52E-08	1.39E-08	1.31E-08	2.89E-08	2.26E-08	3.28E-07	3.58E-08
Ionizing radiation	kBq Co-60 eq	4.93E-05	2.04E-03	1.05E-03	5.55E-03	1.66E-03	2.99E-03	1.06E-03	1.66E-03	2.20E-03	1.07E-02	9.30E-02	1.10E-03
Ozone formation (human health)	kg NO_X eq	6.51E-05	2.03E-04	1.16E-04	2.85E-04	7.24E-05	6.69E-05	8.22E-05	9.13E-05	2.56E-04	1.32E-04	1.96E-03	3.72E-04
Fine particulate matter formation	kg $PM_{2.5}$ eq	3.97E-05	1.63E-04	5.84E-05	1.54E-04	5.30E-05	6.57E-05	4.82E-05	5.90E-05	1.14E-04	9.06E-05	2.21E-03	5.87E-04
Ozone formation (ecosystems)	kg NO_X eq	6.85E-05	2.13E-04	1.25E-04	2.93E-04	7.79E-05	6.78E-05	8.69E-05	9.56E-05	2.67E-04	1.37E-04	1.99E-03	3.87E-04
Terrestrial acidification	kg SO_2 eq	1.51E-04	6.16E-04	1.61E-04	2.91E-04	1.24E-04	1.24E-04	1.02E-04	1.04E-04	3.27E-04	1.79E-04	4.38E-03	1.93E-03
Freshwater eutrophication	kg P eq	1.54E-07	2.42E-05	5.94E-06	3.09E-05	6.64E-06	1.30E-05	6.41E-06	2.27E-05	1.21E-05	3.97E-05	3.69E-04	8.97E-06
Marine eutrophication	kg N eq	2.74E-06	2.67E-04	6.17E-07	1.14E-05	6.58E-07	3.31E-06	6.80E-07	3.61E-06	1.37E-06	4.86E-06	2.58E-05	1.80E-06
Terrestrial ecotoxicity	kg 1,4-DCB	9.86E-03	1.29E-01	2.04E-02	2.05E-01	1.13E-02	2.62E-02	2.00E-02	1.56E-01	1.47E-01	1.85E-01	5.16E-01	1.77E-01
Freshwater ecotoxicity	kg 1,4-DCB	1.04E-05	2.07E-03	9.73E-04	3.47E-03	4.60E-04	1.35E-03	7.75E-04	1.48E-02	4.62E-03	1.71E-02	1.29E-02	9.38E-03
Marine ecotoxicity	kg 1,4-DCB	1.36E-04	2.47E-03	1.31E-03	4.64E-03	6.65E-04	1.75E-03	1.01E-03	1.82E-02	5.92E-03	2.12E-02	1.79E-02	1.17E-02
Human carcinogenic toxicity	kg 1,4-DCB	1.46E-05	3.30E-03	2.20E-03	6.82E-03	1.66E-03	1.98E-03	1.42E-03	4.47E-02	9.32E-03	5.09E-02	3.38E-02	2.84E-02
Human non-carcinogenic toxicity	kg 1,4-DCB	2.23E-02	1.33E-01	1.84E-02	1.67E-01	1.36E-02	2.70E-02	1.63E-02	7.25E-02	7.00E-02	1.02E-01	5.50E-01	4.89E-02
Land use	m^2a crop eq	1.66E-02	2.44E-01	6.13E-04	2.53E-01	3.99E-04	4.92E-03	2.82E-04	2.49E-03	1.48E-03	3.17E-03	1.04E-02	1.66E-03
Mineral resource scarcity	kg Cu eq	1.22E-05	2.16E-04	8.61E-05	2.48E-04	3.01E-05	5.37E-05	4.22E-05	7.36E-04	5.50E-04	8.36E-04	6.32E-03	6.48E-03
Fossil resource scarcity	kg oil eq	5.33E-02	1.41E-02	7.75E-02	1.92E-02	5.60E-02	1.02E-02	3.39E-02	8.44E-03	8.03E-02	1.40E-02	3.27E-01	1.42E-01
Water consumption	m^3	5.72E-07	2.03E-03	4.49E-04	1.28E-03	1.05E-04	2.15E-04	8.90E-04	5.73E-04	5.23E-03	1.48E-03	5.66E-03	2.31E-04
		Fuel oil		**Methanol**		**LNG**		**Liq. hydrogen**		**Ammonia**		**Elec. + LIB**	
Endpoint area of protection	Unit	Diesel	Bio diesel	Methanol	Bio meth.	LNG	Bio LNG	LH_2	eLH_2	NH_3	eNH_3	E.mix + LIB	E.renew + LIB
Human health	DALY	1.99E-07	2.68E-07	1.34E-07	2.26E-07	2.38E-07	1.54E-07	4.72E-08	2.80E-08	2.16E-07	4.69E-08	2.75E-06	9.01E-07
Natural environment	Species x yr	6.97E-10	2.73E-09	4.05E-10	2.59E-09	6.37E-10	3.90E-10	1.42E-10	8.44E-11	6.53E-10	1.42E-10	4.93E-09	1.78E-09
Resource scarcity	USD (2013)	2.38E-02	4.80E-03	5.00E-04	5.02E-03	1.96E-02	2.54E-03	3.89E-15	2.31E-15	1.78E-14	3.87E-15	9.31E-02	5.97E-02
Power plant efficiency	-	49.34%		49.34%		48.55%		43.88%		51.33%		85.70%	
Total powering impact	-	0.0%		+1.6%		+0.8%		+7.4%		+3.2%		+234.4%	

1 MJ = 0.2778 kWh

Table F.3: Total environmental impact container ships [LCIA/MJ shaft output]

		Fuel oil		Methanol		LNG		Liq. hydrogen		Ammonia		Elec. + LIB	
Midpoint impact category	Unit	Diesel	Bio diesel	Methanol	Bio meth.	LNG	Bio LNG	LH_2	eLH_2	NH_3	eNH_3	E.mix + LIB	E.renew + LIB
Global warming	kg CO_2 eq	1.81E-01	1.32E-01	2.14E-01	7.17E-02	1.72E-01	6.81E-02	5.13E-02	3.04E-02	2.37E-01	5.14E-02	1.04E+00	3.98E-01
Stratospheric ozone depletion	kg CFC11 eq	3.70E-08	8.58E-07	3.66E-08	5.38E-08	2.41E-08	2.52E-08	1.40E-08	1.33E-08	2.93E-08	2.29E-08	2.85E-07	3.10E-08
Ionizing radiation	kBq Co-60 eq	4.93E-05	2.04E-03	1.06E-03	5.60E-03	1.66E-03	2.99E-03	1.07E-03	1.67E-03	2.24E-03	1.08E-02	8.06E-02	9.55E-04
Ozone formation (human health)	kg NO_X eq	6.51E-05	2.03E-04	1.17E-04	2.88E-04	7.26E-05	6.71E-05	8.30E-05	9.21E-05	2.60E-04	1.34E-04	1.70E-03	3.23E-04
Fine particulate matter formation	kg $PM_{2.5}$ eq	3.97E-05	1.63E-04	5.90E-05	1.55E-04	5.31E-05	6.59E-05	4.86E-05	5.95E-05	1.16E-04	9.21E-05	1.92E-03	5.09E-04
Ozone formation (ecosystems)	kg NO_X eq	6.85E-05	2.13E-04	1.27E-04	2.96E-04	7.80E-05	6.80E-05	8.77E-05	9.64E-05	2.71E-04	1.39E-04	1.72E-03	3.36E-04
Terrestrial acidification	kg SO_2 eq	1.51E-04	6.16E-04	1.62E-04	2.93E-04	1.24E-04	1.24E-04	1.03E-04	1.05E-04	3.32E-04	1.82E-04	3.80E-03	1.67E-03
Freshwater eutrophication	kg P eq	1.54E-07	2.42E-05	5.99E-06	3.12E-05	6.66E-06	1.31E-05	6.46E-06	2.29E-05	1.23E-05	4.03E-05	3.20E-04	7.78E-06
Marine eutrophication	kg N eq	2.74E-06	2.67E-04	6.23E-07	1.15E-05	6.60E-07	3.31E-06	6.86E-07	3.65E-06	1.39E-06	4.94E-06	2.24E-05	1.56E-06
Terrestrial ecotoxicity	kg 1,4-DCB	9.86E-03	1.29E-01	2.06E-02	2.06E-01	1.13E-02	2.62E-02	2.02E-02	1.57E-01	1.49E-01	1.88E-01	4.47E-01	1.53E-01
Freshwater ecotoxicity	kg 1,4-DCB	1.04E-05	2.07E-03	9.82E-04	3.50E-03	4.61E-04	1.36E-03	7.82E-04	1.49E-02	4.70E-03	1.74E-02	1.12E-02	8.13E-03
Marine ecotoxicity	kg 1,4-DCB	1.36E-04	2.47E-03	1.33E-03	4.69E-03	6.67E-04	1.75E-03	1.02E-03	1.84E-02	6.02E-03	2.15E-02	1.55E-02	1.01E-02
Human carcinogenic toxicity	kg 1,4-DCB	1.46E-05	3.30E-03	2.22E-03	6.89E-03	1.66E-03	1.98E-03	1.43E-03	4.51E-02	9.47E-03	5.17E-02	2.93E-02	2.46E-02
Human non-carcinogenic toxicity	kg 1,4-DCB	2.23E-02	1.33E-01	1.86E-02	1.68E-01	1.36E-02	2.70E-02	1.65E-02	7.32E-02	7.11E-02	1.04E-01	4.77E-01	4.24E-02
Land use	m^2a crop eq	1.66E-02	2.44E-01	6.19E-04	2.55E-01	4.00E-04	4.93E-03	2.84E-04	2.51E-03	1.50E-03	3.22E-03	9.05E-03	1.44E-03
Mineral resource scarcity	kg Cu eq	1.22E-05	2.16E-04	8.69E-05	2.51E-04	3.01E-05	5.38E-05	4.26E-05	7.42E-04	5.59E-04	8.50E-04	5.48E-03	5.62E-03
Fossil resource scarcity	kg oil eq	5.33E-02	1.41E-02	7.82E-02	1.93E-02	5.61E-02	1.02E-02	3.42E-02	8.52E-03	8.16E-02	1.42E-02	2.84E-01	1.23E-01
Water consumption	m^3	5.72E-07	2.03E-03	4.53E-04	1.29E-03	1.05E-04	2.16E-04	8.98E-04	5.79E-04	5.32E-03	1.51E-03	4.91E-03	2.00E-04
		Fuel oil		**Methanol**		**LNG**		**Liq. hydrogen**		**Ammonia**		**Elec. + LIB**	
Endpoint area of protection	Unit	Diesel	Bio diesel	Methanol	Bio meth.	LNG	Bio LNG	LH_2	eLH_2	NH_3	eNH_3	E.mix + LIB	E.renew + LIB
Human health	DALY	1.99E-07	2.68E-07	1.35E-07	2.28E-07	2.39E-07	1.54E-07	4.76E-08	2.82E-08	2.20E-07	4.77E-08	2.38E-06	7.82E-07
Natural environment	Species x yr	6.97E-10	2.73E-09	4.09E-10	2.61E-09	6.38E-10	3.91E-10	1.44E-10	8.52E-11	6.64E-10	1.44E-10	4.28E-09	1.54E-09
Resource scarcity	USD (2013)	2.38E-02	4.80E-03	5.05E-04	5.06E-03	1.96E-02	2.55E-03	3.92E-15	2.33E-15	1.81E-14	3.93E-15	8.08E-02	5.18E-02
Power plant efficiency	-	49.34%		49.34%		48.55%		43.88%		51.33%		85.70%	
Total powering impact	-	0.0%		+2.6%		+1.0%		+8.4%		+4.9%		+190.1%	

1 MJ = 0.2778 kWh

Table F.4: Total environmental impact TSHDs [LCIA/MJ shaft output]

		Fuel oil		Methanol		LNG		Liq. hydrogen		Ammonia		Elec. + LIB	
Midpoint impact category	Unit	Diesel	Bio diesel	Methanol	Bio meth.	LNG	Bio LNG	LH_2	eLH_2	NH_3	eNH_3	E.mix + LIB	E.renew + LIB
Global warming	kg CO_2 eq	1.81E-01	1.32E-01	2.12E-01	7.09E-02	1.76E-01	6.98E-02	5.12E-02	3.04E-02	2.38E-01	5.17E-02	1.26E+00	4.81E-01
Stratospheric ozone depletion	kg CFC11 eq	3.70E-08	8.58E-07	3.62E-08	5.32E-08	2.47E-08	2.58E-08	1.40E-08	1.33E-08	2.95E-08	2.31E-08	3.44E-07	3.74E-08
Ionizing radiation	kBq Co-60 eq	4.93E-05	2.04E-03	1.05E-03	5.54E-03	1.70E-03	3.07E-03	1.07E-03	1.67E-03	2.25E-03	1.09E-02	9.73E-02	1.15E-03
Ozone formation (human health)	kg NO_X eq	6.51E-05	2.03E-04	1.16E-04	2.85E-04	7.43E-05	6.87E-05	8.29E-05	9.20E-05	2.62E-04	1.35E-04	2.05E-03	3.89E-04
Fine particulate matter formation	kg $PM_{2.5}$ eq	3.97E-05	1.63E-04	5.84E-05	1.54E-04	5.44E-05	6.75E-05	4.86E-05	5.95E-05	1.17E-04	9.27E-05	2.31E-03	6.14E-04
Ozone formation (ecosystems)	kg NO_X eq	6.85E-05	2.13E-04	1.25E-04	2.93E-04	7.99E-05	6.96E-05	8.77E-05	9.64E-05	2.73E-04	1.40E-04	2.08E-03	4.05E-04
Terrestrial acidification	kg SO_2 eq	1.51E-04	6.16E-04	1.61E-04	2.90E-04	1.27E-04	1.27E-04	1.03E-04	1.05E-04	3.34E-04	1.83E-04	4.59E-03	2.02E-03
Freshwater eutrophication	kg P eq	1.54E-07	2.42E-05	5.93E-06	3.09E-05	6.82E-06	1.34E-05	6.46E-06	2.29E-05	1.23E-05	4.06E-05	3.86E-04	9.38E-06
Marine eutrophication	kg N eq	2.74E-06	2.67E-04	6.16E-07	1.14E-05	6.76E-07	3.39E-06	6.85E-07	3.65E-06	1.40E-06	4.97E-06	2.70E-05	1.88E-06
Terrestrial ecotoxicity	kg 1,4-DCB	9.86E-03	1.29E-01	2.04E-02	2.04E-01	1.16E-02	2.69E-02	2.02E-02	1.57E-01	1.50E-01	1.89E-01	5.39E-01	1.85E-01
Freshwater ecotoxicity	kg 1,4-DCB	1.04E-05	2.07E-03	9.72E-04	3.46E-03	4.72E-04	1.39E-03	7.82E-04	1.49E-02	4.73E-03	1.75E-02	1.35E-02	9.81E-03
Marine ecotoxicity	kg 1,4-DCB	1.36E-04	2.47E-03	1.31E-03	4.64E-03	6.83E-04	1.79E-03	1.02E-03	1.84E-02	6.05E-03	2.17E-02	1.88E-02	1.22E-02
Human carcinogenic toxicity	kg 1,4-DCB	1.46E-05	3.30E-03	2.20E-03	6.82E-03	1.70E-03	2.03E-03	1.43E-03	4.51E-02	9.53E-03	5.20E-02	3.54E-02	2.97E-02
Human non-carcinogenic toxicity	kg 1,4-DCB	2.23E-02	1.33E-01	1.84E-02	1.67E-01	1.40E-02	2.77E-02	1.65E-02	7.31E-02	7.16E-02	1.05E-01	5.75E-01	5.12E-02
Land use	m^2a crop eq	1.66E-02	2.44E-01	6.13E-04	2.53E-01	4.10E-04	5.05E-03	2.84E-04	2.51E-03	1.51E-03	3.24E-03	1.09E-02	1.74E-03
Mineral resource scarcity	kg Cu eq	1.22E-05	2.16E-04	8.60E-05	2.48E-04	3.08E-05	5.51E-05	4.26E-05	7.42E-04	5.62E-04	8.55E-04	6.61E-03	6.78E-03
Fossil resource scarcity	kg oil eq	5.33E-02	1.41E-02	7.74E-02	1.91E-02	5.75E-02	1.05E-02	3.42E-02	8.51E-03	8.21E-02	1.43E-02	3.43E-01	1.48E-01
Water consumption	m^3	5.72E-07	2.03E-03	4.48E-04	1.28E-03	1.08E-04	2.21E-04	8.97E-04	5.78E-04	5.35E-03	1.52E-03	5.92E-03	2.42E-04
		Fuel oil		**Methanol**		**LNG**		**Liq. hydrogen**		**Ammonia**		**Elec. + LIB**	
Endpoint area of protection	Unit	Diesel	Bio diesel	Methanol	Bio meth.	LNG	Bio LNG	LH_2	eLH_2	NH_3	eNH_3	E.mix + LIB	E.renew + LIB
Human health	DALY	1.99E-07	2.68E-07	1.34E-07	2.26E-07	2.45E-07	1.58E-07	4.76E-08	2.82E-08	2.21E-07	4.80E-08	2.87E-06	9.43E-07
Natural environment	Species x yr	6.97E-10	2.73E-09	4.05E-10	2.58E-09	6.54E-10	4.01E-10	1.44E-10	8.52E-11	6.68E-10	1.45E-10	5.16E-09	1.86E-09
Resource scarcity	USD (2013)	2.38E-02	4.80E-03	4.99E-04	5.01E-03	2.01E-02	2.61E-03	3.92E-15	2.33E-15	1.82E-14	3.96E-15	9.74E-02	6.25E-02
Power plant efficiency	-	49.34%		49.34%		48.55%		43.88%		51.33%		85.70%	
Total powering impact	-	0.0%		+1.5%		+3.4%		+8.4%		+5.5%		+249.9%	

1 MJ = 0.2778 kWh